

Electronic Thesis and Dissertation Repository

5-24-2012 12:00 AM

Complementary and Self-Complementary Hydrogen Bond Double Helical Complexes

Bhanu P. Mudraboyina
The University of Western Ontario

Supervisor
James A. Wisner
The University of Western Ontario

Graduate Program in Chemistry
A thesis submitted in partial fulfillment of the requirements for the degree in Doctor of
Philosophy
© Bhanu P. Mudraboyina 2012

Follow this and additional works at: <https://ir.lib.uwo.ca/etd>

 Part of the [Materials Chemistry Commons](#), and the [Organic Chemistry Commons](#)

Recommended Citation

Mudraboyina, Bhanu P., "Complementary and Self-Complementary Hydrogen Bond Double Helical Complexes" (2012). *Electronic Thesis and Dissertation Repository*. 548.
<https://ir.lib.uwo.ca/etd/548>

This Dissertation/Thesis is brought to you for free and open access by Scholarship@Western. It has been accepted for inclusion in Electronic Thesis and Dissertation Repository by an authorized administrator of Scholarship@Western. For more information, please contact wlsadmin@uwo.ca.

**COMPLEMENTARY AND SELF-COMPLEMENTARY HYDROGEN BOND
DOUBLE HELICAL COMPLEXES**

(Spine title: Complementary and Self-Complementary Double Helical Complexes)

(Thesis format: Integrated Article)

by

Bhanu Prakash Mudraboyina

Graduate Program in Chemistry

A thesis submitted in partial fulfillment
of the requirements for the degree of
Doctor of Philosophy

The School of Graduate and Postdoctoral Studies
The University of Western Ontario
London, Ontario, Canada

© Bhanu Prakash Mudraboyina 2012

THE UNIVERSITY OF WESTERN ONTARIO
School of Graduate and Postdoctoral Studies

CERTIFICATE OF EXAMINATION

Supervisor

Examiners

Dr. James A. Wisner

Dr. Ken Maly

Dr. Brian L. Pagenkopf

Dr. Leonard G. Luyt

Dr. Gerasimos Moschopoulos

The thesis by

Bhanu Prakash Mudraboyina

entitled:

**COMPLEMENTARY AND SELF-COMPLEMENTARY HYDROGEN
BONDED DOUBLE HELICAL COMPLEXES**

is accepted in partial fulfillment of the
requirements for the degree of
Doctor of Philosophy

Date

Chair of the Thesis Examination Board

Abstract

The design of artificial or synthetic strands that self-assemble to form double-helical complexes have been of great interest to chemists and researchers since the discovery of the double helical DNA structure in 1953 by Watson and Crick. Most of the complexes were self-complementary double-helical homodimers and while few heterodimer complexes are also known. The present thesis describes the design, synthesis and characterization of complementary and self-complementary hydrogen bond arrays built from heterocycles such as pyridine, thiazine dioxide and indole connected in different sequences. The sequence-based stabilities, insolubility issues, substitution and preorganization effects in these arrays have been studied in detail.

The design and syntheses of four self-complementary oligomers that contain an underlying AADD hydrogen bond Donor/Aceptor sequence are presented and their self-association examined in the solution and solid states. Substitution with electron donating and withdrawing groups and the influence of preorganization had a large effect on the overall stabilities of the complexes studied. A wide range ($>10^5 \text{ M}^{-1}$) of stabilities were demonstrated and in the most extreme case, the dimerization constant measured ($K_{\text{dimer}} \geq 4.5 \times 10^7 \text{ M}^{-1}$) is comparable to the most stable homodimers of neutral coplanar AADD arrays reported to date.

Two sets of DDD hydrogen bond arrays were synthesized that form triply hydrogen bonded double helical complexes with an AAA array when combined in CDCl_3 solution. In contrast to the detrimental effect of appended alkyl chain arrays containing tethers between donor heterocycles displayed an increased stability in their association constants (K_a).

The effect of introduction of a hexyl chain on the solubility of an originally insoluble (in CDCl_3) DDD array based on three thiazine dioxides was studied. The association constants measured based on NMR titrations and ITC titrations demonstrate formation of a highly stable double-helical pair with a K_a value of $1.4 \times 10^5 \text{ M}^{-1}$. A self-complementary double helical complex based on six hydrogen bond AAADDD array was also synthesized and displays very strong dimerization ($K_{\text{dimer}} > 4.5 \times 10^7 \text{ M}^{-1}$ in CDCl_3) examined by NMR dilution and mixed solvent studies. These findings establish the high potential of the DDD array and the AAADDD array as monomer components to build supramolecular architectures or polymers.

Keywords

Complementary, Self-Complementary, Hydrogen Bond, Double Helix, Substituent Effect, Preorganization, NMR Dilutions, NMR Titrations, Isothermal Titration Calorimetry, X-ray analysis.

Co-Authorship Statement

Dr. Jiaxin Li and Dr. Hong-Bo Wang have synthesized **4-1** and **3-1a-h**, respectively.
Doug Hairsine (manager, mass spectrometry) has collected all the mass spectrometry data.
All of the remaining work in this thesis has been done by the author himself.

Acknowledgments

I would like to take this opportunity to thank everyone who has helped me to reach this point and travel through my graduate program. Firstly, I acknowledge my supervisor Prof. James A Wisner, for providing me with an opportunity to pursue my doctoral studies, and his guidance through the years. He has been very supportive during the entire period of my Ph.D. program, especially through the “not so productive” time and has given me the freedom to extend my research project in right direction. He patiently demonstrated valuable lab techniques from simple flash column chromatography to running sensitive titrations on ITC calorimeter for which I am very grateful. I am fortunate to work with him as he is not only a great supervisor but also a marvellous being. I have learnt a lot from him regarding chemistry and the academic world.

I want to thank my examiners, Dr. Ken Maly, Dr. Brian L. Pagenkopf, Dr. Len G. Luyt and Dr. Gerasimos Moschopoulos for reviewing my thesis work.

I am thankful to all the past and present graduate students of the Wisner lab; Dr. Barry Blight, Dr. Jiaxin Li, Dr. Hong-Bo Wang, Fatimah Al-garni, Jeff Pleizier, Iamnica Linares Mendez. Being an international student, I greatly appreciate my lab mates for providing a friendly atmosphere. Besides passing on the techniques, I have learnt about being a good team leader and a colleague while supervising few 490 students during the term of my Ph.D. program. I extend my thanks to all the 490 students; Melissa McDonald, Stephanie Holborne and Brian Ngo.

I am grateful to Prof. Nicholas Payne for teaching me X-ray crystallography and to Dr. Guerman Popov and Dr. Benjamin Cooper for helping me with valuable discussions to

solve our research lab X-ray data. I am thankful to Prof. Stephen Loeb for arranging to collect one of my crystal data when the X-ray facility at UWO ceased to work for a while. Special thanks to Dr. Hudson and Dr. Workentein for permissions to use their UV, Mass and HPLC spectrophotometers.

I would like to extend my appreciation to all the departmental staff members, especially: Mathew Willans for helping me out with several NMR experiments, Doug Hairsine for the timely mass spectrums; Yves Rambour for fixing the broken glassware; Darlene McDonald for her duties as a Graduate Coordinator; Monika Chirigel, Don Yakobchuk, Marylou Hart and Sherrie McPhee at the chem-bio-stores for their respective services.

I am indebted to my family; Dad and Ma for giving me the freedom to make my own decisions and encouraging me to pursue my dreams; brothers Madhukar and Anil for their loving support. My wife, Preeti has been with me all through my journey as a graduate student and before. I am thankful for having such a delightful person as best friend and wife, who's constant support has made my life easier and cheerier. Without her, my life would not be as wonderful. I also take the opportunity to thank my parent in-laws and all my family and friends in India and abroad for their continuous love, support and understanding. Last but not least, I thank God for giving me the determination and strength to diligently pursue my goals.

THANK YOU EVERYONE

Table of Contents

CERTIFICATE OF EXAMINATION	ii
Abstract	iii
Co-Authorship Statement.....	v
Acknowledgments.....	vi
Table of Contents.....	viii
List of Tables	xiii
List of Figures	xiv
List of Schemes.....	xxii
List of Abbreviations and Symbols.....	xxiv
Chapter 1	
1 Introduction.....	1
1.1 Significance and Occurrence of Hydrogen Bonds.....	2
1.2 Hydrogen Bonding.....	5
1.2.1 Definition	5
1.2.2 Characteristics of Hydrogen Bonds.....	7
1.2.2.1 Strength of a Single Hydrogen Bond.....	7
1.2.2.2 Directionality of Single Hydrogen Bonding.....	9
1.2.2.3 Specificity of Hydrogen Bonds.....	11
1.3 Hydrogen Bonded Complexes	12
1.3.1 Design Parameters of Hydrogen Bonded Complexes.....	13

1.3.1.1	Functional Groups and Substituents.....	14
1.3.1.2	Preorganization.....	17
1.3.1.3	Tautomers.....	20
1.3.1.4	Solubility.....	22
1.3.1.5	Fidelity.....	25
1.3.1.6	Number of Hydrogen Bonds and Secondary Interactions.....	27
1.3.2	Complementary and Self-Complementary Hydrogen Bonded Complexes ..	28
1.3.2.1	Self-Complementary or Homodimer Complexes.....	29
1.3.2.1.1	ADAD Complexes.....	30
1.3.2.1.2	AADD Complexes.....	31
1.3.2.1.3	Six-Membered Self-Complementary Complexes.....	35
1.3.2.2	Complementary or Heterodimer Complexes.....	36
1.3.2.2.1	AAD•DDA Complementary Complexes.....	36
1.3.2.2.2	AAA•DDD Complementary Complexes.....	37
1.3.2.2.3	ADDA•DAAD Complementary Complexes.....	38
1.3.2.2.4	AAAA•DDDD Complementary Complexes.....	39
1.3.2.2.5	Unusual Complementary Complexes.....	41
1.3.3	Double-Helical Complexes	42
1.3.3.1	Design of Double-Helical Arrays.....	47
1.4	Scope of the Thesis	48
1.5	References.....	49
 Chapter 2		
2	Synthesis and Self-Association of Double Helical AADD Arrays.....	56
2.1	Hydrogen Bonded Supramolecular Polymers.....	56

2.2	AADD Arrays as Components of Hydrogen Bonded Materials.....	58
2.3	Design of Double-Helical AADD Arrays.....	61
2.4	Synthesis of Double Helical AADD Arrays.....	66
2.5	X-ray Analysis of AADD Arrays.....	84
2.6	Solution Characterization of the Dimerization of 2-1a-d	95
2.6.1	Analysis of Complex Stability.....	96
2.6.2	¹ H NMR Studies of 2-1a-d	100
2.7	Conclusion.....	107
2.8	Experimental.....	108
	General.....	108
2.8.1	¹ H NMR Dilution Procedure.....	109
2.8.2	General Synthetic Methods.....	110
2.8.3	Synthetic Methods.....	111
2.9	References.....	132

Chapter 3

3	The Effect of Sterics and Preorganization on Stability in Double-Helical AAA-DDD Complexes.....	140
3.1	Contiguous Arrays for Hydrogen Bonded Complex Formation.....	140
3.2	Results and Discussion.....	145
3.2.1	Design of the donor Arrays.....	145
3.2.2	Synthesis of 3-3a-c Donor Arrays.....	147
3.2.3	Synthesis of Single Trimethylene Tethered DDD Arrays.....	149
3.2.4	Synthesis of Dissymmetric Soluble DDD arrays 3-5a-b and 3-6a-b	152
3.3	Solid State X-Ray Studies of the DDD arrays 3-4a , 3-4b and 3-5b	153

3.4 NMR Titration Studies of DDD Arrays.....	160
3.4.1 NMR Titration Studies of DDD Array 3-4b	162
3.4.2 NMR Studies of Soluble DDD Arrays 3-5a,b and 3-6a,b :.....	165
3.5 Conclusion	169
3.5.1 Experimental	169
General.....	169
3.5.2 ¹ H NMR Titration Procedure	170
3.5.3 Synthetic Procedures.....	171
3.6 References.....	183
 Chapter 4	
4 Synthesis and Binding Studies of a Complementary DDD•AAA Complex and a Self-Associated Double-Helical AAADDD•DDDAAA Complex	187
4.1 Synthesis of Alkylated DDD Array 4-4	190
4.2 NMR Titration Studies of the AAA•DDD Array.....	192
4.3 Synthesis of a Double Helical Self-Complementary AAADDD Array.....	196
4.4 Self-Association of the Double-Helical AAADDD•DDDAAA Complex	200
4.5 Conclusion	202
4.6 Experimental	203
4.6.1 Isothermal Titration Calorimetry Procedure	203
4.6.2 Synthetic Procedures.....	204
4.7 References.....	215
 Chapter 5	
5 Conclusions.....	219
5.1 Scope for Future Work.....	221

5.2 References.....	223
Appendices.....	224
Permission to Reproduce Material from the Literature	224
Curriculum Vitae	229

List of Tables

Chapter 2

Table 2-1 Cyanide reagents and stoichiometries used and yields observed in the cyano-dehalogenation reaction of 2-3 . Reaction conditions as in Figure 2-6.....	71
Table-2-2 Trials of the bromination of 2-9a using different reaction conditions.....	73
Table 2-3 Crystallographic parameters for 2-1a•2-1a and 2-1b•2-1b crystals.....	85
Table 2-4 Crystallographic data for 2-1c•2-1c and 2-1d•2-1d	86
Table 2-5 Summary of bond distances and angles of 2-1b•2-1b , 2-1c•2-1c and 2-1d•2-1d from their X-ray crystal structure data.....	94

Chapter 3

Table 3-1 Trials of reactions attempted for last step of scheme 3-1.....	150
Table 3-2 Four sets of complementary AAA•DDD complexes (3-5a•3-2a , 3-5b•3-2a , 3-6a•3-2a and 3-6b•3-2a) compared with the association constants, free energies, their differences and net difference in energies with that of 3-1a•3-2a and 3-1b•3-2a respectively.....	168

Table of Figures

Chapter 1

Figure 1-1	Interaction of enzyme with substrate by a lock and key mechanism to give an enzyme–substrate complex.....	1
Figure 1-2	A cartoon representation of DNA double helical structure with specific base pairing projected as an inset. Keratin (below) displaying α -helix and a β -pleated sheet secondary structures.....	3
Figure 1-3	A two dimensional array of melamine and cyanuric acid hydrogen bonding assembly.....	4
Figure 1-4	Hydrogen bonding between two electronegative heteroatoms X and Y.....	5
Figure 1-5	Molecular electrostatic potential surfaces plotted on the van der Waals' surface of the molecule calculated by using AM1.	9
Figure 1-6	Hydrogen bonding between the acceptor (A) and the hydrogen of donor (D).. .	10
Figure 1-7	Arrangement of complementary sites leads to specifically attractive or repulsive interactions as demonstrated using 2-aminopyridine molecules.	11
Figure 1-8	Common complementary hydrogen bonding arrays developed that resemble base pairs.....	12
Figure 1-9	(i) Hydrogen bonding in an anti-parallel β sheet and (ii) Bing Gong's hydrogen bonded complex which resembles the β sheet.....	13
Figure 1-10	AAA-DDD Model system investigated by Boyd and coworkers.	15
Figure 1-11	Substituent effects of the heterocyclic based array AAA-DDD complementary system on the association constants.....	15
Figure 1-12	Possible tautomeric and conformational configurations of arrays 1-3 and 1-4 ..	16
Figure 1-14	Conformational equilibrium of ethoxynaphthyridine 1-5 and its complex with array 1-6	18

Figure 1-15 Imide-urea strands that pair into self-complementary duplexes 1-8•1-8 via bifurcated hydrogen bonds.....	19
Figure 1-16 The tautomeric and self-association equilibria observed in a solution of 2-ureido-4-pyrimidone 1-9	21
Figure 1-17 Zimmerman's AADD array 1-10a that can only form a tautomeric AADD array 1-10b thereby maximising the association constant values possible for the complex.....	22
Figure 1-18 Intermolecular interactions in solution are a competition between solute–solvent interactions in the free state, and solute–solute and solvent–solvent interactions in the bound state.....	22
Figure 1-19 Results of ³¹ P NMR titration experiments displaying the association constant for formation of a 1:1 complex between perfluoro-tert-butyl alcohol and tri-n-butyl phosphine oxide.	24
Figure 1-20 DAN•UG complex formed due to high fidelity between the two arrays.	26
Figure 1-21 Secondary interactions shown in four different modules, DAD•ADA, ADD•DAA and DDD•AAA motifs	28
Figure 1-22 Dimers of acylated diaminotriazine and diaminopyrimidine ADAD modules.....	30
Figure 1-23 Diacylpyrimidine 1-11 and ureidoacylpyrimidine 1-12 as ADAD bonding motifs according to Meijer and co-workers.....	31
Figure 1-24 Meijer's AADD motifs displaying extreme complex stabilities.....	31
Figure 1-25 Amidinourea-based self-complementary modules with preorganized linear hydrogen-bonding arrays..	32
Figure 1-26 A highly selective, neutral, fluorescent sensor based on 2-ureido-4[1H]-pyrimidinone quadruple hydrogen-bonded AADD motif.....	33

Figure 1-27 Design and self-assembly of general-purpose Bis-DeAP module.....	33
Figure 1-28 Structure of an AADD array based on ureidoimidazo[1,2-a]pyrimidine UImp-2 , forming a stable dimer.	35
Figure 1-29 The design of the self-complementary duplex forming a AADADD-DDADAA complex in the solution state.....	35
Figure 1-30 Assorted complexes containing the AAD•DDA motif. The K_a values are measured in $CDCl_3$	36
Figure 1-32 Extremely stable complexes of both neutral and ionic types.....	38
Figure 1-33 Highly stable complexes exhibiting ADDA•DAAD hydrogen bond arrays.	38
Figure 1-34 Formation of the putative heterodimer AAAA•DDDD with four hydrogen bonds and six attractive secondary interactions.....	39
Figure 1-35 1H NMR spectra of DDDD ⁺ , complex DDDD ⁺ •AAAA and AAAA	40
Figure 1-36 Oligoamide strands containing both benzene and naphthalene spacers sharing AADD sequences that heterodimerize.....	42
Figure 1-37 Structure of an oligopyridinecarboxamide and the crystal structures of its single helix foldamer and double helix dimer.	43
Figure 1-38 Schematic illustration of the heteroduplex formation of 9merH with oligosaccharides.....	44
Figure 1-39 Structures of <i>m</i> -terphenyl-based molecular strands bearing amidine and/or carboxyl groups.....	45
Figure 1-40 Fluoro-substituted quinoline oligoamide that forms cross-hybridized double helical complex.....	46
Figure 1-41 A and D subunits form components of a supramolecular “toolbox” which can be used to construct arrays that undergo hydrogen bonding to form complementary complexes.	47

Chapter 2

- Figure 2-1** A plot of the relation between association constant K_a and the degree of polymerization of idealized monomers at two different concentrations..... 57
- Figure 2-2** Changing the macroscopic properties of a telechelic poly(ethylene/ butylene) copolymer (left) by end-group modification..... 58
- Figure 2-3** Examples of AADD arrays and designs with K_{dimer} values and supporting solvents at room temperature. 59
- Figure 2-4** Biomimetic linear modular polymer based on the Upy AADD array, mimicking titin, a skeletal muscle protein. 60
- Figure 2-5** Basic design of the arrays with a simple donor (D) and acceptor (A) pair leading to an oligomeric strand..... 62
- Figure 2-6** The AADD complex design as a hybrid of alternating ADADA and contiguous AAA•DDD sequences. 63
- Figure 2-7** Design attributes of the AADD array outlined using different colors. 64
- Figure 2-8** Four different AADD arrays **2-1a-d** highlighting the progressive changes made to the basic design that may lead to increased stability of the complexes..... 65
- Figure 2-9** ^1H NMR spectrum of the substitution reaction using $\text{Zn}(\text{CN})_2$ as cyanide reagent, displaying resonances corresponding to the two products **2-4** and **2-5** and the starting material **2-3**..... 69
- Figure 2-10** ^1H NMR of the mixture of mono and dibrominated acetyl skatole before (a) and after (b) washing with ice cold methanol shows considerable reduction of the dibromide contaminant compared to the mono brominated product. 80
- Figure 2-11** Stick representation of X-ray crystal structure of array **2-1a** with intermolecular (dashed orange lines) as well as intramolecular (dashed purple lines) hydrogen bonds” indicated.....87

Figure 2-12	Stick representation of the X-ray crystal structure of array 2-1b with intermolecular (dashed orange lines) hydrogen bonds indicated.....	88
Figure 2-13	Stick representation of the X-ray crystal structure of dimer 2-1c•2-1c with intermolecular hydrogen bonds indicated (dashed orange lines).....	90
Figure 2-14	Stick representation of the X-ray crystal structure of dimer 2-1d•2-1d with intermolecular hydrogen bonds indicated (dashed orange lines).....	92
Figure 2-15	(A) Schematic diagram of ITC; (B) An example of isotherms obtained and plotting of the isotherm for determination of ΔG , ΔH and ΔS	97
Figure 2-16	^1H NMR spectra displaying the concentration dependant behaviour of 2-1a in CDCl_3	100
Figure 2-17	NMR dilution curve of array 2-1a (following N-H ^b) with K_{dimer} value and free energies calculated from fitting of the data to a 1:1 dimerization model.	101
Figure 2-18	Stacked plot of ^1H NMR dilutions of 2-1b in CDCl_3 at concentrations of 6.0×10^{-3} M, 1.5×10^{-3} M, 7.2×10^{-4} M, 2.8×10^{-4} M, 8.6×10^{-5} M.....	102
Figure 2-19	Dilution curve of array 2-1b (following N-H ^b) in CDCl_3 with K_{dimer} value and free energy calculated from fitting of the data to the 1:1 dimerization model.....	103
Figure 2-20	Stacked plot of ^1H NMR dilutions of 2-1c in CDCl_3 at concentrations of 26.0×10^{-3} M, 4.2×10^{-3} M, 6.5×10^{-4} M, 1.3×10^{-4} M, 9.8×10^{-5} M.....	104
Figure 2-21	Dilution curve of array 2-1c (following N-H ^b) with K_{dimer} value and free energy calculated from fitting of the data to a 1:1 dimerization model.....	105
Figure 2-22	(i) 600 MHz ^1H NMR spectrum of 2-1d at 2.5×10^{-3} M in CDCl_3 ; (ii) and (iii) Downfield portion of the ^1H NMR spectra of 2-1d (in ppm) at 100 μM and 1 μM dilutions, respectively.	106

Chapter 3

- Figure 3-1** Early experimental examples of AA•DDD and AAA•DDD hydrogen bonding arrays reported by Zimmerman's group (left and middle) and Bell and Anslyn (right)..... 141
- Figure 3-2** Two examples of complementary AAAA•DDDD⁺ hydrogen bonding complexes and their K_a values determined in CDCl₃ (left side)⁵ and CH₂Cl₂ (right side)..... 142
- Figure 3-3** A very stable complementary double helical AAA•DDD hydrogen bond complex with a K_a value > 10⁵ M⁻¹ in CDCl₃ 143
- Figure 3-4** Complexes **1a-h•2a-c** displaying the increase in the association constants by up to a factor of 30 in the cases studied 144
- Figure 3-5** DDD arrays originally designed for the current study 146
- Figure 3-6** Synthesis of methyl 2-acetyloctanoate, for the incorporation of a pentyl chain at the 3-position of the indole heterocycle..... 155
- Figure 3-7** Stick representations of X-ray crystal structure of DDD array **3-4a**..... 155
- Figure 3-8** Stick representation of X-ray crystal structure of array **3-4b**..... 157
- Figure 3-9** Stick representations of X-ray crystal structure of array **3-5b**..... 159
- Figure 3-10** Titration curves measured at six different percentages of added CH₃OH (v/v) in CDCl₃..... 163
- Figure 3-11** (i) K_a and ΔG values measured in solutions with different percentages of added CH₃OH for complex **3-4b•3-2a**; Plots of K_a (ii) and ΔG values (iii) vs. % CH₃OH in CDCl₃..... 164
- Figure 3-12** Titration curves for three different types of complexes **3-5a,b•3-2a**, **3-6a,b•3-2a** and **3-1a,b•3-2a**..... 166

Chapter 4

- Figure 4-1** An AAA•DDD complementary complex with high stability ($K_a \geq 10^5 \text{ M}^{-1}$) in CDCl_3 . Stick representation of X-ray crystal structure of **4-1.4-2** displaying the double helical arrangement of the complex. 187
- Figure 4-2** (i) Thiazine dioxide and indole containing DDD arrays. (ii) Crystal structure of the insoluble array **4-3a** 188
- Figure 4-3** (i) Terthiazine dioxide based DDD array **4-4** including a hexyl chain attached to the central donor heterocycle to induce solubility in CDCl_3 ; (ii) a six-hydrogen bonded self-complementary AAADDD array **4-5**. 189
- Figure 4-4** Stacked plot of the downfield region of the ^1H NMR spectra of alkylated donor array **4-4**, acceptor array **4-2** and the complex **4-4.4-2** in CDCl_3 at room temperature 193
- Figure 4-5** Titration curve displaying the concentration dependent chemical shifts of the amine proton of thiazine dioxide of **4-4** when titrated with **4-2** 194
- Figure 4-6** ITC data for the binding of **4-4** and **4-2** in CDCl_3 at 22°C 195
- Figure 4-7** A double-helical six hydrogen bonded self-complementary system **4-5.4-5** based on thiazine dioxide, indole and pyridine heterocycles. 196
- Figure 4-8** ^1H NMR spectrum of the double-helical AAADDD•DDDAAA **4-5.4-5** Complex, in CDCl_3 at room temperature. 200
- Figure 4-9** ^1H NMR dilution curve of array **4-5** with a K_{dimer} value of $1.2 \times 10^4 \text{ M}^{-1}$, calculated from fitting of the data to a 1:1 dimerization model with 5% DMSO in CDCl_3 201
- Figure 4-10** Examples of dimers with their definitive K_{dimer} values determined in 5% DMSO (v/v)/ CDCl_3 solvent mixture. 202

Chapter 5

Figure 5-1 Propyl chain incorporated DDD arrays.....	221
Figure 5-2 <i>N,N'</i> -dimethylamine functionalized and preorganized DDD arrays.....	221
Figure 5-3 : Supramolecular polymers formed on the basis of DDD-Linker-DDD and AAA-Linker-AAA.....	222

List of Schemes

Chapter 2

- Scheme 2-1** Retrosynthetic pathways leading from the series of AADD arrays.....67
- Scheme 2-2** Synthesis of acceptor components **2-10a-c**.....69
- Scheme 2-3** Direct incorporation of bromide and tributyltin groups to 4-picoline and 3,4-lutidine.....72
- Scheme 2-4** Synthesis of α -haloacylpyridyl fragments **2-11a,b** of the AADD arrays.....73
- Scheme 2-5** Synthesis of **2-11a,b** from 2,6-dibromo-3,5-lutidine.....74
- Scheme 2-6** Direct acetylation of skatole using AlCl_3 as Lewis acid resulting in mixture of by-products.....77
- Scheme 2-7** Synthesis of the indole containing fragments of AADD arrays.....77
- Scheme 2-8** Synthetic schemes of nitro substituted donor units reflecting poor yields and synthetic difficulties obtaining acyclic nitro skatoles compared to the facile formation of cyclic nitroindole **2-16**.....78
- Scheme 2-9** Mechanistic details of the diazonium salt of nitroaniline undergoing Japp-Klingemann reaction followed by Fisher Indole cyclization.....79
- Scheme 2-10** Final steps in the synthetic route to AADD arrays **2-1a-d**.....83

Chapter 3

- Scheme 3-1** Retrosynthetic pathway leading from the preparation of doubly di/trimethylene tethered DDD arrays **3-3a-c** to commercially available anilines and cyclic ketones.....148
- Scheme 3-2** General synthetic scheme to construct the singly tethered DDD arrays...151-151

Chapter 4

- Scheme 4-1** Synthetic pathway for the preparation of alkylated DDD array **4-4** which undergoes complementary helical complex formation with **4-2**.....192
- Scheme 4-2** Synthetic scheme leading to preparation of acceptor component **4-19**..... 198
- Scheme 4-3** Synthetic scheme leading to **4-2**.....199
- Scheme 4-4** Synthetic scheme leading to preparation of **4-5** and its homodimer.....199

List of Abbreviations and Symbols

A	acceptor
α	alpha
AcOH	acetic acid
AT	adenine-thymine
β	beta
ⁿ BuLi	ⁿ butyl lithium
°C	celsius degree
CG	cytosine-guanine
δ	chemical shift
D	donor
d	doublet
DMAP	4-dimethylaminopyridine
DMF	dimethylformamide
DMSO	dimethylsulfoxide
DNA	deoxyribonucleic acid
EI	electron impact ionization
ESI	electrospray ionization
ES	enzyme- substrate
<i>et al.</i>	and others
γ	gamma
g	gram
ΔG	change in Gibbs free energy
ΔH	enthalpic change

h	hour
HRMS	high resolution mass sepectrometry
Hz	hertz
IN	indole
ITC	isothermal titration calorimetry
K	kelvin
K_a	association constant
K_{dimer}	dimerization constant
kCal	kilo Calorie
kJ	kilo Joule
KSAc	potassium thioacetate
Lu	lutidine
m	multiplet
M^{-1}	$(\text{mol/liter})^{-1}$
<i>m</i> CPBA	metachloroperoxybenzoic acid
MeCN	acetonitrile
min	minute
mL	milliliter
mmol	millimole
mol^{-1}	/mol
m.p.	melting point
N/A	not available/not applicable
NMR	nuclear magnetic resonance
NOESY	nuclear overhauser effect spectroscopy
P	product

Ph	phenyl
ppm	part per million
Py	pyridine
RNA	ribonucleic acid
σ	Hammett substituent constant
s	singlet
ΔS	entropic change
t	triplet
T	temperature
TFAA	trifluoroacetic anhydride
THF	tetrahydrofuran
TH	thiazine dioxide
UHP	urea-hydrogen peroxide
Vs.	versus

Chapter 1

1 Introduction

The concept that the complementarity of interacting sites forms the basis for molecular recognition was first introduced by the Dutch chemist Emil Fischer,¹ who proposed in 1894 that an enzyme and substrate fit together "like a lock and key". A contemporary view on molecular recognition, termed induced fit, considers that the interacting molecules are flexible and can change their shape during the recognition process (Figure 1-1).² Induced fit has been observed experimentally for many protein-ligand interactions. At the molecular level, the factors that contribute to the complementarity between two molecules include the shape of the interacting sites, their various non-covalent interactions and the chemical as well as physical environment.

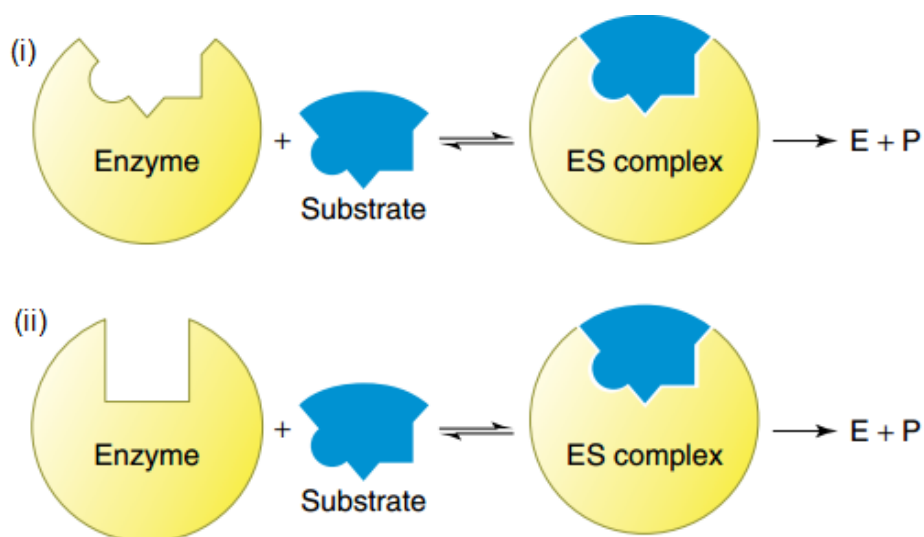


Figure 1-1 (i) Interaction of an enzyme with a substrate by a lock and key mechanism to give an enzyme–substrate complex. (ii) Interaction of an enzyme with a substrate by an induced fit mechanism to give an enzyme–substrate complex.

The essential processes of life such as self-replication, information transportation and metabolisms occur largely by site-specific interactions between biological molecules. Therefore understanding how molecules recognize each other is one of the fundamental issues in biochemical processes. Molecules can be engineered to self-assemble into higher order complexes by arranging the “codes” or information placed on these sites *via* non-covalent bonds. Although single and discrete non-covalent interactions are usually weak in nature and often do not withstand the thermal collisions of molecules that keep them apart, the effects of their cumulative strength are evident in both natural and synthetic materials. The profound effect of these secondary interactions that are used to build „smart materials“³ has a range of interacting energies that gives rise to a flexible array of interesting properties in contexts as diverse as the vital functions of living organisms to data storage in novel materials.⁴ While molecular recognition is broadly based on non-covalent interactions such as hydrogen bonding, π - π stacking,⁵ pre-organizational effects,⁶ ion-dipole interactions,⁷ hydrophobic⁸ and lipophilic interactions,⁹ it is hydrogen bonding that often forms the basis for a recognition process that requires specificity, directionality and stability in complex formation.

1.1 Significance and Occurrence of Hydrogen Bonds

Indeed, hydrogen bonds provide directional interactions that support not only molecular recognition but a wide range of self-assembly. The cores of most proteins are composed of hydrogen bonded secondary structures such as α -helices and β -sheets (Figure 1-2 (below)).¹⁰ Among natural or designed substrate receptors, complementary hydrogen bonded duplexes have been recognized from the commencement of this field.

DNA is one central and remarkable example of two different oligomeric molecular strands coming together in an intertwined, highly specific and reversible manner.

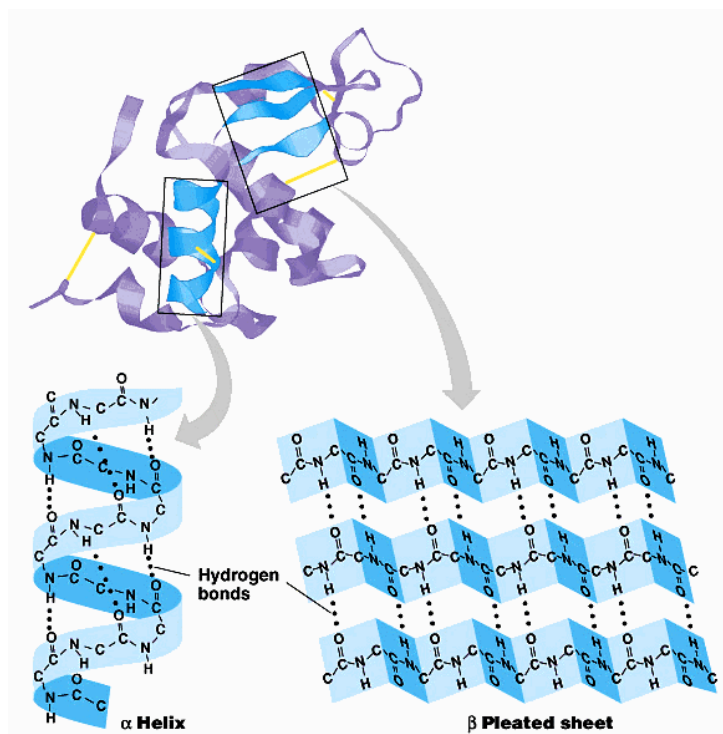
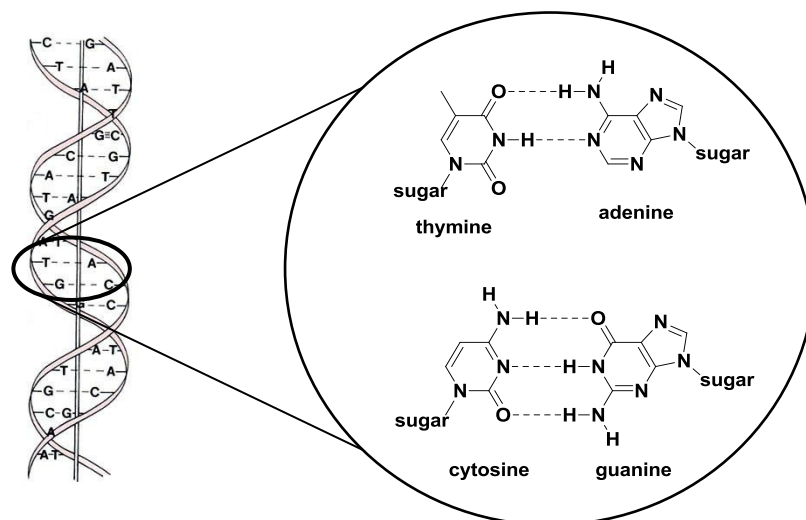


Figure 1-2 (above) A cartoon representation of DNA double helical structure with specific base pairing projected as an inset. Keratin (below) displaying α -helix and a β -pleated sheet secondary structures.

If not for hydrogen bonding, water would not have its special role as a solvent that boils at a high temperature of 100 °C. The hydrogen bonding makes the water molecules “stick” together. In contrast to the desirable qualities, unwanted effects can be seen when cyanuric acid and melamine are brought together (Figure 1-3) leading to kidney stone formation and renal damage.¹¹ Thus this concept of weak interactive forces is very powerful as a cumulative effect and needs to be well studied and understood.

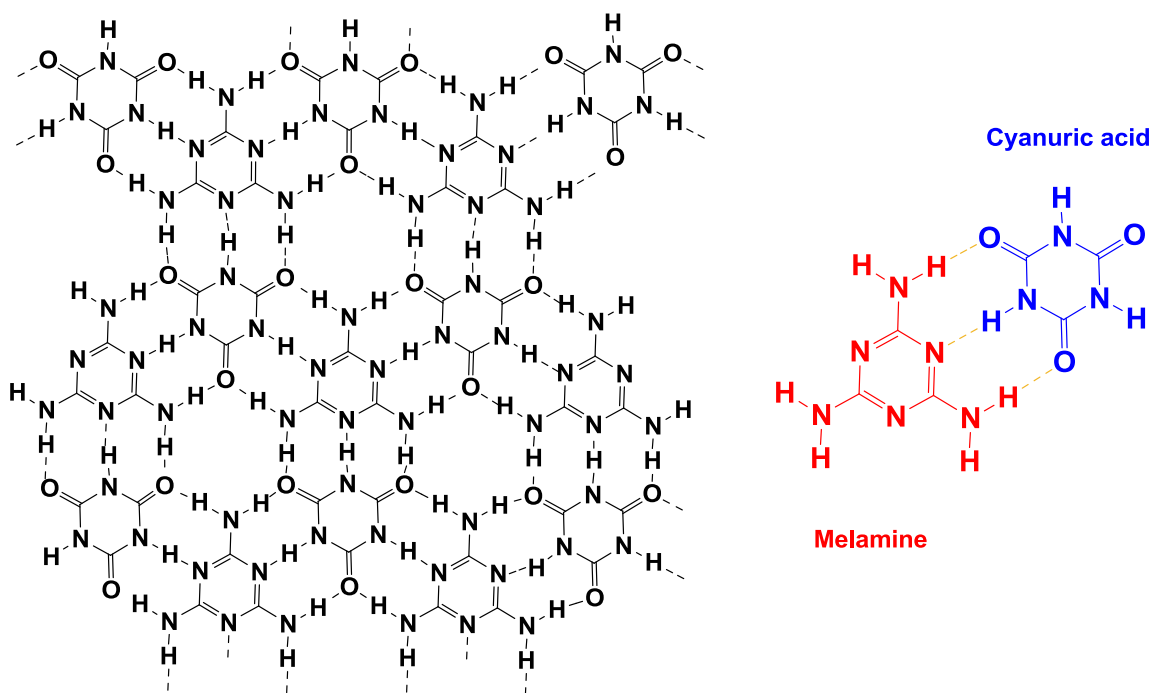


Figure 1-3 A two dimensional array of melamine and cyanuric acid assembled due to the intermolecular attractions of hydrogen bonding that form an insoluble crystal lattice.

Hydrogen bonding can be used to construct larger molecules from smaller ones and thus can be used as „molecular Velcro“ to glue molecules together in a highly specific manner. The stability of such supramolecules in turn rests on the strength of the net hydrogen bonding, the type of modules taking part in hydrogen bonding to bringing about such assemblies and also is often proportional to the number of hydrogen bonds.

1.2 Hydrogen Bonding

Hydrogen bonding is a complex interaction that consists of at least four types of chemical characteristics: electrostatics (acid/base), polarization (soft/hard), van der Waals (repulsion/dispersion), and covalency (charge transfer).¹² The division into these components has been well studied and reported though polarization is not completely independent of the other three components.

1.2.1 Definition

Pauling, in 1939, stated in his book *The Nature of the Chemical Bond* “*under certain conditions an atom of hydrogen is attracted by rather strong forces to two atoms, instead of only one, so that it may be considered to be acting as a bond between them*”. Thus an H atom is the key element that brings a hydrogen bonding donor (X) and hydrogen bonding acceptor (Y) together (Figure 1-4). Depending on the nature of X and Y, the energy of hydrogen bond lies in the range of 2.1 to 167 kJ mol⁻¹. The strongest hydrogen bonds are stronger than the weakest covalent bonds while the weakest hydrogen bonds are practically indistinguishable from van der Waals interactions.

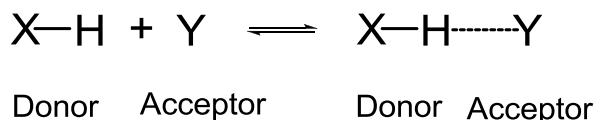


Figure 1-4 Hydrogen bonding between two electronegative heteroatoms X and Y mediated by a hydrogen atom.

In the recent past (1997), IUPAC defined hydrogen bonding in its Gold Book. The definition states that a hydrogen bond is “... *a form of association between an electronegative atom and a hydrogen atom attached to a second, relatively*

electronegative atom. It is best considered as an electrostatic interaction, heightened by the small size of hydrogen, which permits proximity of the interacting dipoles or charges. Both electronegative atoms are usually (but not necessarily) from the first row of the Periodic Table, i.e., N, O or F. Hydrogen bonds may be intermolecular or intramolecular. With a few exceptions, usually involving fluorine, the associated energies are less than $20\text{--}25\text{ kJ mol}^{-1}$ ($5\text{--}6\text{ kcal mol}^{-1}$) ...". The evidence for hydrogen-bond formation may be experimental or theoretical, or ideally, a combination of both. Some criteria useful as evidence and some typical characteristics for hydrogen bonding, not necessarily exclusive, are listed in a recent essay by Desiraju, in detail.^{13,14}

These two definitions do serve to describe hydrogen bonds in their own manner but in simpler parlance we will define it as: the attractive force between the electropositive hydrogen interceding between two electronegative species such as X and Y. Usually the electronegative species X and Y are heteroatoms such as oxygen, nitrogen, or fluorine, which have a partial negative charge and the hydrogen a partial positive charge. In supramolecular terms, the electronegative heteroatom to which the hydrogen is covalently bound is called the hydrogen bond donor (denoted by D). The other electronegative atom must have one or more unshared electron pairs as in the case of oxygen and nitrogen, have a negative partial charge and will be called a hydrogen bond acceptor (denoted by A). The hydrogen on the donor, which has a partial positive charge binds to another atom of oxygen or nitrogen with excess electrons to share and is attracted to the partial negative charge of the acceptor. This forms the basis for a hydrogen bond.

1.2.2 Characteristics of Hydrogen Bonds

Hydrogen bonding is ubiquitous in nature and is characterized mainly by three qualities : strength, directionality and specificity. These unique qualities distinguish it from other types of non-covalent interactions that are generally lacking in at least one of these characteristics. The variance of these qualities in single hydrogen bonds as well as on hydrogen bonded complementary complexes are discussed in the further sections of this chapter.

1.2.2.1 Strength of a Single Hydrogen Bond

The strength of a single hydrogen bond depends on the electronegativity of D and A heteroatoms and the influence of the adjacent functional groups they are connected to. This results in a wide range of energies observed starting from $< 2 \text{ kJ mol}^{-1}$ to $> 170 \text{ kJ mol}^{-1}$.¹⁵ A weak hydrogen bond can be characterized by bond energies less than 16 kJ mol^{-1} , an angle less than 110° and a very long bond length between the heteroatoms ($> 3.6 \text{ \AA}$). On the other hand strong hydrogen bonds are easy to distinguish with energies $> 40 \text{ kJ mol}^{-1}$, short bond distances ($< 3.2 \text{ \AA}$) and angles from 150° 180° .¹⁶ The strength of a hydrogen bonding is a direct outcome of both the electronegativities of the donor and the acceptor as well as the linearity of the hydrogen bond.

Physical organic chemists have determined the association constants K_a for a very large number of intermolecular interactions in the solution phase. For simple molecules, Abraham has developed an equation that relates the $\log K$ for a hydrogen bond interaction between two functional groups and their empirically determined donor or acceptor properties expressed as α_2^H and β_2^H values.

where $\log K = C_1 \alpha_2^H \beta_2^H + C_2$

C_1 is a solvent dependent constant and C_2 is the entropic cost of bringing two neutral molecules together (approximately 6 kJ mol^{-1}).^{17a}

The relationship between pK_a values of a given functional group and the ability to hydrogen bond is not directly applicable to all the functional groups. The relationship may hold among a set of similar functional group derivatives but not for comparisons between different functional groups. For example, relative to alcohols, thiols are fairly acidic. Butanethiol has a pK_a of 10.5 vs 15 for butanol. Thiophenol has a pK_a of 6 vs 10 for phenol. However, alcohols are fairly good hydrogen bond donors whereas thiols are very poor hydrogen bond donors.

In 2004, Hunter developed a new pair of quantities (α and β)^{17b} that describe hydrogen bond donor and acceptor ability respectively:

$$\alpha = E_{\max}/52 \text{ kJ mol}^{-1} = 4.1(\alpha_2^H + 0.33)$$

$$\beta = E_{\min}/52 \text{ kJ mol}^{-1} = 10.3(\beta_2^H + 0.06)$$

where E_{\max} and E_{\min} are the potential minima and maxima on the molecular electrostatic potential surfaces of the molecules as determined by AM1 calculations (Figure-5). Based on Abraham's examples of simple common molecules participating in hydrogen bonding, Hunter has published scatter plots of α_2^H and β_2^H values vs E_{\min} and E_{\max} per kJ mol^{-1} and correlated α and β with α_2^H and β_2^H values. The results are surprisingly linear and form the basis for a reasonably accurate estimation of the strength of a hydrogen bond between two functional groups.

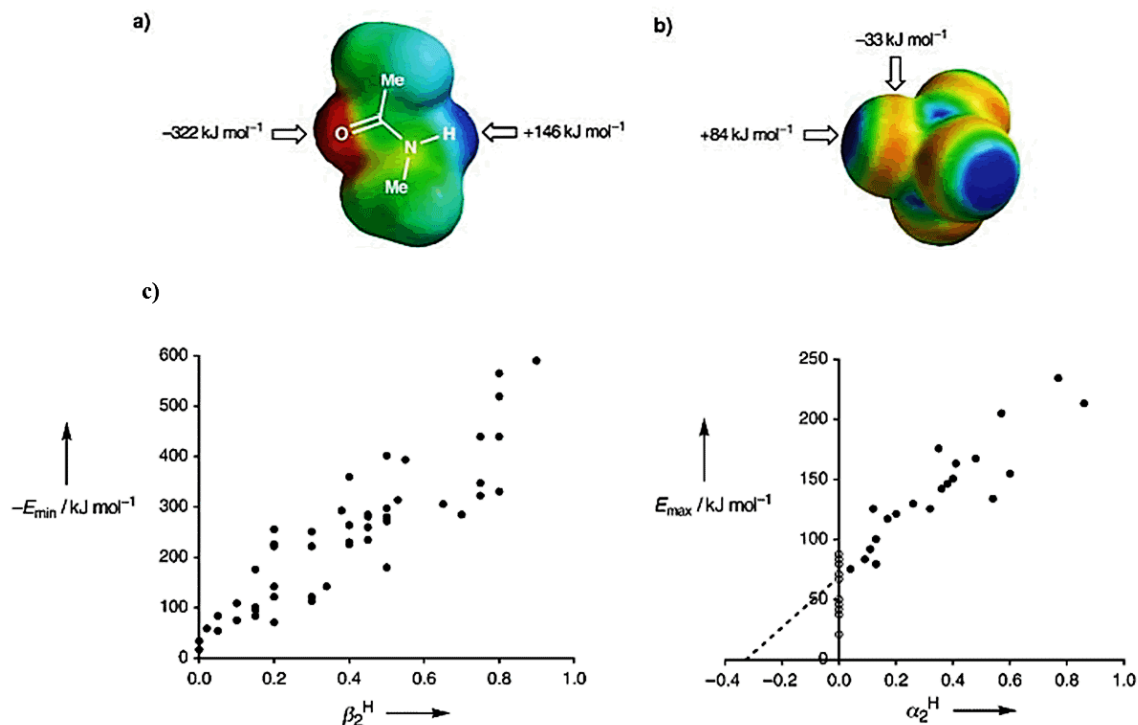


Figure 1-5 Molecular electrostatic potential surfaces plotted on the van der Waals surface of the molecule calculated by using AM1 and a positive point charge in a vacuum as the probe. a) *N*-methyl acetamide; b) Carbon tetrachloride. Positive regions are shown in blue, negative regions are shown in red and green is neutral and c) The maxima (E_{\max}) and minima (E_{\min}) in the AM1 molecular electrostatic potential surfaces of a range of simple molecules containing only one functional group plotted against the corresponding experimentally determined values of α_2^{H} and β_2^{H} from Abraham's examples.^{17c}

1.2.2.2 Directionality of Single Hydrogen Bonding

Directionality is one widely accepted aspect of hydrogen bonding. Although secondary interactions in a system may force the angle D–H⋯A away from linearity, it is the directionality in hydrogen bonding that develops from an anisotropic intermolecular potential that separates it from the more general van der Waals forces, which are likely to be isotropic. They are very different from non-polar interactions in terms of this

directional aspect and they do not arise from point charges as in case of ionic interactions. The forces are the direct result of the tendency of charge separation between an electronegative atom and the hydrogen connected to it. The hydrogen being partially electropositive at a point on its electrostatic surface directly opposite to the donor heteroatom, seeks association with a partially electronegative area of interaction located on A. Linkage through these electronegative regions provides the directionality, as only a particular area and orientation (Figure 1-6) is actually available for interaction and not the entire spherical space around A. The hydrogen bond is strongest when the hydrogen forms the „bridge“ between the two electronegative atoms in aligned linearly with an angle θ , close to 180° with a short bond length. There may be slight deviation from linearity but cannot form or hydrogen bond where $\theta < 110^\circ$ as it will lead an acute angle with lesser compatibility for hydrogen bond formation. Ideally the angles $> 150^\circ$ are generally considered best for hydrogen bonding even though the bond lengths may be longer than usual.¹⁸



Figure 1-6 Hydrogen bonding between the acceptor (A) and the hydrogen atom of the donor (D). The directionality of the (head-on or end-on binding, not side-on binding) electrostatic surface dictates the directionality of the hydrogen bonding which is not observed on the right resulting from an acute bond angle and where there is no contact with the electrostatic potential area of interaction (shown in red in potential map).

1.2.2.3 Specificity of Hydrogen Bonds

Specificity may be defined as the ability to distinguish or discriminate between the arrangement of complementary surfaces and their complementary sites on these surfaces based on strength and orientation of interactions (Figure 1-7). Due to the presence of partial charges that give rise to intermolecular interactions, recognition may occur in a highly specific manner. The partial charges act as electrostatic map i.e. a partially electronegative species or atoms will selectively attract a partially electropositive species or atoms. The specificity of the interaction (similar to a binary code) is enhanced by the proper alignment which gives the interaction a high degree of selectivity in terms of binding.

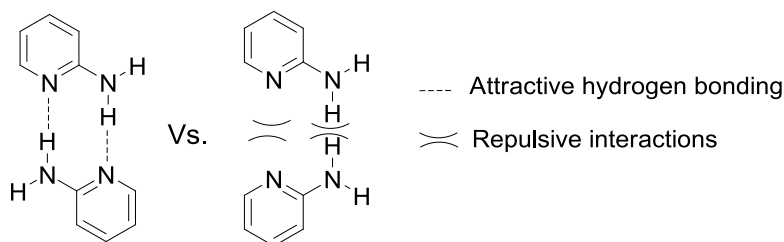


Figure 1-7 Arrangement of complementary sites leads to specifically attractive or repulsive interactions as demonstrated using 2-aminopyridine molecules.

Depending on the nature and strength of electronegative species participating in hydrogen bonding, these interactions lead to wide variations in selectivity. Proximity of the available partial charges also can affect the specific nature of binding when the partially charged species form side chains on a covalent main chain moiety thus leading to sequence specificity through hydrogen bonding. Sequence specificity was pointed out by Watson and Crick in their double helical DNA model where base pairs display near perfect specificity via hydrogen bonding.¹⁹ The concept leads to the use of sequence

specific hydrogen bond interactions to form complexes where the components are arranged in a specific manner.

1.3 Hydrogen Bonded Complexes

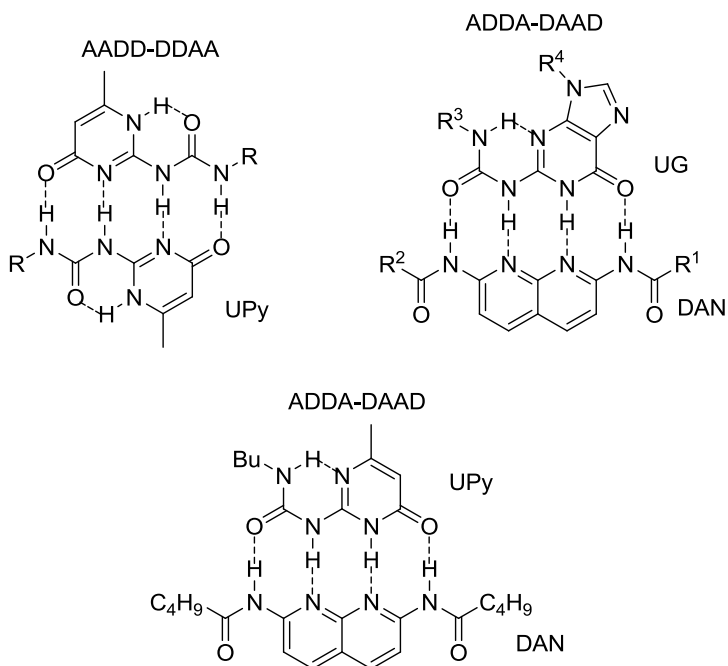


Figure 1-8 Common complementary hydrogen bonding arrays developed that resemble base pairs.

Almost six decades after the discovery of the complementary double-helical DNA complex structure, supramolecular chemists have gained enough information and access to design, synthesis and study the binding patterns of artificial complementary complexes mimicking the base pairs of DNA. Hydrogen bonding serves as the basis for complementary complex formation. Numerous examples of complementary complexes have been reported and various aspects of these complexations have been subjected to analysis. The concept has been extensively studied in linear arrays that may produce

complexes with binding constants on the order of 10^4 M^{-1} and above.²⁰ These motifs are often used in the construction of supramolecular architectures.

Meijer and Zimmerman are two pioneers in the field of development of molecular motifs for complementary hydrogen bonding. Ureido-pyrimidones (UPy),²⁰⁻²¹ the butylurea of guanosine (UG)²² and diamido-naphthyridine (DAN)^{21b,23} derivatives are well known motifs that form hydrogen bonded arrays (Figure 1-8). Most of the existing synthetic hydrogen bond arrays are a result of inspiration from natural complementary complexes such as the DNA base pairs or β pleated sheets of proteins. Gong and coworkers have reported numerous examples that are mimics of the β pleated sheets (Figure 1-9).²⁴

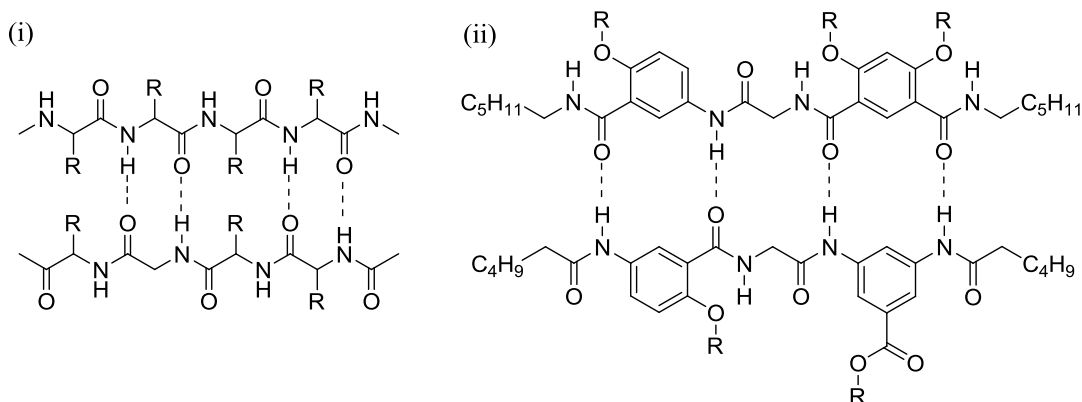


Figure 1-9 (i) Hydrogen bonding in an anti-parallel β sheet and (ii) Bing Gong's hydrogen bonded complex which resembles a β sheet.

1.3.1 Design Parameters of Hydrogen Bonded Complexes

The primary interest in supramolecular systems is the examination of complex formation. Small monomer components that are built to self-assemble hold the information that forms the basis of complex formation. A design involves more than a

synthetic scheme which is often simple and consists of only a few steps. It also takes into account all the plausible geometrical issues of the complexes whether they be steric or electronic effects that dictate the interactions and stabilities of such assemblies.²⁵ The goal of a designer has always been to create these assemblies with minimum number of synthetic steps and generate complexity by assembly of monomer components using molecular recognition into materials with the desired properties. In order to maximize the effects of hydrogen bonding, various types of complexes such as cleft structures, linear or helical complexes have been designed, studied and manipulated to understand the stabilities of these complexes. Often, the starting materials are commercially available and inexpensive. We will discuss several aspects that are important for a well-designed complex system such as functional groups, preorganization, tautomer formation, solubility, fidelity and number of hydrogen bonds and secondary interactions.

1.3.1.1 Functional Groups and Substituents

Hydrogen bonding is often highly sensitive to the nature of the substituents connected to the donor and acceptor components. An electron withdrawing group connected to a donor subunit in an array can make the donor hydrogen atom(s) more highly electropositive. The connection can be in the form of resonance through conjugation or inductively through the σ - framework. Similarly electron donating groups that are connected to an acceptor subunit in an array may improve the acceptor character and tuning of these factors together can significantly improve the overall stabilities of the resulting complexes. Thus a basic design with an accommodation to incorporate functional groups at optimal positions can have a significant effect on stabilities of hydrogen bonded complexation. Boyd *et al.* have examined computationally a contiguous

triply hydrogen bonded system whose binding strengths were studied as a function of various electron withdrawing groups on the donor components and electron donating groups on acceptor components.²⁶ The largest effects were seen when the withdrawing groups acted through resonance (Figure 1-10).

R''	Binding Energy (kJ mol ⁻¹)
NH ₂	31.8
OH	32.2
H	32.6
F	35.6
Cl	41.0
CN	66.9
CHO	73.6
NO ₂	83.7

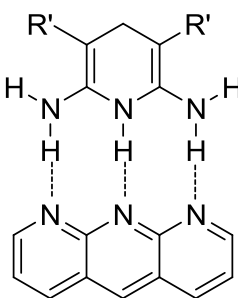


Figure 1-10 AAA-DDD Model system investigated by Boyd and coworkers including the gas phase binding energies stated as function of withdrawing groups on DDD components.

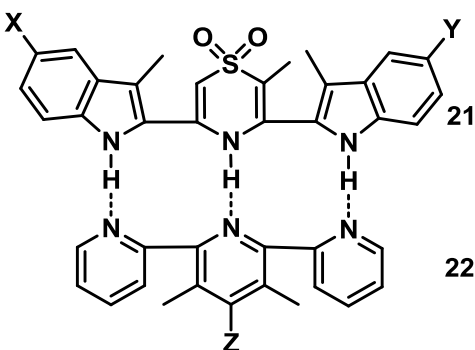
		<i>K_a</i> values in M ⁻¹		
		Z = H	Z = NH ₂	
	21	a: X=H, Y=H	3100	11800
	b: X=Br, Y=H	7000	N/A	
	c: X=H, Y=CO ₂ Et	11000	66000	
	d: X=Br, Y=CO ₂ Et	26000	N/A	
	e: X=H, Y=CN	29000	N/A	
	f: X=CN, Y=Br	49000	N/A	
	g: X=CO ₂ Et, Y=CO ₂ Et	54000	230000	
	h: X=CN, Y=CO ₂ Et	110000	480000	
22				

Figure 1-11 Substituent effects in the complementary AAA-DDD arrays on the association constants (measured in CDCl₃) which are displayed on right hand side; N/A = data not available.

Recently our research group has reported substituent effects on a triply hydrogen bonded system²⁷ (Figure 1-11) incorporating withdrawing substituents such as halogens, esters and nitrile groups on indole hydrogen bond donors. The association constants could be raised from $3.1 \times 10^3 \text{ M}^{-1}$ to $4.8 \times 10^5 \text{ M}^{-1}$ (i.e. by a factor of 30 or 12 kJ mol^{-1} difference) when titrated against substituted (methyl and amino) terpyridyl based acceptor components in CDCl_3 .

Wilson and coworkers have developed AAD•DDA type heterodimers²⁸ based on amidoisocytosine and ureidoimidazole moieties, respectively, that illustrated that remote substituent effects control dimerization affinity in a predictable manner.

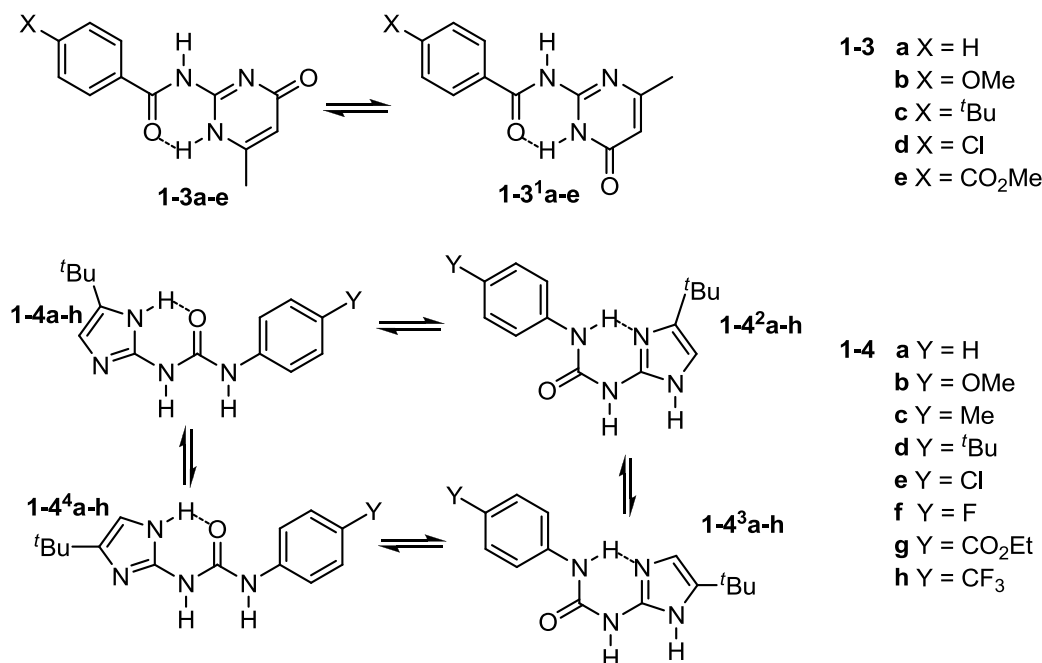


Figure 1-12 Possible tautomeric and conformational states of arrays **1-3** and **1-4**.

The ureidoimidazole motif **1-4** is suitable for studying remote electronic substituent effects because although the hydrogen-bonding array may adopt two tautomeric configurations, these are very similar and either of the conformations that must be

adopted as a consequence of the enforced intramolecular hydrogen bonding presents a DDA array (Figure 1-12). Similarly two tautomeric forms are possible for amidoisocytosine (**1-3**) both stabilized by intramolecular hydrogen bonding among which only one presents the required AAD array. A series of complexes were synthesized with different substituents in the *para* position of the aromatic ureido/amido ring system.

1.3.1.2 Preorganization

Preorganization is a central factor that affects the stability of complexation during molecular recognition. In order to form a complex, the orientation of the non-covalent interactions depends on the geometrical arrangement of the individual components and the way they come together. The degree of freedom to rotate over single bonds in a molecule is what determines its range of conformations. It generally requires energy to bring individual functional groups into the right alignment to form a stable complex. Hence, preorganization can have a great effect in terms of conserving energies which otherwise would be spent bringing the array to its optimal geometrical alignment for complexation. As a design parameter preorganization can be introduced to the participating groups via intramolecular interactions, contributing to the net stability of complex formation.

While preorganization in metal driven coordinated complexes has been extensively studied,²⁹ non-metallic complexation assemblies with preorganizational effects have been gaining importance in recent times. In 1990, Etter framed a set of rules³⁰ as “hydrogen bond rules for organic compounds”. She laid out general rules along with specific ones

for compounds with various functional groups, which can be utilized while designing a complex based from them.

1. All good proton donors and acceptors are used in hydrogen bonding.
2. Six-membered-ring intramolecular hydrogen bonds form in preference to intermolecular hydrogen bonds.
3. The best proton donors and acceptors remaining after intramolecular hydrogen-bond formation form intermolecular hydrogen bonds to one another.

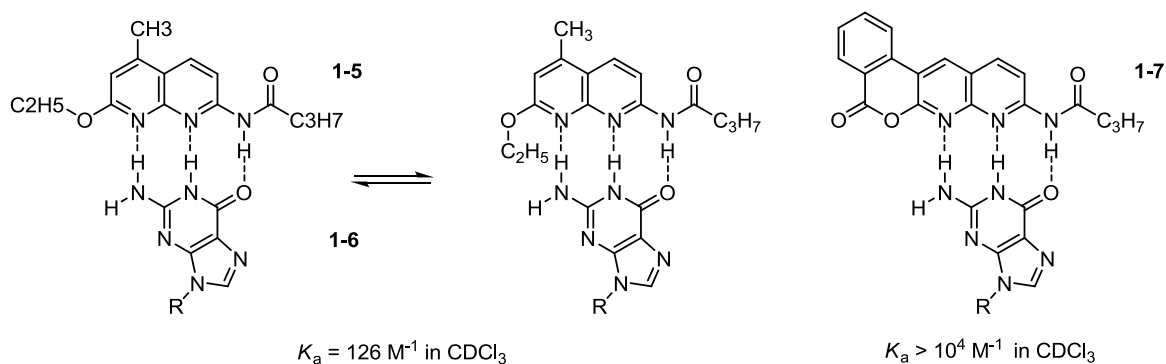
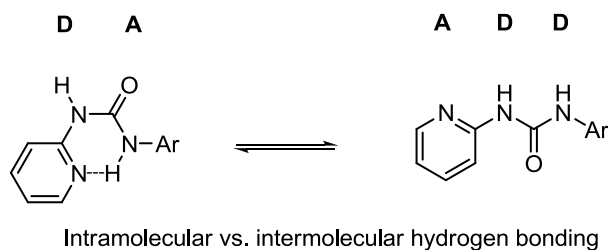


Figure 1-14 Conformational equilibrium of ethoxynaphthyridine **1-5** and its complex with array **1-6**. Array **1-7** contains an oxy substituent but is constrained in a ring. Association constants are measured in CDCl₃.

Along with intramolecular hydrogen bonding, other conformational issues may affect the level of preorganization. Hamilton found that ethoxynaphthyridine **1-5** bound triacetyl guanosine **1-6** with a $K_a = 126 \text{ M}^{-1}$ (Figure 1-14),³¹ which is at least two orders of magnitude lower than the K_a of a very similar complex, **1-6•1-7**. In the example (Figure 1-14) Murray and Zimmerman proposed that the ethoxy group of **1-5** suffers from steric interactions with the guanine amino group. Thus there is an energy cost for producing the less stable conformation of the ethoxy group in **1-5•1-6**. Evidence for this hypothesis was drawn from the studies of **1-7** with an alkoxy group in the 8-position that

is “tied back” in a lactone ring. In contrast to **1-5-1-6** the K_a of **1-6-1-7** is $> 10^4 \text{ M}^{-1}$, which is expected of a DDA•AAD type complex.³²



Although intramolecular hydrogen bonding is a very useful tool to arrange a molecule in a desired conformation, there are also complications that can arise with preorganization via intramolecular hydrogen bonding. The example above demonstrates the unwanted effects of an intramolecular hydrogen bond by clipping a ureido donor to a pyridyl group and bypassing the ADD system intended to produce a DA array instead. This is an undesired result of poor design that introduces intramolecular hydrogen bonding that has a negative effect on the stability of the resulting complex. Thus the example emphasizes the powerful nature of preorganization and how it can be determined by design.

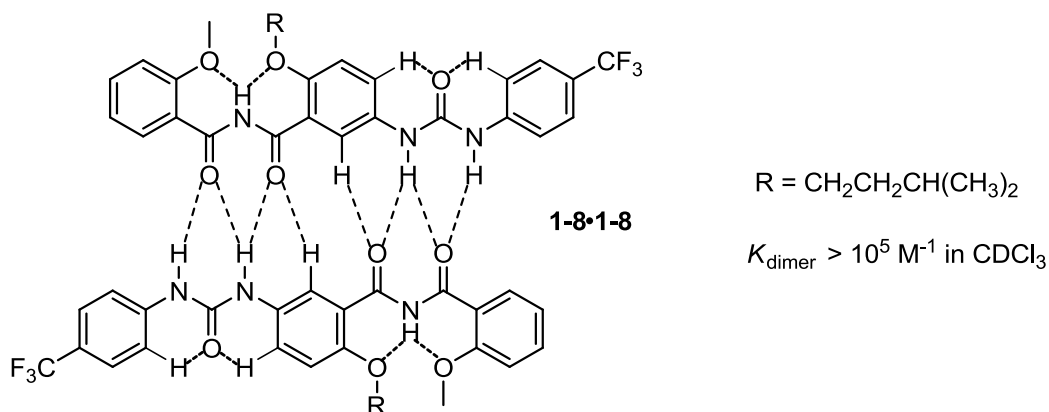


Figure 1-15 Imide-urea strands that pair into self-complementary duplexes **1-8-1-8** via bifurcated hydrogen bonds.

In a recent example,³³ a quadruply hydrogen-bonded duplex (**1-8•1-8**), based on an imide-urea structure preorganized partially by three-center hydrogen bonds was reported to associate via bifurcated hydrogen bonds (Figure 1-15). ¹H NMR dilution experiments revealed the high stability of the homodimer in a non-polar solvent ($K_{\text{dimer}} > 10^5 \text{ M}^{-1}$ in CDCl_3) and enhancement of the association due to electron-withdrawing substituent effects (eg. $-\text{CF}_3$ in Figure 1-15).

1.3.1.3 Tautomers

Tautomers are isomers differing only in the positions of hydrogen atoms and electrons. The carbon skeleton of the compound is unchanged. A reaction which involves simple proton transfer in an intramolecular fashion is called a tautomerism. When designing a complex it is a good idea to pay special attention to the locations of double bonds and functional groups such as carbonyl, amide, amine and lactams so as to avoid unnecessary tautomerism which may affect the overall stability of a complex. In fact, it has been proposed that mutations in DNA may occur as a consequence of mispairing of minor tautomers of the four natural bases,³⁴ indicating the importance of the concept.

Meijer and coworkers have reported a DDA array of 2-ureido-4-pyrimidone (UPy, **1-9**) which tautomerizes to an AADD array (**1-9a**) and ADAD array (**1-9b**) and undergoes self-association (Figure 1-16).^{21a} This is a very good example that demonstrates the role of tautomer formation in determining the overall stability of the complex. The AADD array displays greater stability (over two orders of magnitude) compared to the ADAD array due to the presence of fewer repulsive secondary

interactions. Some tautomers may not even allow the formation of a complex by altering the sequence of the hydrogen bonding array.

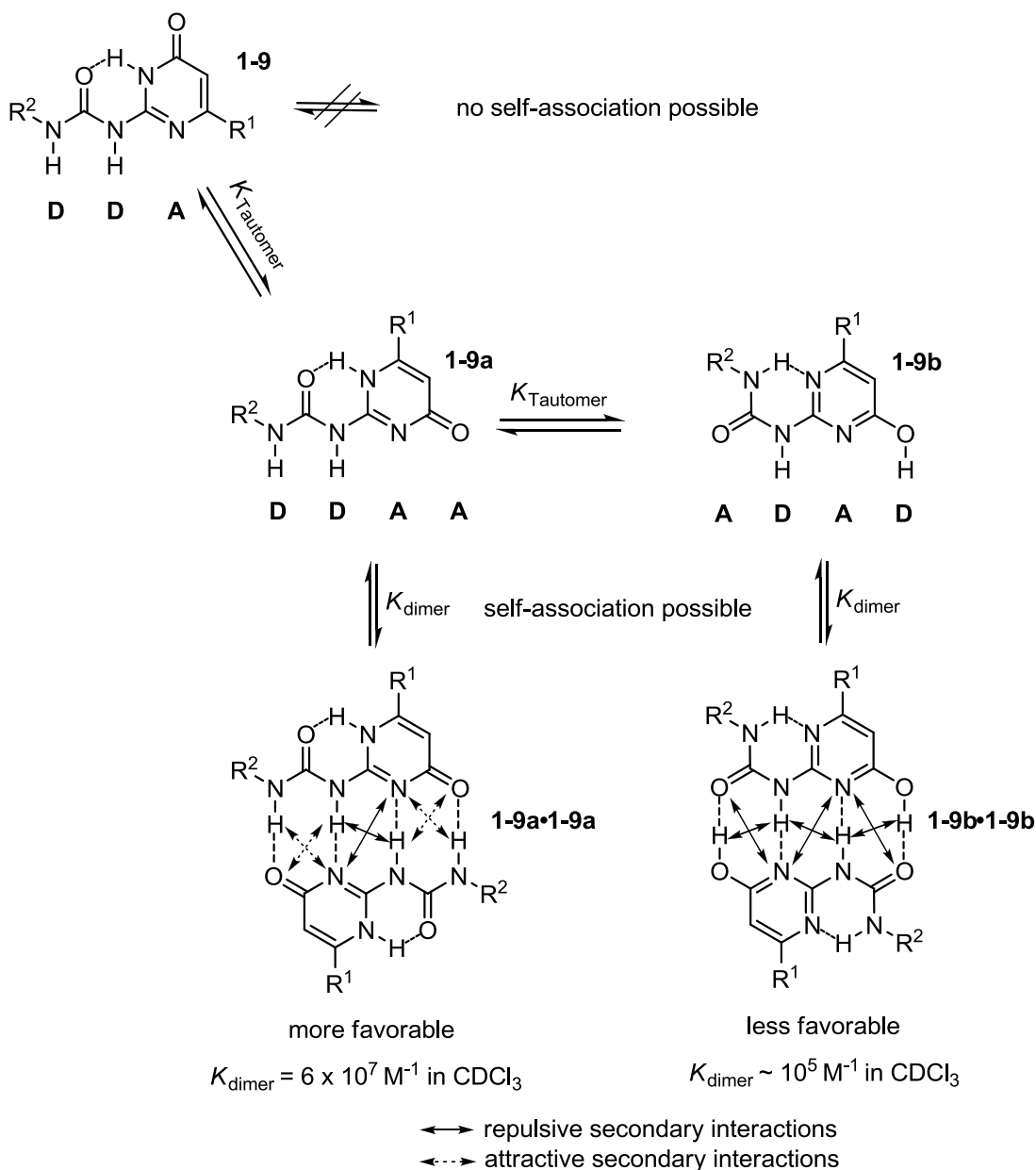


Figure 1-16 The tautomeric and self-association equilibria observed in a solution of 2-ureido-4-pyrimidone (**1-9**). The dimerization values were measured in CDCl_3 .

Zimmerman and coworkers have reported an AADD array **1-10a** that by design forms a tautomer **1-10b** that has the same kind of AADD arrangement and thus avoids

formation of a less favourable array (Figure 1-17).³⁵ Hence, these types of tautomer conflicts can be controlled through careful design if necessary.

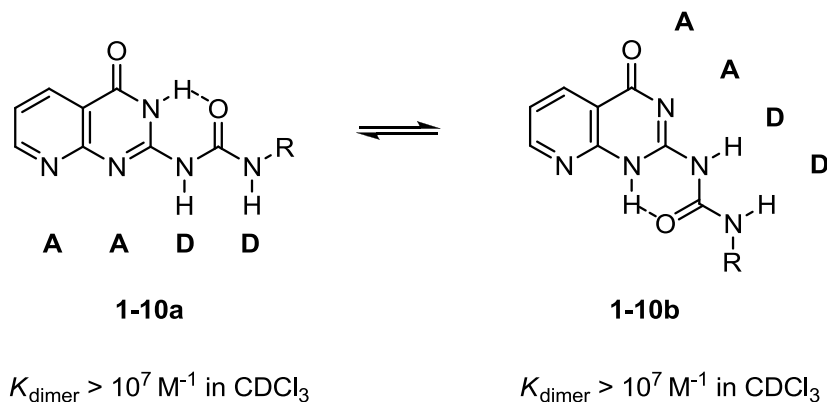


Figure 1-17 Zimmerman's AADD array **1-10a** that can only form a tautomeric AADD array **1-10b** thereby maximising the association constant values possible for the complex.

1.3.1.4 Solubility

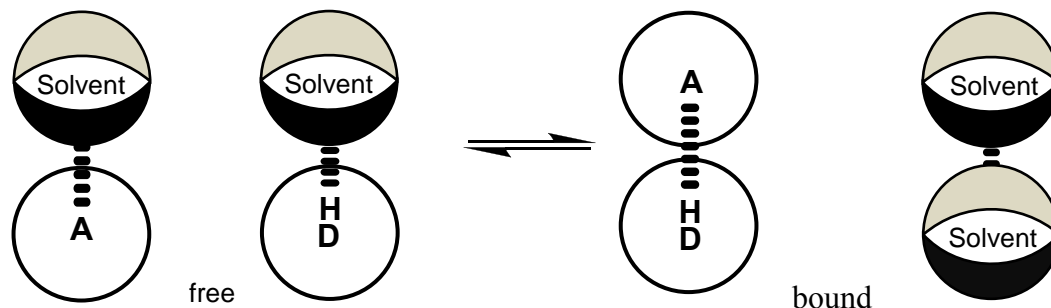


Figure 1-18. Intermolecular interactions in solution are a competition between solute-solvent interactions in the free state, and solute-solute and solvent-solvent interactions in the bound state. For simple functional groups, the primary mode of interaction is hydrogen-bond contacts between the maxima (black) and minima (grey) in the electrostatic potential surfaces of the molecules.³⁶

Solubility plays a central role in many chemical transformations and in the field of molecular recognition, desolvation can be a dominant factor in the stability of non-covalently interacting systems. Polar solvents can bind competitively to hydrogen bond

arrays and may cause a significant decrease in the stability of any complex formation. The analysis of many self-assembled systems are thus restricted to operation in non-competitive, non-polar solvents such as chloroform, toluene and cyclohexane. Solubility is one of the most commonly faced hurdles in terms of the physical properties of supramolecular complexes.

In the solution phase, there is a competition between solute–solute, solvent–solvent, and solute–solvent interactions (Figure 1-18) and Hunter’s universal hydrogen-bond scale can be used to predict the free energy of hydrogen-bonding interactions ($\Delta G_{\text{H-bond}}$ in kJ mol^{-1}) in most solvents.³⁶⁻³⁷

$$-RT \ln K = \Delta G_{\text{H-bond}} = -(\alpha - \alpha_s)(\beta - \beta_s)$$

α and β are hydrogen-bond donor and hydrogen-bond acceptor constants for the solute molecules, and α_s and β_s are the corresponding hydrogen-bond donor and hydrogen-bond acceptor constants for the solvent. The new parameters, α and β correspond to normalized versions of E_{max} and E_{min} [$\alpha = E_{\text{max}}/52 = 4.1(\alpha_2^{\text{H}} + 0.33)$, $\beta = -E_{\text{min}}/52 = 10.3(\beta_2^{\text{H}} + 0.06)$] determined from AM1 electrostatic potential surfaces, as discussed earlier.

Hunter and coworkers have also studied a system for which the association constants were reported in various solvents to highlight the role of competitive solvents and non-competitive solvents play in the determination of the stability of the complexes.^{17b} One of the most polar hydrogen-bond donors known is perfluoro-tert-butyl alcohol and one of the best hydrogen-bond acceptors known is tri-*n*-butylphosphine oxide (Figure 1-19). Experiments on the complexation between these two compounds in comparison to standard reference hydrogen bond acceptors and donors in carbon

tetrachloride suggest that the complex should exhibit extraordinary stability, thereby allowing quantification of the hydrogen bond interaction in competitive polar solvents.³⁷

The results demonstrate the predictable drop in association constants, K_a values with increasing solvent competition/polarity.

Solvent	K_a in M^{-1}
<i>n</i> -decanol	1.6×10^{-1}
DMSO	6.8×10^{-1}
NMF	8.9×10^{-1}
Pyridine	6.5×10^0
pyrrole	1.3×10^1
acetone	6.5×10^1
acetonitrile	1.6×10^2
tetrahydrofuran	2.4×10^2
nitromethane	1.5×10^3
$CHCl_3$	2.7×10^3
Benzene	1.9×10^4
CCl_4	7.6×10^4
Cyclohexane	$> 10^5$

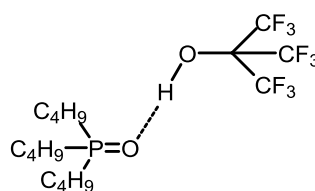


Figure 1-19 Results of ^{31}P NMR titration experiments displaying the association constant for formation of a 1:1 complex between perfluoro-tert-butyl alcohol and tri-*n*-butyl phosphine oxide at 295 K as a function of solvent properties. Errors in K_a are $\pm 20\%$, except for the values in *N*-methylformamide (NMF), dimethyl sulfoxide (DMSO), and *n*-decanol, where only 30–40% of the binding isotherm was accessible and the values are accurate to within an order of magnitude.

There are different ways to overcome solubility issues without disrupting the primary design of a complex. Lengthy alkyl chains, polyethylene glycol units or sterically hindering groups can be incorporated that may improve the solubility of otherwise insoluble components. Alternatively, mixed solvent systems can be used to measure the association constants or for comparative studies of specific interactions. Both of these strategies are employed and discussed in chapter three of this thesis.

1.3.1.5 Fidelity

Fidelity is defined in various fields in different manners. It is the degree or quality of faithfulness toward a particular interaction. The genetic information that is passed on from double helical DNA strands to RNA and subsequently on to proteins is based on the specific recognition of complementary base pairing and such specificity is highly desirable when mimicking nature in order to develop materials for particular applications. In supramolecular terms, fidelity is minimal competition from other recognition events during the process of complex formation. Fidelity has been defined as the ratio of concentration of the desired complexes to the concentration of all associated species. Thus fidelity F , can range from $0 \leq F \leq 1$, where $F = 1$ indicates exclusive formation of the desired complex and $F = 0$ indicates exclusive formation of other undesired complexes.

Zimmerman and coworkers have reported several triple and quadruple hydrogen bonded motifs that form heterodimer complexes with very high fidelity.^{22, 38} Orthogonality has been studied in several examples and a few of them stand out displaying high fidelity. The concept is well demonstrated by complex formation of 2,7-diamido-1,8-naphthyridine (**DAN**) and the butylurea of guanosine (**UG**) in chloroform as **DAN•UG**. The complex is exceptionally strong due to high fidelity between the participating arrays. The association constant for the **DAN•UG** complex was found to be $5 \times 10^7 \text{ M}^{-1}$ by fluorescence energy transfer from the naphthyridine unit of **DAN** to coumarin 343 covalently linked to **UG** (Figure 1-20) and is among the highest reported for a neutral DNA base-pair analogue. The relatively negligible self-association of **DAN**

($K_{\text{dimer}} < 10 \text{ M}^{-1}$) and **UG** ($K_{\text{dimer}} = 300 \text{ M}^{-1}$) strongly suggests that the **DAN•UG** complex forms with unparalleled fidelity.

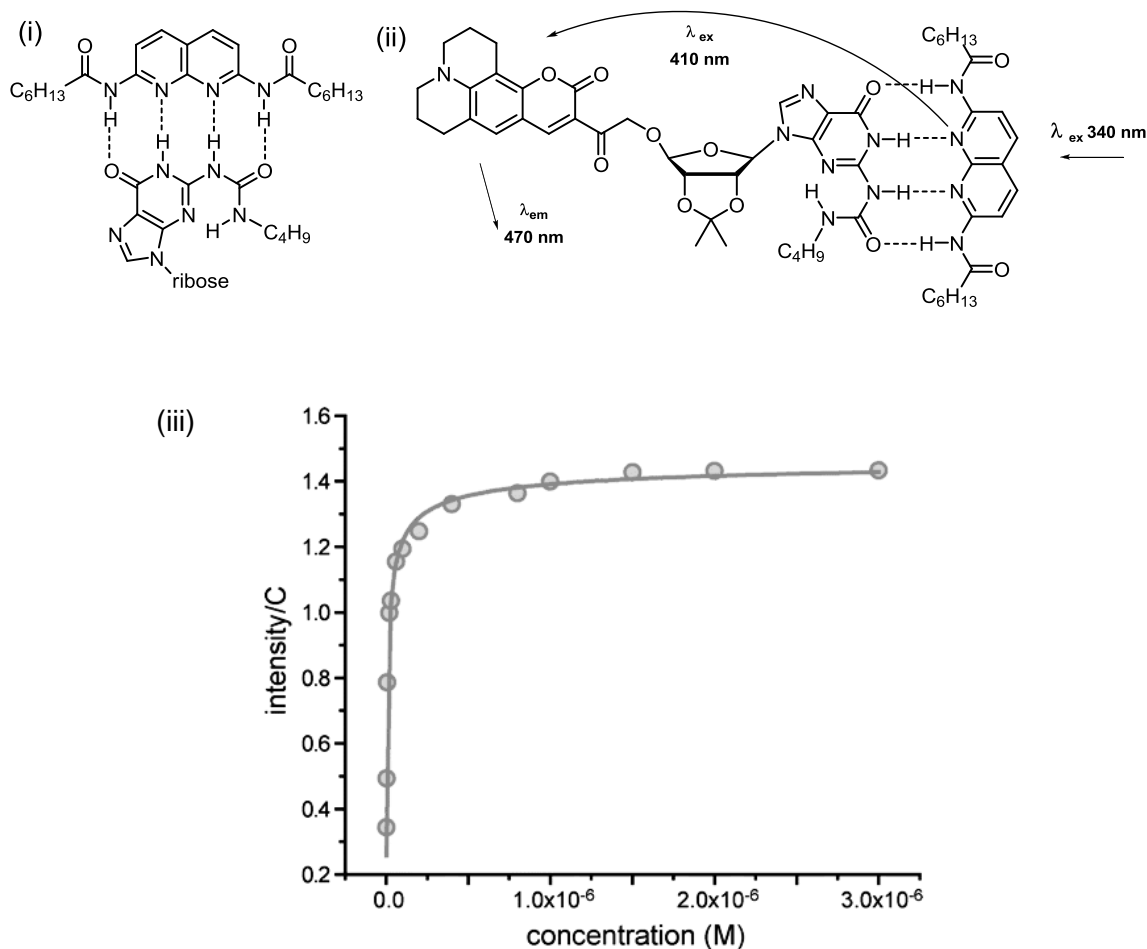


Figure 1-20 (i) **DAN•UG** complex formed due to the high fidelity interaction between the two arrays; (ii) Fluorescence emission of **DAN•UG** complex displaying the fluorescence energy transfer from the naphthyridine unit of **DAN** to a coumarin 343 covalently linked **UG** with dilution in chloroform (background subtracted); (iii) Fluorescence intensity (arbitrary units) plotted against concentration for the association pictured in (ii).

In the above case, F is calculated using the equation:

$$\text{fidelity } (F) = \frac{[\text{DAN}\cdot\text{UG}]}{[(\text{DAN})_2] + [(\text{UG})_n] + [\text{DAN}\cdot\text{UG}]}$$

The **DAN•UG** complex (1:1 stoichiometry) exhibits a nearly perfect fidelity of > 99.9% at 1 M and maintains that level across a 10^6 -fold dilution. Complexes of such high fidelity can be used for highly specific purposes in the field of biochemistry and supramolecular architectures such as reversible polymers constructed using DAN and UG arrays.³⁸

1.3.1.6 Number of Hydrogen Bonds and Secondary Interactions.

Hydrogen bonds are not usually stable individually but cumulatively they can exert a much stabler effect. As the stability of the hydrogen bonded complex is a collective effect, it should be directly proportional to the number of D-A pairs participating in the hydrogen bonding i.e it is expected that a triply hydrogen bonded complex is stronger than a doubly hydrogen bonded complex.

Schneider and coworkers studied the effects of the number of hydrogen bonds and a linear correlation was made between the complexation free energy (ΔG°) in CDCl_3 and number of hydrogen bonds in eight different hydrogen bonded complexes formed from amide or imide and amino- or amidopyridine components.^{39,40} From the correlation, they concluded that each hydrogen bond interaction contributed approximately 5.0 kJ mol^{-1} to the energy of complexation. Furthermore, no such attempts were reported that would generalize the concept and it is arguable that the conclusion made is limited to the carefully chosen complexes with similar types of hydrogen bonded arrays. There are actually a number of examples reported more recently that contain arrays with fewer pairs of hydrogen bonds and significantly higher association or dimerization constants that will be discussed in the subsequent chapters of this thesis.

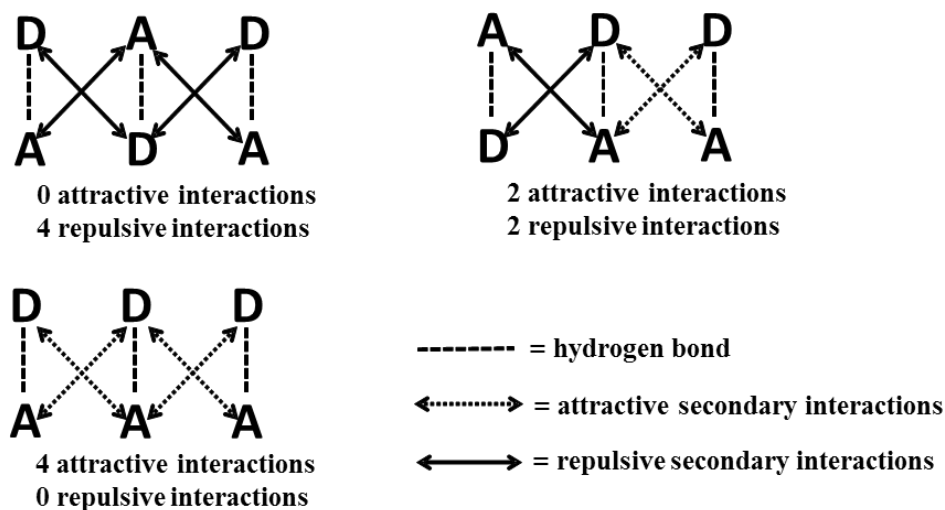


Figure 1-21 Secondary interactions shown in four different modules, DAD•ADA, ADD•DAA and DDD•AAA motifs along with the number of attractive and repulsive interactions in each case.

The strength also depends upon the sequence of the hydrogen bonding arrays as secondary interactions can affect the overall stability of a complex as introduced by Jorgenson and coworkers.⁴¹ Depending upon the sequence one can calculate the number of attractive and repulsive interactions that contribute to the net stability of a complex. Alternating A and D components in an array gives rise to the weakest complexes possible as there are only repulsive secondary interactions present in these type of arrays (Figure 1-21). On the contrary, contiguous arrays give rise to the strongest hydrogen bonded complexes due to the presence of entirely attractive secondary interactions and no repulsive secondary interactions.

1.3.2 Complementary and Self-Complementary Hydrogen Bonded Complexes

Molecular recognition through complementary surfaces bearing complementary sites was developed more out of scientific curiosity to understand the functional aspects

of biochemical processes such as the role of complementarity in translation and replication of nucleotides. Later this understanding has been applied to the development of functional materials with interesting properties. The complementary nature of the duplexes is a manifestation of underlying cooperative action of non-covalent interactions resulting in thermodynamically stable assemblies. An ideal self-assembly involves the associating units that store and retrieve information as the assembly takes place. Hence, “codes”, in form of hydrogen bonding components are the key to complementary complex formation.

1.3.2.1 Self-Complementary or Homodimer Complexes

The development of self-complementary complexes involves the arrangement of intermolecular hydrogen-bonding sites into arrays. Introduction of a sequential arrangement produces a set of hydrogen-bonded duplexes, where the hydrogen bond modules recognize either themselves (self-complementary) or their complements. The number of N duplexes with n intermolecular hydrogen-bonding sites can be calculated as:

$$N = 2^{n-2} + 2^{(n-3)/2} \quad \text{when } n = \text{odd number}$$

$$N = 2^{n-2} + 2^{(n-2)/2} \quad \text{when } n = \text{even number}$$

If n is an odd number, there can be no self-complementary sequences. If n is even, then the number of self-complementary sequences is described by the second term of the equation. Thus, in the set of triple hydrogen bond arrays, there are 3 complementary pairs and in the set of quadruple hydrogen bonded arrays, there are 4 complementary

pairs and 2 self-complementary sequences. The following sections discuss some of the self-complementary arrays reported in the literature that display high stabilities.

1.3.2.1.1 ADAD Complexes

Among self-complementary H-bonded arrays, linear quadruple complexes are well known and studied. Though ADAD modules are expected to be weak hydrogen bonded complexes due to their entirely repulsive secondary interactions that underlie these motifs, there are some interesting examples provided by Meijer and coworkers.

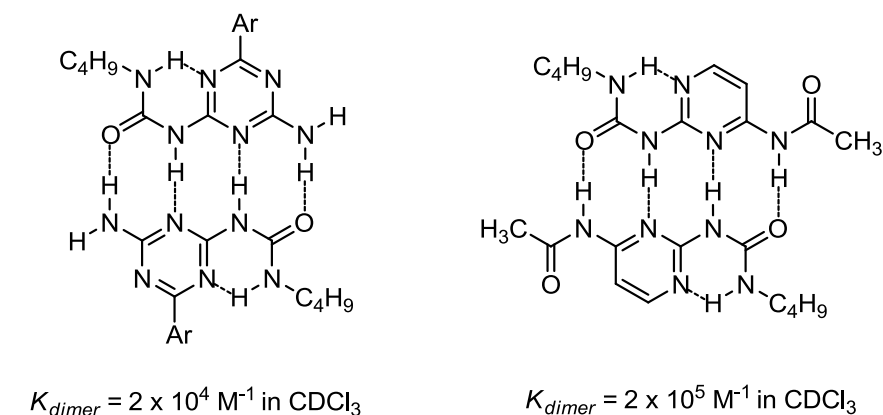


Figure 1-22 Dimers of acylated diaminotriazine and diaminopyrimidine ADAD modules. Association constants are measured in CDCl_3 at room temperature.

Meijer's group was among the first to synthesize self-complementary quadruple hydrogen-bonding motifs with an ADAD array formed by acylation of diaminotriazines and diaminopyrimidines (Figure 1-22).⁴² The dimerization constants for these complexes were measured in CDCl_3 and vary significantly with the corresponding complexation free energies differing by over 17 kJ mol^{-1} from strongest to weakest. The acylated compounds were reported being stabilized by intramolecular hydrogen bonding having association constants up to 10^5 M^{-1} in CDCl_3 (Figure 1-23). They have well demonstrated

the importance of conformational effects and supportive intramolecular hydrogen bonding.

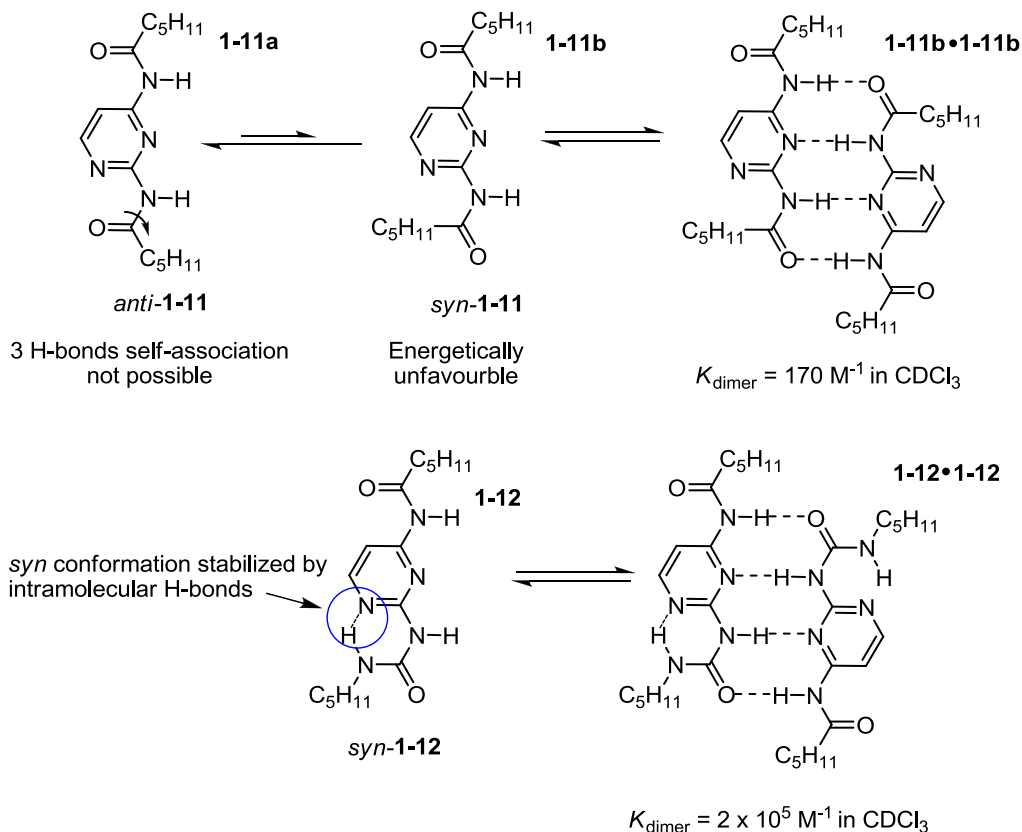


Figure 1-23 Diacylpyrimidine **1-11** and ureidoacylpyrimidine **1-12** as ADAD bonding motifs according to Meijer and co-workers.

1.3.2.1.2 AADD Complexes

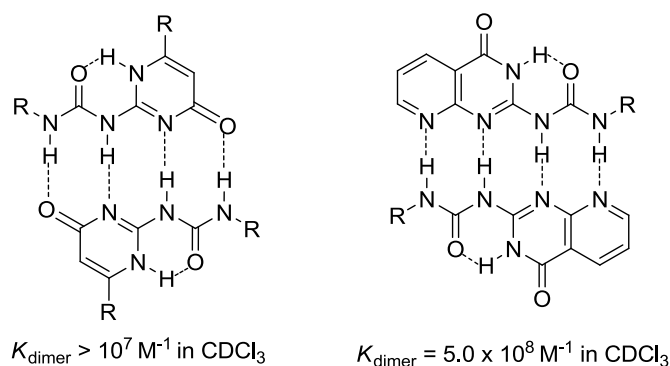


Figure 1-24 Meijer's AADD motifs displaying extreme complex stabilities.

There are numerous examples of AADD self-complementary motifs build by Meijer's group detailed in different sections of this chapter, displaying K_{dimer} values on the order of 10^5 to 10^8 M^{-1} .^{43,43,44}

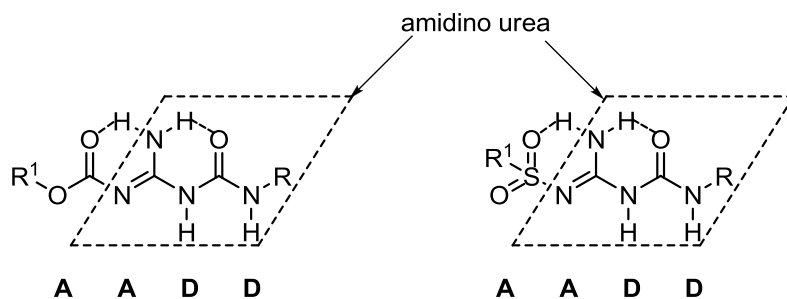


Figure 1-25 Amidino-urea-based self-complementary modules with preorganized linear hydrogen-bonding arrays. The intramolecular hydrogen bonding supports the structural geometry and thereby increase the overall dimerization values.

Inspired from the basic design of Meijer and Zimmerman, Sanjayan and coworkers⁴⁵ have developed sulfonyl based amidino-urea AADD arrays that self-assemble to form the hydrogen bonded complexes. The stability and preorganization in these complexes is augmented by supportive intramolecular hydrogen bonding interactions (Figure 1-25). ESI mass spectroscopy and X-ray diffraction studies were extensively used to investigate the self-assembling propensities of the sulfonyl based AADD array systems.

Tung and coworkers have reported the first example of a fluorescent sensor for fluoride anions based on the 2-ureido-4[1H]-pyrimidinone quadruple hydrogen bonded AADD supramolecular assembly⁴⁶ where the assembly and disassembly processes respond to external stimuli. They employ Meijer's AADD arrays for the self-complementary complex formation and attached an anthracene moiety via a methylene carbon to the AADD array, turning the unit into a fluorescent sensor (Figure 1-26).

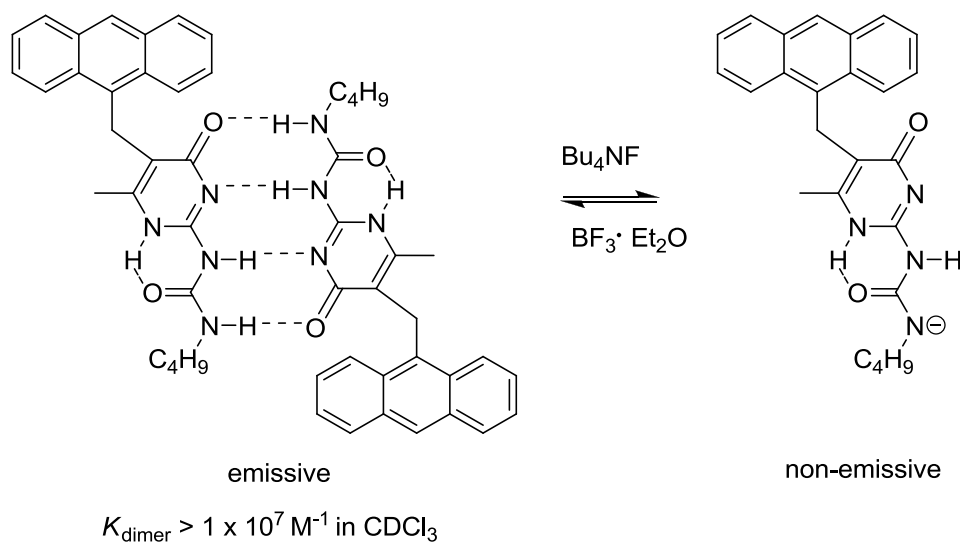


Figure 1-26 A highly selective, neutral, fluorescent sensor based on 2-ureido-4[1H]-pyrimidinone quadruple hydrogen-bonded AADD motif.

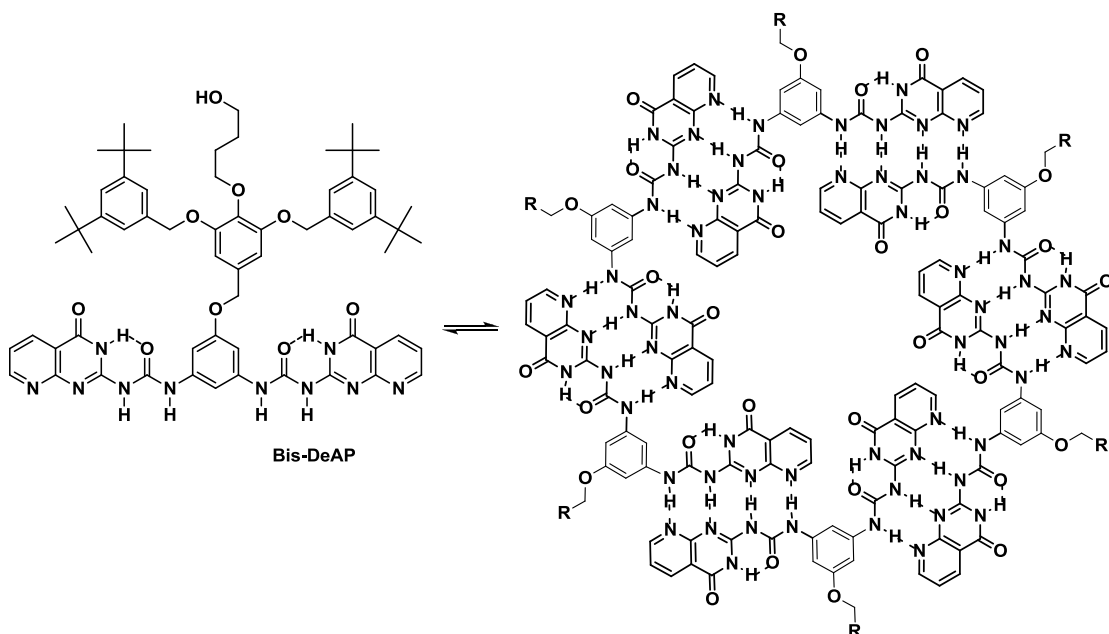


Figure 1-27 Design and self-assembly of general-purpose Bis-DeAP module.

Zimmerman and coworkers have reported a ditopic hydrogen-bonding module bis-ureidodeazaapterin (Bis-DeAP), as a basic AADD-linker-DDAA moiety (Figure 1-27)⁴⁷ for building supramolecular star polymers. It was programmed to self-assemble into

cyclic aggregates. The synthetic ease and scalability are also noteworthy factors. Depending on the flexibility of the linker, different main chain polymers can be drawn. The size of the cyclic assembly is determined by the angle between the hydrogen bonding modules. The scope of the monomer moiety is significant as the terminal hydroxyl group can be attached to polymer initiators which can readily undergo polymerizations, making Bis-DeAP a very valuable addition to the „supramolecular toolbox“ for the generation of ordered nanoscale materials.

The AADD hydrogen-bonding module ureidoimidazo[1,2-a]pyrimidine (**UImp-2**),⁴⁸ developed by Hisamatsu and co-workers forms a highly stable unfolded dimer via an AADD array ($K_{\text{dimer}} > 1.1 \times 10^5 \text{ M}^{-1}$ in CDCl_3) without competition from undesired conformers. This result demonstrates the usefulness of quadruple hydrogen-bonding modules based on five-membered heterocyclic urea structures. When a CDCl_3 solution of **UImp-2** was diluted from 8.0 to 0.40 mM, no changes were observed in chemical shift values of NH^{a} and NH^{b} . This shows that the dimerization of **UImp-2** persists at a low concentration and that the K_{dimer} value is significantly high. Assuming that at this concentration there is less than 10% dissociation that is not detected by ^1H NMR, the K_{dimer} of **UImp-2** was estimated to have a lower limit of $1.1 \times 10^5 \text{ M}^{-1}$. The original arrays that inspired the development of **UImp-2** are based on ureidocytosine **UC**,⁴⁹ which has a much similar $K_{\text{dimer}} > 2.5 \times 10^5 \text{ M}^{-1}$ but due to the ability of **UC** to fold and form an AD array instead of an AADD array there is at least 5% competition from the folded **UC** conformation (Figure 1-28). The **UImp-2** avoids this kind of conformation by switching from ureidocytosine to a five membered ring fused to a six membered heterocycle.

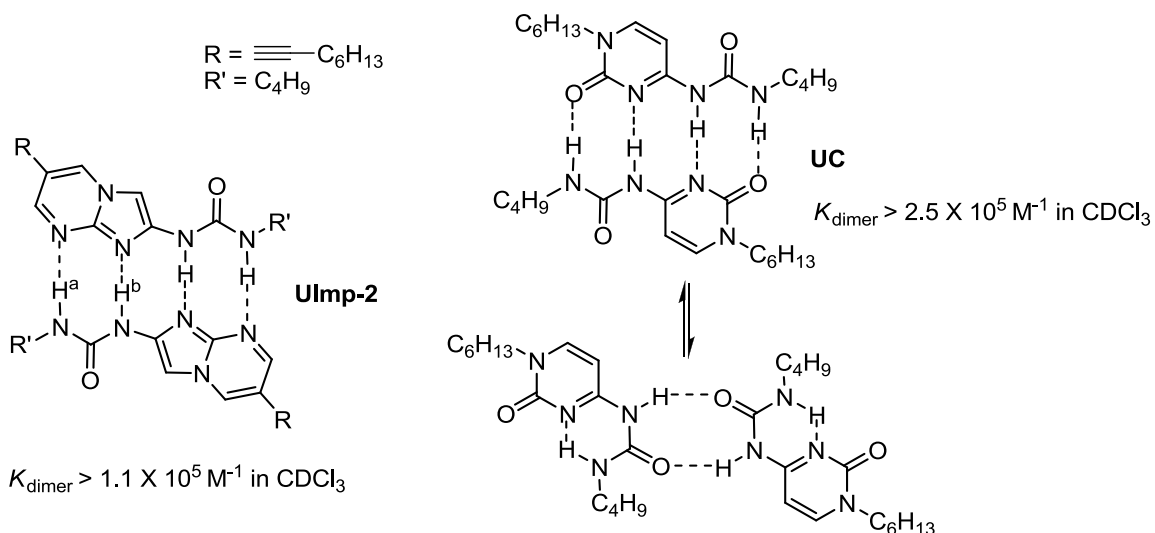


Figure 1-28 Structure of an AADD array (left) based on ureidoimidazo[1,2-a]pyrimidine **UImp-2**, forming a stable dimer. On the right, the ureidocytosine **UC**, a different AADD array can fold up and thus form a duplex with lower stability. All the dimerization constants were determined in CDCl_3 at room temperature.

1.3.2.1.3 Six-membered Self-Complementary Complexes

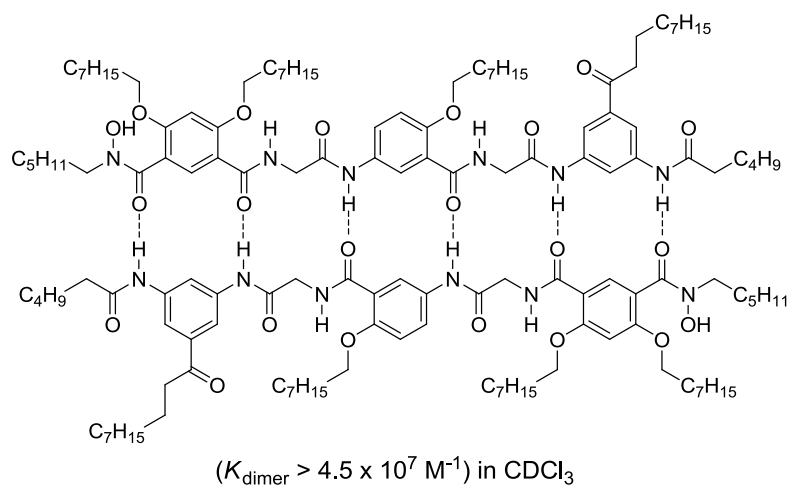


Figure 1-29 The design of the self-complementary duplex forming a AADADD-DDADAA complex in the solution state.

Examples of extremely stable self-complementary six hydrogen bonded AADADD•DDADAA duplexes (Figure 1-29) consisting of amide linkages have been

reported by Gong and coworkers.⁵⁰ The K_{dimer} is reported to be greater than $4.5 \times 10^7 \text{ M}^{-1}$ in CDCl_3 . Due to the high degree of complexation, the chemical shifts of the amine protons do not display any movement either up field or down field, in a wide range of dilutions from 1mmol to 2 μM .

1.3.2.2 Complementary or Heterodimer Complexes

As a result of the influence of positive and negative secondary interactions, the ADA•DAD arrangement is less stable than the AAD•DDA arrangement which is less stable than the AAA•DDD arrangement donor/acceptor arrays. The subsequent examples discussed in this section bear out this general trend where we examine only those complexes with relatively large ($K_a > 10^4 \text{ M}^{-1}$) stabilities.

1.3.2.2.1 AAD•DDA Complementary Complexes

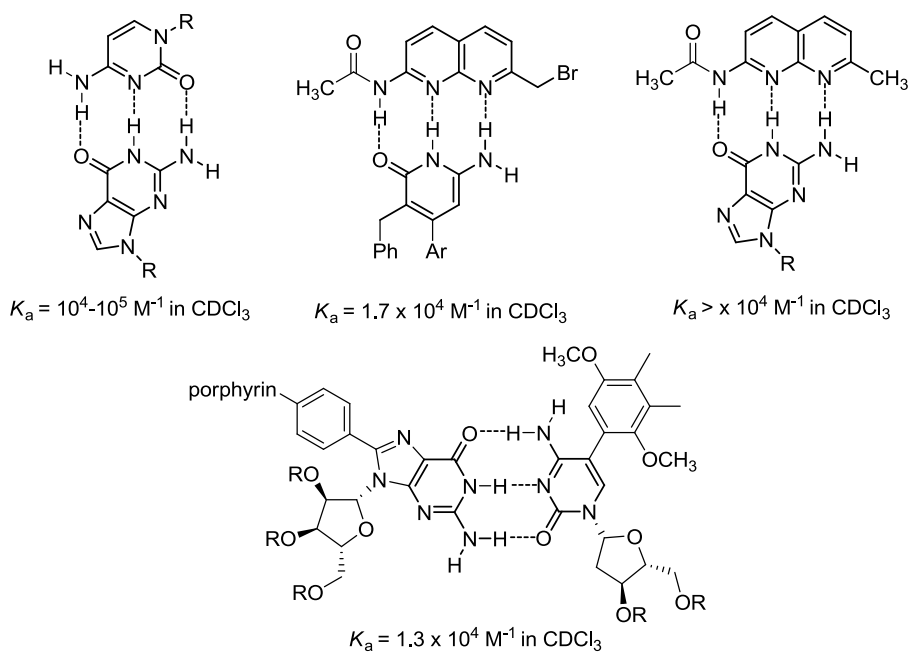


Figure 1-30 Assorted complexes containing the AAD•DDA motif. The K_a values are measured in CDCl_3 .

Compared to ADA•DAD motifs the more stable AAD•DDA arrangement was extensively investigated before the development of quadruple hydrogen bonded complexes. The prototypical example of the naturally occurring AAD•DDA array is the C•G base pair. The association constants (Figure 1-30) lie approximately in the 10^4 - 10^5 M^{-1} range,⁵¹ which are two to three orders of magnitude higher than observed for typical ADA•DAD systems. It is a significant observation as the subunits used to build both motifs are often very similar.

1.3.2.2 AAA•DDD Complementary Complexes

Among triply hydrogen bonded complexes the AAA•DDD arrangement was found to be that with the highest stability due to the presence of entirely attractive secondary interactions.

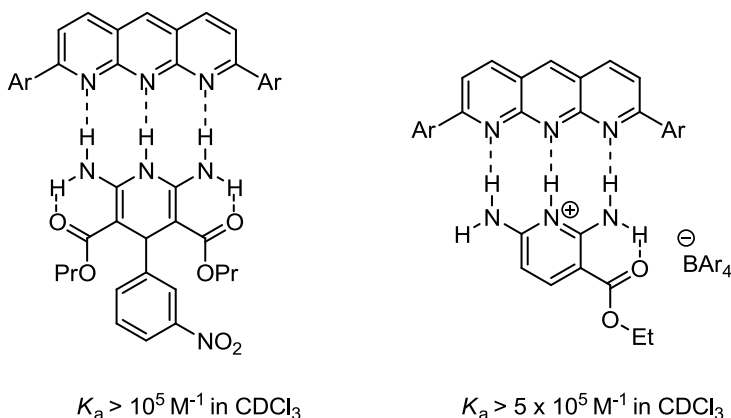


Figure 1-31 A diaryl-1,9,10-anthridine module forming complexes with neutral and cationic DDD arrays in an AAA•DDD arrangement with high stability.⁵² The association constants are measured in $CDCl_3$.

The synthesis of multi-annulated heteroaromatic rings can be difficult and electron withdrawing substituents like nitro- or nitrile groups can cause solubility

problems.⁵³ Though synthetically challenging, the association values of these two examples are in the range required to qualify the monomers to be used to build supramolecular polymers.

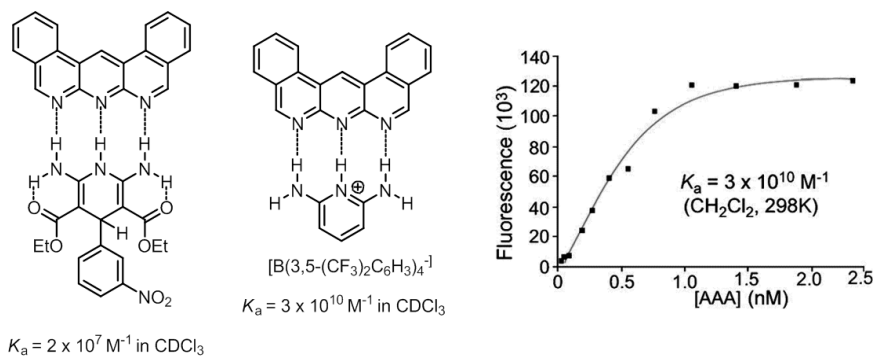


Figure 1-32 Extremely stable complexes of both neutral and ionic types. The association constants are measured in CH_2Cl_2 by using fluorescence spectroscopy. The plot details the fluorescence intensities of AAA array up on addition of ionic DDD array.

More recently, Leigh and coworkers reported a set of extremely strong AAA•DDD complexes including an example that is cationic in nature. They used similar analogs and altered the design of the AAA motif (Figure 1-32) to achieve extremely high stabilities.⁵⁴

1.3.2.2.3 ADDA•DAAD Complementary Complexes

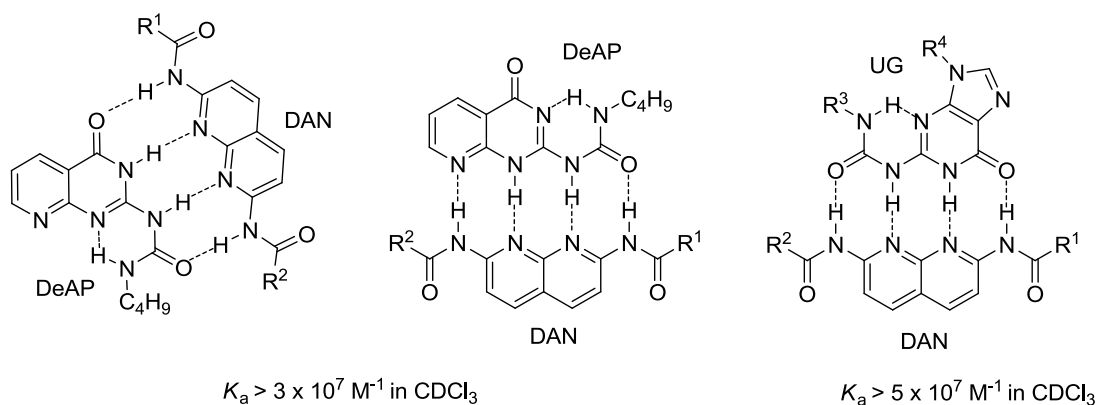


Figure 1-33 Highly stable complexes exhibiting ADDA•DAAD hydrogen bond arrays.

There are very few examples of the ADDA•DAAD type of complexes reported in the literature some of which were discussed in previous sections of the chapter. The two conformers of ureidodeazapterin (DeAP) (Figure 1-33) display a high fidelity towards complex formation with DAN. Computational studies suggested that this is an intrinsic property of the complexes rather than an energetic preference for conformers of the DeAP.⁵⁵

1.3.2.2.4 AAAA•DDDD Complementary Complexes

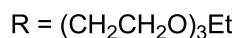
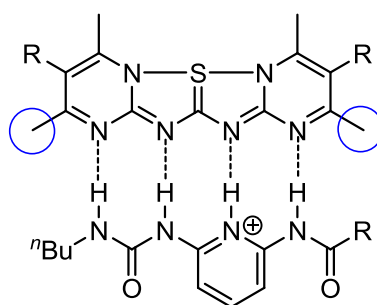


Figure 1-34 Formation of the putative heterodimer AAAA•DDDD with four hydrogen bonds and six attractive secondary interactions.

Extension of these contiguous hydrogen bonded arrays has led to the development of AAAA•DDDD arrays though there are very few examples known. The first example was reported by Luening and coworkers based on the sulfurane AAAA motif and a urea amide based DDAD moiety converted to a DDDD motif upon protonation (Figure 1-34).⁵⁶ The remarkably low association constant observed is attributed to many factors that stem from poor design of the cationic duplex. 2-Pyridinyl ureas can form intramolecular hydrogen bonds that inhibit complexation. In the sulfurane, methyl groups

are attached at the α positions (highlighted in blue circles) that repel the hydrogen bonding partner requiring energy to be expended to form the complex. It has also been reported by Meijer and coworkers that ethylene glycol chains may reduce the association constants of these types of complexes.⁵⁷ Protonation of the AAAA is also yet another possibility to be considered while using a protonated DDDD, which may result in formation of an AADA array and thus form an AADA•DDAD complex which likely has a lower association constant.

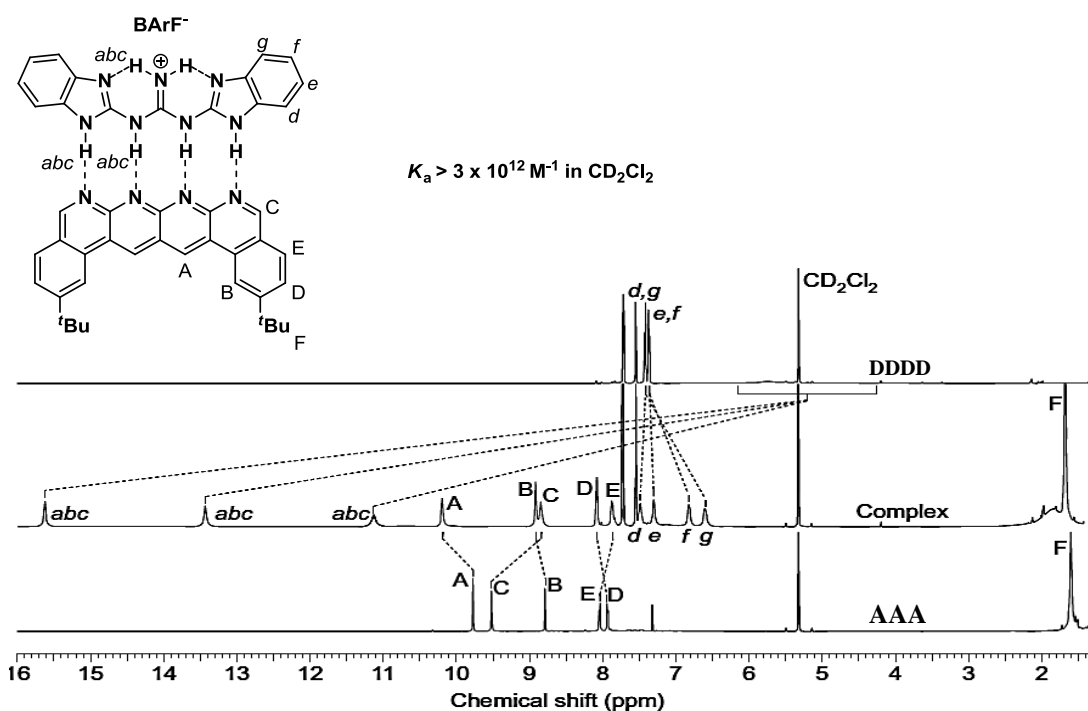


Figure 1-35 ^1H NMR spectra (500 MHz, CD_2Cl_2 , 298 K) of DDDD^+ (top), complex $\text{DDDD}^+\cdot\text{AAAA}$. (middle) and AAAA (bottom). Dashed lines show the changes in chemical shift of the resonances in DDDD^+ and AAAA on formation of complex $\text{DDDD}^+\cdot\text{AAAA}$.

Very recently, surmounting all the negative factors mentioned above, Leigh's group has reported an $\text{AAAA}\cdot\text{DDDD}$ system (Figure 1-35) displaying exceptional

complex stability (in fact the highest to date).⁵⁸ The DDDD⁺ array has two intramolecular hydrogen bonds to help stabilize the cationic guanidinium group, which should also increase the donor strength of the other hydrogen-bond donor groups. The AAAA array is a hexacene system intended to improve its chemical stability compared to underivatized linear arrays of pyridine rings linked through their 2,3/4,5 edges.

The system displays extreme stability in a range of solvent systems ($K_a = 3 \times 10^{12} \text{ M}^{-1}$ in CH_2Cl_2 , $1.5 \times 10^6 \text{ M}^{-1}$ in CH_3CN and $3.4 \times 10^5 \text{ M}^{-1}$ in 10% DMSO/ CHCl_3). The association constant in CH_2Cl_2 corresponds to a binding free energy (ΔG°) in excess of -71 kJ mol^{-1} (more than 20% of the thermodynamic stability of a carbon-carbon covalent bond), which is remarkable for a supramolecular complex held together by just four intercomponent hydrogen bonds. Significantly large downfield shifts of up to 10 ppm of the NH protons of the DDDD⁺ array upon complex formation with the AAAA array and upfield shifts of the benzimidazole CH protons as the NH bonds become more polarized through hydrogen bonding were observed in the ^1H NMR spectra. The broad NH signals in the DDDD⁺ array alone may be the consequence of the interconversion of the possible tautomers that it can form. In contrast, well-resolved signals for three different types of NH protons (H_{abc}) are observed in the spectrum of DDDD⁺•AAAA, as expected for the DDDD⁺ tautomer. With over seven times the order of magnitude required for the complex to qualify for supramolecular polymers, the complex would be very interesting for such extended studies.

1.3.2.2.5 Unusual Complementary Complexes

In a very recent work, Gong and coworkers have reported a strategy for association specificity of hydrogen bonded duplexes by varying the spacings between

adjacent hydrogen bonds (Figure 1-36).⁵⁹ The AADD described in their work are unusual as they do not form the homodimers but still form the AADD arrays bound to DDAA arrays but by heterodimerization. It is a special case of heterodimeric arrays built with what would typically be a homodimeric hydrogen bond sequence.

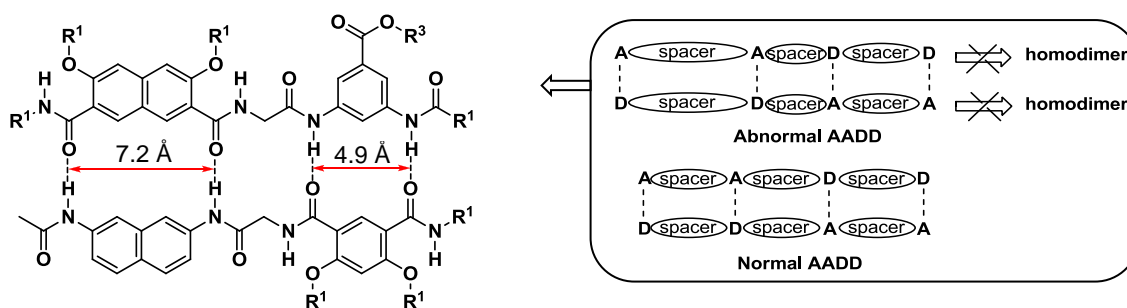


Figure 1-36 Oligoamide strands containing both benzene and naphthalene spacers sharing AADD sequences that heterodimerize.

1.3.3 Double-Helical Complexes

All the discussions so far have centered on linear hydrogen bond arrays. Most of the issues such as unwanted tautomerizations, isomerization conformations are serious considerations when designing a synthetic array for complementary complexation. In an attempt to overcome these hurdles, various attempts have been made by supramolecular chemists to understand some of nature's best complementary systems. The knowledge gained through these studies has enabled them to apply the underlying principles they have uncovered to build artificial double helical complexes.⁶⁰

Helical oligopyridine-dicarboxamide strands⁶¹ (Figure 1-37) were reported by Lehn and coworkers demonstrating the ability of the oligomers to form both single helical foldamers and double helical complexes. The conformations leading to the helical shape of the array result from intramolecular hydrogen bonding within 2'-pyridyl-2-

pyridinecarboxamide units. Extensive intermolecular aromatic stacking was observed stabilizing the double-stranded helices that form through dimerization.

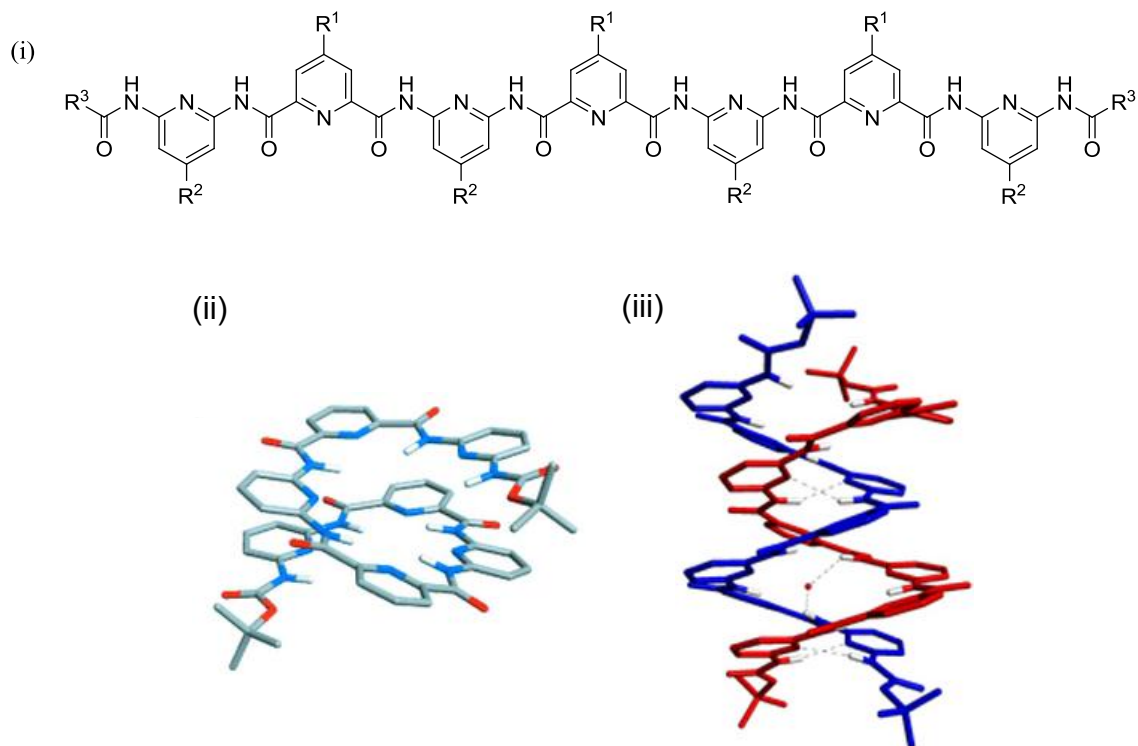


Figure 1-37 Structure of an oligopyridinecarboxamide and the crystal structures of its single helix foldamer and double helix dimer.

A number of complexes have been studied by Yashima and coworkers who have reported double helical oligoresorcinols that specifically recognize oligosaccharides by forming heteroduplexes through noncovalent interactions in water. It is quite difficult to accomplish saccharide recognition in water using artificial receptors because water molecules are such good competitors for the hydrogen bonds. An exception to this is the receptor system relying on covalent sugar-boronate formation, which is truly effective in water.⁶² The oligoresorcinol forms a double helix in water, which unravels and entwines upon complexation with specific oligosaccharides having a particular chain length and glucosidic linkage pattern, thus generating the heteroduplex with an excess one-handed

helical conformation that can be readily monitored and further quantified by absorption, circular dichroism and NMR spectroscopies.

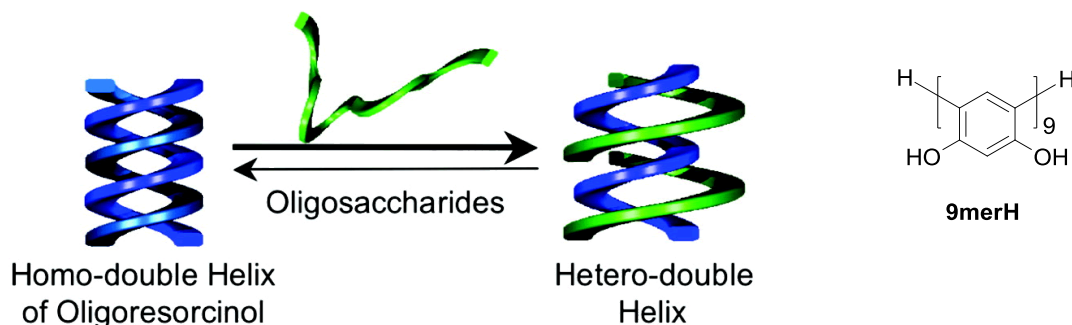


Figure 1-38 Schematic illustration of the heteroduplex formation of **9merH** with oligosaccharides⁶³ and structure of **9merH** (on right).

The oligoresorcinol nonamer **9merH** (Figure 1-28) is long enough to form a double helix as the major species in water, but it dissociates into individual strands in the presence of an increasing volume of organic polar solvents such as methanol at more than 28 vol %, indicating that the double helix formation is highly sensitive to its environment. It starts to unwind as oligosaccharides or polysaccharides are introduced in to the aqueous layer to form the corresponding heterodimer complex whose affinities are measured to be in the range of $3.5 \times 10^3 \text{ M}^{-1}$ in water despite the competition.

The same group has reported an entirely different kind of double helical formation of sequence and chain length specific complementary complexes that are built via amidinium-carboxylate salt bridges (Figure 1-39).⁶⁴ The helical strands consisting of two, three, or four *m*-terphenyl groups attached by diacetylene linkers with complementary binding sites, either the chiral amidine **A** or achiral carboxyl **C** group, were employed. When three dimeric molecular strands (AA, CC, and AC) or six trimeric molecular strands (AAA, CCC, AAC, CCA, ACA, and CAC) were mixed in solution, the

complementary strands were sequence-specifically hybridized to form one-handed double-helical dimers AA•CC and (AC)₂ or trimers AAA•CCC, AAC•CCA, and ACA•CAC, respectively, through complementary amidinium-carboxylate salt bridges.

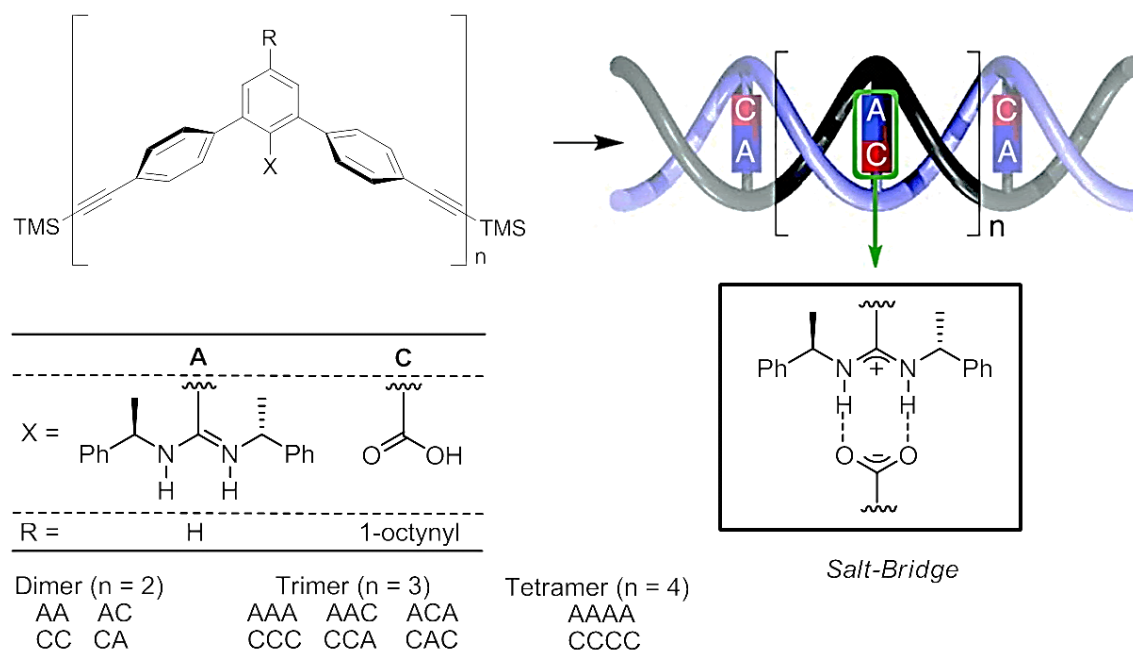


Figure 1-39 Structures of *m*-terphenyl-based molecular strands bearing amidine and/or carboxyl groups and an illustration of double-helical oligomers consisting of complementary molecular strands stabilized by amidinium-carboxylate salt bridges. **A** and **C** denote the monomer units bearing the chiral amidine and achiral carboxyl groups, respectively.

Upon the addition of CCA to a mixture of AAA, AAC, and ACA, the AAC•CCA double helix was selectively formed. Moreover, the homo-oligomer mixtures of amidine or carboxylic acid from the monomers to tetramers (A, AA, AAAA, C, CC, and CCCC) assembled with a precise chain length specificity to form A•C, AA•CC, and AAAA•CCCC, which indicated an extremely specific and well behaved complementary helical system. The high specificity is attributed to the vast gap in binding affinities as

dimerization of carboxylic acid ($\sim 10^2 \text{ M}^{-1}$) is much less than binding constant of amidinium carboxylate salt bridges ($> 10^6 \text{ M}^{-1}$). Based on the success of the salt bridge arrays the group has extended the design to make platinum coordinated polymers⁶⁵ or by incorporating phosphoric acid diesters.⁶⁶

Heteromeric double helices formed by cross-hybridization of chloro and fluoro-substituted quinolone oligoamides have been reported by Huc and coworkers,⁶⁷ whose handedness can be controlled by the chiral substituents on the strands (Figure 1-40). These strands are stabilized by intramolecular N-H \cdots F hydrogen bonds and C=O \cdots F repulsions of the consecutive quinolone units of the sequence.

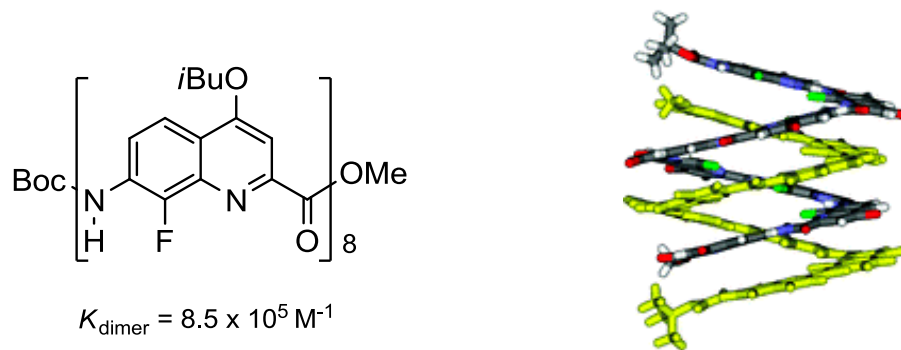


Figure 1-40 Fluoro-substituted quinoline oligoamide that forms cross-hybridized double helical complex. Towards it's right is the crystal structure of the chloro analogue.

Several examples of double helical complexes have been reported from our group that are both self-complementary and complementary arrays built based on pyridyl, thiazine dioxide and indole heterocycles. These examples have demonstrated the importance of considerations of secondary interactions in this context. More will be discussed in detail about these complementary AAA•DDD and self-complementary AADD and AAADDD helical duplexes in the following chapters.

1.3.3.1 Design of Double-Helical Arrays

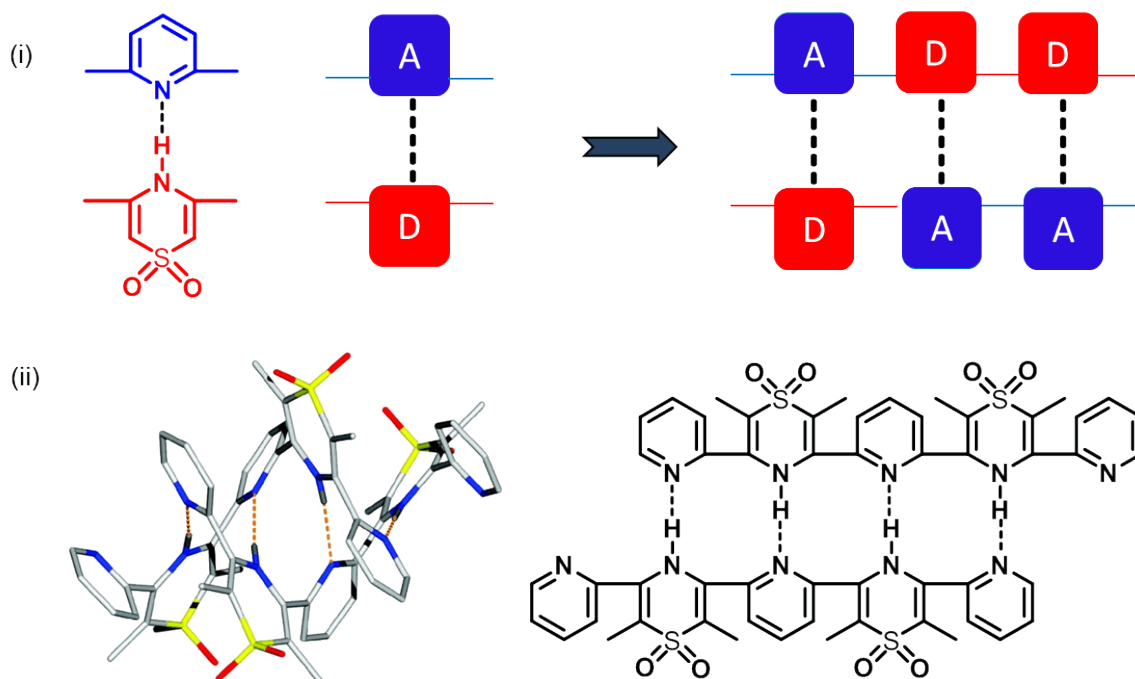


Figure 1-41 (i) A and D subunits form components of a supramolecular “toolbox” which can be used to construct arrays that undergo hydrogen bonding to form complementary complexes; (ii) X-ray crystal structure and schematic representation of a self-complementary double helical ADADA complex developed previously in our research group.

The design of the hydrogen bonding motifs consists of heterocycles such as pyridine, thiazine dioxide and indole derivatives that will form components of our supramolecular „toolbox“. The pyridyl moieties form the acceptor or A units (represented in blue, Figure 1-40) and indole and thiazine dioxides form the donor or D units (represented in red). Pyridine, being easily derivatized, will incorporate methyl groups to enhance the design where required. They serve as electron donating as well as providing steric bias to induce “kink” in the molecule so as to give it a helical geometry. Thiazine dioxide bearing a strong electron withdrawing sulfone group in conjugation with the

amine group, usually forms the central or inner D component. On the other hand, indole being a relatively poor hydrogen donor requires electron withdrawing substituents such as halogens, esters and nitro functional groups (at 5-position) for increased hydrogen bond donor ability and usually forms the terminal or outer D components while designing a complex. Keeping these factors in mind the design is extendable to construction of different arrays merely by changing the sequence of the components. An alternating self-associating pentamer ADADA complex has been reported from our research group serves as an example.

1.4 Scope of the Thesis

The goal of our studies discussed in this thesis was to develop new helical hydrogen bond motifs that are highly specific, soluble in non-competitive solvents and form a variety of double-helical complexes based on hydrogen bonding with a high degree of fidelity. Our intent was to develop a „toolbox“ of heterocyclic acceptor and donor units (pyridine, thiazine dioxide and indole derivatives) use them in different sequences and study the effect of sequence and substitution on complex stability.

Chapter 2 describes the synthesis of self-complementary AADD helical arrays with the added effects of electron donor and acceptor substituents and preorganization. Methyl, ester and nitro functional groups were examined as additions to the acceptor and the donor heterocycles of the arrays. Trimethylene tethers were used to bridge donor heterocycles to provide preorganization. Overall, a wide range ($>10^5 \text{ M}^{-1}$) of stabilities with respect to substitutions at various positions in the AADD oligomers was demonstrated.

Chapter 3 describes the synthesis of some preorganized DDD arrays, substituent effects and accompanying solubility issues encountered. The effect of the addition of pentyl chains to the donor arrays in term of solubilities and overall stabilities was examined by comparison. The extrapolation of these comparative studies gives an estimate of the binding strength of a previously synthesized donor array that was insoluble.

Chapter 4 describes the effects of attachment of alkyl chain to an insoluble (in non-polar solvents such as chloroform and dichloromethane) DDD array and the resulting changes in solubility and binding strength. The chapter also discusses the extended studies of the self-complementary system AADD•DDAA to AAADDD•DDDAAA double helical complementary complex. The longer helical complex provides information about binding propensities ($K_{\text{dimer}} > 4.5 \times 10^7 \text{ M}^{-1}$ in CDCl_3 , and $1.2 \times 10^4 \text{ M}^{-1}$ in 5% DMSO/ CDCl_3 mixture) and the extensibilities of these oligomers which are crucial for using them in developing applications reversible polymers.

1.5 References

1. Fischer, E. *Ber. Dtsch. Chem. Ges.* **1894**, 27 (3), 2985-2993.
2. Wittenberg, J. B.; Isaacs, L., Complementarity and Preorganization. In *Supramolecular Chemistry*, John Wiley & Sons, Ltd: 2012; pp 1-19.
3. (a) Llanes-Pallas, A.; Yoosaf, K.; Traboulsi, H.; Mohanraj, J.; Seldrum, T.; Dumont, J.; Minoia, A.; Lazzaroni, R.; Armaroli, N.; Bonifazi, D. *J. Am. Chem. Soc.* **2011**, 133 (39), 15412-15424; (b) Brinke, G. T.; Ikkala, O. *Chem. Rec.* **2004**,

- 4 (4), 219-230.
4. Tony Jun, H., 3.20 - Molecular Machine-Based NEMS. In *Comprehensive Microsystems*, Hans, Z., Ed. Elsevier: Oxford, 2008; pp 635-656.
 5. (a) Cockroft, S. L.; Hunter, C. A.; Lawson, K. R.; Perkins, J.; Urch, C. J. *J. Am. Chem. Soc.* **2005**, *127* (24), 8594-8595; (b) Wheeler, S. E. *J. Am. Chem. Soc.* **2011**, *133* (26), 10262-10274.
 6. (a) Kierzek, E.; Pasternak, A.; Pasternak, K.; Gdaniec, Z.; Yildirim, I.; Turner, D. H.; Kierzek, R. *Biochemistry* **2009**, *48* (20), 4377-4387; (b) Liu, H.; Wu, J.; Xu, Y.-X.; Jiang, X.-K.; Li, Z.-T. *Tet. Lett.* **2007**, *48* (41), 7327-7331.
 7. Shao, J. D.; Baer, T.; Lewis, D. K. *J. Phys. Chem.* **1988**, *92* (18), 5123-5128.
 8. Ross, P. D.; Rekharsky, M. V. *Biophys. J.* **1996**, *71* (4), 2144-2154.
 9. Jimenez-Barbero, J.; Junquera, E.; Martin-Pastor, M.; Sharma, S.; Vicent, C.; Penades, S. *J. Am. Chem. Soc.* **1995**, *117* (45), 11198-11204.
 10. Kreplak, L.; Doucet, J.; Dumas, P.; Briki, F. *Biophys. J.* **2004**, *87* (1), 640-647.
 11. He, L.; Liu, Y.; Lin, M.; Awika, J.; Ledoux, D.; Li, H.; Mustapha, A. *Sens. Instrum. Food Qual. Saf.* **2008**, *2* (1), 66-71.
 12. (a) Umeyama, H.; Morokuma, K. *J. Am. Chem. Soc.* **1977**, *99* (5), 1316-1332; (b) Desiraju, G. R. *Acc. Chem. Res.* **2002**, *35* (7), 565-573.
 13. Arunan, E.; Desiraju, G. R.; A., K. R.; Sadlej, J.; Scheiner, S.; Alkorta, I.; C., C. D.; Crabtree, R. H.; Danneberg, J. J.; Hobza, P.; Kjaergaard, H. G.; Legon, A. C.;

- Mennucci, B.; Nesbitt, D. J. *Pure Appl. Chem.* **2011**, *83* (8), 1637-1641.
14. Desiraju, G. R. *Angew. Chem. Int. Ed.* **2011**, *50* (1), 52-59.
15. Melandri, S. *Phys. Chem. Chem. Phys.* **2011**, *13* (31).
16. Desiraju, G. R. *Angew. Chem. Int. Ed.* **2007**, *46* (44), 8342-8356.
17. (a) Abraham, M. H. *Chem. Soc. Rev.* **1993**, *22* (2), 73-83; (b) Hunter, C. A. *Angew. Chem. Int. Ed.* **2004**, *43* (40), 5310-5324; (c) Abraham, M. H.; Platts, J. A. *J. Org. Chem.* **2001**, *66* (10), 3484-3491.
18. Resnati, G. *ChemPhysChem* **2002**, *3* (2), 225-226.
19. Watson, J. D.; Crick, F. H. *Nature* **1953**, *171* (4356), 737-738.
20. de Greef, T. F. A.; Meijer, E. W. *Nature* **2008**, *453* (7192), 171-173.
21. (a) Beijer, F. H.; Sijbesma, R. P.; Kooijman, H.; Spek, A. L.; Meijer, E. W. *J. Am. Chem. Soc.* **1998**, *120* (27), 6761-6769; (b) Park, T.; Mayer, M. F.; Nakashima, S.; Zimmerman, S. C. *Synlett* **2005**, *2005* (EFirst), 1435,1436.
22. Park, T.; Todd, E. M.; Nakashima, S.; Zimmerman, S. C. *J. Am. Chem. Soc.* **2005**, *127* (51), 18133-18142.
23. (a) Ghosh, K.; Sen, T.; Fröhlich, R. *J. Inclusion Phenom. Macrocyclic Chem.* **2010**, *68* (1), 193-199; (b) Corbin, P. S.; Zimmerman, S. C.; Thiessen, P. A.; Hawryluk, N. A.; Murray, T. J. *J. Am. Chem. Soc.* **2001**, *123* (43), 10475-10488.
24. (a) Zeng, H.; Yang, X.; Flowers, R. A.; Gong, B. *J. Am. Chem. Soc.* **2002**, *124* (12), 2903-2910; (b) Li, M.; Yamato, K.; Ferguson, J. S.; Gong, B. *J. Am. Chem. Soc.* **2006**, *128* (39), 12628-12629; (c) Sanford, A. R.; Yamato, K.; Yang, X.;

- Yuan, L.; Han, Y.; Gong, B. *Eur. J. Biochem.* **2004**, *271* (8), 1416-1425.
25. Kenny, P. W. *J. Chem. Inf. Model.* **2009**, *49* (5), 1234-1244.
26. Newman, S. G.; Taylor, A.; Boyd, R. J. *Chem. Phys. Lett.* **2008**, *450* (4-6), 210-213.
27. Wang, H.-B.; Mudraboyina, B. P.; Wisner, J. A. *Chem. Eur. J.* **2012**, *18* (5), 1322-1327.
28. Gooch, A.; McGhee, A. M.; Pellizzaro, M. L.; Lindsay, C. I.; Wilson, A. J. *Org. Lett.* **2010**, *13* (2), 240-243.
29. (a) Doxsee, K. M.; Feigel, M.; Stewart, K. D.; Canary, J. W.; Knobler, C. B.; Cram, D. J. *J. Am. Chem. Soc.* **1987**, *109* (10), 3098-3107; (b) Comba, P.; Schiek, W. *Coord. Chem. Rev.* **2003**, *238-239* (0), 21-29; (c) Lim, C. W.; Hong, J.-I. *Bull. Korean Chem. Soc.* **2011**, *32* (3), 1045-1047.
30. Etter, M. C. *Acc. Chem. Res.* **1990**, *23* (4), 120-126.
31. Hamilton, A. D.; Pant, N. *J. Chem. Soc., Chem. Commun.* **1988**, (12).
32. Murray, T. J.; Zimmerman, S. C. *Tet. Lett.* **1995**, *36* (42), 7627-7630.
33. Li, X.; Fang, Y.; Deng, P.; Hu, J.; Li, T.; Feng, W.; Yuan, L. *Org. Lett.* **2011**, *13* (17), 4628-4631.
34. Goodman, M. F. *Nature* **1995**, *378*, 237-238.
35. Corbin, P. S.; Zimmerman, S. C. *J. Am. Chem. Soc.* **1998**, *120* (37), 9710-9711.
36. Hunter, C. A. *Angew. Chem. Int. Ed.* **2004**, *43* (40), 5310-5324.

37. Yang, S.; Wang, C.-F.; Chen, S. *Angew. Chem. Int. Ed.* **2011**, *50* (16), 3706-3709.
38. Park, T.; Zimmerman, S. C. *J. Am. Chem. Soc.* **2006**, *128* (44), 14236-14237.
39. Schneider, H.-J.; Juneva, R. K.; Simova, S. *Chem. Ber.* **1989**, *122*, 1211-1213.
40. Sartorius, J.; Schneider, H.-J. *Chem. Eur. J.* **1996**, *2* (11), 1446-1452.
41. (a) Jorgensen, W. L.; Pranata, J. *J. Am. Chem. Soc.* **1990**, *112* (5), 2008-2010; (b) Pranata, J.; Wierschke, S. G.; Jorgensen, W. L. *J. Am. Chem. Soc.* **1991**, *113* (8), 2810-2819.
42. Beijer, F. H.; Kooijman, H.; Spek, A. L.; Sijbesma, R. P.; Meijer, E. W. *Angew. Chem. Int. Ed.* **1998**, *37* (1-2), 75-78.
43. Söntjens, S. H. M.; Sijbesma, R. P.; van Genderen, M. H. P.; Meijer, E. W. *J. Am. Chem. Soc.* **2000**, *122* (31), 7487-7493.
44. Sijbesma, R. P.; Beijer, F. H.; Brunsveld, L.; Folmer, B. J. B.; Hirschberg, J. H. K. K.; Lange, R. F. M.; Lowe, J. K. L.; Meijer, E. W. *Science* **1997**, *278* (5343), 1601-1604.
45. Prabhakaran, P.; Puranik, V. G.; Sanjayan, G. J. *J. Org. Chem.* **2005**, *70* (24), 10067-10072.
46. Zhao, Y.-P.; Zhao, C.-C.; Wu, L.-Z.; Zhang, L.-P.; Tung, C.-H.; Pan, Y.-J. *J. Org. Chem.* **2006**, *71* (5), 2143-2146.
47. Todd, E. M.; Zimmerman, S. C. *Tetrahedron* **2008**, *64* (36), 8558-8570.
48. Hisamatsu, Y.; Shirai, N.; Ikeda, S.-i.; Odashima, K. *Org. Lett.* **2009**, *11* (19),

4342-4345.

49. (a) Lafitte, V. G. H.; Aliev, A. E.; Horton, P. N.; Hursthouse, M. B.; Bala, K.; Golding, P.; Hailes, H. C. *J. Am. Chem. Soc.* **2006**, *128* (20), 6544-6545; (b) Greco, E.; Aliev, A. E.; Lafitte, V. G. H.; Bala, K.; Duncan, D.; Pilon, L.; Golding, P.; Hailes, H. C. *New J. Chem.* **2010**, *34* (11).
50. Zeng, H.; Yang, X.; Brown, A. L.; Martinovic, S.; Smith, R. D.; Gong, B. *Chem. Commun.* **2003**, (13), 1556-1557.
51. (a) Sessler, J. L.; Wang, B.; Harriman, A. *J. Am. Chem. Soc.* **1993**, *115* (22), 10418-10419; (b) Berman, A.; Izraeli, E. S.; Levanon, H.; Wang, B.; Sessler, J. L. *J. Am. Chem. Soc.* **1995**, *117* (31), 8252-8257.
52. Bell, D. A.; Anslyn, E. V. *Tetrahedron* **1995**, *51* (26), 7161-7172.
53. Murray, T. J.; Zimmerman, S. C.; Kolotuchin, S. V. *Tetrahedron* **1995**, *51* (2), 635-648.
54. Blight, B. A.; Camara-Campos, A.; Djurdjevic, S.; Kaller, M.; Leigh, D. A.; McMillan, F. M.; McNab, H.; Slawin, A. M. Z. *J. Am. Chem. Soc.* **2009**, *131* (39), 14116-14122.
55. Zimmerman, S. C.; Corbin, P., Heteroaromatic Modules for Self-Assembly Using Multiple Hydrogen Bonds. In *Molecular Self-Assembly Organic Versus Inorganic Approaches*, Fuiita, M., Ed. Springer Berlin / Heidelberg: 2000; Vol. 96, pp 63-94.

56. Taubitz, J.; Lüning, U. *Aust. J. Chem.* **2009**, *62* (11), 1550-1555.
57. de Greef, T. F. A.; Nieuwenhuizen, M. M. L.; Sijbesma, R. P.; Meijer, E. W. *J. Org. Chem.* **2010**, *75* (3), 598-610.
58. Blight, B. A.; Hunter, C. A.; Leigh, D. A.; McNab, H.; Thomson, P. I. T. *Nat Chem* **2011**, *3* (3), 244-248.
59. Zhang, P.; Chu, H.; Li, X.; Feng, W.; Deng, P.; Yuan, L.; Gong, B. *Org. Lett.* **2010**, *13* (1), 54-57.
60. Furusho, Y.; Yashima, E. *J. Polym. Sci., Part A: Polym. Chem.* **2009**, *47* (20), 5195-5207.
61. Berl, V.; Huc, I.; Khoury, R. G.; Krische, M. J.; Lehn, J.-M. *Nature* **2000**, *407* (6805), 720-723.
62. Goto, H.; Furusho, Y.; Yashima, E. *J. Am. Chem. Soc.* **2007**, *129* (29), 9168-9174.
63. Goto, H.; Furusho, Y.; Yashima, E. *J. Am. Chem. Soc.* **2007**, *129* (29), 9168-9174.
64. Ito, H.; Furusho, Y.; Hasegawa, T.; Yashima, E. *J. Am. Chem. Soc.* **2008**, *130* (42), 14008-14015.
65. Furusho, Y.; Yashima, E. *Macromol. Rapid Commun.* **2011**, *32* (2), 136-146.
66. Yamada, H.; Maeda, K.; Yashima, E. *Chem. Eur. J.* **2009**, *15* (28), 6794-6798.
67. Gan, Q.; Li, F.; Li, G.; Kauffmann, B.; Xiang, J.; Huc, I.; Jiang, H. *Chem. Commun.* **2010**, *46* (2), 297-299.

Chapter 2

2 Synthesis and Self-Association of Double Helical AADD Arrays

2.1 Hydrogen Bonded Supramolecular Polymers

Synthetic polymeric materials are amongst the most important classes of new materials introduced in the previous century. The impressive recent progress in supramolecular chemistry, has paved the way to design polymers and polymeric materials that lack a formal macromolecular structure.¹ Instead, highly directional secondary interactions are used to assemble the many repeating units into a polymer-like array. Polymers based on this concept hold promise as a unique class of novel materials,² because they combine many of the attractive features of conventional polymers with the reversibility originating from the secondary interactions that assemble them. Hydrogen bond arrays have been used as building blocks for stimuli-responsive polymers and assemblies with nanoscale dimensions.^{3,4} In order to construct a stable reversible polymeric material,⁵ quadruple hydrogen bond arrays with strong binding constants have been employed in the past leading to supramolecular materials. In the polymer phases, weak interactions that are non-directional can give rise to microphase-separated structures or gelation due to network formation.⁶

The degree of polymerization of reversibly interacting “monomers” can be plotted as a function of the stability of their interactions. The diagram (Figure 2-1) indicates that the minimum association or dimerization constant required for a complex to be eligible for formation of supramolecular reversible polymers based on hydrogen bonding is

greater than 10^4 M^{-1} for reaching a degree of polymerization of 100 at 0.05 M or 10^3 M^{-1} at 1 M.⁷

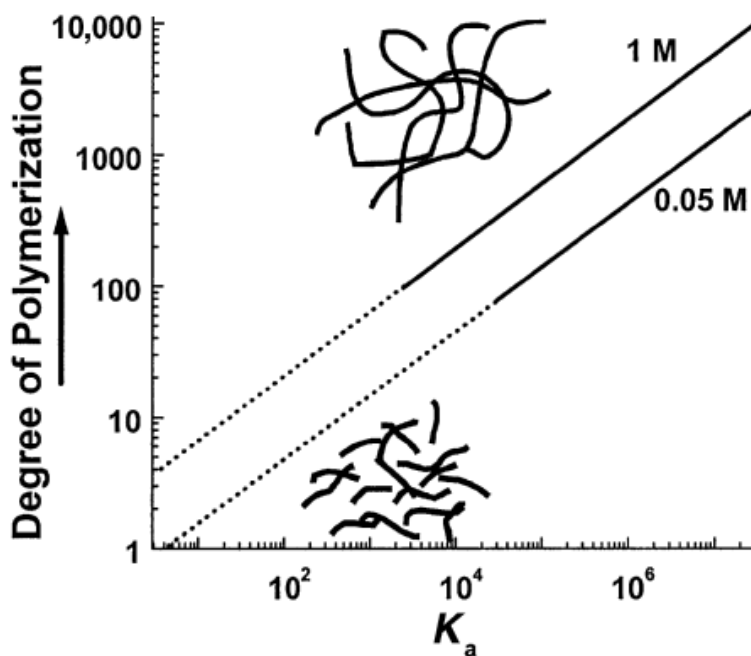


Figure 2-1 A plot of the relation between association constant K_a and the degree of polymerization⁸ of idealized monomers at two different concentrations.

Based on Meijer's UPy-based building blocks, there have been numerous patent applications filed using supramolecular architectures in fields ranging from adhesives,⁹ printing,¹⁰ cosmetics¹¹ and personal care¹² to coatings.¹³

(i)

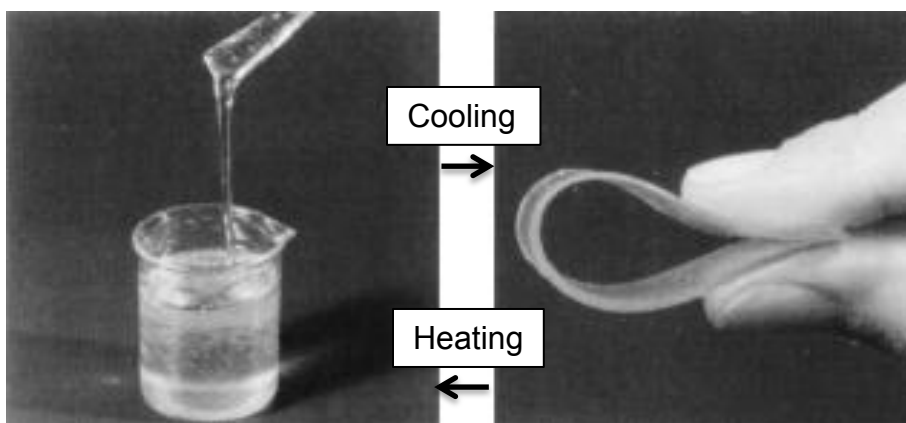


Figure 2-2 continued ...

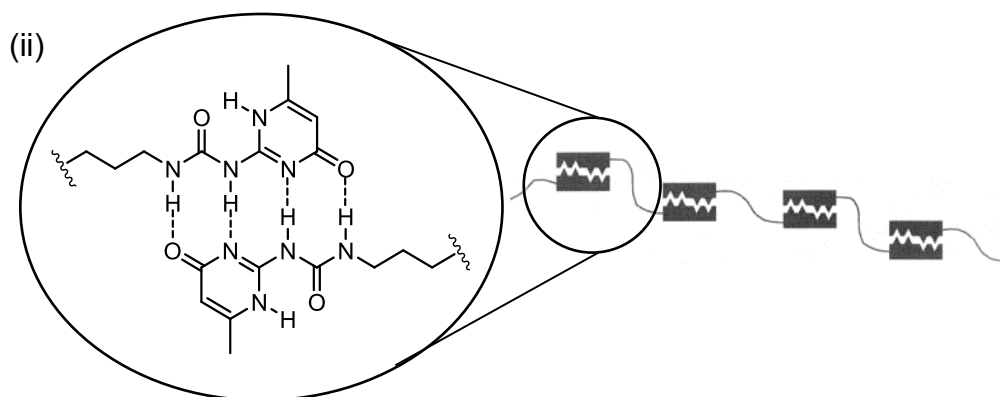


Figure 2-2 (i) Changing the macroscopic properties of a telechelic poly(ethylene/butylene) copolymer (left) by end-group modification with self-associating hydrogen-bonding motifs. The macromolecular structure is a network of monomers connected by hydrogen bonds. (ii) The UPy units form hydrogen bonds to each other and act as monomers in a polymeric chain.¹⁴

One of the salient features of the materials, unique to reversible polymers, is that the supramolecular chains lose strain by breaking, followed by recombination of free chain ends without strain.¹⁵ Breaking rates increase with temperature, and contribute to the temperature-dependent behaviour of supramolecular polymers (Figure 2-2 (i)).^{14, 16}

2.2 AADD Arrays as Components of Hydrogen Bonded Materials

The synthesis and application of self-complementary coplanar AADD hydrogen bond arrays with very large dimerization constants (e.g. 10^7 - 10^8 M^{-1}), originally introduced by the groups of Meijer^{6a} and Zimmerman,¹⁷ stand as a milestone in the development of both supramolecular and materials chemistry. Although there are a great number of advantages of their use in reversible polymeric materials, the materials are based on a very few examples of self-associating quadruple AADD arrays that form highly stable dimers reported in the literature (Figure 2-3).¹⁸

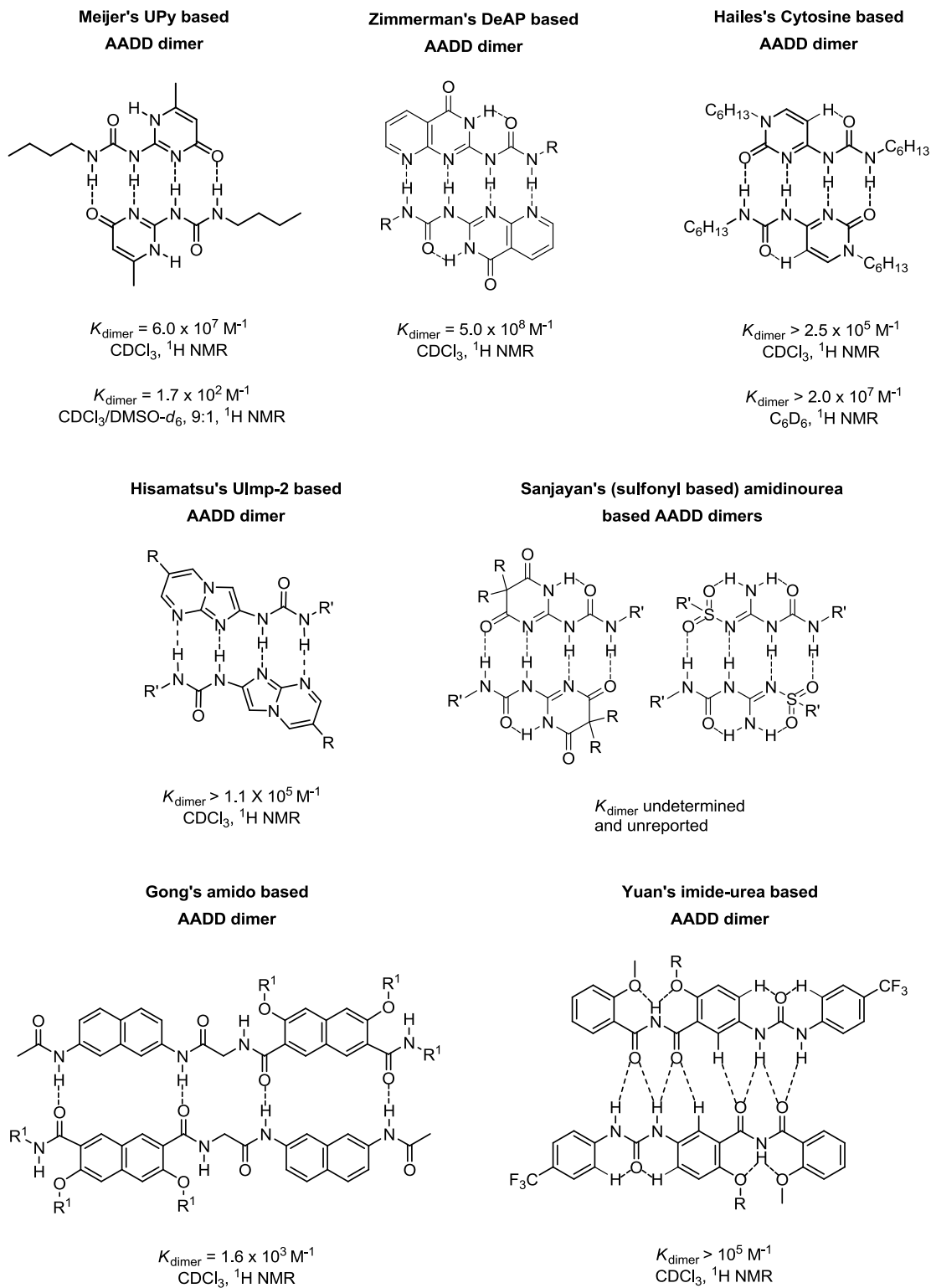


Figure 2-3 Examples of AADD arrays and designs with K_{dimer} values, method used for the analysis and supporting solvents at room temperature.

Well-defined hydrogen bonding arrays have been incorporated in a number of polymers as end groups,^{6a, 19,20} side chains^{21,22} and in the main chains,^{23, 24} in the pursuit of new materials designs. Most of the properties were studied in the solution state.¹⁹⁻²⁵ In an example study, UPy groups were introduced as thermoreversible interaction sites to a chemically cross-linked polymer network, resulting in shape memory properties.²⁶ Guan and co-workers have reported the first biomimetic design of a linear polymer composed of a tandem array of biomimetic cyclic UPy modules, closely mimicking the titin protein architecture, yielding a strong, tough, processable, and highly adaptive material (Figure 2-4).^{3a}

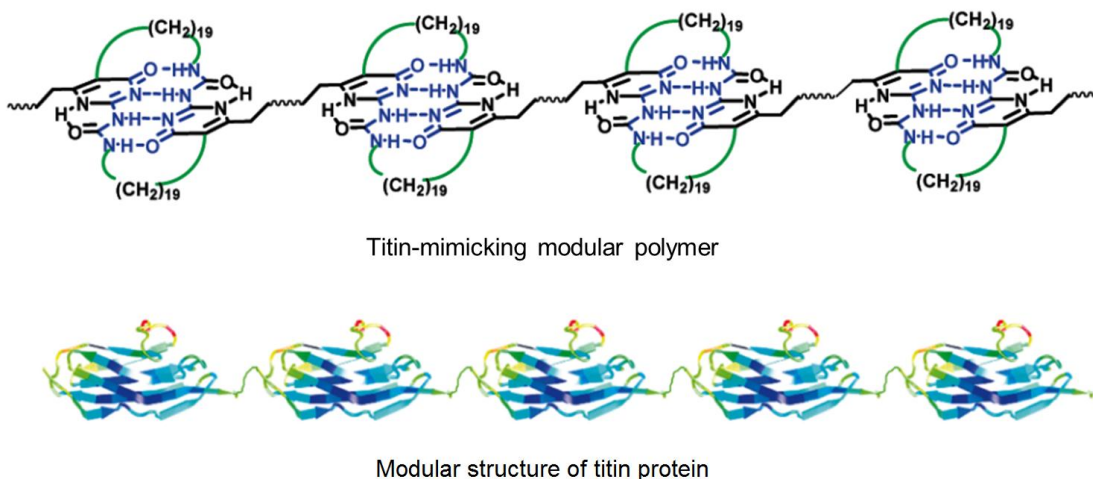


Figure 2-4 Biomimetic linear modular polymer based on the Upy AADD array, mimicking titin, a skeletal muscle protein.

Titin absorbs energy by the reversible rupture of intramolecular secondary interactions, followed by refolding induced recovery, making it an intriguing model for the design of adaptive materials. Experiments were conducted to study the mechanical and adaptive nature of the biomimetic polymer such as incubation in water, heating the polymer and cooling it down to freeze the shape. The results demonstrated valuable

properties such as shape-memory properties, high modulus and toughness, large extensibility, and intriguing adaptive behaviour, whereas similar tests on the control polymer where the dimerization of UPy arrays was blocked completely lacked the above properties, suggesting that the reversible rupture and refolding of UPy dimer modules contributes to the macroscopic properties.

These types of unique materials with excellent qualities of stability and reversibility are an inspiration for the development of new AADD arrays that can be used orthogonally to extend the behaviour to use more than one interaction.²⁷ We anticipated that we could achieve this goal using double helical self-complementary complexes. As discussed, in order to be effective as the monomers of a supramolecular polymer, our AADD arrays should possess a K_{dimer} value of at least 10^4 M^{-1} .⁸ The rest of this chapter discusses the efforts to test the efficacy of our design and also to engineer the highest possible dimer stabilities with this sequence.

2.3 Design of Double-Helical AADD Arrays

Utilizing the acceptor (A) and the donor (D) heterocycles from our supramolecular “tool box” we engineered the basic design to construct our arrays (Figure 2-5). Sequential connection of these heterocycles gives rise to the desired oligomers which self-associate based on the order of connectivity. Before discussing the specificities of our design there are other important factors to be considered from the point view of the AADD arrays. Based on the sequence of the arrangement of heterocycles in an oligomer, attractive or repulsive secondary interactions²⁸ play an important role in determining stabilities of hydrogen bonded complexes.

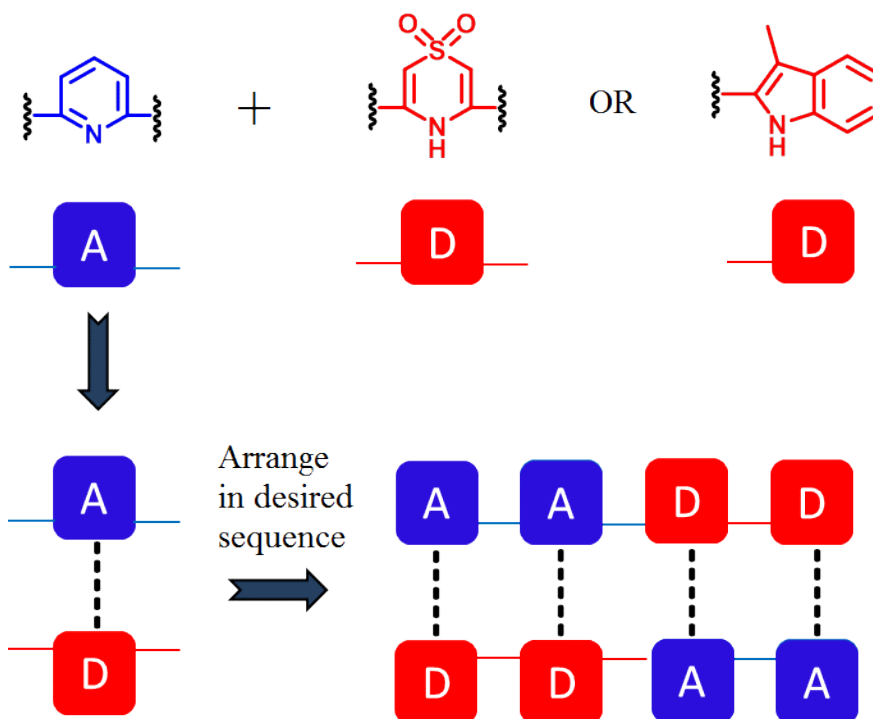


Figure 2-5 Basic design of the arrays with a simple donor (D) and acceptor (A) pair leading to an oligomeric strand. The strands should undergo self-assembly into double-helical self-complementary duplexes.

Generally, in a similar manner to traditional coplanar hydrogen bond arrays, the stability of these complexes is also dependent on the number^{29,30} of hydrogen bonded components in an array, apart from their order of arrangement. The general trend can be greatly disrupted based on the interplay of secondary interactions. The dependence of the stabilities of these complexes due to secondary interactions is aptly demonstrated by the two complexes depicted at the top and bottom left of Figure 2-6.^{31,32} The complex formed by the two contiguous arrays presenting AAA and DDD sequences is several orders of magnitude more stable than that produced by the dimerization of the ADADA array pictured above it, even though it incorporates one less hydrogen bond. Presumably the effect is a result of strong secondary hydrogen bond interactions between the two strands

upon complex formation. The AAA•DDD complex has four attractive secondary interactions and no repulsive secondary interactions whereas the ADADA dimer has six repulsive secondary interactions and no attractive secondary interactions.

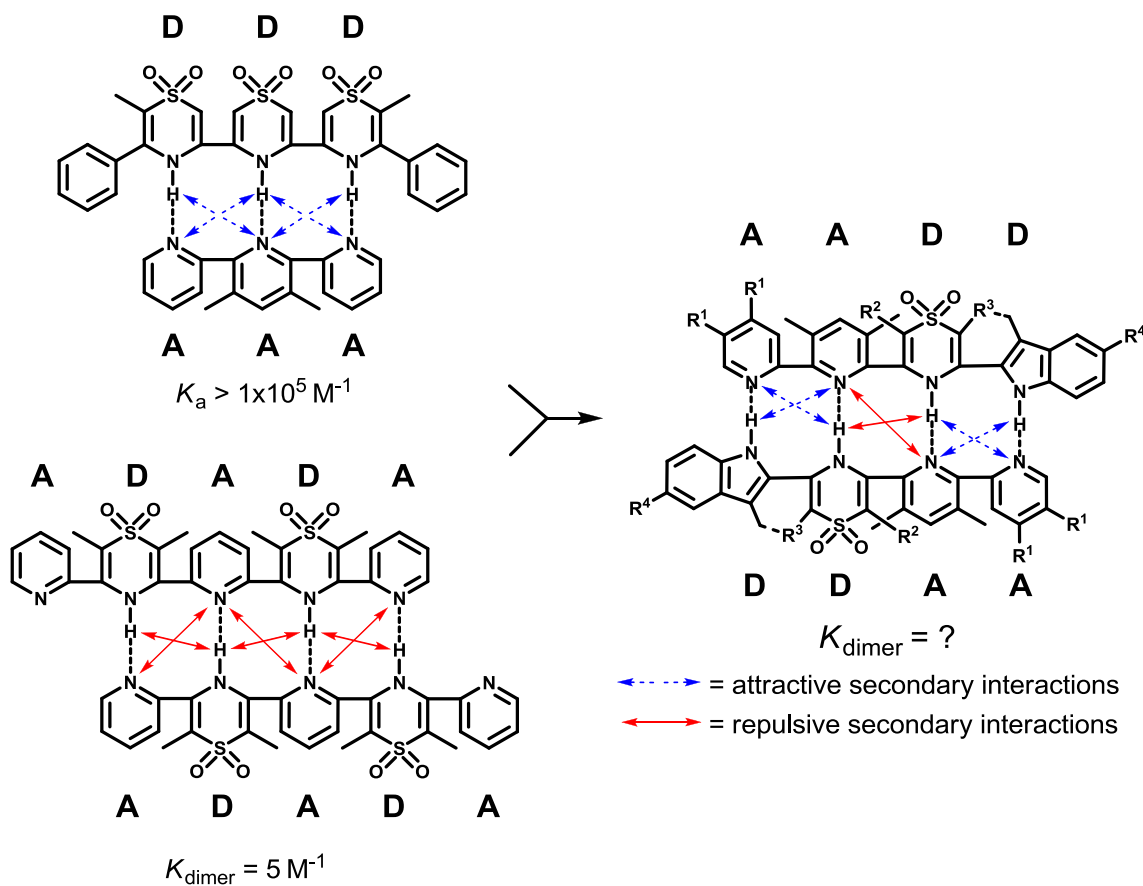


Figure 2-6 The AADD complex design as a hybrid of alternating ADADA and contiguous AAA•DDD sequences.

Given these results, we considered whether the two designs could be amalgamated to generate a hybrid structure (an AADD array) with both contiguous and alternating elements and how stable the resulting complex would be. It would be a very interesting as well as a challenging study particularly with four attractive secondary interactions and two repulsive secondary interactions, whether the quadruple arrays would form highly stable self-complementary double-helical complexes. In view of the

importance and wide utility of coplanar AADD arrays described above in the development of supramolecular polymers and materials,^{6a, 17b, 33} we anticipated an array based on our design containing this sequence could be utilized in similar applications.

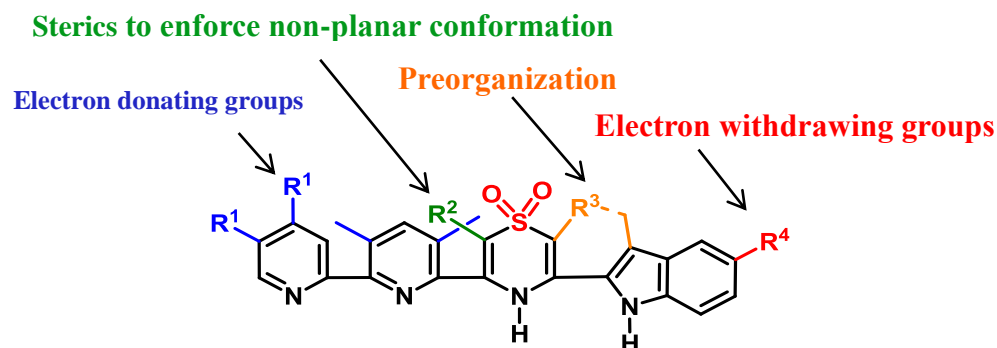


Figure 2-7 Design attributes of the AADD array outlined using different colors.

The acceptor components of the AADD array may contain additional electron donating groups (blue) that improve their hydrogen acceptor character. The (green) methyl component is not desirable as an electron donating group placed on the hydrogen bond donor component (thiazine dioxide) which may reduce the hydrogen bonding donor capacity of the amine proton. However, it is likely necessary to provide a steric “kink” in the molecule so that it undergoes helical complex formation via hydrogen bonding. The alkyl tether (orange) between the hydrogen bond donor heterocycles also provides preorganization in the array and the (red) electron withdrawing group increases the hydrogen bond donor character of the indole N-H.

Following these criteria, a series of AADD arrays were designed by progressively introducing one or more stabilising factors into each motif (Figure 2-7). The stepwise introduction of these strengthening elements was also intended to give an estimation of how much they contribute individually toward the overall stability of the complexes. This

kind of information is essential in order to fine tune the stability of such complexes to function in materials based on them.

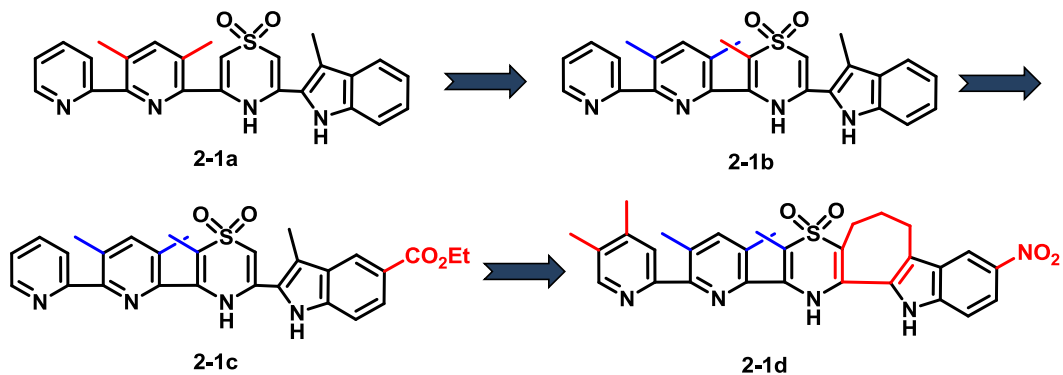
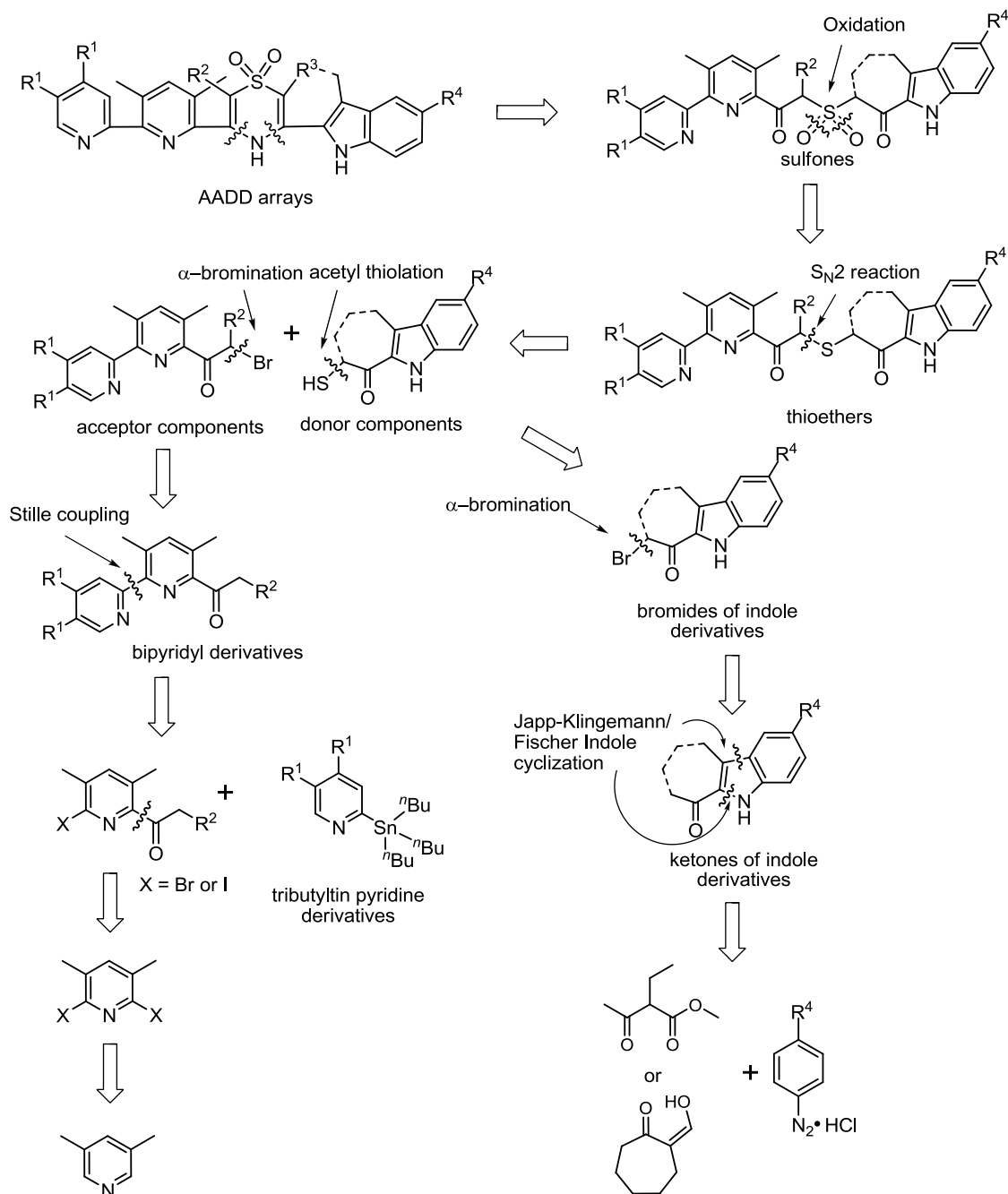


Figure 2-8 Four different AADD arrays **2-1a-d** highlighting the progressive changes made to the basic design that may lead to increased stability of the complexes. Initial changes are in red and blue indicates changes carried forward through the molecular design.

Array **2-1b** has a methyl group introduced to the thiazine dioxide ring between the central acceptor and donor heterocycles. The methyl functional group improves the stability compared to the **2-1a** by preventing unwanted intramolecular and intermolecular hydrogen bonding as explained in the preceding paragraphs. **2-1c** has an electron withdrawing ester functional group introduced at the 5-position of the indole ring. This should provide an idea how such groups can influence the dimerization stability. The last AADD array in the series has three major changes. The first change is the introduction of nitro substituent as a very strong electron withdrawing group. The second change is the introduction of a pre-organizing trimethylene tether between the two donor subunits. The final change is the addition of two more methyl groups at positions 4 and 5 on the terminal pyridine heterocycle thereby improving its hydrogen bond acceptor character. The syntheses of the four AADD arrays may be approached using a simple retrosynthetic

analysis.

2.4 Synthesis of Double Helical AADD Arrays

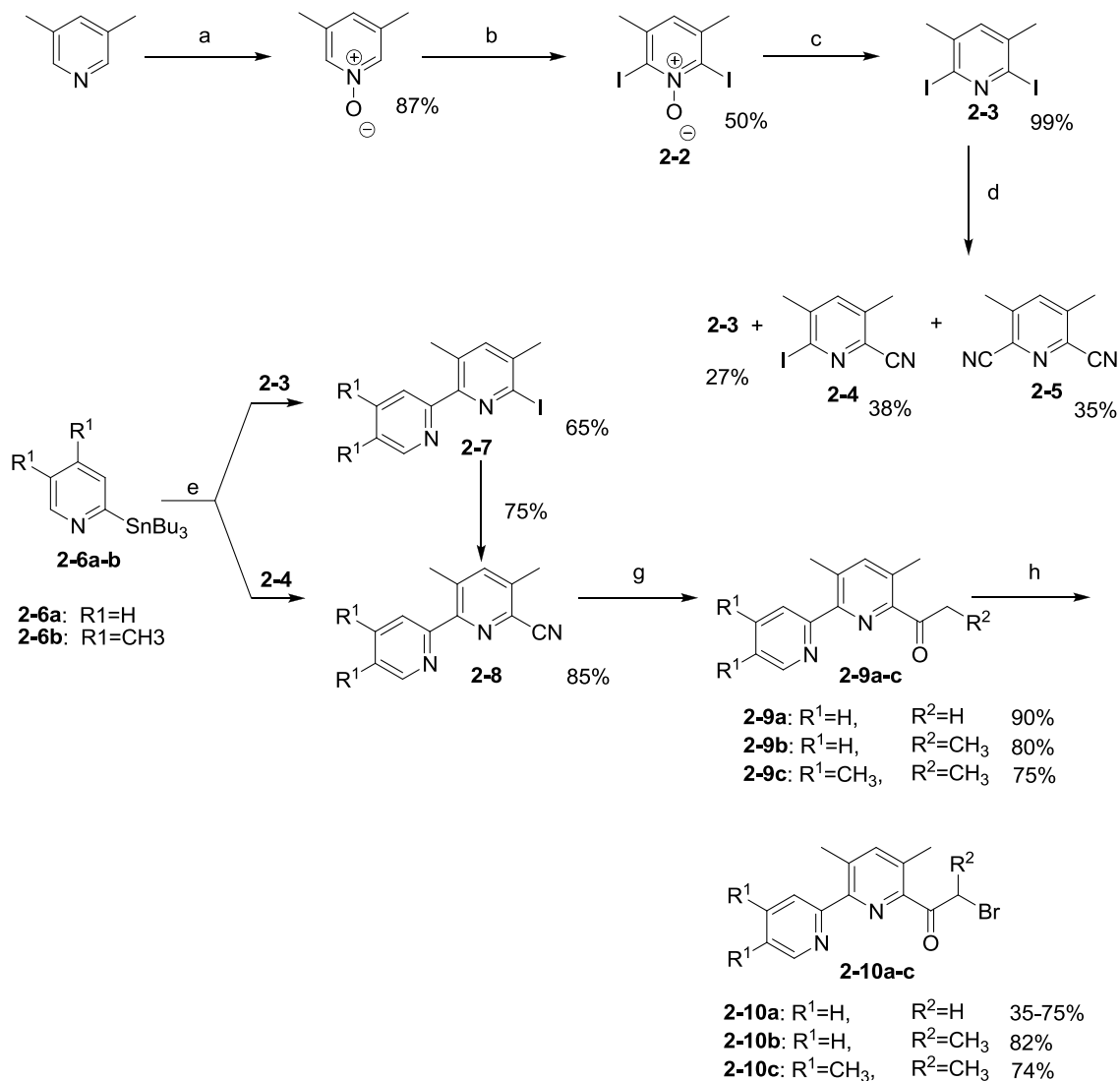


Scheme 2-1 Retrosynthetic pathways leading from the series of AADD arrays. After disconnecting the condensed thioethers into acceptor and donor units, they follow two different retrosynthetic paths to readily available starting materials.

The thiazine dioxide heterocycle can be disconnected on either side of the amine group which may be formed by condensation of a 3-sulfonyl-1,5-dione precursor (Scheme 2-9). The sulfones are the oxidized forms of thioethers which in turn are products from the S_N2 reaction of thiols (referred to as the donor components) and halides (referred to as the acceptor components). The α -bromoketones undergo substitution readily and are simple to synthesize. The acceptor bipyridyl derivatives may be obtained through the corresponding 6-bromo-2-acetyl or propionyl lutidines by Stille coupling with tributyltin pyridines. The thiols of the donor components are generated from the corresponding thioacetates which are products from substitution of the corresponding halides.³⁴ The halides can be obtained from the acyl indoles by α -bromination in a similar fashion to the acceptor components. The acetyl indoles can be synthesized either by acetylating skatole directly (not shown) or constructing them via Japp-Klingemann/Fisher-Indole cyclizations starting from diazonium salts of the corresponding anilines.

The two major subunits in the retrosynthetic scheme are the acceptor and donor components (Scheme 2-1). Synthesis of the bipyridyl fragments was developed earlier in our research group³⁵ and the reported procedures were largely duplicated. The initial synthetic sequence of the acceptor component began with the preparation of 2,6-diiodolutidine. 3,5-Lutidine (Scheme 2-2) was oxidized using an excess of 30% hydrogen peroxide in acetic acid.³⁶ Due to the hygroscopic nature of the *N*-oxide product it was necessary to ensure that the substrate was dry before carrying on to the next step. Purification was carried out using glass vacuum distillation apparatus or Kugelrohr and stored in a desiccator for later use. The distillation step can be eliminated by drying over

excess magnesium sulphate in chloroform, concentrating the compound under reduced pressure for a couple of hours and immediately using it in the dilithiation step.



Scheme 2-2 Synthesis of acceptor components **2-10a-c**. Reaction conditions: (a) 1eq. H₂O₂, CH₃COOH, reflux 12 h, 87%; (b) 2.4eq. ⁿBuLi, THF, -78 °C, 2 h, 2.2 eq. I₂, THF, -78 °C to 21 °C, 8 h, 50%; (c) 2.5 eq. PCl₃, CHCl₃ reflux, 6 h, 99%; (d) 0.75 eq. Zn(CN)₂, 3% Pd(PPh₃)₄, DMF, Microwave, 3 minutes, 200 °C, 27% (**2-3**), 38% (**2-4**), 35% (**2-5**); (e) 3 % Pd(PPh₃)₄, toluene, reflux 26 h, 65-85%; (f) 1.6 eq. Zn(CN)₂, 3% Pd(PPh₃)₄, DMF, Microwave, 3 minutes, 170 °C, 75%; (g) 1.2 eq MeMgBr/EtMgBr, THF, addn at 0 °C, reflux 12 h, 80-90%; (h) 1.2 eq. Br₂, Et₂O, 36 h, 35-82 %.

Oxidation of the 3,5-lutidine nitrogen activates the 2- and 6-positions to undergo lithiation and hence the *N*-oxide was iodinated to give **2-2** as an off-white solid in 45-50% yield.³⁷ The use of different stoichiometries of iodine in the reaction leads to different ratios of products. These include formation of coupled products such as bis(iodolutidine) in minute quantities. In order to get the best yields of diiodolutidine *N*-oxide, 2.2 equivalents of iodine were employed. Compound **2-2** was deoxygenated using phosphorus trichloride in near to quantitative yields. Caution was applied by using ice while quenching and working up as the deoxygenation reaction is highly exothermic and evolves enormous heat due to the reaction of *in situ* formed phosphorous oxychloride with water.

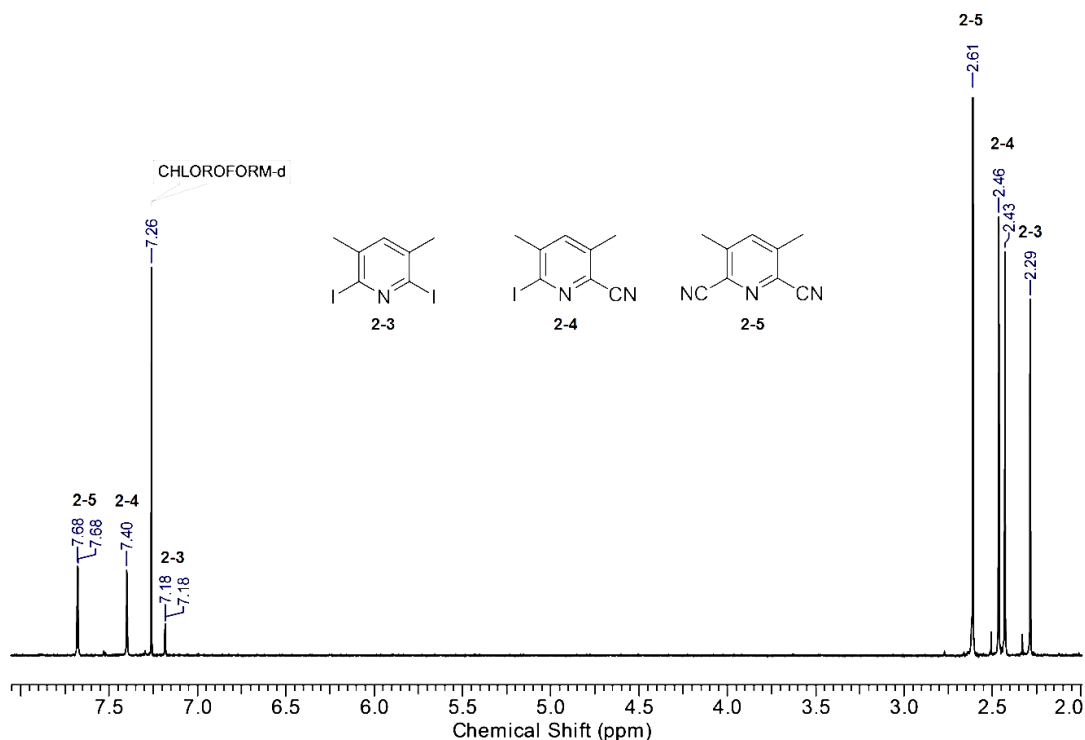


Figure 2-9 ¹H NMR spectrum of the substitution reaction using Zn(CN)₂ as cyanide reagent, displaying resonances corresponding to the two products **2-4** and **2-5** and the starting material **2-3**. Reaction conditions: 0.75 eq. Zn(CN)₂, 3% Pd(PPh₃)₄, DMF, Microwave, 3 minutes, 200 °C, 27% (**2-3**), 35% (**2-4**), 38% (**2-5**).

In order to generate the mono halo-nitrile **2-4**, various stoichiometries of nitrile reagent, zinc cyanide or sodium cyanide (with copper (II) iodide in the presence of Pd [0] catalysts) were explored. Zinc cyanide was a better source of the cyanide reagent in terms of cleanliness of the reaction, work up and yields of **2-4** compared to sodium cyanide.

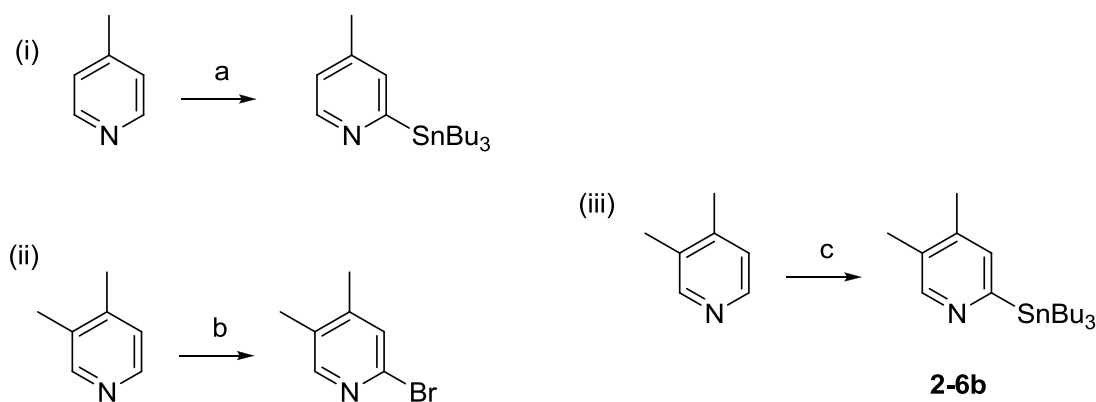
Table 2-1 Cyanide reagents and stoichiometries used and yields observed in the cyano-dehalogenation reaction of 2-3. Reaction conditions as in Figure 2-6.

Eq. of Zn(CN) ₂	Yield % 2-3 : 2-4 : 2-5	Eq. of NaCN	Yield % 2-3 : 2-4 : 2-5
0.50	46 : 36 : 18	0.50	83 : 15 : 02
0.75	27 : 38 : 35	0.80	57 : 25 : 18
1.00	17 : 33 : 50	1.20	31 : 36 : 33

No matter what stoichiometries or the method of heating (refluxing or microwave), this reaction always resulted in mixtures of mono- and di substituted nitrile **2-4** and **2-5** and starting material **2-3**. As the step requires purification using flash column chromatography yielding 38% at the most, it necessitated repeating the substitution reaction step several times to attain a sufficient amount of **2-4** to carry forward in the reaction.

Trimethyltin chloride was initially used to synthesize trimethyltin pyridine but was replaced with tributyltin chloride to avoid the higher toxicity of the former reagent. Though, tributyltin pyridine is well known, 2-tributyltin-4,5-lutidine **2-6b** has not been reported in the literature. Altering the method followed by Yves *et al.*³⁸ provided a route

to the synthesis of **2-6b** in a moderate yield of 45% for the lithiation of 3,4-lutidine followed by addition of tributyl tin halide. The yield is not a surprise considering the two steps in a single pot and as the reaction is carried out directly on the lutidine instead of the 2-substituted halide as normally practiced in the literature. Solvents and stoichiometries of the reagents play an important role in determining the selective formation of the product **2-6b**. The use of excess solvent and reagent improves the selectivity of product formation, as the use of lesser amounts leads to the formation of unwanted 3,4-dimethyl-2-(trimethylstannyl)pyridine. These stannyl compounds are easily purified by column chromatography using silica and are stable to storage for long periods.



Scheme 2-3 Direct incorporation of bromide and tributyltin groups to 4-picoline and 3,4-lutidine. Reaction conditions: (i) 2 eq. 2-(dimethylamino)ethanol in anhyd. hexanes (15 mL per 10.5 mmol), 0 °C, 4 eq. ⁿBuLi in hexanes -0 °C, 0.5 h, 5 eq. tributyltin chloride, THF, -78 °C, 1 h, 80 %; (ii) (b) 2 eq. 2-(dimethylamino)ethanol, 0 °C, 4 eq. ⁿBuLi in hexanes (50 mL per 10 mmol), -0 °C, 30 minutes, 4 eq. CBr₄, THF, -78 °C, 1h, 80 %. (i) and (ii) are reported. (iii) 2 eq. 2-(dimethylamino)ethanol in anhy. Hexanes (25 mL per 10.5 mmol), 0 °C, 4.5 eq. ⁿBuLi in hexanes -0 °C, 0.5 h, 2.6 eq. tributyltin chloride, THF, -78 °C, 1h, 45 %.

At this juncture we explored two ways to synthesize intermediate **2-9**. Tributyltin derivative **2-6** can either be coupled to **2-3** or to **2-4**. Compound **2-7** was synthesized *via* Stille coupling of compound **2-3** directly with the corresponding stannyl pyridines or stannyl lutidines (**2-6a-b**) by refluxing in toluene in the presence of the catalyst tetrakis(triphenyl phosphine)palladium. The reaction gave rise to numerous by-products and was difficult to purify. Though the later step of converting **2-7** to **2-8** was high yielding, this route was unattractive because of these purification problems. Compound **2-8** was synthesized alternatively by coupling **2-6a** to **2-4** using the same Stille conditions to give a clean product. The acetyl bipyridyl **2-9a** was synthesized by subjecting 2-cyanobipyridyl derivative **2-8** to reaction with methylmagnesium bromide solution.

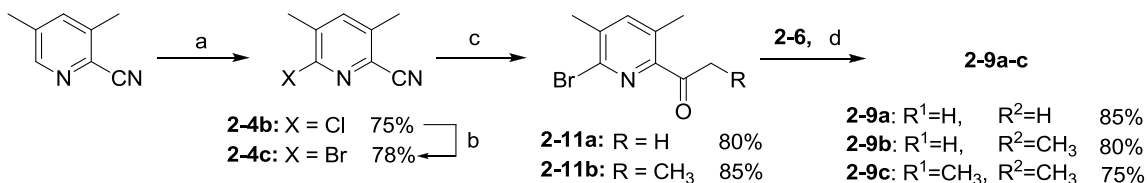
Table-2-2 Trials of the bromination of **2-9a** using different reaction conditions.

Brominating reagent	Solvents and conditions	NMR spectroscopy	% Yield
1 eq. of Bromine	CH ₃ COOH, 23 °C, 4 h	Decomposition	0
1 eq. of <i>N</i> -Bromosuccinimide	CH ₃ CN, 23 °C, 3 h	Decomposition	0
1 eq. of Bromine	THF, 23 °C, 12 h	Decomposition	0
1 eq. of Bromine	Ether, 23 °C, 36 h	2-9 + 2-10	35
1.2 eq. of Bromine and 2 eq. of 33% HBr in acetic acid	CH ₃ COOH, 23 °C, 12 h	No mixtures, only product	75

Bromination of **2-9a** was very difficult and does not go to completion giving product **2-10a** in only 35% yield. Of all the solvents employed, diethyl ether seems to be most advantageous for the reaction. The partial reaction necessitated the repetition of this

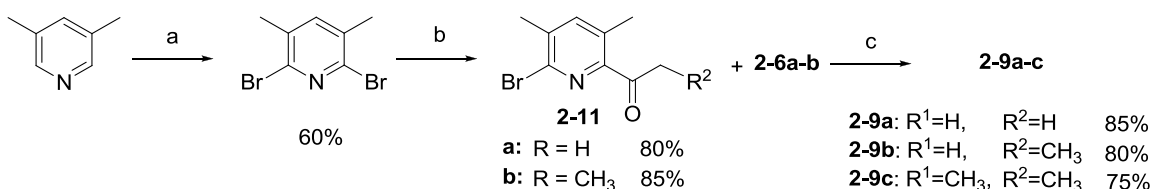
particular step several times to acquire enough of the product for further steps and so a different route to the bromination was sought. Treating the acetyl **2-9a** with 1.2 eq. bromine and 33% HBr in acetic acid solution greatly improved the yield from 35% to 75%. The remaining bottleneck of the synthetic scheme, namely monocyanation of **2-3** prompted us to alter our approach in order to improve yields and cut down on the repetition of steps.

The first alternate route to synthesis of the dipyriddy fragments is outlined in Scheme 2-4. The starting nitrile was obtained according to the procedure of Kokotos³⁹ in 82 % yield. It was then oxygenated using excess hydrogen peroxide in refluxing acetic acid for approximately 16 h, cooling it in ice, then basified and extracted the *N*-oxide product. Treating the *N*-oxide with phosphorus oxychloride produced **2-4b** with elimination of oxygen and was subjected to a halogen exchange reaction using 33% hydrogen bromide in acetic acid solution to produce **2-4c**. Thus one of the bottlenecks of the Scheme 2-2 was eliminated. Also it's noteworthy that none of the reactions up to this point needs to be purified by column chromatography as they are pure enough be carried forward to next step. They also can be recrystallized from ethanol if necessary.



Scheme 2-4 Synthesis of α -haloacylpyridyl fragments **2-11a-b** of the AADD arrays. Reaction conditions: a) (i) Excess H₂O₂/AcOH, reflux, 18 h, 80 %, (ii) Ex. POCl₃, reflux 0.5 h, 75%; (b) 2 eq. 33% HBr, in AcOH, reflux, 78%; (c) 1.25 eq. MeMgBr/EtMgBr, THF, 0 °C, reflux 18 h, 70-85%; (d) 3 % Pd(PPh₃)₄, toluene, reflux 18 h, 75-85%.

Bromide **2-4c** is then reacted with methyl or ethylmagnesium bromide solution producing **2-11a** or **2-11b** in 70-80 % yield. The further bromination is the same as described in the previous scheme. The advantage of the present scheme is the direct development of mononitrile heterocycle **2-4c** which avoids the three step synthesis of diiodolutidine and the messy conversion to **2-4**. This scheme contains fewer steps and the reactions are faster with no or little effort required for purification. Disadvantages are that the initial steps require fuming, toxic reagents involving highly exothermic workups. As an alternative approach, dibromination of 3,5-lutidine in a single step was carried out by modifying the original Dunn *et al.*⁴⁰ procedure using fuming sulphuric acid. Pugh *et al.*⁴¹ brought down the temperature to 160 °C from the originally reported 220 °C and the bromine addition was performed over 3-4 h at the same temperature. The reaction mixture was maintained over a period of 14-16 h at reflux. The reaction was quenched by pouring the reaction mixture into a large beaker (typically a 3 liter beaker for a scale of 10 grams product) filled half way with ice. The quenching process needs to be handled with full protection of eyes and general body parts as the contents are highly fuming and acidic. The direct bromination of 3,5-lutidines gave the desired 2,6-dibromo-3,5-lutidine in 60 % yield after recrystallization from ethanol as colourless needles.

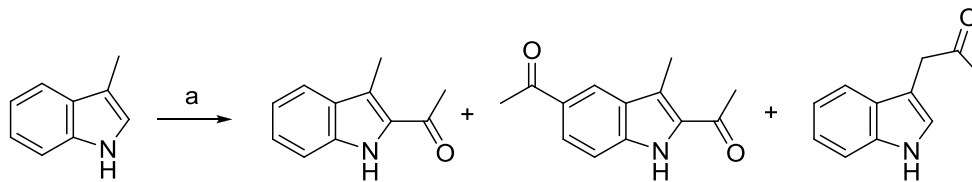


Scheme 2-5 Synthesis of **2-11a,b** from 2,6-dibromo-3,5-lutidine. Reaction condition: a) Fuming H₂SO₄ (20% free SO₃), 0 °C to 160 °C, 1 eq. Br₂, reflux 15 h, 60%; b) 1.2 eq. ^tBuLi / Et₂O, -78 °C, 0.5 h, 1 eq. *N,N*-dimethylacetamide or *N,N*-dimethyl propionamide, -78 °C, 1.5 h, 80-85%; c) 3 % Pd(PPh₃)₄, toluene, reflux 18-36 h, 75-85%.

The preparation of 2,6-dibromo-3,5-lutidine opened a route to selectively monolithiate the dibromolutidine at one of the *ortho* positions and add either an acetyl or propanoyl moiety thereby obviating the cyanation step that produces corresponding **2-11a** and **2-11b**. Monolithiation was not a possibility with the diiodolutidines as lithiating the iodides was very difficult. Though possible in this case, the yields of monolithiated lutidines from their iodide counterparts were very poor (5-12%), even when employing a stronger base such as ^tBuLi as the lithiating reagent.⁴²

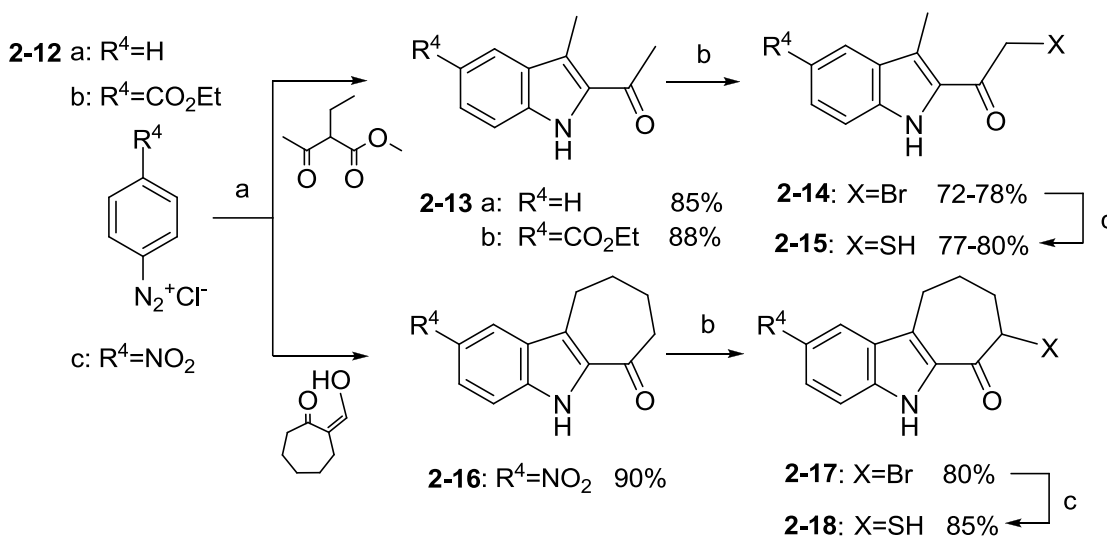
The increased overall yields of **2-11a,b** and elimination of two steps in the reaction scheme is noteworthy. This improvement also shortens the reaction times as the acylations are carried to completion within a period of two and half hours compared to the cyanation reactions that are followed by 16-18 hour Grignard reactions in the previous schemes. Upon synthesizing the coupled products **2-9a-c**, they were subjected to bromination and carried further in the synthesis.

The synthetic scheme for the donor component is relatively straight forward and involves ultimately inexpensive starting materials such as aniline and its 4-substituted derivatives, allowing simple access to 2-acyl-5-functionalized skatoles. Originally skatole, a foul malodorous compound (purchased from Alfa Aesar) was directly used as a starting material for the unsubstituted (5-H) indole derivatives. Acetylating or attaching a propionyl group via electrophilic substitution in the presence of a Lewis acid such as AlCl₃, yielded the desired ketone product along with other by-products (Scheme 2-6).⁴³ The crude material was subjected to tedious flash column chromatography that was required to isolate the pure compound.



Scheme 2-6 Direct acetylation of skatole using AlCl_3 as Lewis acid resulting in mixture of by-products. Reaction conditions: (a) CH_3COCl , AlCl_3 , 1,2-dichloroethane, 25°C , 6 h.

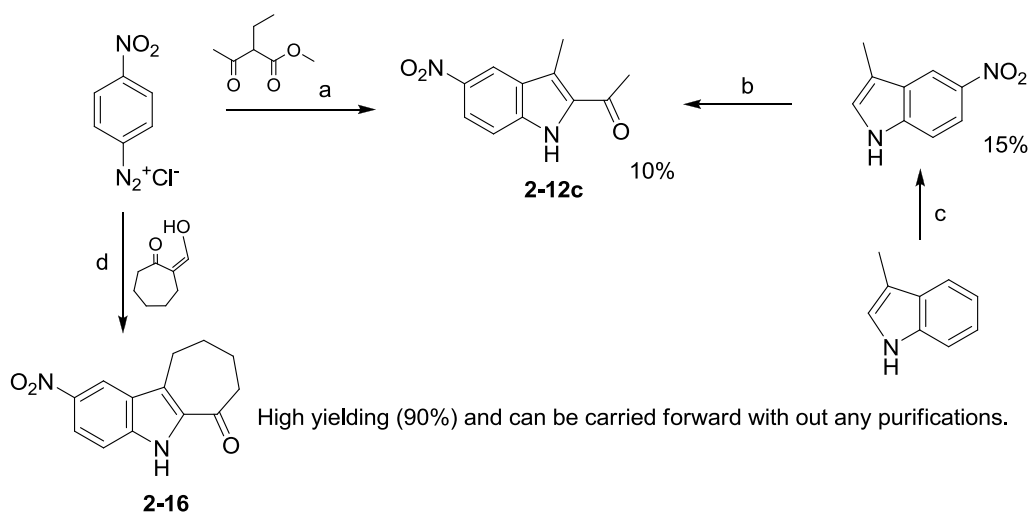
To avoid the nauseating odour of the skatole and purifications, a more economical route was adapted using a Japp-Klingemann/Fisher Indole cyclization to obtain the indoles starting from anilines (see experimental procedures).



Scheme 2-7 Synthesis of the indole containing fragments of AADD arrays. Reaction conditions: a) (i) KOH , EtOH , H_2O , 0°C to room temperature, (ii) HCOOH , reflux 2-20 h, 80-90%; b) 1 eq. PTAP (Phenyltrimethylammonium tribromide), dry THF , 40°C , 1-12 h, 72-80 %; (c) (i) 1 eq. KSAc , Dry DMF , 4-12 h, 90-95%; (ii) 1 eq. Cysteamine.HCl , 1.2 eq. NaHCO_3 , MeCN , 24 h, 77-85%.

Indole subunits were synthesized by reaction of aryl diazonium salts and β -ketoesters to form the corresponding hydrazones. Methyl 2-ethylacetoacetate (Scheme 2-7), a β -ketoester was used as starting material that leads to the formation of

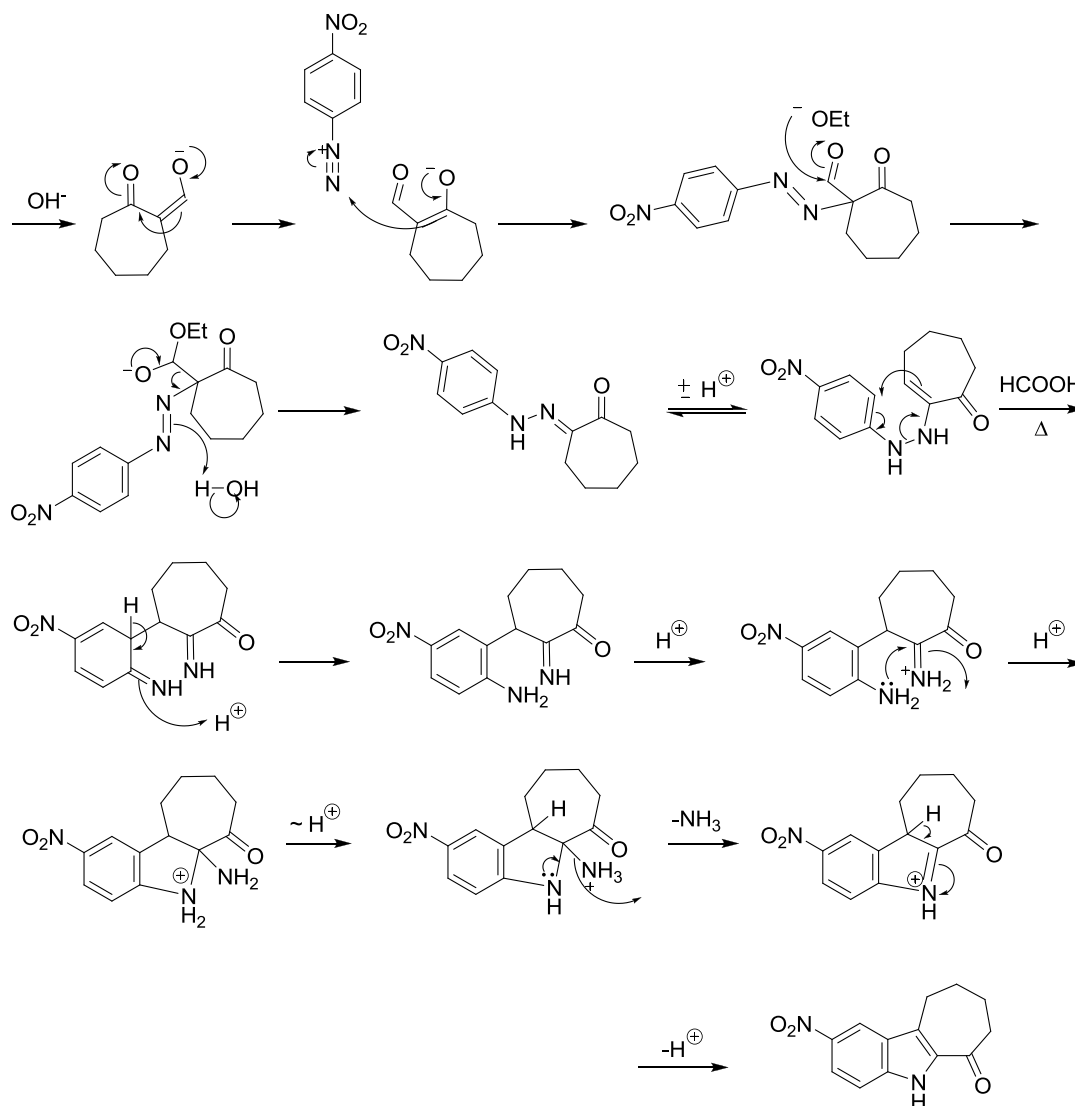
corresponding acetyl hydrazone *via* Japp-Klingemann reaction. The formation of hydrazones was aided by buffering the reaction mixture with sodium acetate and by stirring the buffered mixture vigorously. Ester hydrazones precipitated in non-buffered solutions and required excess stir times to get rid of unwanted salts. The hydrazone undergoes the Fisher Indole when refluxed in formic acid to give the desired acetyl skatole moieties with or without functional groups at the 5th position of indole.



Scheme 2-8 Synthetic schemes of nitro substituted donor units reflecting poor yields and synthetic difficulties obtaining acyclic nitro skatoles compared to the facile formation of cyclic nitroindole **2-16**. Reaction conditions: (a) KOH, EtOH, H₂O, 0 °C to r.t., HCOOH, reflux 20 h, 10%; (b) 1.2 eq AlCl₃, 1 eq. acetyl chloride, 10% and very difficult isolations; (c) H₂SO₄, HNO₃, 15%, difficult isolations; (d) KOH, EtOH, H₂O, 0 °C to r.t., HCOOH, reflux 20 h, 90%.

The 5-nitro-substituted indole was the most challenging to synthesize and isolate. Few trials were attempted to nitrate the skatole units through direct nitration using sulphuric acid and nitric acid at zero to subzero temperatures. The method works, but poor yields (10-15%) and tedious isolations led us to adopt a seven membered cyclic

nitro-skatole **2-16** as a better alternative due to the synthetic ease as well as the preorganization that it provide in the final AADD array contributing to the overall stability of duplex formation.



Scheme 2-9 Mechanistic details of the diazonium salt of nitroaniline undergoing Japp-Klingemann reaction followed by Fischer Indole cyclization in acidic medium with an overall yield of 90%.⁴⁴

Scheme 2-7 requires 2-(hydroxymethylidene)cycloheptanone as the starting material which was synthesized by vigorously stirring the cycloheptanone in the presence

of strong base such as sodium methoxide and ethyl formate for 18 h. The reaction mixture was quenched with 1 M HCl and the product was extracted using ethyl acetate. No purification was required and the product was carried forward as is.

The highly active 2-(hydroxymethylidene)cycloheptanone forms the corresponding hydrazone even with a very strong electron withdrawing nitro group on the aniline in contrary to the acyclic hydrazone formations. The cyclic derivative of the indole hydrazone undergoes cyclization in high purity and yields (Scheme 2-8). Japp-Klingemann/Fischer Indole cyclization proceeds through nucleophilic addition of enolate anion to diazonium salt, followed by hydrolysis of the intermediate to give hydrazone. Fisher Indole mechanism consists essentially of three separate stages: (a) hydrazone-enehydrazine equilibrium; (b) formation of a new C-C bond; (c) loss of ammonia and cyclization.

Bromination of the ketoindoles was achieved using phenyltrimethylammonium tribromide to give products in 75 %-80 % yield.⁴⁵ Various other reagents such as, bromine, *N*-bromosuccinimide, (aq.) HBr solution and pyridinium bromide were explored, unsuccessfully. Moderate to good yields, short reaction times and simple work up procedures are advantages of the reaction with phenyltrimethylammonium tribromide. It is necessary to make sure that the intermediate ketoindoles are completely dry as the bromination reaction is highly sensitive to stoichiometry and any solvent mass in the starting material leads to the formation of dibromide products. The dibromides have very similar *R_F* values with their singly brominated analogues thus making the purification process difficult using column chromatography. Washing the mixtures with an excess of cold methanol dissolves these dibromides to a considerable extent.

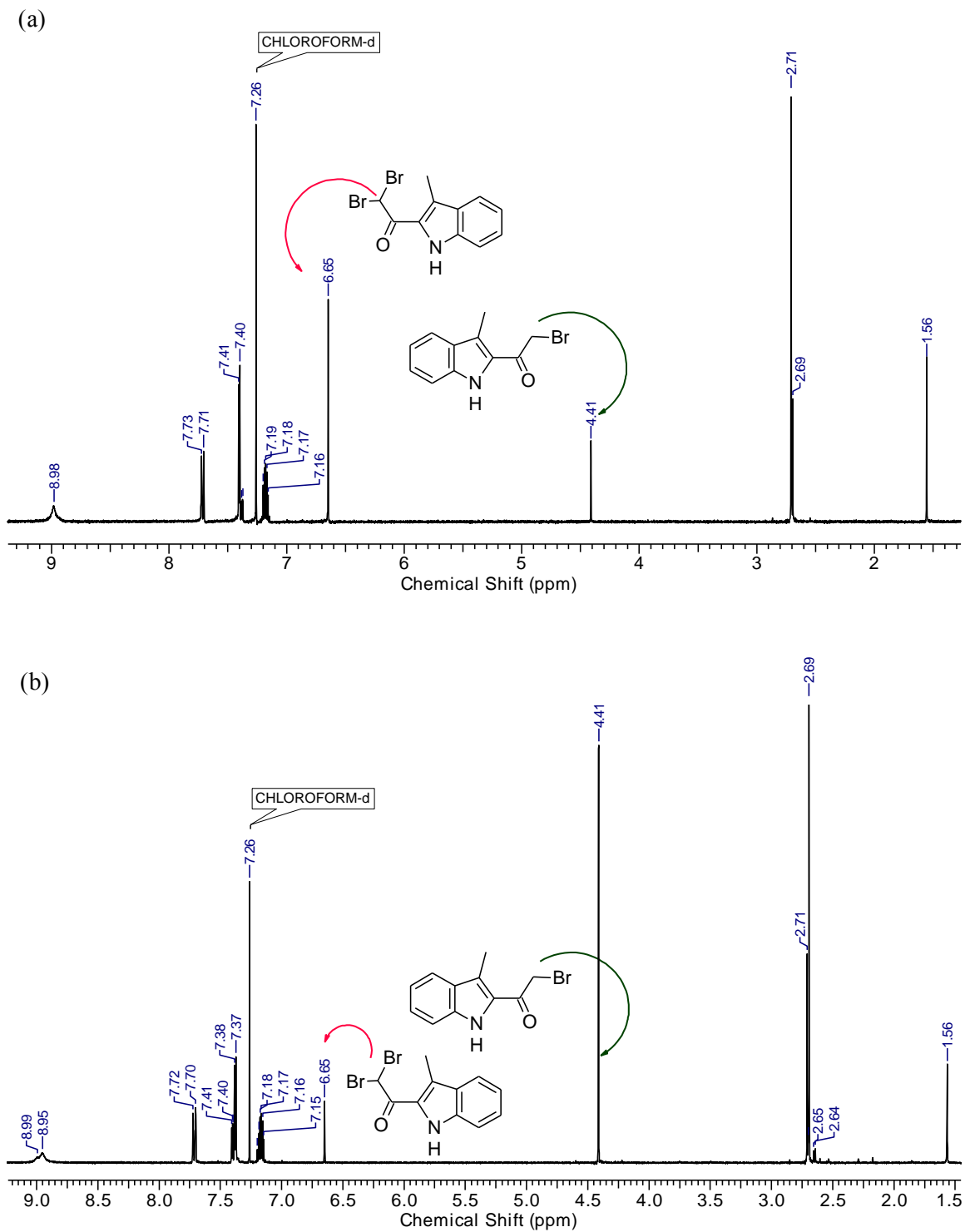


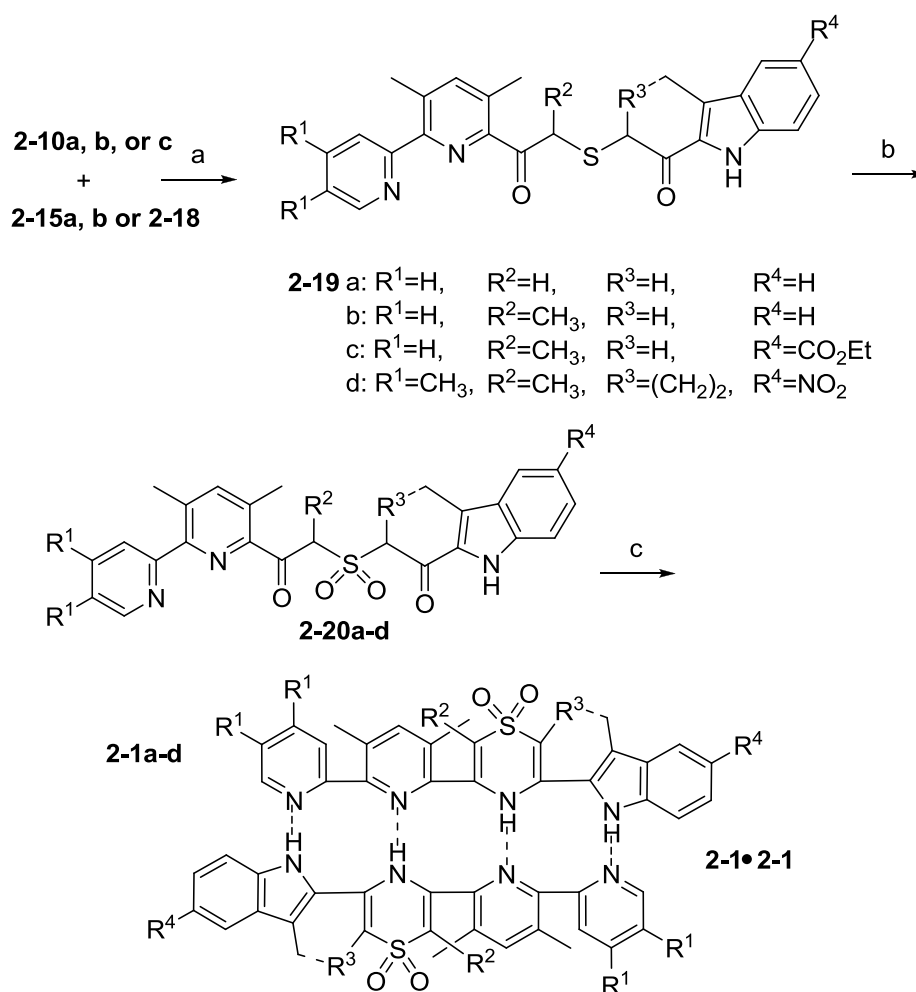
Figure 2-10 ^1H NMR of the mixture of mono and dibrominated acetyl skatole before (a) and after (b) washing with ice cold methanol shows considerable reduction of the dibromide contaminant compared to the mono brominated product.

When such a mixture of mono and dibromides is used to synthesize thioacetates, only mono thioacetates are formed as dithioacetate formation requires attack of the nucleophile at the more sterically congested dibromide. Hence purification does not necessarily need to be performed at the bromination step to isolate reasonable yields of the further thioacetate intermediates. Whether purified or not the bromides are then thioacetylated using potassium thioacetate and hydrolyzed to give the corresponding thiols **2-15a-b** and **2-18**. Various solvents were explored for both these steps. Anhydrous ethanol or dry DMF offer the best yields in the thioacetylations and acetonitrile was found to be the best solvent for the hydrolysis reactions as there are few or no side products formed.

The thioacetate of **2-17** was synthesized in similar manner by using potassium thioacetate in anhydrous DMF and the crude mixture hydrolyzed in the presence of cysteaminehydrochloride. The resulting solution was acidified with 10 % HCl if no precipitation occurred by the addition of water to the reaction. Acetonitrile as solvent medium produced best results with no side products and with no requirement of further purification.

Thiols **2-15** and **2-18** are stable solids and can be shelved for months for later use. Any residue of solvent DMF, from the thioacetate step makes precipitation of the thiols difficult and in these cases large amounts of water are added and the mixtures are vigorously stirred for 12 h to induce precipitate formation. In addition, as a measure of precaution, the aqueous layers are further extracted with dichloromethane, to give reasonably high yields (no other purifications were carried out).

The synthesis of thioethers **2-19** was performed in anhydrous DCM by cooling to zero degrees followed by the slow addition of a solution of bromide **2-10** to a solution of thiol **2-15** and, after 30 minutes, addition of base. The sequence of addition is important for the reaction as addition of base to any one of the components alone did not yield the desired product but gave unidentified by-products even under a nitrogen atmosphere. The formation of **2-19** is also sensitive to the strength of the base used.



Scheme 2-10 Final steps in the synthetic route to AADD arrays **2-1a-d**. Reaction conditions: a) 1 eq. 2,6-Lutidine, MeCN, 2-14 h, 80-85%; b) 4eq. Urea hydrogen peroxide, 3 eq. TFAA, MeCN, 2 h, to 12 h, 80-95%; c) 6-10 eq. NH₄OAc, AcOH, reflux 18-36 h, 70-90%.

Triethylamine and potassium carbonate are the two other typical choices for the base in these reactions, but they proved to be incompatible here. A milder base (2,6-lutidine) was used which was neutralized at the end of reaction using citric acid. One equivalent of the base is required but addition of an extra equivalent does not have any unwanted side reactions and moreover, the reaction is faster with an excess of lutidine. Faster reaction times are observed in DCM and slower reaction times with acetonitrile but cleaner products are obtained with the latter solvent. In either solvent, letting the reaction run a longer time than required to finish has a detrimental effect on yields and purity. Thioethers **2-19b-c** were synthesized in similar manner as described for **2-19a**. **2-19b-d** were all isolated as mixtures of either enantiomers or diastereomers.

Thioethers **2-19** were oxidized using UHP/TFAA mixtures in the ratio 4/3 in acetonitrile solution. UHP has very poor solubility in acetonitrile but upon addition of TFAA becomes soluble. The order of addition to generate the reagent is important, particularly in gram scale or larger reactions. After transferring the UHP to the acetonitrile solution, TFAA is added drop wise to it while stirring. Once the UHP dissolves completely, this reagent solution is added drop wise to the reaction mixture at zero degrees or at room temperature based on the starting material quantity. The thioethers **2-19** gave crude enantiomeric or diastereomeric sulfone mixtures which were isolated using flash column chromatography. These stereoisomeric mixtures were carried forward to the next step of synthesis without resolving them as the chiral center(s) are lost in the cyclization step. The sulfones **2-20a-d** were cyclized using ammonium acetate in acidic medium (AcOH) under reflux to produce the final AADD arrays **2-1**.

2.5 X-ray Analysis of AADD Arrays

Table 2-3 Crystallographic parameters for **2-1a•2-1a** and **2-1b•2-1b** crystals.

Crystal Parameters	2-1a•2-1a	2-1b•2-1b
chemical formula	C ₂₅ H ₂₂ N ₄ O ₂ S	C ₂₇ H ₂₅ Cl ₃ N ₄ O ₂ S
formula weight (g·mol ⁻¹)	442.53	575.92
crystal system	monoclinic	monoclinic
space group	<i>P</i> 2 ₁ / <i>c</i>	Cc
<i>a</i> (Å)	10.515(3)	22.305(5)
<i>b</i> (Å)	20.231(5)	11.774(2)
<i>c</i> (Å)	20.630(6)	21.760(4)
β (°)	97.150(3)	106.73(3)
<i>V</i> (Å ³)	4355(2)	5472.8(19)
<i>T</i> (K)	173(2)	150(2)
<i>Z</i>	8	8
λ (Mo K α) (Å)	0.71073	0.71073
<i>D</i> _{calc} (g·cm ⁻³)	1.350	1.398
μ (mm ⁻¹)	0.179	0.444
<i>F</i> (000)	1856.0	2384.0
reflection collected	37669	13865
unique reflections	7421	8667
absorption correction	multi-scan	multi-scan
refinement on	<i>F</i> ²	<i>F</i> ²
<i>R</i> (<i>F</i> _o) (<i>I</i> > 2 σ (<i>I</i>))	0.0983	0.1307
<i>R</i> _w (<i>F</i> _o ²) (<i>I</i> > 2 σ (<i>I</i>))	0.2371	0.3143
<i>R</i> (<i>F</i> _o) (all data)	0.1073	0.1619
<i>R</i> _w (<i>F</i> _o ²) (all data)	0.2451	0.3410
GOF on <i>F</i> ²	1.397	1.368

Table 2-4 Crystallographic data for **2-1c•2-1c** and **2-1d•2-1d**.

Crystal Parameters	2-1c•2-1c	2-1d•2-1d
chemical formula	C ₆₁ H ₆₀ Cl ₃ N ₉ O ₈ S ₂	C ₃₂ H ₃₁ Cl ₆ N ₅ O ₄ S
formula weight (g·mol ⁻¹)	1217.65	794.38
crystal system	monoclinic	monoclinic
space group	<i>P2₁/n</i>	<i>C2/c</i>
<i>a</i> (Å)	12.8276(8)	26.009(5)
<i>b</i> (Å)	20.8609(13)	12.919(3)
<i>c</i> (Å)	23.0123(13)	23.029(5)
β (°)	106.135(2)	113.26(3)
<i>V</i> (Å ³)	5915.4(6)	7109(2)
<i>T</i> (K)	150(2)	150(2)
<i>Z</i>	4	8
λ (Mo K α) (Å)	0.71073	0.71073
<i>D</i> _{calc} (g·cm ⁻³)	1.367	1.485
μ (mm ⁻¹)	0.289	0.587
<i>F</i> (000)	2544.0	3264.0
reflection collected	138863	12073
unique reflections	12569	6287
absorption correction	multi-scan	multi-scan
refinement on	<i>F</i> ²	<i>F</i> ²
<i>R</i> (<i>F</i> _o) (<i>I</i> > 2 σ (<i>I</i>))	0.0644	0.0617
<i>Rw</i> (<i>F</i> _o ²) (<i>I</i> > 2 σ (<i>I</i>))	0.1442	0.1774
<i>R</i> (<i>F</i> _o) (all data)	0.1318	0.0872
<i>Rw</i> (<i>F</i> _o ²) (all data)	0.1781	0.2071
GOF on <i>F</i> ²	1.023	1.079

Upon successful completion of the synthesis of AADD arrays **2-1a-d** we attempted to crystallize them to observe their behaviour in the solid state. Single crystals suitable for X-ray diffraction were grown for all four of the AADD arrays synthesized. Of the four sets of crystals analysed, satisfactory solutions were obtained for those containing **2-1a**, **2-1c** and **2-1d**. The crystals of **2-1b** were tiny and poorly diffracted resulting in a poor solution that has numerous issues such as twinning and solvent disorder. Nevertheless, the solution is of adequate quality to illustrate a complex topology for this array in the solid state that is very similar to that observed for **2-1c** and **2-1d**. The solid state structures are instructive and shed light on the solution studies that follow.

All four double helical AADD arrays **2-1a-d** were crystallized in a monoclinic crystal system but in four different space groups $P2_1/c$, Cc , $P2_1/n$ and $C2/c$ respectively. Crystals of **2-1a** are merohedral twinned and so further refinement did not lead to a better final R value. The crystallization of **2-1c** was achieved at approximately $-20\text{ }^\circ\text{C}$. The crystals thus grown are stable to air and can be brought to normal temperatures without desolvation or dissolution. With the exception of the uncomplexed **2-1a** crystals (yellow blocks) all the other crystals were colourless.

Crystal **2-1a** has two molecules per asymmetric unit which form zigzag one-dimensional tapes in the lattice through bifurcated hydrogen bonds between the sulfone oxygen atoms of one array and the indole proton of an adjacent molecule ($\text{O1}\cdots\text{N8} = 2.92\text{ \AA}$, $\text{O1}\cdots\text{H8} = 2.12\text{ \AA}$, $\text{O1}\cdots\text{H8-N8} = 158^\circ$, $\text{O2}\cdots\text{N8} = 3.47\text{ \AA}$, $\text{O2}\cdots\text{H8} = 2.80\text{ \AA}$, $\text{O2}\cdots\text{H8-N8} = 139^\circ$; $\text{O3}\cdots\text{N4} = 3.16\text{ \AA}$, $\text{O3}\cdots\text{H4A} = 2.43\text{ \AA}$, $\text{O3}\cdots\text{H4A-N4} = 139^\circ$, $\text{O4}\cdots\text{N4} = 3.18\text{ \AA}$, $\text{O4}\cdots\text{H4A} = 2.46\text{ \AA}$, $\text{O4}\cdots\text{H4A-N4} = 139^\circ$). Aside from this intermolecular interaction,

the two molecules have very similar conformations and do not exhibit the double helical dimer character that one might be expected. Instead, the two molecules both display an electrostatically favourable intramolecular contact between the N-H proton of their thiazine donor and the nitrogen atom of their lutidine acceptor ($N2\cdots H3A = 2.16 \text{ \AA}$, $N2\cdots H3A-N3 = 112^\circ$; $N6\cdots H7 = 2.23 \text{ \AA}$, $N6\cdots H7-N7 = 107^\circ$) resulting in interplanar angles between these two heterocycles of only 22 and 24° ($N2-C12-C13-N3$ and $N7-C38-C37-N6$ respectively).

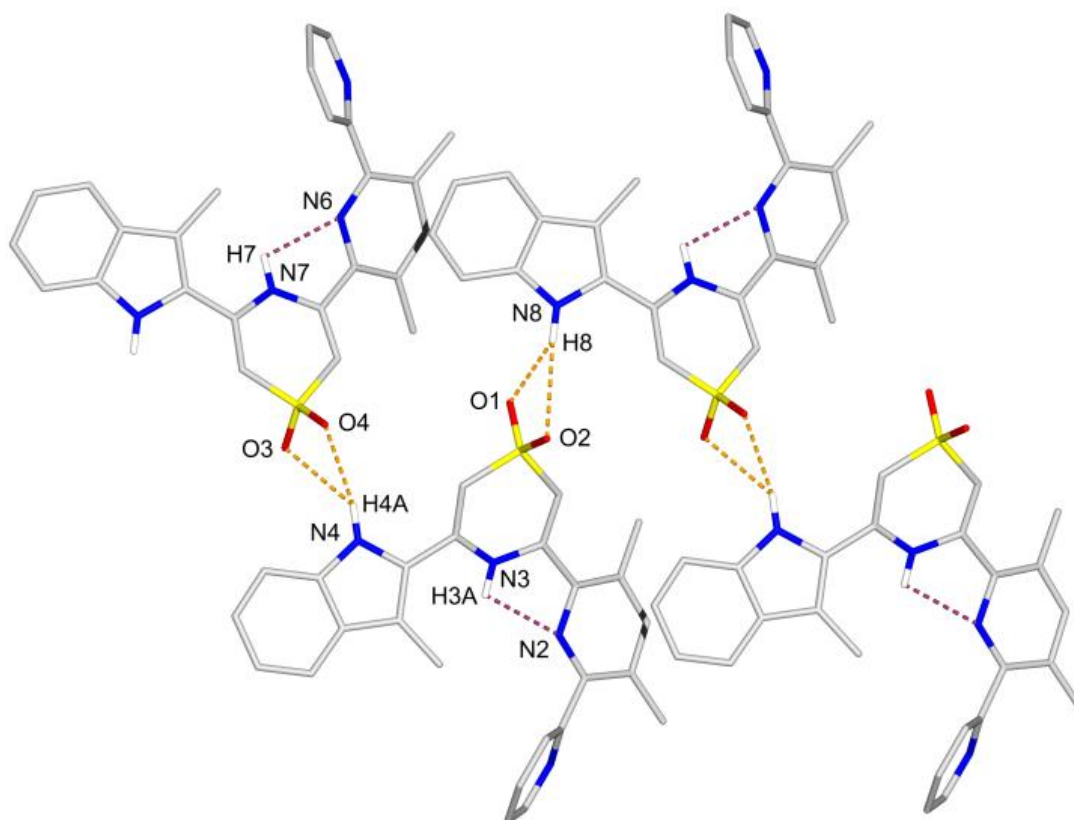


Figure 2-11 Stick representation of X-ray crystal structure of array **2-1a** with intermolecular (dashed orange lines) as well as intramolecular (dashed purple lines) hydrogen bonds” indicated. All C-H hydrogen atoms have been removed for clarity.

The formation of this intramolecular hydrogen bonding can be prevented by introducing a methyl group on the thiazine dioxide between the acceptor unit and donor

unit as demonstrated below in the remaining structure and solution state studies. The methyl group may not only be expected to enforce a dihedral twist between the planes of the lutidine and thiazine dioxide rings, but also to prevent potential intermolecular interactions between the sulfone oxygens and the NH donors of other arrays.

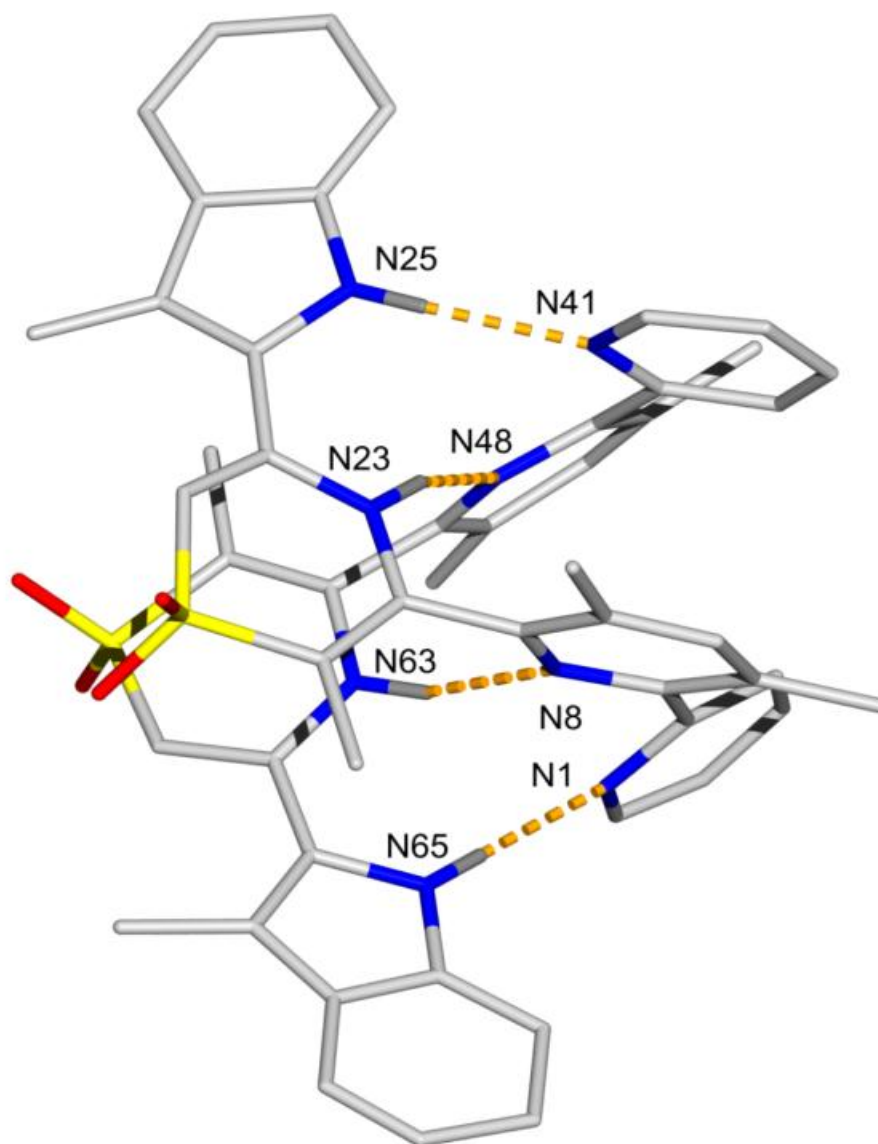


Figure 2-12 Stick representation of the X-ray crystal structure of array **2-1b** with intermolecular (dashed orange lines) hydrogen bonds indicated. All C-H hydrogen atoms have been removed for clarity.

The addition of a methyl group (R^2) to the other three derivatives **2-1b-d** proved very helpful in complexation. In fact, none of these three structures exhibit any intramolecular hydrogen bonds analogous to **2-1a**. Instead, all three undergo the expected double helical dimer arrangement in the solid state.

In this case of **2-1b**, the array crystallizes in space group Cc with a single molecule per asymmetric unit. The molecules are arranged to form four identical double-helical dimeric complexes, each exhibiting C_2 symmetry, in the unit cell (Figure 2-12). The two molecules comprising each dimer are, again, positioned to allow four primary hydrogen bonds ($N1 \cdots N65 = 2.84 \text{ \AA}$, $H1 \cdots N65 = 1.96 \text{ \AA}$, $N1-H1 \cdots N65 = 176^\circ$; $N8 \cdots N63 = 2.93 \text{ \AA}$, $H8 \cdots N63 = 2.14 \text{ \AA}$, $N8-H8 \cdots N63 = 148^\circ$; $N23 \cdots N48 = 2.96 \text{ \AA}$, $H23 \cdots N48 = 2.14 \text{ \AA}$, $N23-H23 \cdots N48 = 153^\circ$; $N25 \cdots N41 = 2.84 \text{ \AA}$, $H25 \cdots N41 = 2.04 \text{ \AA}$, $N25-H25 \cdots N41 = 168^\circ$). Adjacent heterocyclic rings in each molecule are twisted out of plane from one another in order to accommodate the four hydrogen bonds between the two strands ($N1-C6-C7-N8 = 38^\circ$; $N8-C9-C15-N23 = 60^\circ$; $N23-C22-C24-N25 = 28^\circ$; $N41-C46-C47-N48 = 42^\circ$; $N48-C49-C55-N63 = 67^\circ$; $N63-C62-C64-N65 = 24^\circ$). It is notable that the dihedral angle between the thiazine and lutidine rings in each strand is significantly larger (60 and 67°) than those between the other rings ($\leq 42^\circ$). Short secondary hydrogen bond contacts also support the entwined hydrogen bonded geometry ($N1 \cdots N63 = 3.2 \text{ \AA}$, $H1 \cdots N63 = 2.48 \text{ \AA}$, $N1-H1 \cdots N63 = 140^\circ$; $N8 \cdots N65 = 3.10 \text{ \AA}$, $H8 \cdots N65 = 2.72 \text{ \AA}$, $N8-H8 \cdots N65 = 107^\circ$; $N23 \cdots N41 = 3.12 \text{ \AA}$, $H23 \cdots N41 = 2.60 \text{ \AA}$, $N23-H23 \cdots N41 = 135^\circ$; $N25 \cdots N48 = 3.29 \text{ \AA}$, $H25 \cdots N48 = 2.92 \text{ \AA}$, $N25-H25 \cdots N48 = 107^\circ$).

Array **2-1c** crystallized in space group $P2_1/c$ including two molecules per asymmetric unit. Inspection of the lattice reveals a repeating dimer motif in which the

two unique molecules intertwine to form a hydrogen bonded double helix with approximate C_2 symmetry (Figure 2-13).

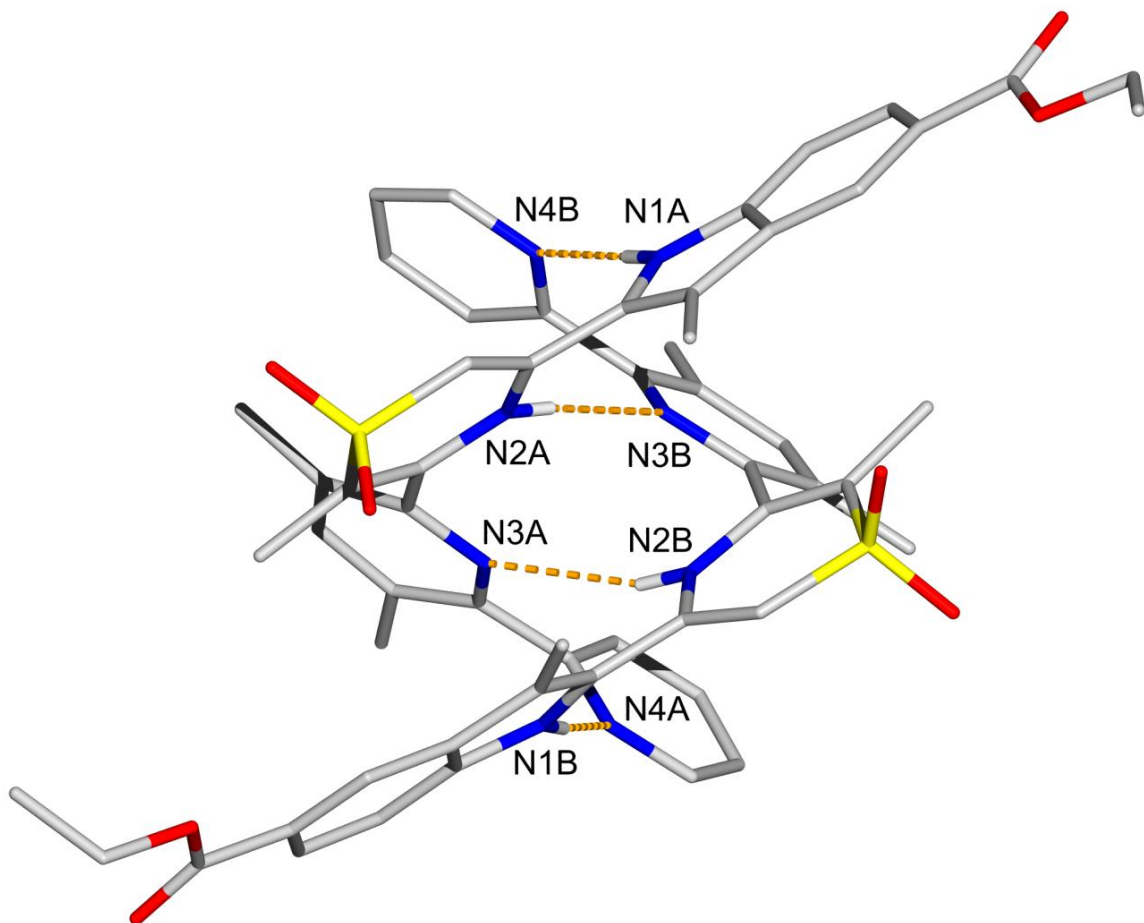


Figure 2-13 Stick representation of the X-ray crystal structure of dimer **2-1c·2-1c** with intermolecular hydrogen bonds indicated (dashed orange lines). All C-H hydrogen atoms have been removed for clarity.

The two molecules assemble in an antiparallel fashion that arranges their hydrogen bond donors and acceptors in register to provide four primary hydrogen bonds between them ($N1B \cdots N4A = 3.00 \text{ \AA}$, $H1B \cdots N4A = 2.10 \text{ \AA}$, $N1B-H1B \cdots N4A = 178^\circ$; $N2B \cdots N3A = 3.17 \text{ \AA}$, $H2B \cdots N3A = 2.35 \text{ \AA}$, $N2B-H2B \cdots N3A = 165^\circ$; $N2A \cdots N3B = 3.11 \text{ \AA}$, $H2A \cdots N3B = 2.24 \text{ \AA}$, $N2A-H2A \cdots N3B = 175^\circ$; $N1A \cdots N4B = 2.92 \text{ \AA}$, $H1A \cdots N4B =$

2.06 Å, N1A-H1A \cdots N4B = 172°). Adjacent heterocyclic rings in each molecule are twisted out of plane from one another in order to accommodate the four hydrogen bonds between the two strands (N1B-C12B-C13B-N2B = 33°; N2B-C17B-C18B-N3B = 60°; N3B-C24B-C25B-N4B = 40°; N1A-C12A-C13A-N2A = 37°; N2A-C17A-C18A-N3A = 56°; N3A-C24A-C25A-N4A = 45°). It is again notable that the dihedral angle between the thiazine and lutidine rings in each strand is significantly larger (60 and 56°) than those between the other rings (< 46°). Whether this is a result of the steric repulsion provided by the two methyl substituents on the adjacent thiazine and lutidine rings, repulsive electrostatics between the two opposing thiazine donors (H2A \cdots H2B = 2.57 Å) and lutidine acceptors (N3A \cdots N3B = 3.11 Å), or both is impossible to distinguish based on the X-ray data alone. Short secondary hydrogen bond contacts also support the entwined hydrogen bonded geometry (N1B \cdots N3A = 3.08 Å, H1B \cdots N3A = 2.68 Å, N1B-H1B \cdots N3A = 107°; N2B \cdots N4A = 3.32 Å, H2B \cdots N4A = 2.75 Å, N2B-H2B \cdots N4A = 127°; N2A \cdots N4B = 3.20 Å, H2A \cdots N4B = 2.68 Å, N2A-H2A \cdots N4B = 119°; N1A \cdots N3B = 3.12 Å, H1A \cdots N3B = 2.71 Å, N1A-H1A \cdots N3B = 111°).⁴⁶

The solid state structure of **2-1d** is similar to that of **2-1c**. In this case, the array crystallizes in space group *C2/c* with a single molecule per asymmetric unit. The molecules are arranged to form four identical double-helical dimeric complexes, each exhibiting *C*₂ symmetry, in the unit cell (Figure 2-14). The two molecules comprising each dimer are, again, positioned to allow four primary hydrogen bonds (N1 \cdots N4 = 2.88 Å, N1 \cdots H4 = 2.18 Å, N1 \cdots H4-N4 = 172°; N2 \cdots N3 = 2.97 Å, N2 \cdots H3 = 2.15 Å, N2 \cdots H3-N3 = 175°) and four secondary hydrogen bond contacts (N1 \cdots N3 = 3.21 Å, N1 \cdots H3 = 2.75 Å, N1 \cdots H3-N3 = 117°; (N2 \cdots N4 = 3.09 Å, N2 \cdots H4 = 2.69 Å, N2 \cdots H4-N4 = 118°) to

stabilize the complex geometry giving rise to non-coplanar orientations of the adjacent heterocyclic rings ($N1-C7-C8-N2 = 42^\circ$; $N2-C14-C15-N3 = 67^\circ$; $N3-C18-C24-N4 = 23^\circ$) in each strand.

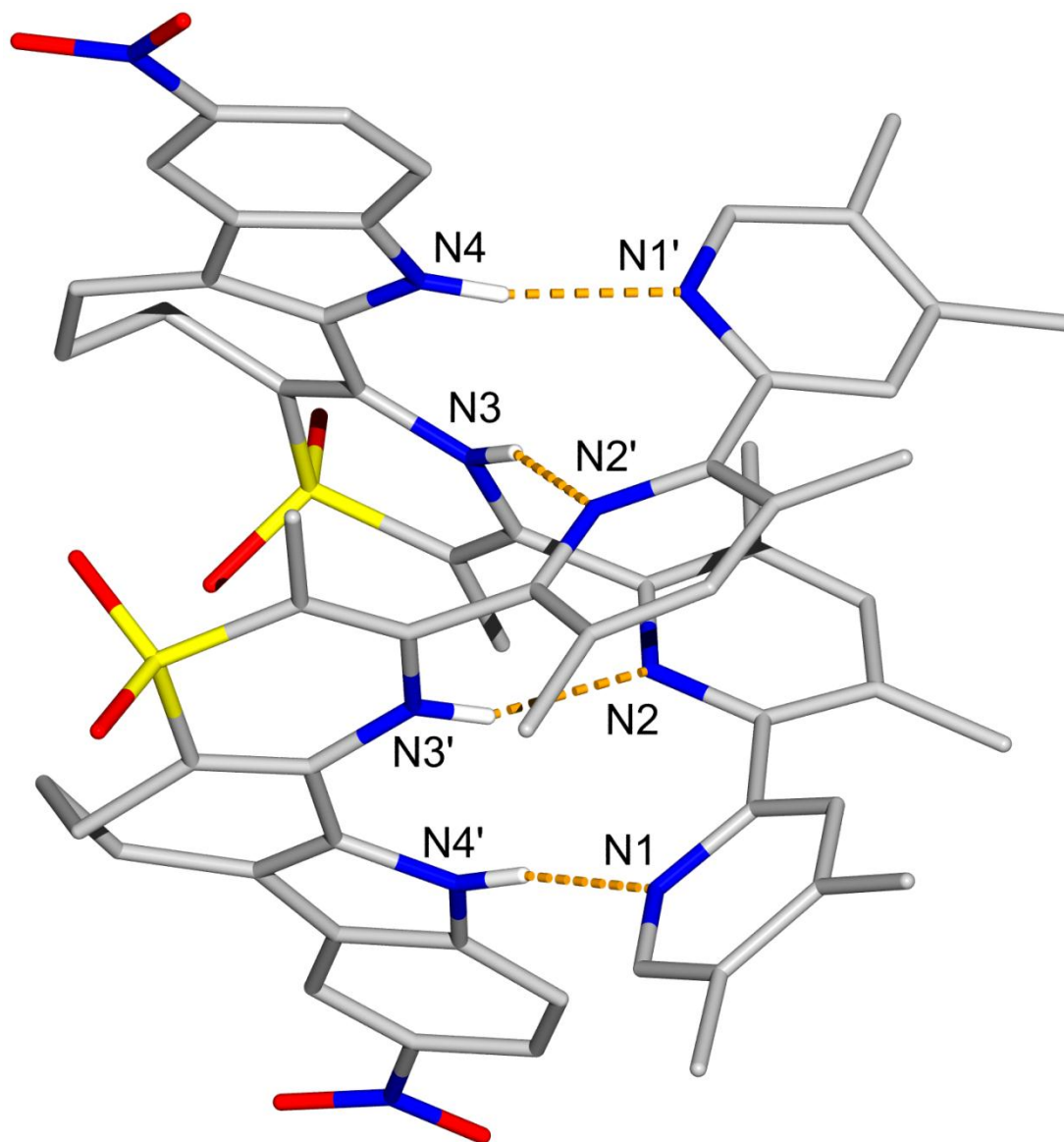


Figure 2-14 Stick representation of the X-ray crystal structure of dimer **2-1d·2-1d** with intermolecular hydrogen bonds indicated (dashed orange lines). All C-H hydrogen atoms have been removed for clarity.

The major contrast between these latter two structures is a compression of the interplanar angles between the indole and thiazine rings (23° versus 33 and 37°) and a concomitant expansion of the interplanar angle between the thiazine and lutidine rings (67° versus 56 and 60°) of **2-1d** versus **2-1c**. Likely, this is a result of the trimethylene tether present in **2-1d** that greatly restricts the conformational freedom of the two donor heterocycles to a narrow range of interplanar angles. The table below summarizes the bond angles and lengths of the three crystal structures that undergo expected double-helical formation using hydrogen bonding in solid state.

Table 2-5 Summary of bond distances and angles of **2-1b**•**2-1b**, **2-1c**•**2-1c** and **2-1d**•**2-1d** from their X-ray crystal structure data.

2-1b	Bonds	Distances	Distances	Distances	Angles ($^\circ$)
		<u>N-H</u>···<u>N</u> (Å)	N-H (Å)	<u>N-H</u>···<u>N</u> (Å)	
In-Py	N1···N65	2.8413 (99)	0.8793 (69)	1.9638 (72)	175.56
Th-Lu	N8···N63	2.9306 (98)	0.8804 (60)	2.1471 (74)	147.91
Lu-Th	N23···N48	2.9546 (99)	0.8803 (69)	2.1419 (72)	153.25
Py-In	N25···N41	2.8413 (98)	0.8802 (66)	2.0364 (86)	168.31
2° Hydrogen Bonding In-Th	N1···N63	3.2066 (94)		2.4818 (76)	140.01
	N8···N65	3.0977 (99)		2.7215 (89)	107.21
	N8···N48	3.0196 (80)		N/A	N/A
	N23···N63	3.2580 (86)		3.0133 (11)	88.98
	N23···N41	3.2855 (99)		2.5998 (84)	135.42
	N25···N48	3.2850 (98)		2.9240 (72)	106.56

Interplanar angles (strand-A)		(°)	Interplanar angles (strand-B)		(°)
Py-Lu	N1-C6-C7-N8	38.20	PY-LU	N41-C46-C47-N48	42.14
Lu-Th	N8-C9-C15-N23	60.02	LU-TH	N48-C49-C55-N63	67.11
Th-In	N23-C22-C24-N25	28.34	TH-IN	N63-C62-C64-N65	23.65

2-1c	Bonds	Distances	Distances	Distances	Angles (°)
		<u>N-H</u>···<u>N</u>(Å)	<u>N-H</u>(Å)	<u>N-H</u>···<u>N</u>(Å)	
In-Py	N1B···N4A	3.0036 (44)	0.9125 (417)	2.0914 (417)	178.21
Th-Lu	N2B···N3A	3.1656 (40)	0.8314 (413)	2.3562 (407)	164.67
Lu-Th	N2A···N3B	3.1123 (40)	0.8806 (29)	2.2346 (27)	174.49
Py-In 2° Hydrogen Bonding In-Th	N1A···N4B	2.9172 (41)	0.8636 (401)	2.0594 (407)	172.05
	N1B···N3A	3.0824 (38)		2.6784 (349)	107.79
	N2B···N4A	3.3166 (45)		2.7462 (385)	127.30
	N2B···N2A	3.2619 (33)		2.9894 (339)	101.75
	N3A···N3B	3.1134 (42)		N/A	N/A
	N2A···N4B	3.2006 (40)		2.8806 (24)	107.99
	N1A···N3B	3.1222 (39)		2.6801 (27)	118.96

Interplanar angles (bent)		(°)	Interplanar angles (straight)		(°)
In-Th	N1B-C12B-C13B-N2B	33.13	IN-TH	N1A-C12A-C13A-N2A	36.68
Th-Lu	N2B-C17B-C18B-N3B	60.02	TH-LU	N2A-C17A-C18A-N3A	55.76
Lu-Py	N3B-C24B-C25B-N4B	40.07	LU-PY	N3A-C24A-C25A-N4A	45.88

2-1d	Bonds	Distances	Distances	Distances	Angles (°)
		<u>N-H</u>···<u>N</u> (Å)	N-H (Å)	<u>N-H</u>···<u>N</u> (Å)	
In-Lu	N4···N1	2.8877 (48)	0.7122 (399)	2.1803 (409)	172.37
Th-Lu	N3···N2	2.9698 (45)	0.8206 (426)	2.1518 (430)	174.69
2° Hydrogen	N3···N1	3.2066 (37)		2.7465 (358)	117.28
Bonding In-Th					
	N4···N2	3.0867 (43)		2.6891 (363)	117.85
	N2···N2	2.9594 (38)		N/A	N/A
	N3···N3	3.2549 (50)		2.9296 (403)	106.16
<hr/>					
Interplanar angles		(°)			
Lu-Lu	N1-C7-C8-N2	41.88			
Th-Lu	N2-C14-C15-N3	67.41			
Th-In	N3-C18-C24-N4	23.1			

Where Py = pyridine; Lu = lutidine; Th = Thiazine dioxide; In = indole derivatives on AADD arrays.

As a final comparison between the complexes, it is interesting to note that the average of the interplanar angles amongst the set of **2-1b•2-1b**, **2-1c•2-1c** and **2-1d•2-1d** crystals was calculated to be 43°, 46° and 44° respectively which might suggest that the angle 45° is the optimal interplanar value for double-helical formation.

2.6 Solution Characterization of the Dimerization of 2-1a-d

One of the primary goals in designing and synthesizing the complementary complexes is to study the stabilities of the duplexes formed. There are a number of

factors that must be considered when measuring complex stabilities such as the appropriate method of analysis, solubilities of the arrays, the presence of tautomers, temperature and other environmental effects. Some of these factors are discussed in the following sections.

2.6.1 Analysis of Complex Stability

General methods of analyzing complex stability use titration or dilution and observe changes in NMR, UV-Vis, fluorescence spectra or changes in enthalpy (ITC). Modern NMR instruments allow titrations to be run at dilutions on the order of $1 \times 10^{-4} \text{ M}$ allowing the measurement of K_a values up to 10^6 M^{-1} . In practicality, K_a values up to $1 \times 10^5 \text{ M}^{-1}$ can be determined with accuracy⁴⁷ and any value that is above this limit is not generally reliable. Typically for data analysis of NMR titrations, the chemical shifts of the participating protons are plotted against the concentrations of the host and guest in solution and fit to a 1:1 binding model using data analysis software. Another consideration is whether the system of interest is in the fast or slow exchange region under the conditions used.

Calorimetry is another powerful method used to determine complex stability. It relies on measuring enthalpy (H) changes on the addition of guest to a host in a specially designed apparatus measuring the heat (Q) formed or absorbed (usually an isothermal calorimeter-ITC, Figure 2-15). ITC has a wider range of detection and can directly measure binding constants in the range of 10^2 to 10^9 M^{-1} .⁴⁸ Larger binding constants of 10^9 to 10^{12} M^{-1} can be measured using competitive binding techniques. The most powerful feature of calorimetric titrations is that not only do they yield the free energy

(ΔG) changes via the association constant according to eqn (1) but also the enthalpy and thus the entropy (ΔS) change can also be obtained from eqn (2). It also provides information regarding the stoichiometry of the complexation.

$$\Delta G = - RT \ln(K) \quad (1)$$

$$\Delta G = \Delta H - T\Delta S \quad (2)$$

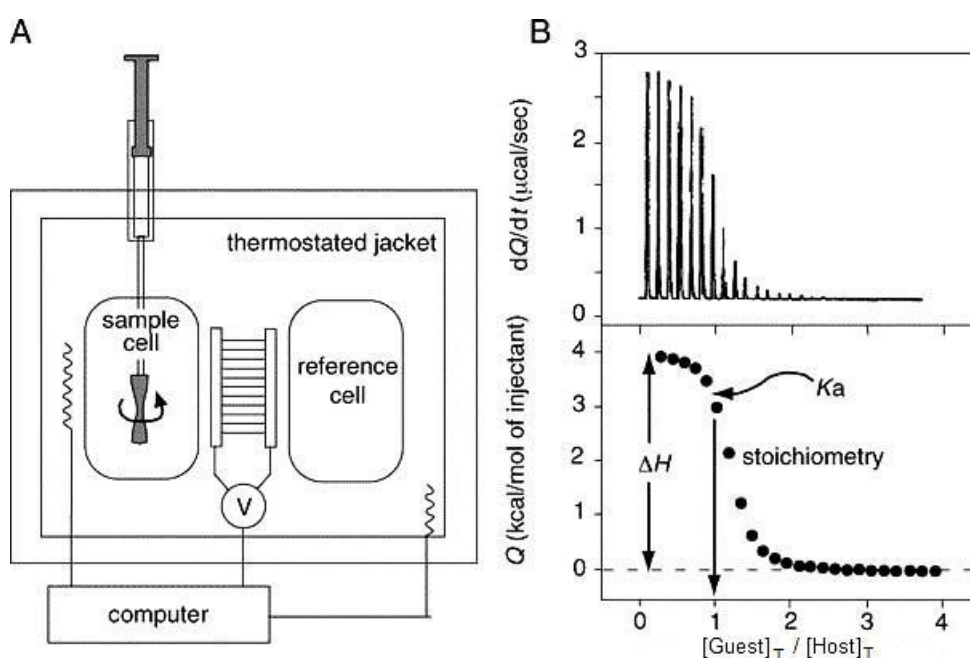


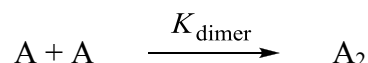
Figure 2-15 (A) Schematic diagram of ITC; (B) An example of isotherms obtained and plotting of the isotherm for determination of ΔG , ΔH and ΔS .

Another common method for studying binding interactions is UV-Vis spectroscopy. A good chromophore, such as a porphyrin, allows host concentrations in the sub-micromolar (10^{-7} M) region, making the determination of association constants as high as 10^9 M^{-1} in simple 1 : 1 systems possible. Larger binding constants of 10^9 to 10^{12} M^{-1} can be measured using competitive binding techniques. The concentrations chosen must lie within the region where the absorption peak(s) of interest in both the host

and its complex are within the limits of the Beer–Lamberts Law ($A = bc\epsilon$, with $A < 1$). There must also be some measureable change in the UV-Vis spectrum upon complex formation. Fluorescence spectroscopy is also a powerful and highly sensitive tool but only those complexes which are fluorescence active can be subjected to these experiments.

In the present study, dilutions studies using NMR spectroscopy are the only applicable method of analyzing the stabilities of **2-1a-d**. This is due to the sparingly soluble nature of the arrays in non-competitive solvents such as CDCl_3 and limited fluorescence of the arrays. Attempts at dilutions using UV-Vis spectroscopy revealed no useful measureable changes, (eg. appearance of a charge transfer band) nor an isosbestic point that could be identified.

Hence, ^1H NMR dilution experiments were used to characterize the dimerizations of **2-1a-d**. As the process of dimerization is a concentration dependent phenomenon, the monomer and dimer concentrations are used to arrive at an equation that would define a dimerization constant K_{dimer} .⁴⁹



$$K_{\text{dimer}} = \frac{[\text{A}_2]}{[\text{A}]^2} \quad (3)$$

$$\delta_{\text{obs}} = \frac{2[\text{A}_2]}{[\text{A}]_0} \delta_{\text{dimer}} + \frac{[\text{A}]}{[\text{A}]_0} \delta_{\text{monomer}} \quad (4)$$

Where,

$[\text{A}]_0$ = total concentration of monomer and dimer

δ_{obs} = observed chemical shift of a donor proton

$[A]$ = concentration of the monomer δ_{dimer} = hydrogen bonded proton chemical shift

$[A]_2$ = concentration of dimer δ_{dimer} = uncomplexed donor proton chemical shift

$$[A] = [A]_0 - 2[A_2] \quad (5)$$

$$\text{From Eq. 3 and 5} \quad [A_2] = K_{\text{dimer}} \left[[A]_0 - 2[A_2] \right]^2 \quad (6)$$

Rearrangement of Eq. 6 to describe $[A_2]$ in terms of $[A]_0$ leads to:

$$[A_2] = \frac{1+4 K_{\text{dimer}} [A]_0 - \sqrt{1+8 K_{\text{dimer}} [A]_0}}{8 K_{\text{dimer}}} \quad (7)$$

Substitution of the Eq. 7 for $[A_2]$ in the first term of Eq. 4 and substitution of Eq. 5 and 7 for $[A]$ in the second term of Eq. 4, eliminates all other concentration terms except known $[A]_0$ leading to the final expression Eq. 8.

$$\begin{aligned} \delta_{\text{obs}} = & \frac{2 \left(\frac{1+4 K_{\text{dimer}} [A]_0 - \sqrt{1+8 K_{\text{dimer}} [A]_0}}{8 K_{\text{dimer}}} \right)}{[A]_0} \delta_{\text{dimer}} \\ & + \frac{[A]_0 - 2 \left(\frac{1+4 K_{\text{dimer}} [A]_0 - \sqrt{1+8 K_{\text{dimer}} [A]_0}}{8 K_{\text{dimer}}} \right)}{[A]_0} \delta_{\text{monomer}} \quad (8) \end{aligned}$$

In our NMR dilution experiments, as the relative concentration of the dimer increases, the chemical shift of the donor proton(s) shifts downfield as a result of participation in hydrogen bonding. We used Origin data analysis software, to plot the dilution curves and calculate the K_{dimer} values based on the above 1:1 dimerization model through non-linear regression.¹⁸

2.6.2 ^1H NMR Studies of 2-1a-d

The self-associating behaviour of all four sets of AADD arrays was investigated using this ^1H NMR method. The concentration-dependent chemical shifts of the thiazine and indole NH protons upon dilution of a concentrated solution in CDCl_3 at room temperature were plotted in three of the four cases **2-1a**, **b** and **c**. The fourth case (**2-1d**) displays extremely strong binding behaviour and therefore the lower limit possible for the binding constant was calculated by a slightly different method which will be discussed in detail later when that dimer is considered.

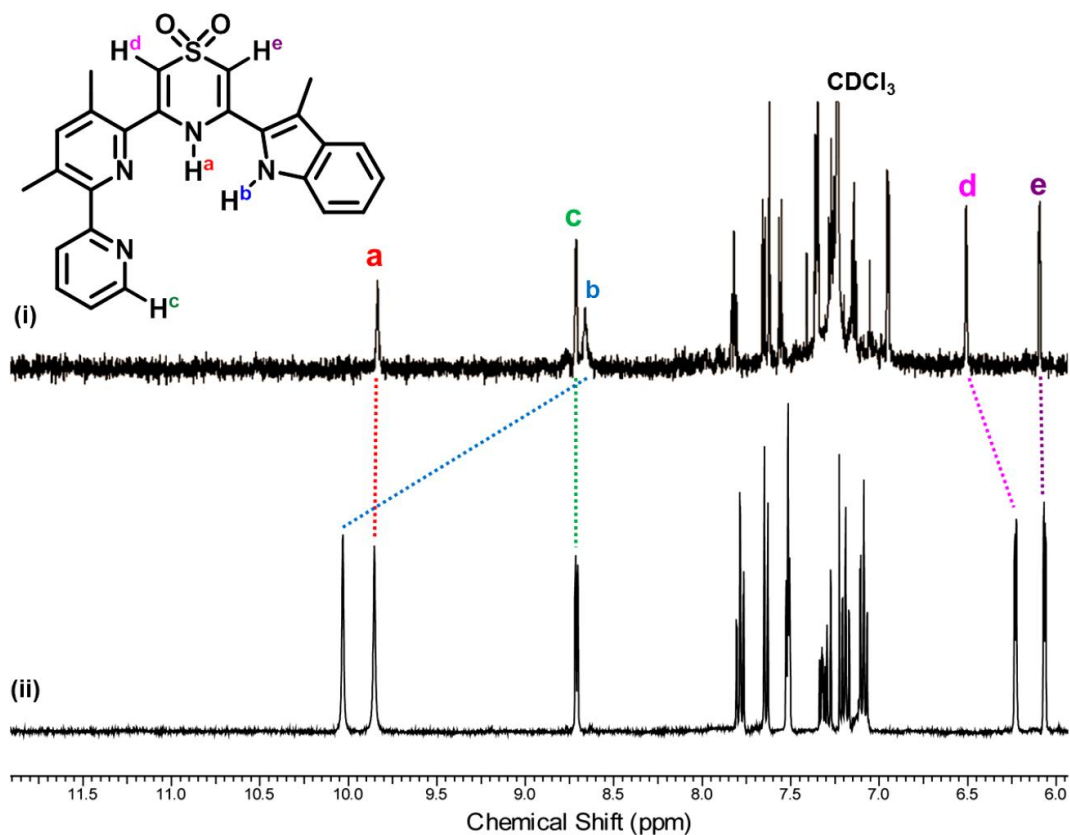


Figure 2-16 ^1H NMR spectra displaying the concentration dependant behaviour of **2-1a** in CDCl_3 . (i) 7×10^{-5} M at 298 K and (ii) 2×10^{-3} M solution at 298 K. While no shift in the NH^a peak is noticeable upon comparison of the two concentrations, the NH^b peak moves down field by approximately 1.5 ppm.

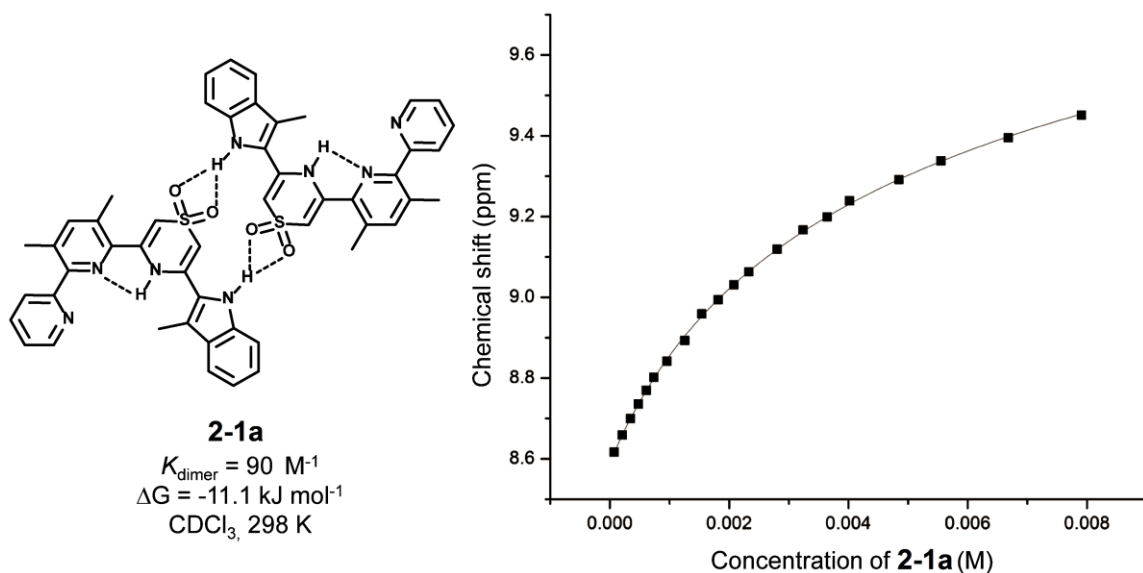


Figure 2-17 NMR dilution curve of array **2-1a** (following N-H^b) with K_{dimer} value and free energies calculated from fitting of the data to a 1:1 dimerization model.⁴⁹ Note that only one of two potential dimers of **2-1a** is depicted.

The spectral behaviour of **2-1a** reveals the presence of unwanted intramolecular hydrogen bonding resulting in a low K_{dimer} value of approximately 90 M^{-1} . The dilution of a sample of **2-1a** (CDCl_3 , 298K) exhibits no change in the chemical shift of the thiazine proton NH^a ($\delta = 9.80 \text{ ppm}$) with respect to concentration (Figure 2-16). This indicates that in both the self-complexed and unassociated states this proton is intramolecularly hydrogen bonded in a manner comparable to that observed in the solid state (Figure 2-11). However, the indole NH^b proton shifts downfield with increasing concentration (Figure 2-17) indicating an intermolecular hydrogen bond interaction as a result of weak self-association ($K_{\text{dimer}} = 90 \text{ M}^{-1}$ $\Delta G = -11.1 \text{ kJ mol}^{-1}$). Examination of molecular models based on the solid-state structure (i.e. intramolecularly hydrogen bonded) does permit the possibility of an antiparallel 1:1 self-associated geometry involving hydrogen bonding between either the two indole and pyridyl termini of the oligomers or the indole donors

and opposing sulfone acceptors (Figure 2-18). Regardless, the K_{dimer} is weak and does not appear to produce the double helical geometry intended in solution.

In case of **2-1b**, the ^1H NMR dilution/concentration studies demonstrated at room temperature, that both peaks corresponding to the NH groups of thiazine dioxide and indole heterocycles were broad and move downfield by 1 ppm.

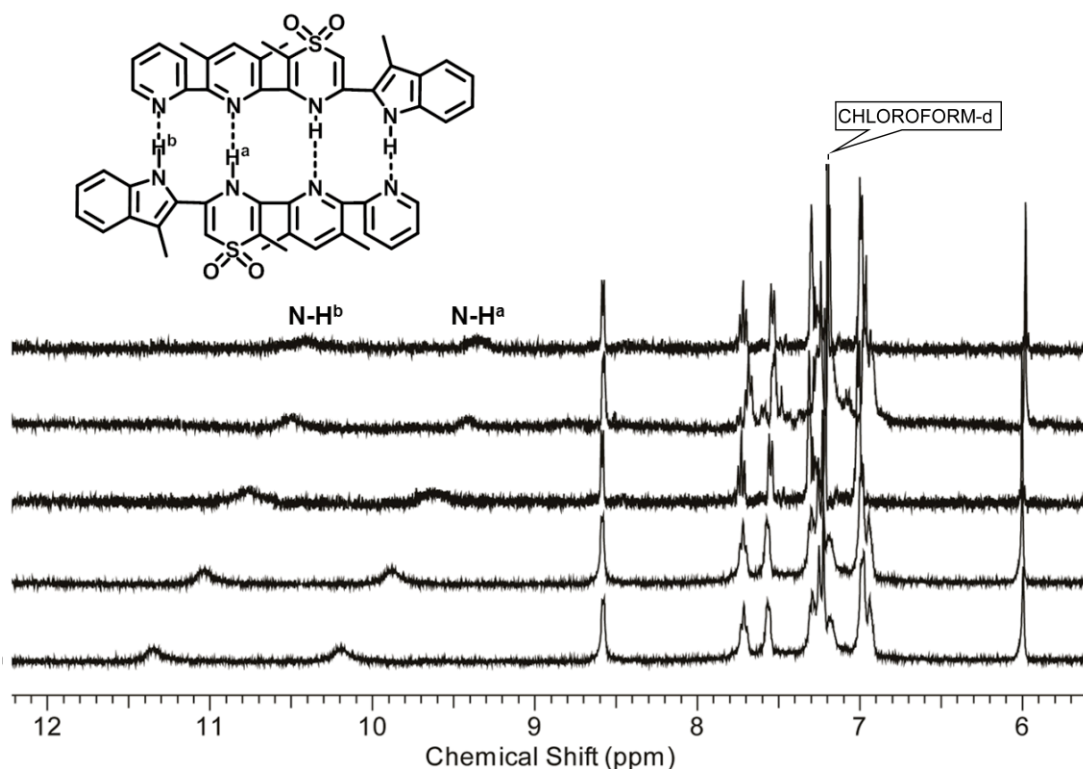


Figure 2-18 Stacked plot of ^1H NMR dilutions of **2-1b** in CDCl_3 at concentrations of 6.0×10^{-3} M, 1.5×10^{-3} M, 7.2×10^{-4} M, 2.8×10^{-4} M, 8.6×10^{-5} M (stacked from bottom to top) at room temperature. Both N-H protons *a* and *b* move downfield at high concentrations.

This indicates (Figure 2-18) that both NH groups are in interaction via hydrogen bonding which was not observed for **2-1a**. The K_{dimer} for **2-1b** was found to be 1400 M^{-1} ($\Delta G = -17.9$) which is a better value compared to that of **2-1a** but not an expected value.

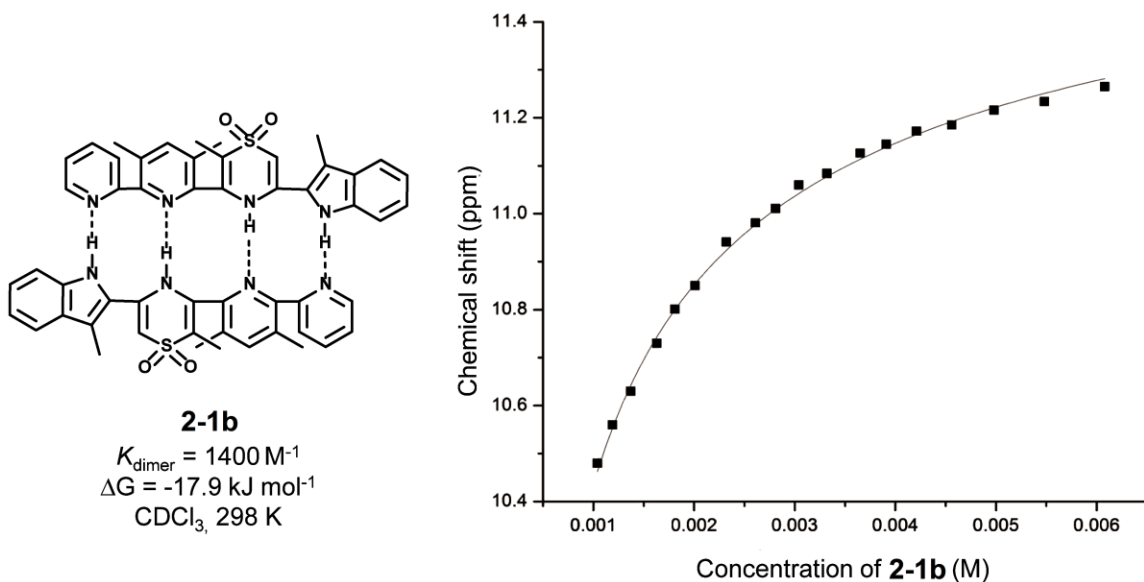


Figure 2-19 Dilution curve of array **2-1b** (following N-H^b) in CDCl_3 with K_{dimer} value and free energy calculated from fitting of the data to the 1:1 dimerization model.

The low value for a quadruple bonding in this case can be accounted for on the basis of two repulsive secondary interactions between the central A and D components of the AADD complex and the poor hydrogen bond donor character of the indole ring.

Concentration of a solution of **2-1c** (CDCl_3 , 298K) produces large downfield shifts of the NH protons (NH^a and NH^b) in the array (Figure 2-20). Fitting of this data (employing N-H^b) to the 1:1 dimerization model yields $K_{\text{dimer}} = 5700 \text{ M}^{-1}$ ($\Delta G = -21.4 \text{ kJ mol}^{-1}$) for **2-10c** (Figure 2-21). The calculated uncomplexed chemical shifts of NH^a ($\delta_{\text{free}} = 7.72 \text{ ppm}$) derived from fitting of the dilution data of **2-1b** and **c** are significantly up field from that measured for solutions of **2-1a** ($\delta = 9.80 \text{ ppm}$ at all concentrations) and indicative of this lack of interaction in their free states. In fact, the δ_{max} (NH^a) calculated for self-association of both **2-1b** and **2-1c** from the dilution data (9.90 and 10.16 ppm

respectively) are very similar to the value for **2-1a**; lending further support for this conclusion.

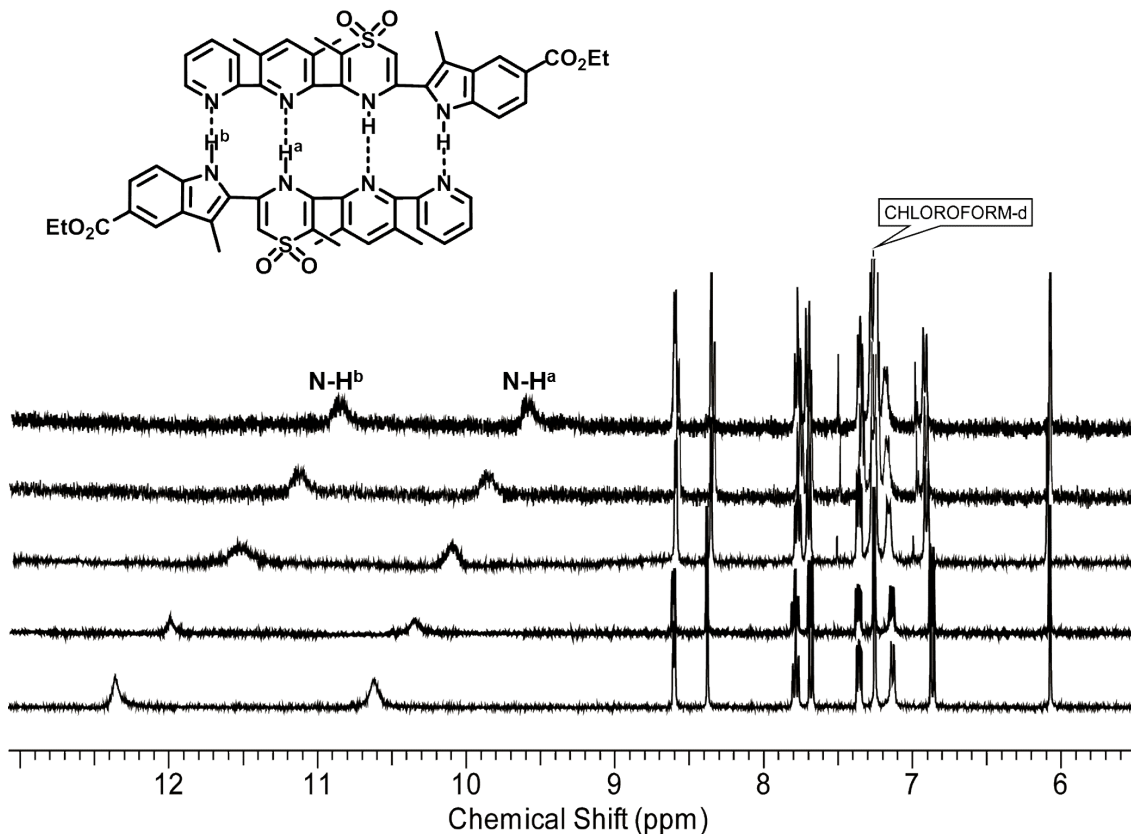


Figure 2-20 Stacked plot of ^1H NMR dilutions of **2-1c** in CDCl_3 at concentrations of 26.0×10^{-3} M, 4.2×10^{-3} M, 6.5×10^{-4} M, 1.3×10^{-4} M, 9.8×10^{-5} M (stacked from bottom to top) at room temperature. Both N-H protons *a* and *b* move downfield at increasing concentrations.

Addition of a moderately electron withdrawing substituent ($\text{R}^4 = -\text{COOEt}$) to the indole ring in **2-1c** increases dimer stability by a modest amount in comparison to **2-1b** ($\Delta\Delta\text{G} = -3.5 \text{ kJ mol}^{-1}$) and with a similar magnitude to that observed in a related system we have recently reported.^{10c}

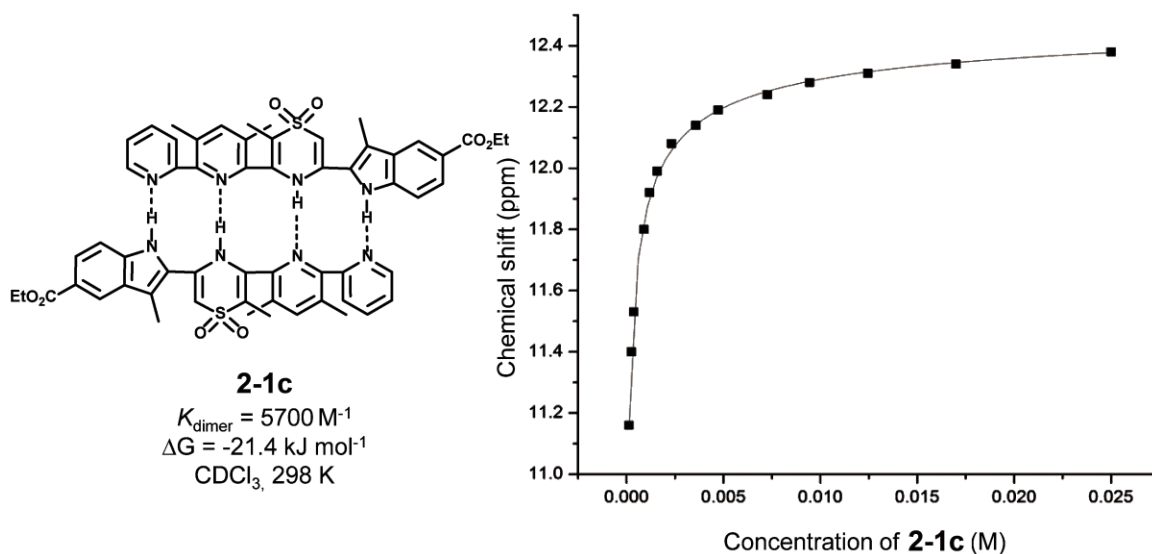


Figure 2-21 Dilution curve of array **2-1c** (following N-H^b) with K_{dimer} value and free energy calculated from fitting of the data to a 1:1 dimerization model.

The structure of **2-1d** incorporates three modifications to the AADD design intended to further increase the stability of the homodimer. Firstly, the two donor heterocycles of the array were restricted to a narrow range of interplanar angles using a trimethylene tether ($R^3 = -\text{CH}_2\text{CH}_2-$). Simple molecular models¹⁹ of the free array indicate that the dihedral angle $\text{HN}-\underline{\text{C}}-\underline{\text{C}}-\text{NH}$ is expected to be $20 \pm 5^\circ$, preorganizing the two NH groups in their approximate binding orientations with respect to one another. Secondly, a more powerful withdrawing group was placed on the indole ring ($R^4 = -\text{NO}_2$) to improve the hydrogen bond donor character of the NH group. Finally, two methyl substituents were placed on the terminal pyridine acceptor ($R^1 = -\text{CH}_3$) in positions that would not sterically perturb the conformation of either the free or self-associated arrays but improve the hydrogen bond acceptor character of the heterocycle.

Indeed, the solution behaviour of **2-1d** upon dilution (CDCl_3 , 298K) is very different in comparison to **2-1a-c**. In this case, self-association appears to be complete in all the

solutions examined down to a minimum concentration practicably measurable by the 600 MHz NMR spectrometer employed in our studies (Figure 2-22).²⁰

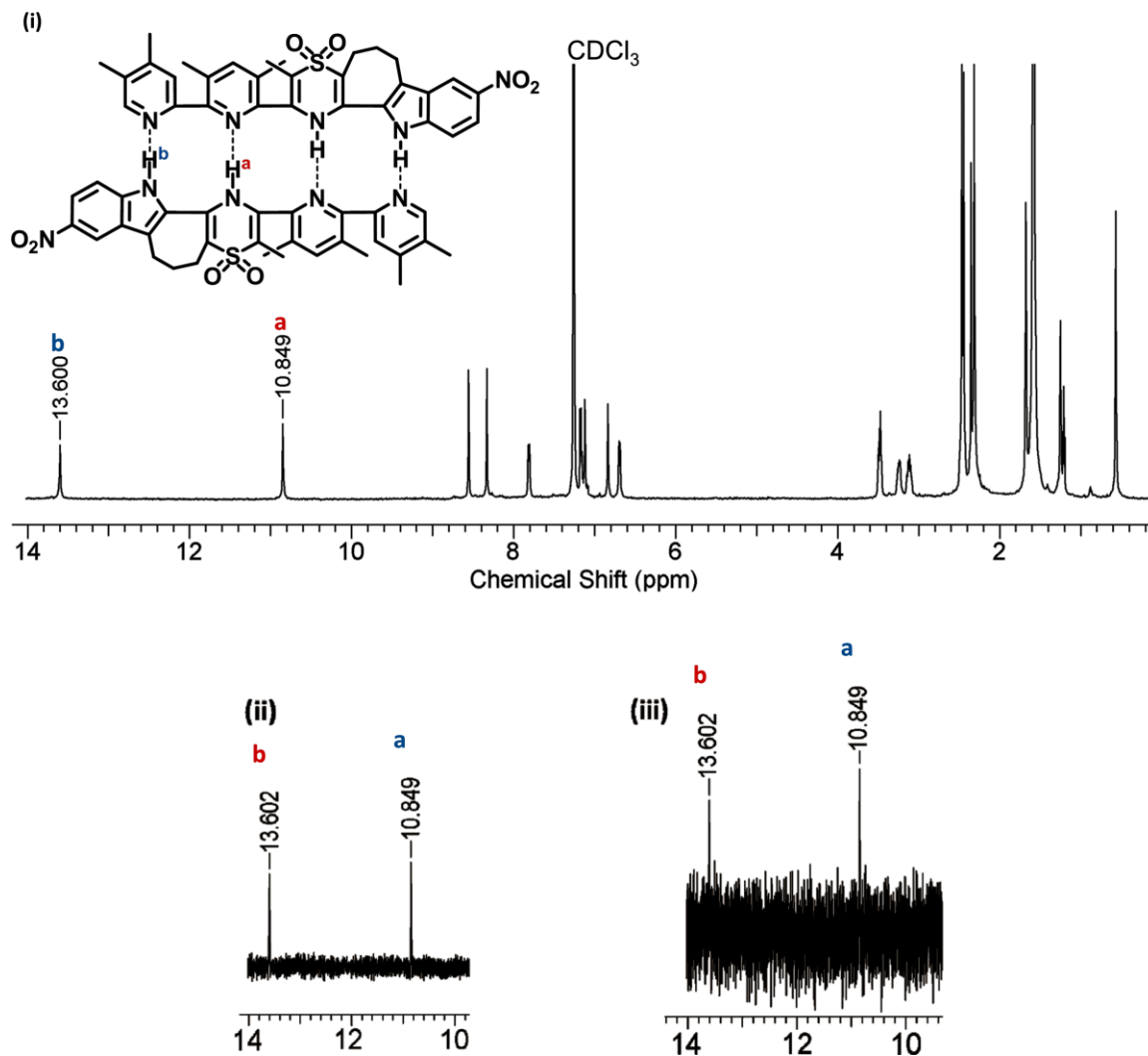


Figure 2-22 (i) 600 MHz ¹H NMR spectrum of **2-1d** at 2.5×10^{-3} M in CDCl₃; (ii) and (iii) Downfield portion of the ¹H NMR spectra of **2-1d** (in ppm) at 100 μM and 1 μM dilutions, respectively.

In an attempt to detect the signals of **2-1d** at 1 μM dilution, the spin-lattice relaxation time (T_1) was experimentally determined to be 0.65 s. The ¹H NMR spectrum at 1 μM dilution was recorded for a period of approximately 15 h 25 m. (acquisition time = 1.708

s; relaxation delay time = 0.5 s; excitation pulse width = 8.3 μ s with a tip angle of 60 degrees; number of acquisitions = 25,000). Due to very strong intermolecular hydrogen bonding, the NH^a and NH^b peaks remained sharp and intact at 10.85 and 13.60 ppm, even at 1 μ M dilution, respectively.

Unfortunately, the absence of any variation in the proton chemical shifts in the concentration range examined precludes fitting of the data to the model used in determining the dimerization constants for **2-1a-c**. However, when we (conservatively) assume 10% dissociation at 1 μ M, a lower limit of $K_{\text{dimer}} \geq 4.5 \times 10^7 \text{ M}^{-1}$ ($\Delta G = -43.7 \text{ kJ mol}^{-1}$) may be calculated for the dimerization of **2-1d** under these conditions.^{17b,50} The dimerization constant exhibited by this array is comparable to the most stable examples of neutral AADD dimers reported in the literature to date. Given the limited increases in dimer stability expected from the incorporation of the electron withdrawing ($R^4 = -\text{NO}_2$) and donating ($R^1 = -\text{CH}_3$) groups to the underlying skeleton,^{10c} a large proportion of this remarkable increase in stability ($\Delta\Delta G \geq -22.3 \text{ kJ mol}^{-1}$) must originate from preorganization by the trimethylene tether. Moreover, it raises the question of what further increases in K_{dimer} might be realized in this system if either or both of the two remaining interplanar degrees of freedom were restrained in a similar manner.

2.7 Conclusion

Four new double-helical AADD hydrogen bond arrays (**2-1a-d**) were designed, synthesized and their self-complementary dimerization examined. Intramolecular hydrogen bonding prevented one of the arrays (**2-1a**) from forming the entwined structure expected. The elimination of this intramolecular interaction through steric interference ($R^2 = -\text{CH}_3$) enabled the remaining three arrays (**2-1b-d**) to assume the double-helical

complex geometry intended in both the solution and the solid state. The stabilities of these dimers, while demonstrably higher than the desmethylated example (**2-1a**), vary greatly depending on their pattern of further substitution. Installation of an electron withdrawing group to the indole ring system increased K_{dimer} (**2-1c**) by a relatively small margin. A much greater increase in stability was observed (**2-1d**) upon introduction of a trimethylene tether between the two donor heterocycles that preorganizes them for binding. This modification, and the incorporation of electron withdrawing/donating substituents to polarize the hydrogen bond donor/acceptor subunits of the array further, produces a complex with an extremely high dimerization constant ($k_{\text{dimer}} \geq 4.5 \times 10^7 \text{ M}^{-1}$) that parallels the most stable literature examples based on neutral hydrogen bond interactions. These studies demonstrate that this type of binding motif can generate complexes with comparable interaction strengths to those observed in rigid coplanar arrays but with very different topologies. The project leaves a promising scope for investigating the integration of these building blocks into higher order assemblies such as supramolecular polymers and copolymers with desirable material properties. An extrapolation of the design into construction of an **AAADDD** array that may self-assemble into longer double helical oligomeric complexes will be discussed in detail in chapter four.

2.8 Experimental

General: All experiments were performed under an atmosphere of nitrogen unless otherwise indicated. Chemicals were purchased from Aldrich and Alfa aesar and used as received. Solvents (THF, hexanes, dichloromethane, toluene and diethyl ether) were obtained from Caledon Laboratories and dried using an Innovative Technology Inc.

Controlled Atmospheres Solvent Purification System that utilizes dual alumina columns (SPS-400-5), or purchased from Aldrich and used as is. Reactions were monitored by thin layer chromatography (TLC) performed on EM 250 Kieselgel 60 F254 silica gel plates. Column chromatography was performed with 240-400 mesh silica gel-60. Nuclear magnetic resonance spectra were recorded on an INOVA and Mercury 400 MHz spectrometer ($^{13}\text{C} = 100.52$ MHz). Proton and $^{13}\text{C}\{^1\text{H}\}$ NMR spectra were referenced relative to Me_4Si using the NMR solvent (^1H : CHCl_3 , $\delta = 7.26$ ppm, $\text{C}_3\text{HD}_5\text{O}$, $\delta = 2.05$ ppm,; $^{13}\text{C}\{^1\text{H}\}$: CHCl_3 , $\delta = 77.16$ ppm, $\text{C}_3\text{HD}_5\text{O}$, $\delta = 29.84, 206.26$ ppm). Solvents for ^1H NMR spectroscopy ($\text{CHLOROFORM-}d$, $\text{ACETONE-}d_6$, $\text{DMSO-}D_6$) were purchased from Cambridge Isotope Laboratories. Mass spectra were recorded using an, electron ionization Finnigan MAT 8200 mass spectrometer and PE-Sciex API 365. X-ray diffraction data were collected on a Bruker Nonius Kappa CCD X-ray diffractometer using graphite monochromated Mo-K_α radiation ($\gamma = 0.71073 \text{ \AA}$).

2.8.1 ^1H NMR Dilution Procedure

An accurately measured amount (0.50 mL) of CDCl_3 was injected into a NMR tube via syringe, and a ^1H NMR spectrum was then recorded. A sample (**2-1a-c**) of known weight was dissolved in 2.0 mL CDCl_3 to produce a 1×10^{-3} M solution. Aliquots of the prepared solution were added successively to the NMR tube containing the CDCl_3 solution ($0.5 \mu\text{L} \times 8$, $10.0 \mu\text{L} \times 6$, $20.0 \mu\text{L} \times 5$, $50.0 \mu\text{L} \times 4$), the tube was well shaken each time to mix the contents, and the ^1H NMR spectrum was recorded after each addition. The chemical shifts of the N-H protons from the two hydrogen bond donors in each sample were recorded and fit satisfactorily to 1:1 binding model using Origin data analysis software

(Microcal, USA). The average of the two K_{dimer} values determined from these two protons was used as the value for that dilution run.

2.8.2 General Synthetic Methods

General Synthesis of Thioacetates: To a solution of potassium thioacetate (20.98 mmol) dissolved in 50 mL of anhydrous DMF (degassed for 10 minutes) was added a solution of the alkyl halide (20.98 mmol) dissolved in 50 mL of anhydrous DMF (degassed for 10 minutes) drop wise over a period of 20 minutes. The reaction mixture was stirred for 4 h and filtered through celite. The filtrate was poured into 100 mL water and extracted with DCM 3x50 mL, washed with water 2x100 mL and the organic layers were combined, dried over MgSO_4 . The solvent was concentrated under reduced pressure to obtain the corresponding thioacetates.

General Synthesis of Thiols: To a degassed solution of thioacetate (6.78 mmol) dissolved in 50 mL of anhydrous acetonitrile, cysteamine (6.78 mmol) was added under a blanket of nitrogen and stirred for 5 minutes. Sodium bicarbonate (6.78 mmol) was added to the reaction mixture and stirred for 4 h. The reaction was quenched with 30 mL of 10 % HCl solution. The reaction mixture was poured in to 100 mL of water and if precipitated, the mixture is stirred and the product was filtered and dried under vacuum. If the product does not precipitate then it was extracted with 2x50 mL of DCM, washed with 2x50 mL of water and dried over MgSO_4 . The solvent was removed by rotary evaporation, giving corresponding thiols.

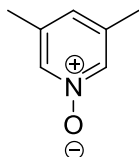
General Synthesis of Thioethers: To a solution of thiol (6.47 mmol) in 10 mL of dry DCM, a solution of halide (6.47 mmol) in 10 mL of dry DCM was added drop wise over

a period of 20 minutes. 2,6-lutidine (6.47) was added *via* syringe to the reaction mixture and stirred for 3 h. The reaction mixture was concentrated and subjected to flash column chromatography, affording corresponding pure thioethers.

General Synthesis of Sulfones: Thioether (2.33 mmol) was dissolved in acetonitrile followed by the addition of urea hydrogen peroxide (UHP) (9.32 mmol) and trifluoroacetic anhydride, (TFAA) (7.00 mmol) at 0 °C. The reaction mixture was brought to room temperature and stirred for 2 h, diluted with water. Most of the sulfones were precipitated out and the sulfones that were not precipitated were extracted with 2 x 40 mL dichloromethane. The organic layers were combined and washed with 2x50 mL of water and dried over MgSO₄. The solvent was removed by rotary vaporation and the residue was washed with methanol, affording almost quantitative yields of purified sulfones.

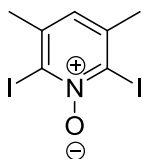
General Synthesis of thiazine dioxide derivatives: Sulfone (2.19 mmol) was dissolved in 10 mL of acetic acid and 5 to 10 equivalents of ammonium acetate were added. The reaction mixture was refluxed overnight or longer based on the completion of reaction (monitored by TLC). The reaction mixture is poured on ice to precipitate out the product. The precipitate is filtered and washed with 2x50 mL water and air dried to afford powdery solids of corresponding thiazine dioxides.

2.8.3 Synthetic Methods



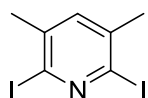
Synthesis of 3,5-Dimethylpyridine-1-oxide: Hydrogen peroxide (1.33 mL, 30 % H₂O₂, 11.61 mmol) was added drop wise to the solution of 3,5-Lutidine (1.25 g, 11.61 mmol) dissolved in 10 mL of glacial acetic acid and refluxed after 5 h. A second portion of hydrogen peroxide (1.33 mL, 30 % H₂O₂, 11.61

mmol) was added to the solution and refluxing was continued overnight. The pH of the solution was adjusted to 8-9 by adding concentrated sodium hydroxide solution and extracted with 2x50 mL of dichloromethane (DCM) and washed with 40 mL of water. The organic layer is dried over MgSO₄ and solvent was removed under reduced pressure, afforded a colourless crystalline solid (87%, 1.25 g, 10.13 mmol). ¹H NMR (CDCl₃, 400 MHz) δ ppm 7.96 (s, 2H), 6.98 (s, 1H), 2.27 (s, 6H). ¹³C NMR (100MHz, CDCl₃) δ, 136.6, 136.0, 128.5, 18.2.

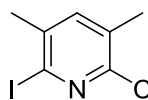


Synthesis of 2-2: 3,5-Dimethyl pyridine-1-oxide (5.6 g, 45.53 mmol) was dissolved in 30 mL of tetrahydrofuran (THF), and cannula transferred into a solution of *n*-butyl lithium (*n*BuLi) (2.5 M in hexanes, 45.79 mL), cooled to -78 °C, over a period of half an hour. The solution was stirred for an hour and half, at -78 °C. Iodine (11.56 g, 90.09 mmol) dissolved in 25 mL of THF was added drop wise to the reaction mixture at -78 °C. After an hour of stirring at -78 °C, the reaction mixture was allowed to warm up to room temperature and stirred overnight. The mixture was washed with 30 mL of saturated solution of sodium thiosulfate and the pale yellow solid was filtered and washed with a small portion of cold methanol. The filtrate was collected, extracted with 2 x 50 mL of DCM and washed with water and dried over MgSO₄, solvent removed using roto-vaporation gave a dirty light brown solid. The solid was recrystallized in cold methanol. The Residue from the first filtration and the solid from the recrystallization were identified to be same compound (45%, 7.22 g, 22.31 mmol) by NMR analysis. ¹H NMR (400 MHz, CDCl₃) δ ppm 6.87 (s, 1H), 2.45 (s, 6H). ¹³C NMR

(100 MHz, CDCl₃) δ 148.4, 137.5, 132.3, 16.8. EI-HRMS calcd. for C₇H₇I₂NO (M)⁺: 374.8617, found: 374.8630.

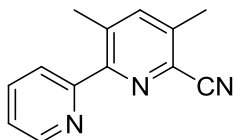


Synthesis of 2-3 : To a solution of **2-2** (1.72 g, 4.59 mmol) in 25 mL of chloroform, phosphorous trichloride (1.18 mL, 13.77 mmol) dissolved in 10 mL of chloroform was added drop wise and refluxed overnight. The reaction mixture was basified to a pH of 9 and extracted with 2x30 mL of DCM, washed with water and dried over MgSO₄. The solvent was removed by rotary evaporation afforded pale yellowish white crystalline solid. The crude product was further purified by flash column chromatography using 3 : 7; EtOAc : Hexane, as eluent system, to give colourless crystalline solid (98.75%, 1.63 g, 4.53 mmol). ¹H NMR (400 MHz, CDCl₃) δ ppm 7.18 (s, 1H), 2.28 (s, 6H). ¹³C NMR (100 MHz, CDCl₃) δ 138.2, 137.0, 118.9, 24.7. EI-HRMS calcd. for C₇H₇I₂N (M)⁺: 358.8668, found: 358.8665.

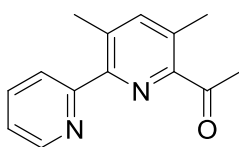


Synthesis of 2-4: To a solution of 2,6-diiodo-3,5-lutidine (1.01 g, 2.82 mmol), sodium cyanide (0.12 g, 2.54 mmol) and cuprous iodide (0.05 g, 0.25 mmol, 10%) in 10 mL of dry acetonitrile, 10 % palladium over carbon was added. The reaction solution was refluxed overnight. The resulting mixture was then filtered through celite and the filtrate was portioned between mL of distilled water and mL of dichloromethane and extracted with 2x30 mL of dichloromethane. The organic layers were combined and washed with 2x40 mL of distilled water, brine and dried over MgSO₄, concentrated using reduced pressure. Column chromatography using 100% DCM as eluent system, gave white needle like crystals (35%, 0.2545 g, 0.9864 mmol). ¹H

NMR (400 MHz, CDCl₃) δ ppm 7.40 (s, 1H), 2.46 (s, 3H), 2.43 (s, 3H); ¹³C NMR (100MHz, CDCl₃) δ 143.73, 138.40, 138.14, 131.68, 121.83, 115.43, 26.58, 18.10. EI-HRMS calcd. for C₈H₇IN₂ [M]⁺ : 257.9654, found : 257.9652.

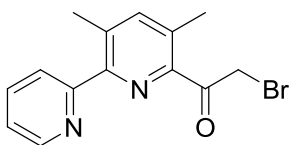


Synthesis of 2-8: Compound **2-4** (0.61 g, 2.37 mmol) was dissolved in 20 mL of dry toluene followed by addition of 2-trimethyltin pyridine (0.57 g, 2.37 mmol) and tetrakis(triphenylphosphine) palladium [0] (0.082 g, 3%), under nitrogen. The reaction mixture was refluxed for a period of about 26 h and filtered. After removing the solvent by reduced pressure, flash column chromatography is done on the residue, using 1 : 1 ; EtOAc : Hexanes, as eluent system, yielded white needle like crystals (85%, 0.42 g, 2.01 mmol). ¹H NMR (400 MHz, CDCl₃) δ ppm 8.67 (d, *J*=4.88 Hz, 1H), 7.88 (dt, *J*=8.01 Hz, 1H), 7.84 (td, *J*=8.01 Hz, 1H), 7.58 (s, 1H), 7.33 (dd, *J*=4.88 Hz, 1H), 2.60 (s, 3H), 2.57 (s, 3H); ¹³C NMR (100MHz,) δ CDCl₃ 157.4, 155.5, 148.6, 141.4, 139.0, 137.7, 137.0, 130.9, 124.6, 123.5, 116.8, 20.8, 18.4. ESI HRMS calcd. for C₁₃H₁₁N₃ *m/z* : 209.0953, found : 209.0951.

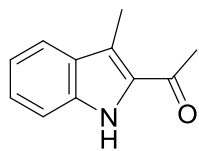


Synthesis of 2-9a: To a solution of methyl magnesium bromide (3.5 mL, 8.98 mmol) in 50 mL of tetrahydrofuran (THF), a solution of **2-8** (1.87 g, 8.93 mmol) in 50 mL of THF was added drop wise at 0 °C, over 15 minutes. The reaction mixture was refluxed overnight followed by neutralization with 10% HCl solution and extraction with 2x40 mL of dichloromethane. The organic layer was washed with 2x40 mL of water dried over MgSO₄. The solvent was removed by reduced pressure to yield pale yellow crude product which is subjected to flash column chromatography using EtOAc : Hexanes; 2 : 3, as eluent system, afforded white

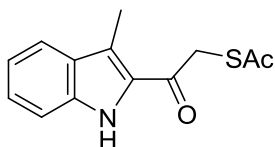
needle like crystals (90%, 1.82 g, 8.04 mmol). ^1H NMR (400 MHz, CDCl_3) δ ppm 8.67 (d, $J=4.88$ Hz, 1H), 7.97 (t, $J=8.01$, 1H), 7.83 (t, $J=8.01$, 1H), 7.48 (s, 1H), 7.30 (d, $J=4.88$ Hz, 1H), 2.74 (s, 3H), 2.61 (s, 6H); ^{13}C NMR (100MHz, CDCl_3) δ 202.5, 158.8, 152.5, 148.5, 148.4, 143.7, 136.7, 136.2, 134.2, 124.4, 122.91, 28.3, 20.5, 20.2. ESI HRMS calcd. for $\text{C}_{14}\text{H}_{14}\text{N}_2\text{O}$ m/z : 226.1106, found : 226.1105.



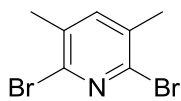
Synthesis of 2-10a: White crystalline needles of **2-9a** (0.68 g, 3.01 mmol) were dissolved in dry diethyl ether followed by addition of 2% AlCl_3 under nitrogen. Liquid bromine (0.16 mL, 3.12 mmol), partially dissolved in dry diethyl ether, was added drop wise to the reaction mixture over 15 minutes. The reaction mixture was stirred for 36 h. The mixture was washed with sodium bicarbonate solution and extracted with 2x30 mL of dichloromethane. The organic layers were combined washed with 2x30 mL of water and dried over MgSO_4 . The solvent is removed by roto-vaporation and flash column chromatography was done using EtOAc : DCM; 1: 9, as eluent system. The product was obtained in the form of whitish yellow crystals (35%, 0.3213 g, 1.0534 mmol). ^1H NMR (400 MHz, CDCl_3) δ ppm 8.68 (dq, $J=4.88$ Hz, 1H), 7.94 (dt, $J=8.01$ Hz, 1H), 7.85 (td, $J=8.01$ Hz, 1H), 7.53 (s, 1H), 7.33 (dd, $J=4.88$ Hz, 1H), 4.92 (s, 2H), 2.65 (s, 3H), 2.63 (s, 3H); ^{13}C NMR (100MHz, CDCl_3) δ 193.7, 158.3, 152.8, 148.4, 146.4, 144.0, 137.5, 136.9, 135.8, 124.4, 123.1, 35.4, 20.7, 20.1. ESI HRMS calcd. for $\text{C}_{14}\text{H}_{14}\text{BrN}_2\text{O}$ m/z : 304.0211, found : 304.0213.



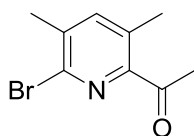
Synthesis of 2-13a: 1-(3-Methyl-1*H*-indol-2-yl)-ethanone was prepared in accordance with the R. Dakarapu *et al.*²⁹ method, in 76 % yield. The crude was purified by flash column chromatography using EtOAc : Hexanes; 2 : 3, as eluent system affording pale yellow crystalline solid.



Synthesis of S-2-(3-methyl-1*H*-indol-2-yl)-2-oxoethyl ethanethioate: To a solution of potassium thioacetate (0.6042 g, 5.3004 mmol) dissolved in 3.0 mL of dry DMF, **2-13a** (1.34 g, 5.30 mmol) dissolved in 3.0 mL of dry DMF was added drop wise and stirred for 4 h. The crude product was precipitated out by adding 30 mL of ice cold water to the reaction mixture and filtered. Residue was air dried and purified by flash column chromatography, using 100% DCM as eluent, affording reddish yellow powdery solid (94%, 1.24 g, 5.00 mmol). ¹H NMR (400 MHz, CDCl₃) δ ppm 9.09 (s, br, 1H), 7.70 (dd, *J* = 8.01 Hz, 1H), 7.37 (m, 2H), 7.15 (dd, *J* = 8.01 Hz, 1H), 4.33 (s, 2H), 2.70 (s, 3H), 2.44 (s, 3H); ¹³C NMR (100MHz, CDCl₃) δ 196.3, 177.2, 138.9, 134.0, 129.6, 127.1, 125.4, 121.5, 120.5, 112.2, 41.1, 24.2, 7.9. EI HRMS calcd. for C₁₃H₁₃NO₂S *m/z* : 247.0667, found : 247.0669.

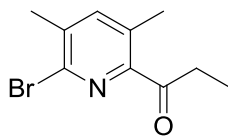


Synthesis of 2,6-Dibromo-3,5-dimethylpyridine: The title compound was synthesized in accordance with the procedure of Dunn *et al.*⁴⁰ and Pugh *et al.*⁴¹ in 60% yield, using bromine and fuming sulphuric acid refluxing at 160 °C.

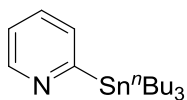


Synthesis of 2-11a: To a stirred solution of 2,6-Dibromo-3,5-dimethylpyridine (1.05 g, 3.96 mmol) in diethylether (25 mL) at -78 °C was added drop wise a 1.7 M solution of ^tBuLi (2.7 mL, 4.75 mmol) in *n*-pentane over 10 min. After 30 minutes stirring at -78 °C, *N,N*-dimethylacetamide (0.42

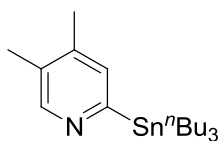
mL, 3.95 mmol) was added and stirring maintained further 1.5 h. The resulting mixture was allowed to warm to room temperature and treated with water (5 mL). The formed bilayers were separated, and the organic phase was washed with water (2 X 10 mL). The aqueous layer was extracted with Et₂O (3 X 10 mL). The combined organic layers were dried over MgSO₄. Removal of the solvent under reduced pressure gave yellow oil that was further purified by chromatography using 0.5 : 9.5; EtOAc : Hexanes as eluent system affording white crystalline solid (80 %, 0.7672 g, 3.17 mmol). ¹H NMR (400 MHz, CDCl₃) δ ppm 7.38 (s, 1H), 2.65 (s, 3H), 2.50 (s, 3H), 2.38 (s, 3H); ¹³C NMR (100MHz, CDCl₃) δ 200.7, 149.5, 142.8, 140.0, 138.5, 134.0, 27.9, 21.8, 19.5. ESI HRMS calcd. for C₉H₁₀BrNO *m/z* : 226.9945, found : 226.9939.



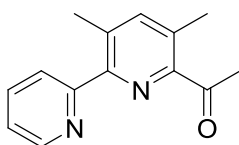
Synthesis of 2-11b: The title compound **2-11b** is synthesized in the similar fashion as of **2-11a**, except that *N,N*-dimethylpropamide is used in the place of *N,N*-dimethylacetamide, with 85% yield. ¹H NMR (400 MHz, CDCl₃) δ ppm 7.39 (s, 1H), 3.17 (q, *J*=7.23 Hz, 2H), 2.50 (s, 3H), 2.39 (s, 3H), 1.15(t, *J*=7.23 Hz, 3H); ¹³C NMR (100MHz, CDCl₃) δ 203.3, 149.6, 142.7, 141.1, 138.2, 133.8, 32.9, 212.8, 19.4, 7.9. ESI HRMS calcd. for C₁₀H₁₂BrNO *m/z* : 241.0102, found : 241.0106.



Synthesis of 2-6a: Prepared according to the literature procedure of Shin *et al.*^{38a} in almost quantitative yield. The crude is passed through neutral alumina loaded with 1 : 24; EtOAc : Hexanes as eluent system to give pale yellowish oil in 96% yield.

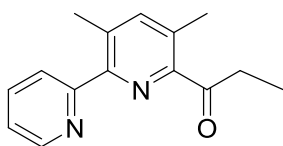


Synthesis of 2-6b: The synthesis of the **2-6b** was carried through extrapolation and modification of the synthetic methods followed by Y. Fort *et al.*^{38b} of lithiations of lutidines. A solution of 2-(dimethylamino)ethanol (1.06 mL, 10.5 mmol) in dry hexanes (25 mL) was treated with *n*BuLi (8.5 mL, 22.1 mmol) drop wise at 0 °C. After the mixture was stirred for 15 minutes in ice bath, a solution of 3,4-lutidine (0.6 mL, 5.3 mmol) in 5 mL of hexanes was added drop wise. After 1 h at 0 °C, the orange solution was cooled to -78 °C and treated with a solution of tributyltin chloride (3.7 mL, 13.64 mmol) in THF (12.5 mL). After 1 h at -78 °C, the reaction mixture was warmed to room temperature. Hydrolysis was carried at 0 °C with water (20 mL). The organic layer was then extracted with diethyl ether (2x15 mL) and dried over MgSO_4 , and the solvents were evaporated under vacuum. The crude product was then purified by column chromatography with hexanes:EtOAc, 4:1 mixtures as eluents giving pure product as yellow liquid in 45% (0.96 g, 24.2 mmol). ^1H NMR (400 MHz, CDCl_3) δ ppm 8.46 (s, 1H), 7.14 (s, 1H), 2.22 (s, 3H), 2.20 (s, 3H), 1.60-1.44 (m, 6H), 1.38-1.25 (m, 8H) 1.11-1.07 (m, 4H) 0.88 (t, 9H); ^{13}C NMR (100MHz, CDCl_3) δ 169.7, 151.0, 142.8, 133.4, 130.5, 29.3, 29.1, 27.8, 27.3, 26.8, 18.9, 17.5, 16.3, 13.7, 9.7, 8.7. ESI HRMS calcd. for $\text{C}_{19}\text{H}_{35}\text{NSn}$ m/z : 397.1791, found : 397.1794.

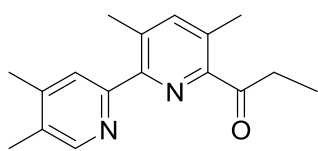


Synthesis of 2-9a: White crystalline needles of **2-11a** (0.64 g, 2.81 mmol) were dissolved in 30 mL of dry toluene followed by addition of tributyltin pyridine (1.03 g, 2.81 mmol) and tetrakis triphenylphosphine palladium [0] (0.097 g, 3%), under nitrogen. The reaction mixture was refluxed for a period of about 18 h and filtered. After removing the solvent by reduced pressure, flash column chromatography was done on the residue, using 1 : 1 ; EtOAc : Hexanes, as eluent

system, yielded white needle like crystals (85%, 0.57 g, 2.38 mmol). The data matches with the set of data reported for the same compound but synthesized using a different route. ^1H NMR (400 MHz, CDCl_3) δ ppm 8.67 (dq, $J=4.88$ Hz, 1H), 7.97 (dt, $J=8.01$, 1H), 7.83 (td, $J=8.01$, 1H), 7.48 (s, 1H), 7.30 (dd, $J=4.88$ Hz, 1H), 2.74 (s, 3H), 2.61 (s, 6H); ^{13}C NMR (100MHz, CDCl_3) δ 202.5, 158.8, 152.5, 148.5, 148.4, 143.7, 136.7, 136.2, 134.2, 124.4, 122.91, 28.3, 20.5, 20.2. ESI HRMS calcd. for $\text{C}_{14}\text{H}_{14}\text{N}_2\text{O}$ m/z : 226.1106, found : 226.1105.

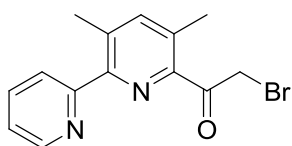


Synthesis of 2-9b: The propanone **2-9b** is prepared in 80 % yield via the above mentioned procedure of **2-9a**. ^1H NMR (400 MHz, CDCl_3) δ ppm 8.67 (d, $J=4.88$ Hz, 1H), 7.97 (d, $J=7.81$ Hz, 1H), 7.83 (t, $J=7.81$ Hz, 1H), 7.48 (s, 1H), 7.30 (dd, $J=4.88$ Hz, 1H), 3.27 (q, $J=7.42$ Hz, 2H), 2.61 (s, 3H), 1.18 (t, $J=7.42$ Hz, 3H); ^{13}C NMR (100MHz, CDCl_3) δ 204.9, 158.7, 152.3, 148.9, 148.3, 143.6, 136.6, 135.8, 133.9, 124.3, 122.8, 33.0, 20.4, 20.0, 8.3. ESI HRMS calcd. for $\text{C}_{15}\text{H}_{16}\text{N}_2\text{O}$ m/z : 240.1263, found : 240.1261.

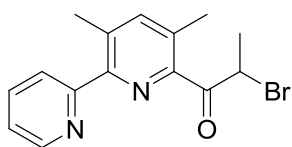


Synthesis of 2-9c: The title compound is synthesized according to the procedure of **2-9b** and whitish yellow crude product is subjected to flash column chromatography using EtOAc : dichloromethane; 1 : 4, as eluent system, affording white needle like crystals in 75% yield. ^1H NMR (400 MHz, CDCl_3) δ ppm 8.36 (s, 1H), 7.65 (s, 1H), 7.43 (s, 1H), 3.25 (q, $J=7.42$ Hz, 2H), 2.56 (s, 3H), 2.54 (s, 3H), 2.34 (s, 3H), 2.28 (s, 3H) 1.16 (t, $J=7.42$ Hz, 3H); ^{13}C NMR (100MHz, CDCl_3) δ 204.8, 156.3, 152.6, 148.7, 148.5, 146.0,

143.1, 135.4, 133.2, 131.4, 124.8, 32.8, 20.1, 19.7, 19.4, 16.2, 8.0. ESI HRMS calcd. for $C_{17}H_{20}N_2O$ m/z : 268.1576, found : 268.1572.

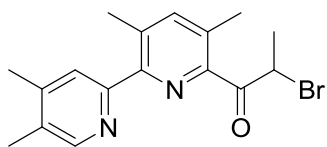


Synthesis of 2-10a: White crystalline needles of **2-9a** (0.68 g, 3.01 mmol) were dissolved in 5 mL of acetic acid followed by addition of 2% $AlCl_3$ under nitrogen. HBr solution, 33 wt% in acetic acid (0.77 mL, 3.13 mmol) was added drop wise to the reaction mixture over 15 minutes. The reaction mixture was stirred for 18 h and was washed with sodium bicarbonate solution followed by extraction with 2x30 mL of dichloromethane. The organic layers were combined washed with 2x30 mL of water and dried over $MgSO_4$. The solvent is removed by roto-vaporation and subjected to flash column chromatography using EtOAc : DCM; 1: 9, as eluent system. The product was obtained in the form of whitish yellow crystals (75 %, 0.64 g, 2.11 mmol). The data matches with the set of data reported for the same compound but synthesized using a different route. 1H NMR (400 MHz, $CDCl_3$) δ ppm 8.68 (dq, $J=4.88$ Hz, 1H), 7.94 (dt, $J=8.01$ Hz, 1H), 7.85 (td, $J=8.01$ Hz, 1H), 7.53 (s, 1H), 7.33 (dd, $J=4.88$ Hz, 1H), 4.92 (s, 2H), 2.65 (s, 3H), 2.63 (s, 3H); ^{13}C NMR (100MHz, $CDCl_3$) δ 193.7, 158.3, 152.8, 148.4, 146.4, 144.0, 137.5, 136.9, 135.8, 124.4, 123.1, 35.4, 20.7, 20.1. ESI HRMS calcd. for $C_{14}H_{14}BrN_2O$ m/z : 304.0211, found : 304.0213.



Synthesis of 2-10b: The bromide **2-10b** is synthesized according to the procedure for synthesis of **5a** except for the reagent and solvent is replaced by bromine and dry THF, respectively and the reaction was carried under nitrogen. Flash column chromatography was done on crude using EtOAc : DCM; 1: 9, as eluent system. to give the product in 82%. 1H NMR (400 MHz,

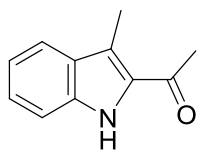
CDCl₃) δ ppm 8.68 (d, $J=4.88$ Hz, 1H), 7.97 (dt, $J=7.81$ $J=1.17$, Hz, 1H), 7.85 (td, $J=7.81$ $J=1.95$, Hz, 1H), 7.54 (s, 1H), 7.33 (d, $J=4.88$ Hz, 1H), 6.15 (q, $J=7.03$ Hz, 1H), 2.63 (s, 3H), 1.88 (d, $J=7.03$ Hz, 3H); ¹³C NMR (100MHz, CDCl₃) δ 195.6, 158.2, 152.3, 148.1, 146.3, 143.5, 136.7, 136.6, 135.5, 124.3, 122.8, 43.5, 20.3, 19.7, 19.5. ESI HRMS calcd. for C₁₅H₁₅BrN₂O m/z : 318.0367, found : 318.0364.



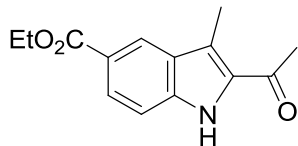
Synthesis of 2-10c: The bromide **2-10c** is synthesized under same conditions of **2-10b** and flash column chromatography was done using EtOAc : hexanes; 1: 4, as eluent system. The

product was obtained in the form of whitish yellow crystals in 74% yield. ¹H NMR (400 MHz, CDCl₃) δ ppm 8.38 (s, 1H), 7.67 (s, 1H), 7.50 (s, 1H), 6.15 (q, $J=6.64$ Hz, 1H), 2.59 (s, 3H), 2.57 (s, 3H), 2.37 (s, 3H), 2.30 (s, 3H), 1.87 (d, $J=6.64$ Hz, 3H); ¹³C NMR (100MHz, CHLOROFORM-d) δ 195.7, 160.0, 152.9, 148.5, 146.2, 143.3, 136.5, 135.2, 131.6, 125.0, 43.8, 20.2, 19.8, 19.5, 16.3. ESI HRMS calcd. for C₁₇H₁₉BrN₂O m/z : 346.0681, found : 346.0669.

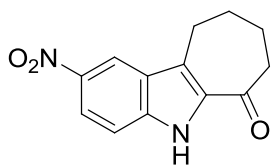
Synthesis of 2-12a-c: The compounds 6a-c are synthesized according to standard procedure of diazonium salts preparations as described by the Hillier M. C. *et al.* in *J. Org. Chem.* 70 (21) **2005**,8385-8394 and then subjected to Japp-Klingemann reaction to produce the corresponding hydrazones which were carried forward to Fisher Indole Cyclization process to obtain the corresponding indoles. No purifications required in any of the steps involved. If desired, recrystallizations can be carried out in cold ethanol to yield pure crystalline products.



Synthesis of 2-13a: The hydrazone obtained by the Japp-Klingemann reaction of **2-12a** and methyl 2-ethyl-3-oxobutanoate was refluxed in formic acid yielding fisher indole product **2-13a** in 85% and the nmr data matched with the literature data^{S6}.

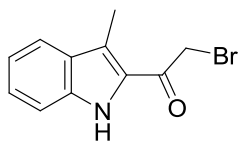


Synthesis of 2-13b: Compound **2-13b** was prepared in similar manner as of **32a** by using the corresponding hydrazone in 88% yield. M.P. 198.2-200.6 °C. ¹H NMR (400 MHz, DMSO-*d*₆, 298 K) δ (ppm) = 11.81(s, 1H), 8.37-8.34 (m, 1H), 7.87-7.84 (m, 1H), 7.49-7.45 (m, 1H), 4.31 (q, *J* = 7.0 Hz, 2H), 2.59 (s, 3H), 2.58 (s, 3H), 1.34 (t, *J* = 7.0 Hz, 3H); ¹³C NMR (100 MHz, DMSO-*d*₆, 298 K) δ (ppm) = 190.7, 166.3, 138.5, 133.6, 127.5, 125.7, 123.6, 121.2, 119.0, 112.4, 60.3, 29.1, 14.3, 10.4, EI HRMS *m/z* calculated for C₁₄H₁₅NO₃ : 245.1052, found 245.1056.

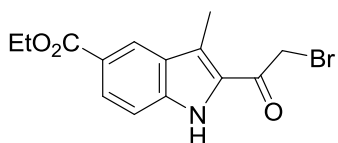


Synthesis of 2-16: The title compound was synthesized by refluxing the cyclic hydrazone, 2-(2-(4-nitrophenyl)hydrazono)cycloheptanone (2.00 g, 7.65 mmol) in 25 mL of formic acid for about 20 h and quenching the reaction by adding water to the reaction mixture. The contents were then allowed to stir for about 20 minutes and then filtered off to give the yellowish crude product (1.69 g, 6.92 mmol, 90%) and the crude is carried forward without any purifications. M.P. 268.8-271.2 °C. ¹H NMR (400 MHz, CDCl₃, 298 K) δ (ppm) = 9.48 (s, br, 1H), 8.67 (d, *J* = 1.9 Hz, 1H), 8.23 (d, *J* = 9.4 Hz, 1H), 7.44 (d, *J* = 9.4 Hz, 1H), 3.26 (t, *J* = 5.8 Hz, 2H), 2.90 (t, *J* = 5.8 Hz, 2H), 2.20-2.10 (m, 2H), 2.09-2.00 (m, 2H). ¹³C NMR (100MHz, CDCl₃, 298 K) δ (ppm) = 194.9, 141.9,

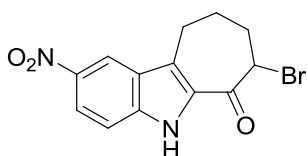
139.0, 135.0, 127.4, 126.3, 121.6, 119.0, 112.1, 42.9, 26.4, 25.7, 22.5. HRMS m/z calculated for $C_{13}H_{12}N_2O_3$: 244.0848, found 244.0838.



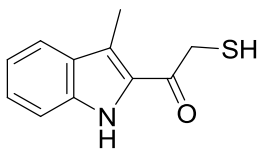
Synthesis of 2-14a: 2-Bromo-1-(3-methyl-1H-indol-2-yl)ethanone was made in accordance with the A.N. Kost *et al.*⁴⁵ method in 72 % yield.



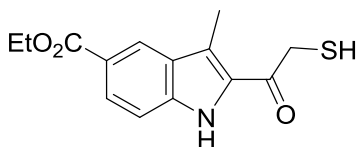
Synthesis of 2-14b: The title compound was synthesized by following the same method as described for **2-14a** and obtained the product in 78% yield as light yellowish green solid. M.P. 184.5-186.0 °C. 1H NMR (400 MHz, DMSO- d_6 , 298 K) δ (ppm) = 11.96 (s, 1H), 8.39-8.37 (m, 1H), 7.91-7.88 (m, 1H), 7.52-7.48 (m, 1H), 4.80 (s, 2H) 4.31 (q, J = 7.0 Hz, 2H), 2.63 (s, 3H), 1.34 (t, J = 7.0 Hz, 3H); ^{13}C NMR (100 MHz, DMSO- d_6 , 298 K) δ (ppm) = 190.7, 166.3, 138.5, 133.6, 127.5, 125.7, 123.6, 121.2, 119.0, 112.4, 60.3, 29.1, 14.3, 10.4; EI-HRMS (m/z) calculated for $C_{14}H_{14}BrNO_3$: 323.0157, found : 323.0165.



Synthesis of 2-17: The bromide was made in accordance with the A.N. Kost *et al.*⁴⁵ method in 80 % yield. M.P. 272.5-275.2 °C. 1H NMR (400 MHz, DMSO- d_6 , 298 K) δ (ppm) = 12.00 (s, br, 1H), 9.15 (d, J = 2.3 Hz, 1H), 8.64 (dd, J = 8.9 Hz, J = 2.3 Hz, 1H), 8.10 (d, J = 8.9 Hz, 1H), 5.64-5.62 (m, 1H), 3.98-3.90 (m, 1H), 3.75-3.66 (m, 1H), 3.11-3.03 (m, 1H), 2.96-2.85 (m, 2H), 2.72-2.61 (m, 1H). ^{13}C NMR (100MHz, DMSO- d_6 , 298 K) δ (ppm) = 187.5, 141.0, 140.0, 132.8, 126.1, 125.8, 120.8, 119.1, 113.0, 56.3, 31.7, 24.5, 22.8. EI HRMS m/z calculated for $C_{13}H_{11}BrN_2O_3$: 321.9953, found : 321.9958.

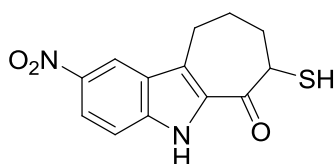


Synthesis of 2-15a: To a solution of potassium thioacetate (2.39 g, 20.98 mmol) dissolved in 15 mL of anhydrous DMF was added a solution of the bromide **2-14a** (5.28 g, 20.98 mmol) dissolved in 25 mL of anhydrous DMF drop wise over a period of 5 minutes. The reaction mixture was stirred for 4 h and quenched with 50 mL of water. The mixture was extracted with 3x15 mL of DCM and washed with 3 x 25 mL of water. The organic layers were combined and concentrated by rotary evaporation, to obtain the corresponding thioacetate (4.61 g, 18.74 mmol, 90%). The crude thioacetate was dissolved in 75 mL of dry acetonitrile and an equivalent of cysteamine hydrochloride was added to the solution followed by addition of an equivalent of sodium bicarbonate. The reaction mixture was stirred for 8-10 h and the reaction was quenched by 10% hydrochloride solution followed by the addition of 100 mL of water. Then, 3 x 40 mL of DCM was used to extract the organic layers and washed with 3 x 50 mL of water before the organic layers were pooled and dried over MgSO₄. Reduction of solvent was carried out under reduced pressure to yield the title compound **2-15a** (3.32 g, 16.20 mmol, 85% or 77% overall yield) as a pale yellow solid. M.P. 180.6-182.2 °C. ¹H NMR (400 MHz, CDCl₃, 298 K) δ (ppm) = 8.94 (s, br, 1H), 7.70 (d, *J* = 8.2 Hz, 1H), 7.39-7.36 (m, 2H), 7.19-7.13 (m, 1H), 3.92 (d, *J* = 7.5 Hz, 2H), 2.66 (s, 3H), 2.17 (t, *J* = 7.5 Hz, 1H); ¹³C NMR (100MHz, CDCl₃ with few drops of DMSO-*d*₆, 298 K) δ (ppm) = 187.5, 136.7, 130.2, 128.0, 125.9, 120.6, 119.5, 119.2, 112.1, 32.3, 10.7. EI HRMS *m/z* calculated for C₁₁H₁₁NOS: 205.0561, found : 205.0565.



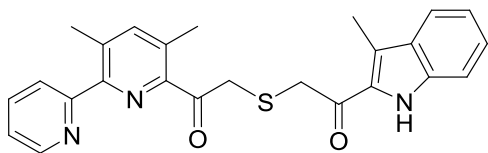
Synthesis of 2-15b: The title compound was synthesized in a similar manner as described for compound **2-15a** in an

overall yield of 80 %. M.P. 201.2-204.0 °C. ^1H NMR (400 MHz, CDCl_3 , 298 K) δ (ppm) = 9.14 (s, br, 1H), 8.51-8.49 (m, 1H), 8.04 (dd, $J = 8.6$ Hz, $J = 1.6$ Hz, 1H), 7.40-7.38 (m, 1H), 4.41 (q, $J = 7.0$ Hz, 2H), 3.92 (d, $J = 6.6$ Hz, 2H), 2.70 (s, 3H), 2.16 (t, $J = 6.6$ Hz, 1H), 1.43 (t, $J = 7.0$ Hz, 3H); ^{13}C NMR (100MHz, CDCl_3 , 298 K) δ (ppm) = 187.6, 167.1, 138.7, 131.8, 128.4, 127.7, 124.6, 122.9, 120.6, 111.7, 60.9, 32.8, 14.4, 11.2. ESI HRMS m/z calculated for $\text{C}_{14}\text{H}_{15}\text{NO}_3\text{S}$: 277.0773, found : 277.0785.



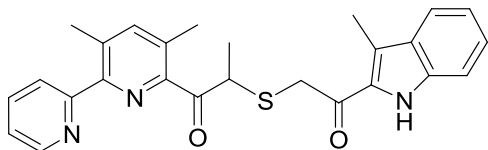
Synthesis of 2-18: To a solution of Potassium thioacetate

(0.97 g, 8.51 mmol) in 10 mL dry DMF, was added a solution of bromide (2.75 g, 8.51 mmol) in 15 mL dry DMF, drop wise over a period of 15 min. and stirred at room temperature for 16 h The reaction mixture was poured in to 50 mL water and stirred for 20 minutes before filtering the thioacetate as yellow solid. To the solution of thioacetate (2.5 g, 7.86 mmol) in 100 mL of dry acetonitrile, was added cysteamine hydrogen chloride (0.89 g, 7.86 mmol) followed by the addition of sodium bicarbonate (0.66 g, 7.86 mmol). The mixture was stirred for 28 h and then treated with 30 mL of 10% HCl solution. The resultant mixture was stirred for 15 minutes and filtered off to collect the yellowish green thiol as solid (1.99 g, 7.23 mmol, 85%). M.P. 210.5-212.2 °C. ^1H NMR (400 MHz, $\text{DMSO}-d_6$, 298 K) δ (ppm) = 12.22 (s, br, 1H), 8.72 (d, $J = 2.0$ Hz, 1H), 8.13 (dd, $J = 8.9$ Hz, $J = 2.0$ Hz, 1H), 7.53 (d, $J = 8.9$ Hz, 1H), 4.38-4.32 (m, 1H), 3.36-3.25 (m, 1H), 3.13-3.00 (m, 1H), 2.50-2.43 (m, 2H), 2.10-1.95 (m, 2H). ^{13}C NMR (100MHz, $\text{DMSO}-d_6$, 298 K) δ (ppm) = 191.4, 140.9, 139.7, 133.9, 126.1, 125.5, 120.5, 118.8, 113.0, 47.6, 31.7, 24.2, 22.9. EI HRMS m/z calculated for $\text{C}_{13}\text{H}_{12}\text{N}_2\text{O}_3\text{S}$: 276.0569, found : 276.0558.



Synthesis of 2-19a: To a solution of **2-15a** (1.33 g, 6.47 mmol) in 10 mL of dry DCM, a solution of **2-10a** (1.97 g, 6.47 mmol) in 10 mL of dry DCM was added drop wise over a period of 10

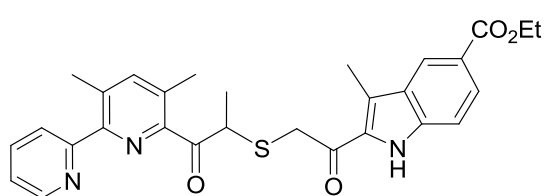
minutes. 2,6-lutidine (0.75 mL, 6.47 mmol) was added *via* syringe to the reaction mixture and stirred for 3 h. The reaction mixture was quenched using citric acid solution and re-extracted with 15 mL of DCM. The organic layers are combined and dried over MgSO₄ and concentrated under reduced pressure. Thus obtained crude is subjected to flash column chromatography (1:4, EtOAc:DCM) affording the pure thioether, **2-19a** as a yellow solid (2.22 g, 5.18 mmol, 80 %). M.P. 185.0-188.2 °C. ¹H NMR (400 MHz, CDCl₃, 298 K) δ (ppm) = 9.39 (s, 1H), 8.63 (dq, *J* = 4.9 Hz, *J* = 0.7 Hz, 1H), 7.90 (dt, *J* = 8.0 Hz, *J* = 0.7 Hz, 1H), 7.74-7.78 (m, 1H), 7.66 (d, *J* = 8.0 Hz, 1H), 7.49 (s, 1H), 7.35-7.30 (m, 2H), 7.24 (dd, *J* = 4.9 Hz, 1H), 7.13 (dd, *J* = 8.0 Hz, 1H), 4.28 (s, 2H), 3.95 (s, 2H), 2.65 (s, 3H), 2.60 (s, 3H), 2.59 (s, 3H). ¹³C NMR (100MHz, CDCl₃, 298 K) δ (ppm) = 197.6, 187.5, 158.3, 152.6, 148.4, 147.3, 144.0, 137.0, 136.8, 136.7, 135.7, 131.3, 129.0, 126.9, 124.45, 123.0, 121.5, 120.4, 120.1, 112.2, 40.0, 38.0, 20.6, 20.1, 11.3. EI HRMS *m/z* calculated for C₂₅H₂₃N₃O₂S : 429.1511, found : 429.1509.



Synthesis of 2-19b: The title compound **2-19b** was synthesized in the same manner as described for **2-19a** in 80 % yield. M.P. 188.8-190.4 °C. ¹H

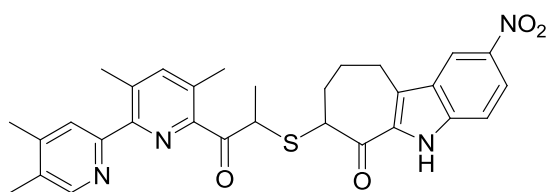
NMR (400 MHz, CDCl₃, 298 K) δ (ppm) = 9.45 (s, br, 1H), 8.58 (dq, *J* = 4.7 Hz, *J* = 0.8 Hz, 1H), 7.85 (dt, *J* = 7.8 Hz, *J* = 1.2 Hz, 1H), 7.68 (td, *J* = 7.8 Hz, *J* = 2.0 Hz, 1H), 7.60

(d, $J = 8.2$ Hz, 1H), 7.42 (s, 1H), 7.29-7.27 (m, 2H), 7.18-7.15 (m, 1H), 7.10-7.08 (m, 1H), 5.31 (q, $J = 7.4$ Hz, 1H), 3.87 (dd, $J = 32.0$ Hz, $J = 15.6$ Hz, 2H), 2.58 (s, 3H), 2.51 (s, 3H), 2.45 (s, 3H), 1.56 (d, $J = 7.4$ Hz, 3H); ^{13}C NMR (100MHz, CDCl_3 , 298 K) δ (ppm) = 198.4, 187.3, 158.0, 152.1, 148.1, 147.6, 143.4, 136.5, 136.4, 136.0, 135.4, 131.0, 128.6, 126.4, 124.1, 122.7, 121.1, 120.0, 119.5, 111.8, 41.3, 39.1, 20.1, 19.7, 16.7, 10.9. EI HRMS m/z calculated for $\text{C}_{26}\text{H}_{25}\text{N}_3\text{O}_2\text{S}$: 443.1667, found : 443.1658.



Synthesis of 2-19c: The title compound **2-19c** was synthesized in the same manner as described for **2-19a** in 82% yield. M.P.

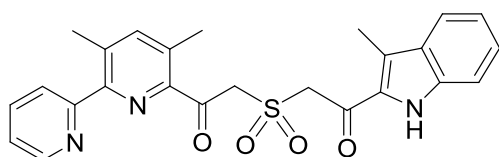
175.2-177.8 °C. ^1H NMR (400 MHz, CDCl_3 , 298 K) δ (ppm) = 9.55 (s, br, 1H), 8.62 (d, $J = 4.7$ Hz, 1H), 8.42 (s, 1H), 8.00 (d, $J = 8.2$ Hz, 1H), 7.84 (d, $J = 7.8$ Hz, 1H), 7.74 (t, $J = 7.8$ Hz, 1H), 7.44 (s, 1H), 7.30 (d, $J = 8.2$ Hz, 1H), 7.22 (t, $J = 6.6$ Hz, 1H), 5.32 (q, $J = 7.0$ Hz, 1H), 4.41 (q, $J = 7.0$ Hz, 2H), 3.89 (dd, $J = 39.5$ Hz, $J = 15.2$ Hz, 2H), 2.59 (s, 3H), 2.50 (s, 6H), 1.57 (d, $J = 7.0$ Hz, 3H), 1.43 (t, $J = 7.0$ Hz, 3H); ^{13}C NMR (100MHz, CDCl_3 , 298 K) δ (ppm) = 198.9, 187.6, 167.4, 158.4, 152.6, 148.6, 148.0, 143.8, 138.8, 136.8, 136.4, 135.9, 132.5, 128.6, 127.6, 124.9, 124.5, 123.2, 122.9, 121.1, 111.8, 61.2, 41.7, 39.6, 20.4, 20.4, 20.1, 16.6, 14.8, 11.3. EI HRMS m/z calculated for $\text{C}_{29}\text{H}_{29}\text{N}_3\text{O}_4\text{S}$: 515.1879, found : 515.1886.



Synthesis of 2-19d: The title compound **2-19d** was synthesized in the same manner as described for **2-19a** except that acetonitrile

was used as solvent giving 85% product yield. M.P. 205.8-207.5 °C. ^1H NMR (400 MHz, CDCl_3 , 298 K) δ (ppm) = 9.62 (s, br, 1H), 8.58 (s, 1H), 8.32 (s, 1H), 7.72 (d, $J = 8.6$ Hz,

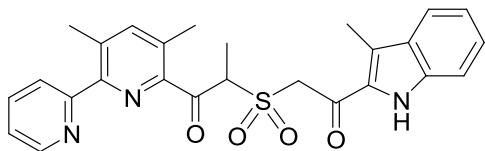
1H), 7.48 (s, 1H), 7.40 (s, 1H), 3.84 (q, $J = 7.0$ Hz, 1H), 3.22-3.16 (m, 1H), 2.88-2.67 (m, 2H), 2.64 (s, 3H), 2.54 (s, 3H), 2.23 (s, 3H), 2.17 (s, 3H), 2.19-2.07 (m, 2H), 1.93-1.87 (m, 2H), 1.51 (d, $J = 7.0$ Hz, 3H); ^{13}C NMR (100MHz, CDCl_3 , 298 K) δ (ppm) = 199.2, 191.2, 155.2, 148.5, 143.6, 141.8, 139.8, 136.1, 134.5, 132.3, 127.1, 125.3, 121.3, 120.3, 118.8, 112.1, 52.8, 43.9, 29.5, 25.8, 22.8, 22.6, 19.9, 19.5, 16.6, 16.4. ESI HRMS m/z calculated for $\text{C}_{30}\text{H}_{30}\text{N}_4\text{O}_4\text{S}$: 542.1988, found : 542.1996.



Synthesis of 2-20a: The thioether **2-19a** (1.00 g, 2.34 mmol) was dissolved in 15 mL of acetonitrile followed by the addition mixture of urea hydrogen peroxide, (UHP) (0.88 g, 9.32 mmol) and trifluoroacetic anhydride, (TFAA) (0.99 mL, 6.99 mmol) in 10 mL acetonitrile at 0 °C. The reaction mixture was brought to room temperature and stirred for 120 minutes and diluted with 40 mL of water. The sulfone was extracted with 2 x 40 mL DCM, the organic layers were combined and washed with 2 x 50 mL of water and dried over MgSO_4 . The solvent was removed by rotary evaporation affording the desired product. Flash column chromatography was carried out using 2% methanol in DCM to elute the pure sulfone **2-20a** (0.97 g, 2.11 mmol, 90%). M.P. 188.8-190.3 °C. ^1H NMR (400 MHz, CDCl_3 , 298 K) δ (ppm) = 9.21 (s, 1H), 8.62 (d, $J = 4.9$ Hz, 1H), 7.89 (d, $J = 7.8$ Hz, 1H), 7.76 (dt, $J = 7.8$ Hz, $J = 1.2$ Hz, 1H), 7.66 (d, $J = 8.0$ Hz, 1H), 7.53 (s, 1H), 7.36-7.31 (m, 2H), 7.22 (dd, $J = 4.9$ Hz, $J = 0.7$ Hz, 1H), 7.14 (dd, $J = 8.0$ Hz, $J = 1.2$ Hz, 1H), 5.44 (s, 2H), 4.96 (s, 2H), 2.66 (s, 3H), 2.61 (s, 3H), 2.61 (s, 3H). ^{13}C NMR (100MHz, CDCl_3 , 298 K) δ (ppm) = 191.6, 180.9, 157.6, 153.1, 148.3, 146.4, 144.1, 138.2, 137.3, 136.9, 136.5,

131.6, 128.8, 127.9, 124.4, 123.2, 122.5, 121.7, 120.8, 112.3, 62.0, 61.0, 20.5, 20.1, 11.3.

EI HRMS m/z calculated for $C_{25}H_{23}N_3O_4S$: 461.1409, found : 461.1407.

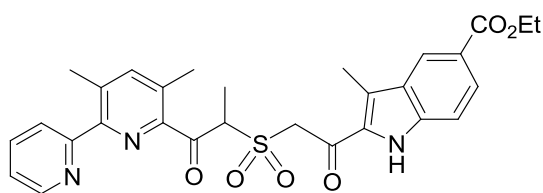


Synthesis of 2-20b: The title compound **2-20b**

was synthesized in the same manner as described

for **2-20a** in 85% yield. M.P. 195.0-197.2 °C. 1H

NMR (400 MHz, $CDCl_3$, 298 K) δ (ppm) = 9.42 (s, 1H), 8.52 (d, $J = 4.7$ Hz, 1H), 7.8 (dt, $J = 7.8$ Hz, $J = 1.2$ Hz, 1H), 7.63 -7.59 (m, 2H), 7.5 (s, 1H), 7.34-7.27 (m, 2H), 7.13-7.05 (m, 2H), 6.41 (q, $J = 7.4$ Hz, 1H), 4.76 (dd, $J = 124.5$ Hz, $J = 14.8$ Hz, 2H), 2.64 (s, 3H), 2.54 (s, 3H), 2.48 (s, 3H), 1.77 (d, $J = 7.4$ Hz, 3H); ^{13}C NMR (100MHz, $CDCl_3$, 298 K) δ (ppm) = 194.3, 180.1, 157.3, 153.7, 148.2, 146.3, 144.0, 143.8, 137.5, 136.4, 136.3, 131.4, 128.4, 124.1, 122.7, 122.5, 121.4, 121.2, 120.4, 112.1, 63.6, 63.5, 20.2, 19.9, 11.7, 10.8. EI HRMS m/z calculated for $C_{26}H_{25}N_3O_4S$: 475.1566, found : 475.1562.



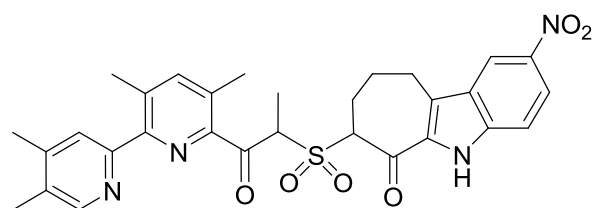
Synthesis of 2-20c: The title compound **2-**

20c was synthesized in the same manner as

described for **2-20a** in 95% yield. M.P.

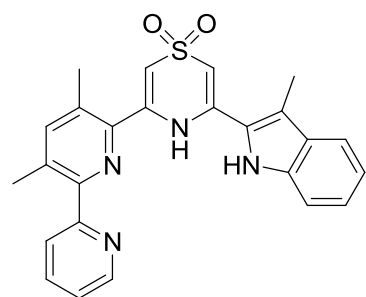
182.6-185.0 °C. 1H NMR (400 MHz, $CDCl_3$, 298 K) δ (ppm) = 9.55 (s, 1H), 8.56 (d, $J = 4.7$ Hz, 1H), 8.44 (s, 1H), 8.04-8.01 (m, 1H), 7.80 (d, $J = 7.6$ Hz, 1H), 7.70 (t, $J = 7.6$ Hz, 1H), 7.54 (s, 1H), 7.32 (d, $J = 8.8$ Hz, 1H), 7.16 (t, $J = 7.6$ Hz, 1H), 6.38 (q, $J = 7.0$ Hz, 1H), 4.76 (dd, $J = 176.9$ Hz, $J = 14.6$ Hz, 2H), 4.42 (q, $J = 7.0$ Hz, 2H), 2.67 (s, 3H), 2.58 (s, 3H), 2.55 (s, 3H), 1.77 (d, $J = 7.0$ Hz, 3H), 1.43 (t, $J = 7.0$ Hz, 3H); ^{13}C NMR (100MHz, $CDCl_3$, 298 K) δ (ppm) = 194.4, 180.1, 166.9, 157.2, 152.6, 148.2, 146.4, 144.1, 139.2, 137.7, 136.8, 136.6, 132.6, 128.2, 124.8, 124.2, 123.1, 111.9, 63.8, 60.9,

20.2, 14.4, 11.9, 10.9. EI HRMS m/z calculated for $C_{29}H_{29}N_3O_6S$: 547.1777, found : 547.1784.



Synthesis of 2-20d: The title compound **2-20d** was synthesized in the same manner as described for **2-20a** in 96%

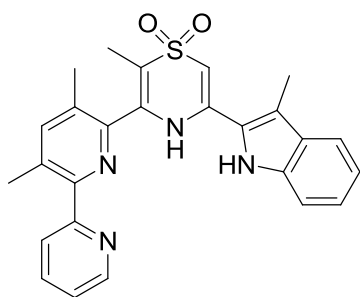
yield. M.P. 210.5-213.2 °C. 1H NMR (400 MHz, $CDCl_3$, 298 K) δ (ppm) = 10.08 (s, br, 1H), 8.59 (s, 1H), 8.37 (s, 1H), 8.21 (d, J = 8.6 Hz, 1H), 7.57 (s, 1H), 7.50 (s, 1H), 4.86 (q, J = 7.0 Hz, 1H), 4.41 (q, J = 7.0 Hz, 1H), 3.22-3.12 (m, 2H), 2.87-2.75 (m, 2H), 2.66 (s, 3H), 2.48 (s, 3H), 2.21-2.19 (m, 2H), 2.18 (s, 3H), 2.02 (s, 3H), 1.74 (d, J = 7.0 Hz, 3H); ^{13}C NMR (100MHz, $CDCl_3$, 298 K) δ (ppm) = 193.6, 187.4, 155.1, 153.1, 149.0, 146.8, 144.1, 143.0, 139.4, 137.2, 134.2, 132.1, 127.1, 124.9, 122.2, 119.2, 119.0, 112.5, 71.0, 64.9, 59.7, 26.6, 25.2, 22.8, 22.8, 19.9, 19.1, 16.6, 16.0, 10.8. EI HRMS m/z calculated for $C_{30}H_{30}N_4O_6S$: 574.1886, found : 574.1882.



Synthesis of 2-1a: Compound **2-1a** was synthesized by refluxing the solution of compound **2-20a** (1.2 g, 2.60 mmol) in acetic acid in the presence of ammonium acetate (1.2 g, 15.62 mmol) for 18 h before the mixture was poured in to ice and stirred to precipitate. The crude was

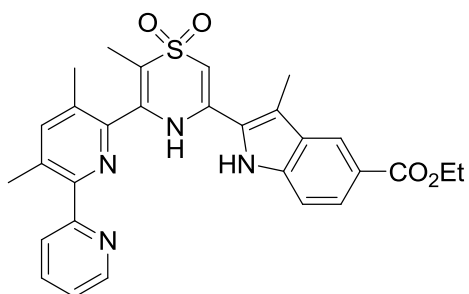
purified by using flash column chromatography using a solvent system of 3% methanol in dichloromethane yielding pure pale yellow crystals (0.92 g, 2.08 mmol, 80 %). 1H NMR (400 MHz, $CDCl_3$, 298 K) δ (ppm) = 10.01 (s, 1H), 9.83 (s, 1H), 8.66 (d, J = 4.9 Hz, 1H), 7.81 (td, J = 7.8 Hz, J = 1.2 Hz, 1H), 7.66 (dt, J = 7.8 Hz, J = 1.2 Hz, 1H), 7.55 (d, J = 8.0 Hz, 1H), 7.51 (s, 1H), 7.37 (d, J = 4.8 Hz, 1H), 7.34 (dd, J = 7.6 Hz, J = 1.2

Hz, 1H), 7.25 (dd, $J = 7.6$ Hz, $J = 1.2$ Hz, 1H), 7.12 (dd, $J = 8.0$ Hz, 1H), 6.22 (d, $J = 3.7$ Hz, 1H), 6.09 (d, $J = 3.7$ Hz, 1H), 2.50 (s, 3H), 2.49 (s, 3H), 2.39 (s, 3H). ^{13}C NMR (100MHz, CDCl_3 , 298 K) δ (ppm) = 157.2, 153.3, 148.8, 144.4, 143.9, 139.5, 137.4, 137.0, 136.6, 134.2, 132.5, 129.1, 126.0, 124.4, 123.5, 121.1, 119.8, 113.5, 111.7, 103.9, 99.6, 21.0, 19.5, 9.9. ESI HRMS m/z calculated for $\text{C}_{25}\text{H}_{22}\text{N}_4\text{O}_2\text{SNa}$: 465.1371, found : 465.1361.



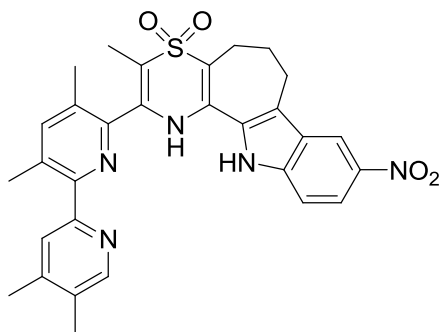
Synthesis of 2-1b: Compound **2-1b** was made in accordance with the synthesis of **2-1a**, using 10 equivalents of Ammonium acetate, in 85 % yield, upon refluxing for 36 h. ^1H NMR (400 MHz, CDCl_3 , 298 K) δ (ppm) = 11.41 (s, br, 1H), 10.01 (s, br, 1H), 8.62 (d, $J =$

4.9 Hz, 1H), 7.75 (t, $J = 7.8$ Hz, 1H), 7.65-7.56 (m, 1H), 7.40-7.30 (m, 1H), 7.29 (s, 1H), 7.23-7.18 (m, 1H), 7.09-7.01 (m, 2H), 6.99-6.93 (m, 1H), 6.03 (s, 1H), 2.52 (s, 3H), 2.41 (s, 3H), 1.87 (s, 3H), 1.08 (s, 3H). ^{13}C NMR (100MHz, CDCl_3 , 298 K) δ (ppm) = 152.1, 149.2, 148.0, 142.1, 137.5, 136.5, 136.2, 135.7, 133.2, 132.3, 129.0, 125.7, 124.3, 123.6, 123.2, 120.0, 119.4, 113.6, 111.7, 110.8, 109.8, 98.5, 19.8, 17.4, 10.4, 7.0. EI HRMS m/z calculated for $\text{C}_{26}\text{H}_{24}\text{N}_4\text{O}_2\text{S}$: 456.1620, found : 457.1626.



Synthesis of 2-1c: Compound **2-1c** was made in accordance with the synthesis of **2-1a**, using 10 equivalents of ammonium acetate, in 82 % yield, upon refluxing for 28 h. ^1H NMR (400 MHz,

CDCl₃, 298 K) δ (ppm) = 12.37 (s, br, 1H), 10.62 (s, br, 1H), 8.60 (d, J = 3.9 Hz, 1H), 8.38 (s, 1H), 7.80 (t, J = 7.8 Hz, 1H), 7.69-7.67 (m, 1H), 7.38-7.35 (m, 1H), 7.26-7.25 (m, 1H), 7.14 (d, J = 7.8 Hz, 1H), 6.87 (d, J = 8.6 Hz, 1H), 6.07 (s, 1H), 4.35 (q, J = 7.0 Hz, 2H), 2.58 (s, 3H), 2.41 (s, 3H), 1.76 (s, 3H), 1.40 (t, J = 7.0 Hz, 3H), 0.84 (s, 3H). ¹³C NMR (100MHz, CDCl₃, 298 K) δ (ppm) = 167.6, 149.3, 148.0, 142.3, 138.5, 136.9, 136.6, 135.3, 133.3, 132.1, 128.5, 126.9, 124.4, 123.8, 123.0, 121.6, 115.2, 111.9, 110.3, 109.8, 98.9, 60.6, 42.13, 19.9, 17.3, 14.4, 10.7, 6.8. ESI HRMS m/z calculated for C₂₉H₂₈N₄O₄S : 528.1831, found : 528.1838.



Synthesis of 2-1d: Compound **2-1d** was made in accordance with the synthesis of **2-1a**, using 10 equivalents of ammonium acetate, in 82 % yield, upon refluxing for 28 h. ¹H NMR (400 MHz, CDCl₃, 298 K) δ (ppm) = 13.60 (s, br, 1H), 10.85 (s, br, 1H),

8.56 (s, 1H), 8.33 (s, 1H), 7.82 -7.80 (m, 1H), 7.26-7.22 (m, 1H), 7.19-7.16 (m, 1H), 7.12 (s, 1H), 6.85-6.83 (m, 1H), 6.72-6.66 (m, 1H), 3.53-3.42 (m, 2H), 3.32-3.12 (m, 2H), 2.47-2.44 (m, 6H), 3.34-2.31 (m, 6H), 1.26-1.18 (m, 2H), 0.57 (s, 3H), 1.40 (t, J = 7.0 Hz, 3H), 0.84 (s, 3H). ¹³C NMR (100MHz, DMSO-*d*₆, 298 K) δ (ppm) = 154.3, 151.1, 150.8, 149.2, 147.5, 139.2, 138.5, 133.7, 133.3, 128.7, 127.6, 124.4, 124.1, 123.4, 121.9, 121.6, 120.8, 118.4, 112.3, 111.8, 110.5, 108.3, 31.3, 29.6, 24.2, 17.8, 16.5, 14.7, 13.4, 6.9. EI HRMS m/z calculated for C₃₀H₂₉N₅O₄S : 555.1940, found : 555.1946.

2.9 References

1. Scherman, O. A.; Ligthart, G. B. W. L.; Ohkawa, H.; Sijbesma, R. P.; Meijer, E.

- W. *PNAS* **2006**, *103* (32), 11850-11855.
2. (a) Aida, T.; Meijer, E. W.; Stupp, S. I. *Science* **2012**, *335* (6070), 813-817; (b) De Greef, T. F. A.; Smulders, M. M. J.; Wolffs, M.; Schenning, A. P. H. J.; Sijbesma, R. P.; Meijer, E. W. *Chem. Rev.* **2009**, *109* (11), 5687-5754.
 3. (a) Kushner, A. M.; Vossler, J. D.; Williams, G. A.; Guan, Z. *J. Am. Chem. Soc.* **2009**, *131* (25), 8766-8768; (b) Shi, L.; Wang, X.; Sandoval, C. A.; Li, M.; Qi, Q.; Li, Z.; Ding, K. *Angew. Chem. Int. Ed.* **2006**, *45* (25), 4108-4112; (c) Huerta, E.; Metselaar, G. A.; Fragoso, A.; Santos, E.; Bo, C.; de Mendoza, J. *Angew. Chem. Int. Ed.* **2007**, *46* (1-2), 202-205.
 4. Appel, W. P. J.; Portale, G.; Wisse, E.; Dankers, P. Y. W.; Meijer, E. W. *Macromolecules* **2011**, *44* (17), 6776-6784.
 5. (a) Hirata, S.; Lee, K.-S.; Watanabe, T. *Adv. Funct. Mater.* **2008**, *18* (19), 2869-2879; (b) El-ghayoury, A.; Schenning, A. P. H. J.; van Hal, P. A.; van Duren, J. K. J.; Janssen, R. A. J.; Meijer, E. W. *Angew. Chem. Int. Ed.* **2001**, *40* (19), 3660-3663; (c) Lange, R. F. M.; Van Gurp, M.; Meijer, E. W. *J. Polym. Sci., Part A: Polym. Chem.* **1999**, *37* (19), 3657-3670.
 6. (a) Sijbesma, R. P.; Beijer, F. H.; Brunsveld, L.; Folmer, B. J. B.; Hirschberg, J. H. K. K.; Lange, R. F. M.; Lowe, J. K. L.; Meijer, E. W. *Science* **1997**, *278* (5343), 1601-1604; (b) Yan, X.; Xu, D.; Chi, X.; Chen, J.; Dong, S.; Ding, X.; Yu, Y.; Huang, F. *Adv. Mater.* **2012**, *24* (3), 362-369.

7. Brunsveld, L.; Folmer, B. J. B.; Meijer, E. W.; Sijbesma, R. P. *Chem. rev.* **2001**, *101* (12), 4071-4098.
8. Brunsveld, L.; Folmer, B. J. B.; Meijer, E. W. *MRS Bull.* **2000**, *25* (04), 49-53.
9. Eling, B.; Lindsay, C. I. Supramolecular polymer forming polymer. US7919110, 2002.
10. (a) Goodbrand, H. B. Phase change ink composition. US2003/0105185 A1, 2003; (b) Smith, T. W. Aqueous ink compositions. US2003/0079644, 2003; (c) Vanmaele, L.; Locculier, J.; Meijer, E. W.; Fransen, F.; Janssen, H. M. Ink composition containing a particular type of dye, and corresponding ink jet printing process. EP1310533 A2, 2003; (d) Asawa, Y.; Ishizuka, Y.; Hayakawa, E.; Pappas, S. P. Two-layer imageable element comprising thermally reversible polymers. WO02053627 A1, 2002; (e) Pappas, S. P.; Monk, A.; Saraiya, S.; Huang, J. Imageable element and composition comprising thermally reversible polymers. WO02053626 A1, 2002.
11. (a) Mouglin, N.; Livoreil, A.; Mondet, J. Cosmetic composition forming after application a supramolecular polymer. WO02098377 A1 2002; (b) Cooper, J. H. Cosmetic and personal care compositions. WO03032929 A2, 2003.
12. Goldoni, F. Laundry composition. WO02092744 A1, 2002.
13. Loontjens, J. A. Supramolecular Compound. EP1031589 A1, 2000.
14. Folmer, B. J. B.; Sijbesma, R. P.; Versteegen, R. M.; van der Rijt, J. A. J.; Meijer,

- E. W. *Adv. Mater.* **2000**, *12* (12), 874-878.
15. Bosman, A. W.; Sijbesma, R. P.; Meijer, E. W. *Mater. Today* **2004**, *7* (4), 34-39.
16. van Gemert, G. M. L.; Peeters, J. W.; Söntjens, S. H. M.; Janssen, H. M.;
Bosman, A. W. *Macromol. Chem. Phys.* **2012**, *213* (2), 234-242.
17. (a) Beijer, F. H.; Kooijman, H.; Spek, A. L.; Sijbesma, R. P.; Meijer, E. W.
Angew. Chem. Int. Ed. **1998**, *37* (1-2), 75-78; (b) Beijer, F. H.; Sijbesma, R. P.;
Kooijman, H.; Spek, A. L.; Meijer, E. W. *J. Am. Chem. Soc.* **1998**, *120* (27),
6761-6769.
18. de Greef, T. F. A.; Meijer, E. W. *Nature* **2008**, *453* (7192), 171-173.
19. Hirschberg, J. H. K. K.; Beijer, F. H.; van Aert, H. A.; Magusin, P. C. M. M.;
Sijbesma, R. P.; Meijer, E. W. *Macromolecules* **1999**, *32* (8), 2696-2705.
20. Mather, B. D.; Elkins, C. L.; Beyer, F. L.; Long, T. E. *Macromol. Rapid Commun.*
2007, *28* (16), 1601-1606.
21. S n t j e n s, S. H. M.; Renken, R. A. E.; van Gemert, G. M. L.; Engels, T. A. P.;
Bosman, A. W.; Janssen, H. M.; Govaert, L. E.; Baaijens, F. P. T. *Macromolecules*
2008, *41* (15), 5703-5708.
22. Guan, Z.; Roland, J. T.; Bai, J. Z.; Ma, S. X.; McIntire, T. M.; Nguyen, M. *J. Am.*
Chem. Soc. **2004**, *126* (7), 2058-2065.
23. Yamauchi, K.; Lizotte, J. R.; Long, T. E. *Macromolecules* **2003**, *36* (4), 1083-
1088.

24. Park, T.; Zimmerman, S. C. *J. Am. Chem. Soc.* **2006**, *128* (35), 11582-11590.
25. Rieth, L. R.; Eaton, R. F.; Coates, G. W. *Angew. Chem. Int. Ed.* **2001**, *40* (11), 2153-2156.
26. Li, J.; Viveros, J. A.; Wrue, M. H.; Anthamatten, M. *Adv. Mater.* **2007**, *19* (19), 2851-2855.
27. Wisse, E.; Spiering, A. J. H.; Dankers, P. Y. W.; Mezari, B.; Magusin, P. C. M. M.; Meijer, E. W. *J. Polym. Sci., Part A: Polym. Chem.* **2011**, *49* (8), 1764-1771.
28. (a) Kuhn, B.; Fuchs, J. E.; Reutlinger, M.; Stahl, M.; Taylor, N. R. *J. Chem. Inf. Model.* **2011**, *51* (12), 3180-3198; (b) Pranata, J.; Wierschke, S. G.; Jorgensen, W. L. *J. Am. Chem. Soc.* **1991**, *113* (8), 2810-2819; (c) Jorgensen, W. L.; Pranata, J. *J. Am. Chem. Soc.* **1990**, *112* (5), 2008-2010.
29. Schneider, H.-J.; Juneva, R. K.; Simova, S. *Chem. Ber.* **1989**, *122*, 1211-1213.
30. Sartorius, J.; Schneider, H.-J. *Chem. Eur. J.* **1996**, *2* (11), 1446-1452.
31. Wang, H.-B.; Mudraboyina, B. P.; Li, J.; Wisner, J. A. *Chem. Commun.* **2010**, *46* (39), 7343-7345.
32. Li, J.; Wisner, J. A.; Jennings, M. C. *Org. Lett.* **2007**, *9* (17), 3267-3269.
33. (a) Gröger, G.; Meyer-Zaika, W.; Böttcher, C.; Grün, F.; Ruthard, C.; Schmuck, C. *J. Am. Chem. Soc.* **2011**, *133* (23), 8961-8971; (b) Sun, H.; Lee, H. H.; Blakey, I.; Dargaville, B.; Chirila, T. V.; Whittaker, A. K.; Smith, S. C. *J. Phys. Chem. B* **2011**, *115* (38), 11053-11062; (c) Tang, Q.; Liang, Z.; Liu, J.; Xu, J.;

- Miao, Q. *Chem. Commun.* **2010**, 46 (17), 2977-2979; (d) Greco, E.; Aliev, A. E.; Lafitte, V. G. H.; Bala, K.; Duncan, D.; Pilon, L.; Golding, P.; Hailes, H. C. *New J. Chem.* **2010**, 34 (11); (e) Lafitte, V. G. H.; Aliev, A. E.; Horton, P. N.; Hursthouse, M. B.; Bala, K.; Golding, P.; Hailes, H. C. *J. Am. Chem. Soc.* **2006**, 128 (20), 6544-6545; (f) Spencer, E. C.; Howard, J. A. K.; Baruah, P. K.; Sanjayan, G. J. *CrystEngComm* **2006**, 8 (6); (g) Zhao, Y.-P.; Zhao, C.-C.; Wu, L.-Z.; Zhang, L.-P.; Tung, C.-H.; Pan, Y.-J. *J. Org. Chem.* **2006**, 71 (5), 2143-2146; (h) Schmuck, C.; Wienand, W. *Angew. Chem. Int. Ed.* **2001**, 40 (23), 4363-4369; (i) Lange, R. F. M.; Van Gorp, M.; Meijer, E. W. *J. Polym. Sci. A Polym. Chem.* **1999**, 37 (19), 3657-3670.
34. Chi, D. Y.; O'Neil, J. P.; Anderson, C. J.; Welch, M. J.; Katzenellenbogen, J. A. *J. Med. Chem.* **1994**, 37 (7), 928-937.
35. Li, J. The design of hydrogen bonded double helices. monograph, University of Western Ontario, London Ontario, 2009.
36. Hershenson, F. M.; Bauer, L. *J. Org. Chem.* **1969**, 34 (3), 655-660.
37. (a) Denmark, S. E.; Fan, Y. *Tetrahedron: Asymmetry* **2006**, 17 (4), 687-707; (b) Mongin, O.; Rocca, P.; Thomas-dit-Dumont, L.; Trecourt, F.; Marsais, F.; Godard, A.; Queguiner, G. *J. Chem. Soc., Perkin Trans. 1* **1995**, (19), 2503-2508.
38. (a) Shin, D.; Switzer, C. *Chem. Commun.*, **2007**, (42), 4401-4403; (b) Kaminski, T.; Gros, P.; Fort, Y. *Eur. J. Org. Chem.* **2003**, (19), 3855-3860.

39. Moutevelis-Minakakis, P.; Sinanoglou, C.; Loukas, V.; Kokotos, G. *Synth.* **2005**, *2005*, 933,938.
40. Dunn, A. D.; Guillermic, S. *Zeitschrift für Chemie* **1988**, *28* (2), 59-60.
41. Pugh, D. *Acta Crystallogr. C* **2006**, *62* (10), o590-o592.
42. Lyubov, D. M.; Fukin, G. K.; Cherkasov, A. V.; Shavyrin, A. S.; Trifonov, A. A.; Luconi, L.; Bianchini, C.; Meli, A.; Giambastiani, G. *Organometallics* **2009**, *28* (4), 1227-1232.
43. Pal, M.; Dakarapu, R.; Padakanti, S. *J. Org. Chem.* **2004**, *69* (8), 2913-2916.
44. Robinson, B. *Chem. Rev.* **1963**, *63* (4), 373-401.
45. Kost, A. N.; Gorbunova, S. M.; Budylin, V. A. *Khim. Geterotsikl+* **1971**, *11* (Journal Article), 1522-1526.
46. (a) Blight, B. A.; Camara-Campos, A.; Djurdjevic, S.; Kaller, M.; Leigh, D. A.; McMillan, F. M.; McNab, H.; Slawin, A. M. Z. *J. Am. Chem. Soc.* **2009**, *131* (39), 14116-14122; (b) Quinn, J. R.; Zimmerman, S. C.; Del Bene, J. E.; Shavitt, I. *J. Am. Chem. Soc.* **2007**, *129* (4), 934-941; (c) Murray, T. J.; Zimmerman, S. C. *J. Am. Chem. Soc.* **1992**, *114* (10), 4010-4011.
47. Lüning, U. *Angew. Chem.* **1991**, *103* (10), 1417-1418.
48. (a) Velazquez-Campoy, A.; Freire, E. *Nat. Protocols* **2006**, *1* (1), 186-191; (b) Thordarson, P. *Chem. Soc. Rev.* **2011**, *40* (3).
49. Bisson, A. P.; Carver, F. J.; Eggleston, D. S.; Haltiwanger, R. C.; Hunter, C. A.;

Livingstone, D. L.; McCabe, J. F.; Rotger, C.; Rowan, A. E. *J. Am. Chem. Soc.*

2000, *122* (37), 8856-8868.

50. (a) Li, X.; Fang, Y.; Deng, P.; Hu, J.; Li, T.; Feng, W.; Yuan, L. *Org. Lett.* **2011**, *13* (17), 4628-4631; (b) Zeng, J.; Wang, W.; Deng, P.; Feng, W.; Zhou, J.; Yang, Y.; Yuan, L.; Yamato, K.; Gong, B. *Org. Lett.* **2011**, *13* (15), 3798-3801; (c) Zeng, H.; Miller, R. S.; Flowers, R. A.; Gong, B. *J. Am. Chem. Soc.* **2000**, *122* (11), 2635-2644.

Chapter 3

3 The Effect of Sterics and Preorganization on Stability in Double-Helical AAA-DDD Complexes.

3.1 Contiguous Arrays for Hydrogen Bonded Complex Formation

Contiguous arrays have been reported as the ideal arrangement of hydrogen bond donor/acceptor pairs to build some of the most stable hydrogen bonded complexes known. As hypothesized initially by Jorgenson, secondary hydrogen bond interactions may contribute significantly to complex stability in these cases.¹ Therefore, in systems containing two, three or four hydrogen bonds, sequences with AA•DD, AA•DDD, AAA•DDD and AAAA•DDDD arrangements are expected to result in the most stable complexes² as a result of multiple attractive secondary interactions. Fused ring heterocyclic arrays have been well studied as frameworks for contiguous arrays in hydrogen bonded complexes.³

As outlined in the first chapter, the first experimental systems containing contiguous arrays were synthesized by Murray and Zimmerman⁴ who reported the association constants of an AA•DDD complex (Figure 3-1) to be $K_a = 3 \times 10^3 \text{ M}^{-1}$ and that of an AAA•DDD complex to be $K_a \geq 10^5 \text{ M}^{-1}$ in CDCl_3 . However, the AAA•DDD system examined was chemically unstable in the presence of acid. The system required addition of a proton scavenger (1,8-bis(dimethylamino)naphthalene) to solution during the binding studies to prevent a facile hydride shift occurring from C-4 of the DDD array to C-10 of the AAA array. Bell and Anslyn's positively charged AAA•DDD⁺ complex was synthesized by protonating the central pyridyl nitrogen of a

diaminopyridine derivative to form a pyridinium ion which also contributed to large values of the association constants ($K_a > 5 \times 10^5 \text{ M}^{-1}$) determined by UV-Vis titration experiments.

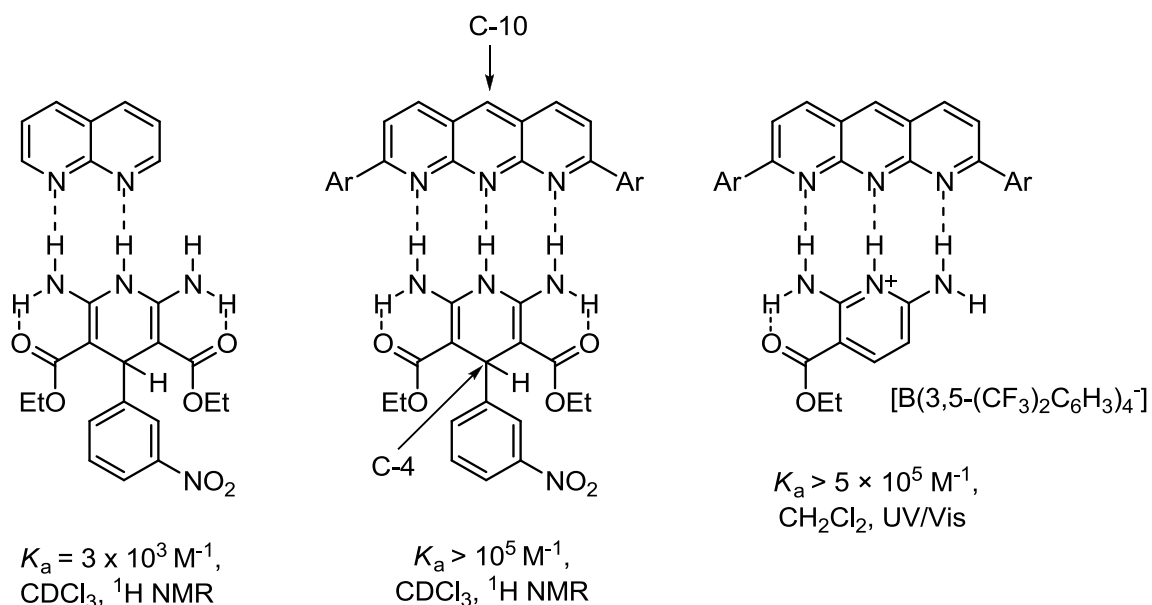


Figure 3-1 Early experimental examples of AA•DDD and AAA•DDD hydrogen bonding arrays reported by Zimmerman's group (left and middle) and Bell and Anslyn (right).

Neutral (AAA-DDD) and cationic (AAA•DDD⁺) complexes reported by David Leigh and co-workers,^{2c} based on triple hydrogen bonding have displayed exceptional K_a values on the order of 10^7 M^{-1} and 10^{10} M^{-1} , respectively. The binding constants were determined by fluorescence spectroscopy in dichloromethane (CH₂Cl₂). The first quadruple contiguous array AAAA•DDDD⁺ complex was reported by Lünig⁵ (as detailed in chapter one) with a very low association constant of 525 M^{-1} (Figure 3-2) due to numerous factors impeding complexation. Leigh's group has reported an extremely stable AAAA•DDDD⁺ complex with an association constant greater than $3 \times 10^{12} \text{ M}^{-1}$ determined using UV-Vis competition experiments in CH₂Cl₂. While any hydrogen bond

complex with an association constant approximately above 10^5 M^{-1} can be used as a motif for supramolecular architectures such as reversible polymers,⁶ these complexes that have K_a values much greater than 10^5 M^{-1} and may possess very interesting properties in supramolecular materials.

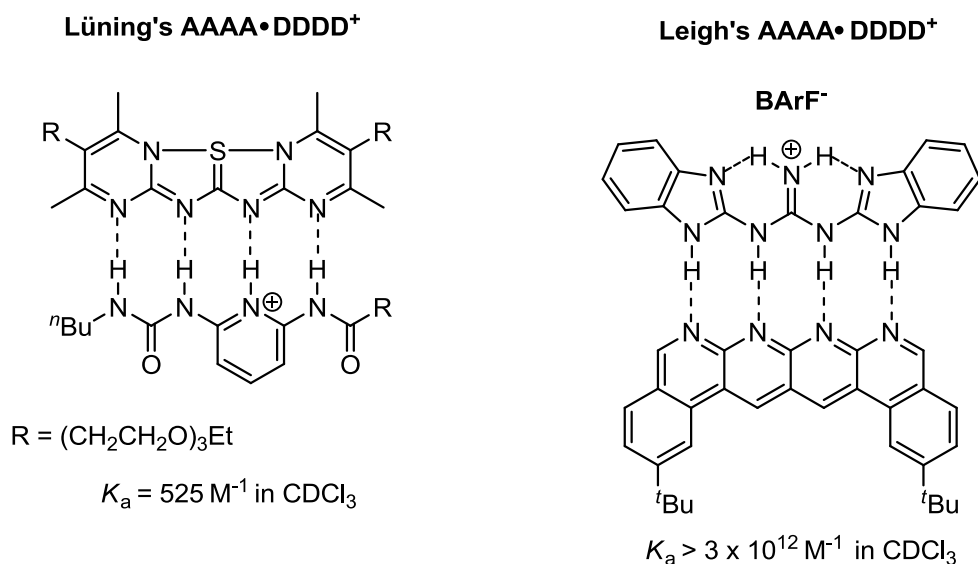


Figure 3-2 Two examples of complementary AAAA•DDDD⁺ hydrogen bonding complexes and their K_a values determined in CDCl_3 (left side)⁵ and CH_2Cl_2 (right side)^{2d}.

In the previous chapter, the synthesis and self-association of AADD arrays based on a double helical complex geometry were discussed in detail. The repulsive secondary interactions between the central A and D heterocycles (avoided by default in AAA•DDD complexes), the effects of substituents and the preorganizing effect of the trimethylene tether between the donor heterocycles on the overall stabilities were important factors to consider in the AADD array design that can be utilized while designing a new set of complementary helical hydrogen bonded complexes. As stated earlier, our research group reported a complementary double-helical system (Figure 3-3) where the DDD array was insoluble in CDCl_3 alone, but was drawn into solution to form a complex upon

addition of a terpyridyl derived AAA array. The lower limit for the association constant of the complex was calculated to be 10^5 M^{-1} in CDCl_3 .⁷ The calculated complexation induced shifts in the DDD arrays as a result of hydrogen bonding were $\Delta\delta = 5.60$ (N-H^a) and 4.73 (N-H^b) ppm supporting the formation of a very strong complex between the two arrays.

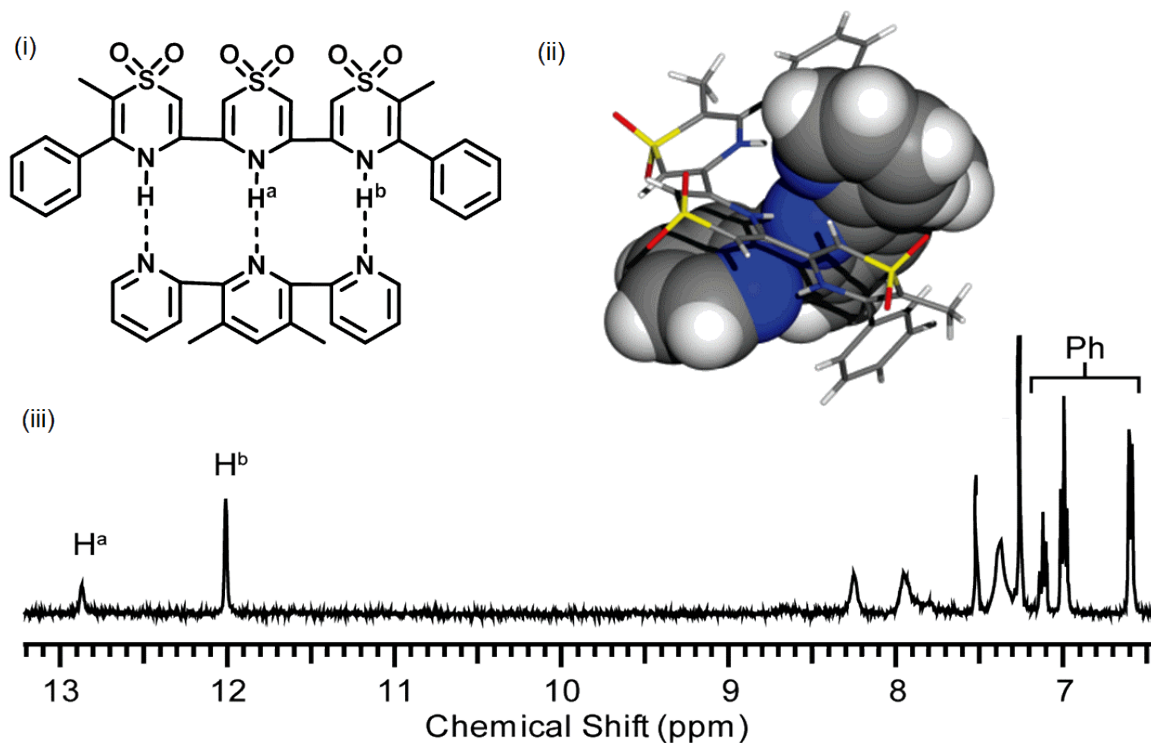


Figure 3-3 (i) A very stable complementary double helical AAA•DDD hydrogen bond complex with a K_a value $> 10^5 \text{ M}^{-1}$ in CDCl_3 ; (ii) solid state X-ray structure displaying the double-helical nature of the complex; (iii) Downfield region of the partial ^1H NMR spectrum of the AAA•DDD complex in CDCl_3 at room temperature indicating the complexation induced shifts of N-H^a and N-H^b.⁷

The high stability of the AAA•DDD complex motivated us to design and synthesize other AAA•DDD motifs using the same pyridine acceptors and mixed indole

and thiazine dioxide oligoheterocycles as DDD arrays (Figure 3-4). The K_a value of the original unsubstituted complex (**3-1a**•**3-2a**) was measured as $3.1 \times 10^3 \text{ M}^{-1}$ in CDCl_3 .

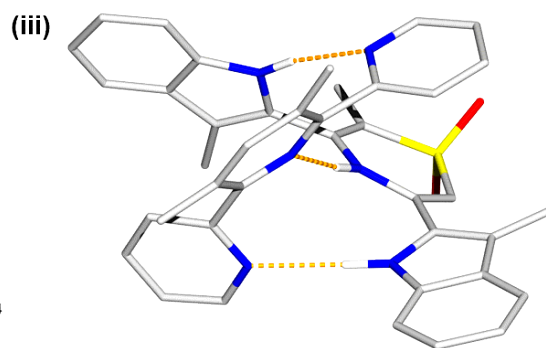
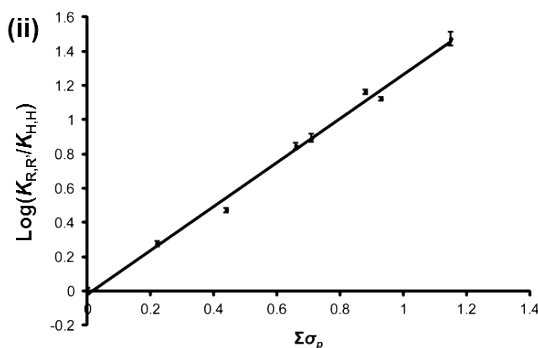
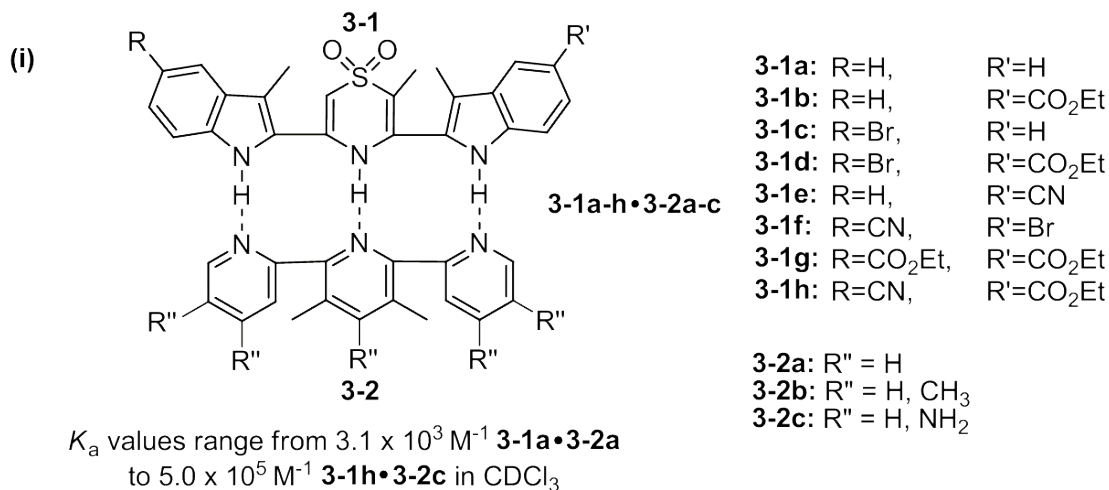


Figure 3-4 (i) Complexes **3-1a-h**•**3-2a-c** displaying an increase in the association constants by up to a factor of 30 in the cases studied; (ii) Plot of $\log(K_{R,R'}/K_{H,H})$ versus $\Sigma\sigma_p$ for the interaction of **3-1a-h** with **3-2a**; (iii) Optimized (HF 6-31G*) molecular model of the **3-1a**•**3-2a** complex.⁸

For a triply hydrogen bonded contiguous AAA•DDD system this value is lower than that measured for the ter(thiazine dioxide) complex by at least two orders of magnitude which may be attributed to the poor hydrogen bond donor character of the terminal indole heterocycles. The addition of electron withdrawing groups at the 5-position of the indole rings, increase the K_a value to $1.1 \times 10^5 \text{ M}^{-1}$ in CDCl_3 . Electron

donating functional groups were also incorporated with the pyridine acceptors demonstrating a similar trend in improving the stabilities of the complexes formed (**3-1h**•**3-2c**; $K_a = 5.0 \times 10^5 \text{ M}^{-1}$ in CDCl_3). A few DDD arrays were prepared incorporating electron withdrawing groups (eg. **3-1i** X = CN, Y = CN) that were insoluble and prevented the determination of binding constants, even at very low dilutions. Though there was a linear free energy relationship between the functional group Hammett values and the binding constants in all the cases examined there appeared to be no straightforward enthalpy-entropy compensation effect in the complexation.⁸

Overall, the various combinations of these modifications demonstrated a control over complex affinities of more than three orders of magnitude from 10^2 to $>10^5 \text{ M}^{-1}$ (or $> 20 \text{ kJ mol}^{-1}$) within the same underlying recognition motif. The predictable nature of these effects could be used to easily tailor a particular stability complex for applications where complementary hydrogen bond association is desirable as a design feature (e.g. supramolecular polymerization).

3.2 Results and Discussion

3.2.1 Design of the Donor Arrays

A combination of the substitutions discussed above and the preorganizational effect demonstrated in the previous chapter applied in our AAA•DDD system would presumably result in the formation of extremely stable complexes. In order to study this combination, a di/trimethylene tether was introduced between the central thiazine dioxide heterocycle and one of the terminal indole heterocycles (Figure 3-5). The DDD arrays can be oriented in a particular conformation by restricting the dihedral freedom of

adjacent donor heterocycles in this manner. This preorganization maintains the helical geometry of the DDD array, saving energy which otherwise would be spent bringing the molecule into the optimal conformation for binding.

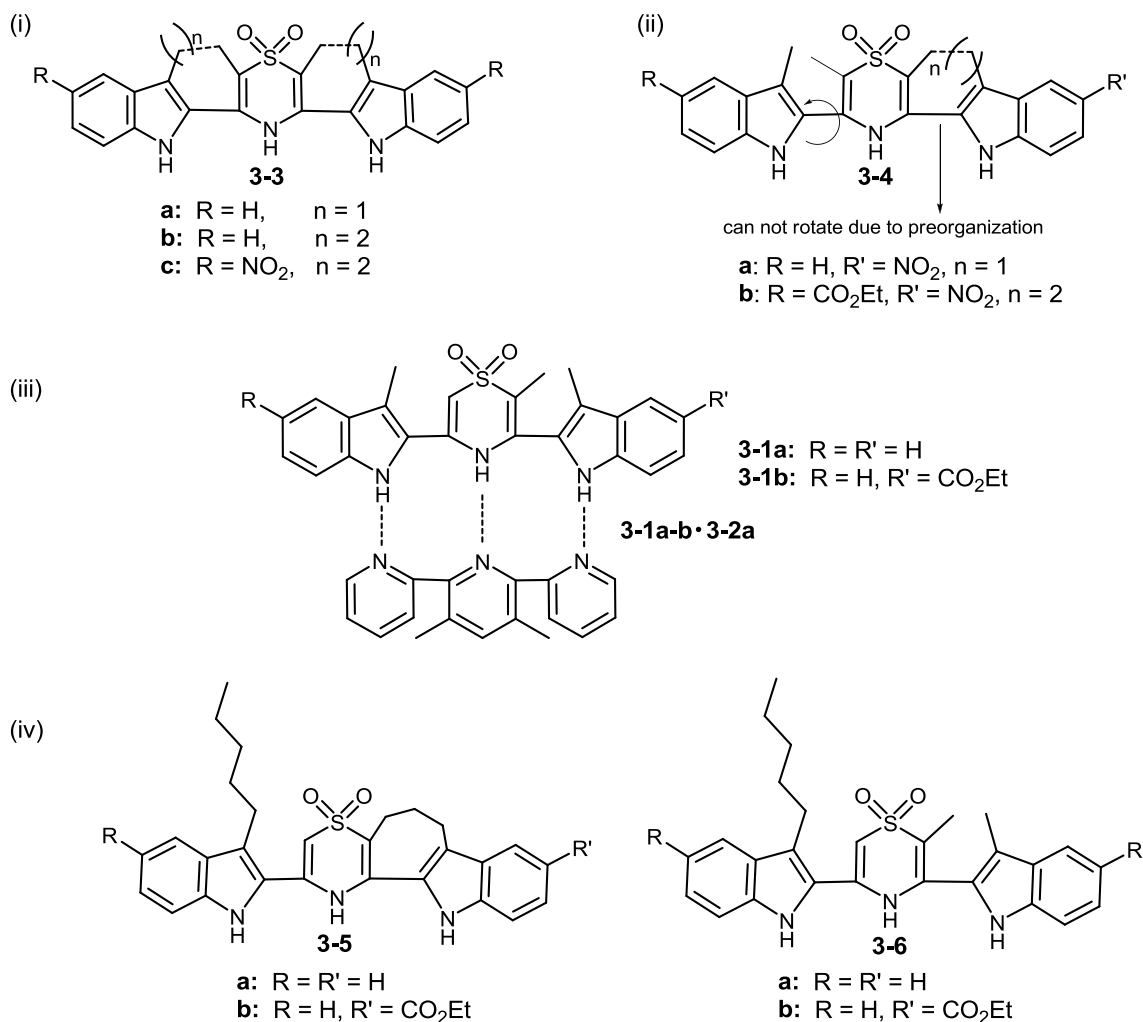


Figure 3-5 DDD arrays originally designed for the current study (i) The doubly-tethered symmetrical DDD arrays **3-3a-c**; (ii) The singly di/trimethylene tethered DDD arrays **3-4a-b**; (iii) Complex **3-1a,b•3-2a** used as a comparison in complex studies; (iv) Alkylated singly tethered and non-tethered DDD arrays **3-5a,b** and **3-6a,b**.

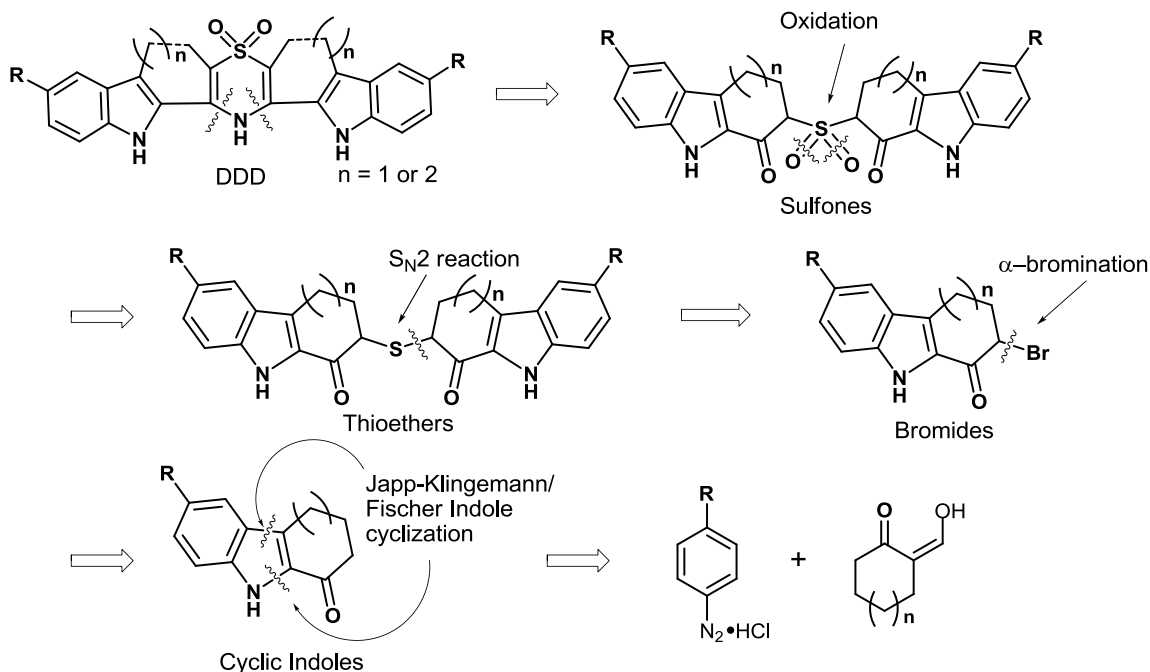
The previous chapter's results demonstrated that preorganization brought about by a di/trimethylene tether can increase the association constants by at least an order of

magnitude per tether. We intended to construct donor strands **3-3a-c** that would form exceptionally strong contiguous complementary complexes. Arrays **3-3a,b** were meant to probe the basic unsubstituted DDD skeleton and **3-3c** to study one of the strongest hydrogen bond donor arrays we could easily synthesize. Concurrently, the syntheses of **3-4a,b** was designed to explore a single preorganization (with both di/trimethylene tethers) and the effect of the two electron withdrawing groups (ester and nitro) on these donor arrays. As the trimethylene tether was expected to provide similar or even more demanding sterics compared to a methyl group attached to the thiazine dioxide, we anticipated that the presence of this group would avoid unwanted intermolecular hydrogen bonding between the DDD arrays thereby avoiding the problems with solubility previously encountered. Finally, the four alkylated DDD arrays, **3-5a-b** and **3-6a-b** were not originally part of the synthetic plan but were included later as a solution to accompanying insolubility issues that will be discussed later in this chapter. The binding studies of these alkylated contiguous complexes display interesting results upon comparison with those of **3-1a-b** and **3-2a**. The contiguous AAA array **3-2a** was used in the complexation studies with all the above DDD arrays to provide a consistent comparison.

3.2.2 Synthesis of 3-3a-c Donor Arrays

The synthesis of the symmetric DDD arrays **3-3a-c** consisting of di/trimethylene tethers on either side of the central donor heterocycle was planned through the retrosynthetic pathway pictured in Scheme 3-1. It would be realized through cyclization of a 3-sulfonyl-1,5-dione precursor. Sulfones are the oxidized forms of thioethers which can be oxidized using *m*CPBA or urea hydrogen peroxide and trifluoroacetic anhydride mixture. The condensation of α -ketobromides could be achieved by employing sodium

sulphide nonahydrate or sodium hydrogensulphide, forming the corresponding thioethers and sodium bromide. The rest of the intermediates are familiar from chapter 2.



Scheme 3-1 Retrosynthetic pathway leading from the preparation of doubly di/trimethylene tethered DDD arrays **3-3a-c** to commercially available anilines and cyclic ketones.

The initial reactions to synthesize the doubly tethered DDD arrays were carried out in a similar manner to those detailed in chapter two; Japp-Klingemann/Fischer Indole synthesis⁹ followed by bromination of the α -ketobromides using phenyl trimethylammonium tribromide.¹⁰ The reaction times were generally longer compared to the acyclic indole analogues. The bromination reactions took 12-16 h to reach completion. Condensation of the α -ketobromides took approximately 3 days (versus 3 h in the case of acyclic indole analogues) to yield the products in 85 - 90%. The thioethers were oxidized using *m*CPBA as an oxidant in DMF¹¹ as the thioethers were sparingly soluble in non-polar and most polar solvents except DMF and DMSO. Unfortunately all

the attempts for the final cyclization of the sulfone precursors to produce **3-3** were unsuccessful regardless of the reagents and conditions used (Table 3-1).

Table 3-1 Trials of reactions attempted for last step of scheme 3-1.

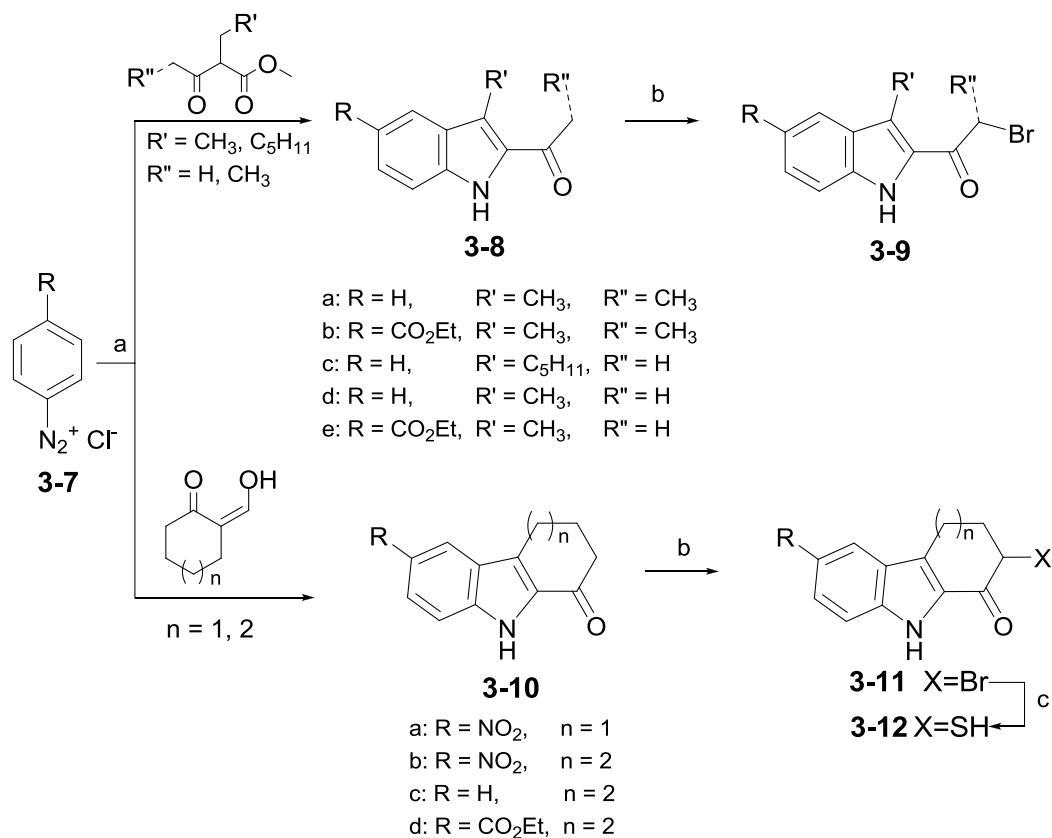
Reagent	Reaction Conditions	Results
6 to 25 eq. of ammonium acetate	Glacial acetic acid, reflux for 16 h. to 7 days	No reaction, starting materials recovered
6 to 8 eq. of ammonium acetate	Methanol, reflux 16 h. to 48 h.	Decomposed
6 to 8 eq. of ammonium acetate	Ethanol, reflux 16 h. to 48 h.	Decomposed
6 to 10 eq. of ammonium formate	Formic acid, N ₂ , reflux 16 h. to 48 h.	Decomposed
2 to 6 eq. of hydrazine	Ethanol, reflux 16 h. to 48 h.	No reaction, starting materials recovered

3.2.3 Synthesis of Single Trimethylene Tethered DDD Arrays

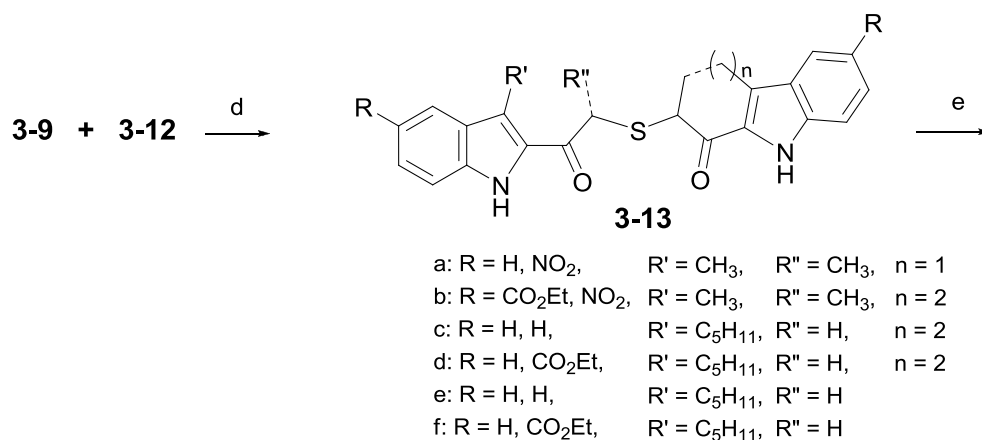
The failure of the last synthetic step to produce doubly trimethylene bridged DDD arrays left the remaining synthesis of singly di/trimethylene tethered DDD arrays **3-4a,b** (Scheme 3-2). Diazonium salts **3-7** of unsubstituted and substituted anilines were synthesized using sodium nitrite and hydrochloric acid at 0 °C, which readily react with a methyl oxopentanoate derivative¹² or formylated cyclic ketones¹³ to give corresponding hydrazone intermediates that were subjected to Fischer Indole cyclization requiring

approximately 24 to 36 h for reaction completion.

(i)

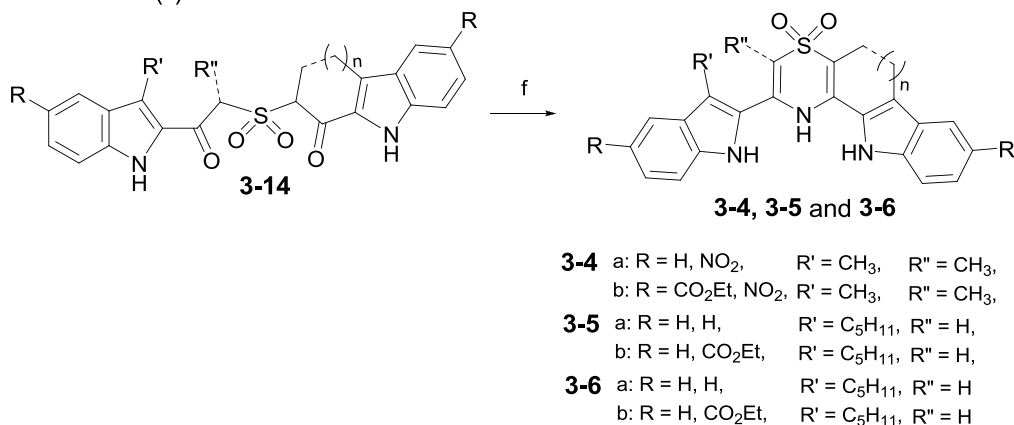


(ii)



Rest of the Scheme 3-2, continued on the following page...

Scheme 3-2 (ii) continued...



Scheme 3-2 General synthetic scheme to construct the singly tethered DDD arrays; Reaction conditions: (a) (i) HCl, H₂O, NaNO₂, KOH, EtOH, 0 °C to room temperature, (ii) HCOOH, reflux 2 h. - 36 h., 90%-almost quantitative yields; (b) Trimethylphenyl ammonium tribromide, dry THF, 40 °C 1.5 h. - 12 h., 75-80 % (c) (i) KSAc, Dry DMF, 4 h. 90-95% (ii) Cysteamine.HCl, NaHCO₃, MeCN, 24 hr. 85-92% (d) K₂CO₃, MeCN, H₂O, 2days, 80-85% (e) 2.1 eq. *m*CPBA, DMF, 0 °C to room temperature, 12 h. to 18 hr., 75-85% (f) 5 eq. NH₄OAc, AcOH, reflux 1day to 2 days, 70-80 %.

Bromides **3-9** and **3-11** are obtained by reaction of the indoles and with the quaternary bromide salt trimethylphenylammonium tribromide for 1.5 (**3-8**) to 12-16 (**3-10**) h respectively. The bromides **3-11** were converted to the corresponding thiols **3-12** through hydrolysis of their thioacetate substitution products. The thiol and bromide intermediates **3-9** and **3-12** are condensed using potassium carbonate (in place of 2,6-lutidine) in excess (3 eq.). These reaction conditions gave cleaner thioethers **3-13** which did not require any column chromatography for purification. If desired, recrystallization may be carried out in ethanol to give yellowish-orange crystals. Oxidations of **3-13** employing the urea hydrogen peroxide and trifluoroacetic anhydride mixture (4:3) resulted in decompositions. The oxidations were instead performed using an excess of 2.1 eq. *m*CPBA in DMF (at 0 °C).⁸ The reaction mixture was brought to room temperature

slowly and stirred more than 12 h to give the desired sulfones, **3-14**. Sodium bicarbonate solution was used to neutralize the *m*CBA by-product at the completion of reaction. A saturated solution of sodium sulfite is more effective in the neutralization process but could be harsh on the sulfones and led to formation of disconnected by-products such as acetyl or propionyl skatoles observed in the ^1H NMR spectra. Column chromatography is required at this stage to purify most of the sulfones which are then subjected to cyclizations employing 6 to 8 eq. of ammonium acetate refluxed in glacial acetic acid. In contrast to the doubly tethered sulfone precursors, these sulfones undergo relatively facile cyclizations giving the desired arrays **3-4a,b**. Unfortunately, both of these DDD arrays were insoluble in non-polar solvents such as CDCl_3 and DCM. They do however display good solubilities in more polar solvents such as acetonitrile, acetone, methanol and DMSO.

3.2.4 Synthesis of Dissymmetric Soluble DDD Arrays 3-5a,b and 3-6a,b

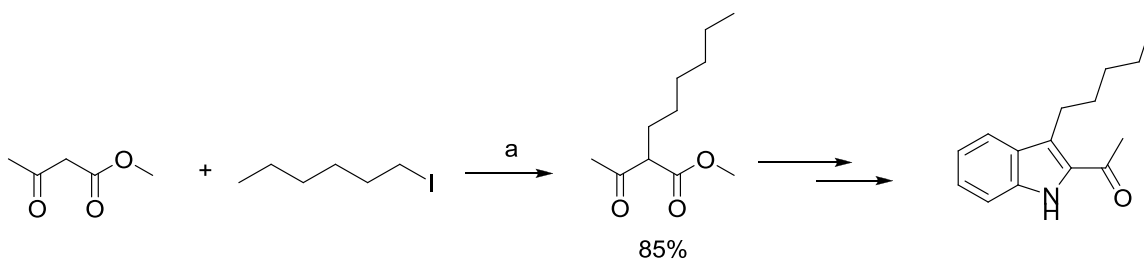


Figure 3-6 Synthesis of methyl 2-acetyloctanoate, for the incorporation of a pentyl chain at the 3-position of the indole heterocycle; Reaction conditions: (a) 3 eq. K_2CO_3 , THF, reflux for 36 h followed by Japp-Klingemann/Fischer Indole synthesis of alkylated acyl Indoles.

In order to make relevant comparisons to our own and literature values of association constants these measurements should be made in typical non-polar solvents

such as CDCl_3 and CD_2Cl_2 . Our strategy to induce solubility¹⁴ and retain the trimethylene tether between an indole and the central thiazine dioxide heterocycles was to attach a pentyl chain to the other indole at the 3-position. This may be accomplished by simply employing methyl 2-acetyloctanoate¹⁵ in place of methyl 2-ethyl-3-oxobutanoate as the starting material for the Japp-Klingemann reaction followed by the Fisher Indole synthesis (Figure 3-6). The rest of the steps are similar to those discussed in Scheme 3-2. Fortunately the arrays **3-5** and **3-6** were remarkably soluble in CDCl_3 compared to arrays **3-4**. Four DDD arrays are synthesized, two with a single trimethylene tether but retaining the pentyl chain (**3-5a,b**) and the other two without the tether but retaining the pentyl chain (**3-6a,b**). Comparisons of their binding behaviours were drawn with the corresponding complexes **3-1a,b** and **3-2a**.

3.3 Solid State X-Ray Studies of the DDD Arrays **3-4a,b** and **3-5b**.

All attempts to cocrystallize the complexes were unsuccessful, as the DDD arrays formed powders or amorphous solids before any crystallization occurred. However, single crystals of **3-4a** (Figure 3-7) were grown by the slow diffusion of diisopropyl ether into the concentrated solution of DCM. Although **3-4a** was not soluble in non-competitive solvents it was nevertheless an illuminating structure as the solid state structure might indicate the effects of both preorganization and reasons for insolubility.

The lattice is composed of antiparallel C_2 symmetric 1-D chains (Figure 3-7) that lie along the *c* direction of the unit cell. The chains are held together by two intermolecular hydrogen bonds between the donor N-H groups (N3-H3 and N2-H2) of one molecule of **3-4a** and one of the sulfone oxygen atoms (O4) of the next in the chain.

Table 3-2: Summary of the crystallographic data of the all three crystal structures **3-4a·CH₂Cl**, **3-4b** and **3-5b·DMSO**.

Crystal	3-4a·CH₂Cl₂	3-4b	3-5b·DMSO
Parameters			
chemical formula	C ₂₅ H ₂₂ Cl ₂ N ₄ O ₄ S	C ₂₈ H ₂₆ Cl ₃ N ₄ O ₆ S	C ₃₃ H ₃₉ N ₃ O ₅ S ₂
Formula weight	545.43	546.59	621.79
crystal system	monoclinic	Triclinic	Orthorhombic
space group	<i>P</i> 2 ₁ / <i>c</i>	P -1	Pna2(1)
<i>a</i> (Å)	12.241(1)	10.846(2)	30.553(1)
<i>b</i> (Å)	16.713(1)	12.315(3)	10.465(4)
<i>c</i> (Å)	12.689(1)	14.506(3)	9.980(4)
α , β and γ (°)	90, 111.062(5), 90	111.1(1), 98.8(1), 109.5(1)	90, 90, 90
<i>V</i> (Å ³)	2422.5(3)	1618.2(6)	3190.9(2)
<i>T</i> (K)	150(2)	293(2)	150(2)
<i>Z</i>	4	2	4
λ (Mo K α) (Å)	0.71073	0.71073	0.71073
<i>D</i> _{calc} (mg·cm ⁻³)	1.495	1.122	1.294
μ (mm ⁻¹)	0.396	0.141	0.212
<i>F</i> (000)	1128	572	1320
total reflections	34030	13351	16485
unique reflections	5549	7473	4863
absorption	multi-scan	multi-scan	multi-scan
refinement on	<i>F</i> ²	<i>F</i> ²	<i>F</i> ²
<i>R</i> (<i>F</i> _o) (<i>I</i> > 2 σ (<i>I</i>))	0.0468	0.0534	0.0350
<i>Rw</i> (<i>F</i> _o ²) (<i>I</i> > 2 σ (<i>I</i>))	0.1085	0.1038	0.0828
<i>R</i> (<i>F</i> _o) (all data)	0.0787	0.0952	0.0452
<i>Rw</i> (<i>F</i> _o ²) (all data)	0.1225	0.1493	0.0881
GOF on <i>F</i> ²	1.021	1.067	0.884

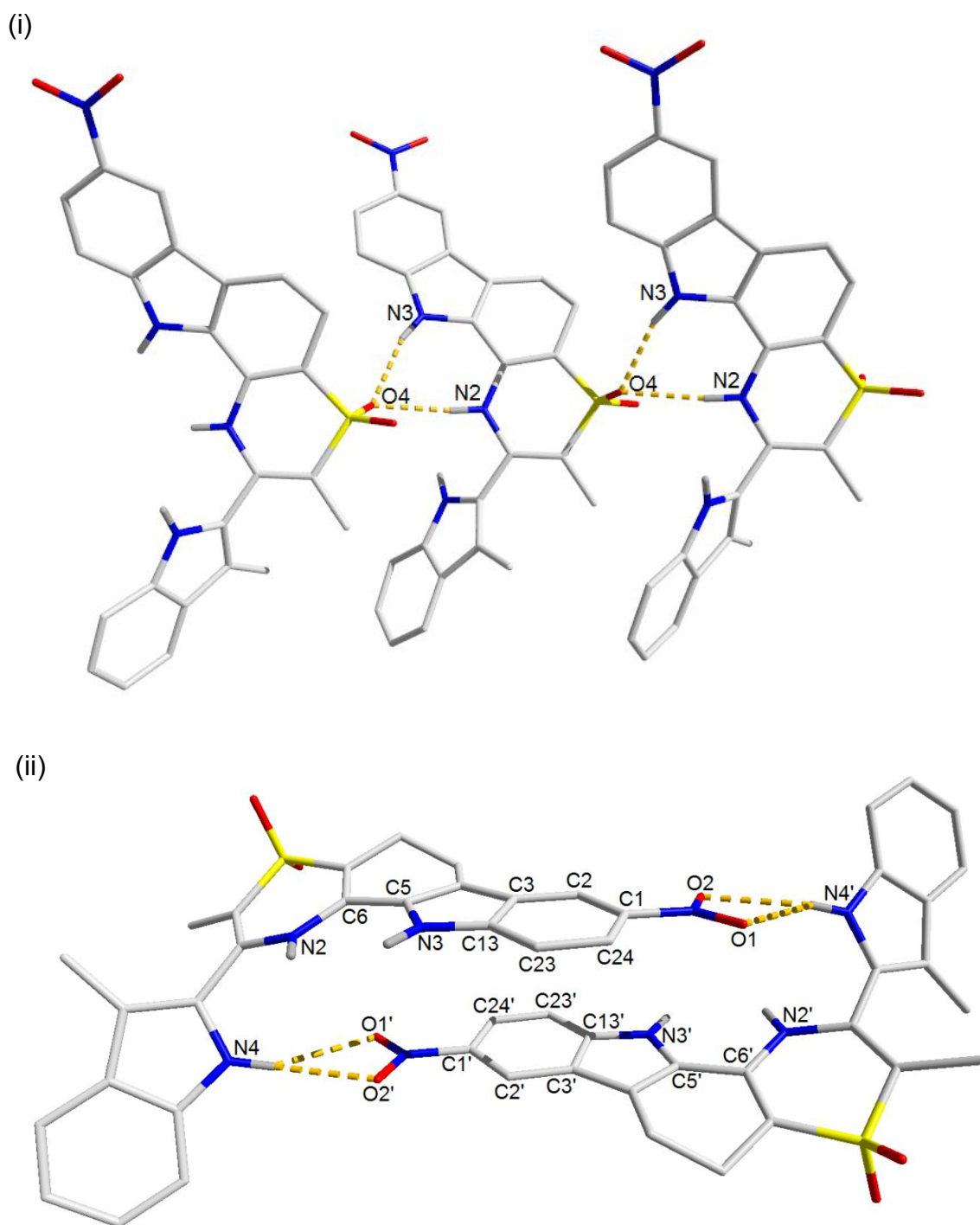


Figure 3-7 Stick representations of X-ray crystal structure of DDD array **3-4a**. (i) The intermolecular hydrogen bonding interactions between O4 atoms and donor N-H groups N2-H2 and N3-H3. (ii) The dihedral angle between the tethered indole and thiazine dioxide is $N2-C6-C5-N3 = 15^\circ$. All C-H hydrogen atoms have been removed for clarity.

The individual molecules reside in a helical conformation such that the tethered indole donor N-H group N3-H3 forms a hydrogen bond with O4 (sulfone oxygen atom) in the adjacent molecule ($\text{N3-H3}\cdots\text{O4} = 2.89 \text{ \AA}$ and $\text{N3-H3}\cdots\text{O4} = 162^\circ$). The thiazine NH donor group N2-H2 participates in hydrogen bonding with the same oxygen atom O4 ($\text{N2-H2}\cdots\text{O4} = 2.99 \text{ \AA}$ and $\text{N2-H2}\cdots\text{O4} = 171^\circ$). The Donor N4-H4 group participates in a bifurcated hydrogen bonding arrangement with both oxygen atoms O1 and O2 of the nitro-functional group ($\text{N4-H4}\cdots\text{O1} = 3.27 \text{ \AA}$, $\text{N4-H4}\cdots\text{O2} = 3.15 \text{ \AA}$, $\text{N4-H4}\cdots\text{O1} = 148^\circ$ and $\text{N4-H4}\cdots\text{O2} = 154^\circ$).

The dihedral angle between the the two donor heterocycles that are connected through dimethylene tether was measured to be 14° , which is likely too acute for efficient formation of a double helical complex. The small dihedral angle is due to the rigidity induced by the six membered ring between the two donor heterocycles. Examination of molecular models suggests a dihedral angle between these two heterocycles of 30° to 60° would be optimal in this case.

Apart from the hydrogen bonding interactions and preorganization, the solid state structure also displays π - π interactions between the benzene ring of the tethered indole of a DDD array with benzene ring of the tethered indole of adjacent DDD array. The distance between the centroid of the C1-C2-C3-C13-C23-C24 ring to the centroid of the C1'-C2'-C3'-C13'-C23'-C24' ring is $3.542(1) \text{ \AA}$, strongly indicating favourable π - π interactions between the two ring systems. The presence of these intermolecular interactions in the solid state is a reasonable basis for the insolubility of these arrays in non-polar solution due to aggregation.

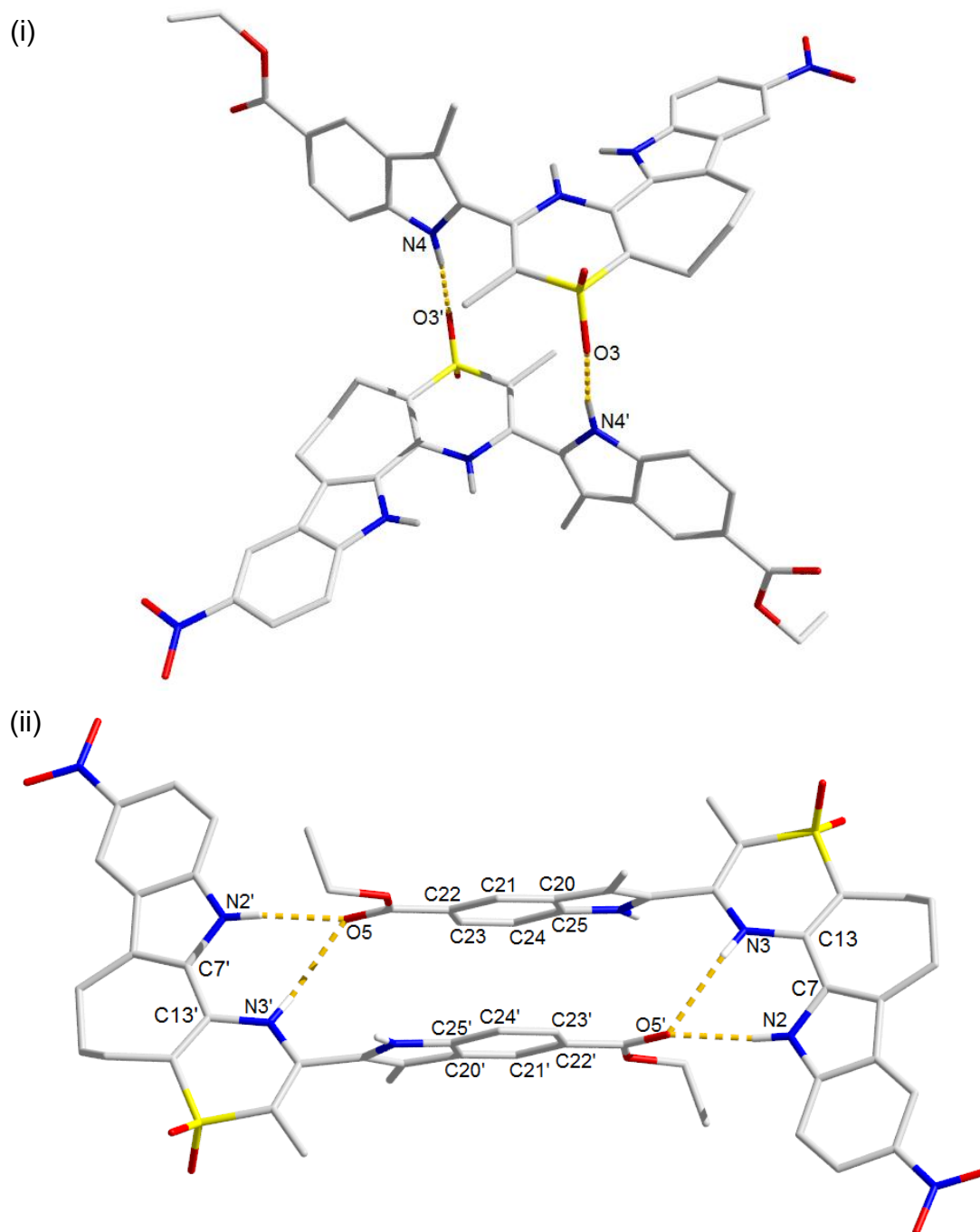


Figure 3-8 Stick representation of X-ray crystal structure of array **3-4b**. (i) Supramolecular dimers from intermolecular hydrogen bonding between amine donors and the sulfonyl oxygens of the thiazine dioxide heterocycles. (ii) Supramolecular dimers from intermolecular hydrogen bonding between amine donors and the carbonyl oxygen of the ester functional group. The dihedral angle between the tethered indole and thiazine dioxide rings is $N2-C7-C-13-N3 = 25^\circ$.

Though the solid state structure of the **3-4b** does not form 1-D chains through hydrogen bonding, the single X-ray structure demonstrates similar hydrogen bonding interactions, preorganization and moderate π - π interactions. There are two modes of hydrogen bonding interactions that can be observed as depicted in Figure 3-8 (i) and (ii) which together create supramolecular crosslinks in the lattice. The untethered indole donor group N4-H4 hydrogen bonds with O3 of the sulfone group ($\text{N4-H4}\cdots\text{O3} = 2.79 \text{ \AA}$ and $\text{N4-H4}\cdots\text{O} = 157^\circ$) the carbonyl oxygen O5 of the ester group participate in a bifurcated hydrogen bonding arrangement ($\text{N2-H2}\cdots\text{O5} = 2.80 \text{ \AA}$, $\text{N3-H3}\cdots\text{O5} = 3.00 \text{ \AA}$, $\text{N2-H2}\cdots\text{O5} = 161^\circ$ and $\text{N3-H3}\cdots\text{O5} = 152^\circ$). Each of the DDD arrays likely participates in both types of interactions in solution thereby rendering them insoluble. The increase in the tether by one carbon in **3-4b** has resulted in a higher dihedral of 25° which is much closer to the optimal range of dihedral angle than **3-4a** and so the arrays with trimethylene tether bridges between one of the terminal donor heterocycle and the central heterocycle (Figure 3-8) are likely capable of forming very stable double helical complementary complexes. In the solution state, indeed the DDD array **3-4b** forms a very stable double-helical complex with AAA array **3-2a** (see section 3.4.1). The solid state structure of **3-4b** also displays π - π interactions between the benzene ring of the untethered indole of a DDD array with benzene ring of the untethered indole of an adjacent DDD array. The distance between the centroid of the C20-C21-C22-C23-C24-C25 ring to the centroid of the C20''-C21''-C22''-C23''-C24''-C25'' ring is $3.732(1) \text{ \AA}$, strongly indicating favourable π - π interactions between the two aryl ring systems.

Numerous attempts have been made to co-crystallize the complexes **3-5a-b.3-2a** and **3-6a-b.3-2a** unsuccessfully. However, single crystals of **3-5b** alone were grown by

slow evaporation of concentrated solution in chloroform (Figure 3-9). There are negligible weak interactions observed in the crystal structure of **3-5b**.

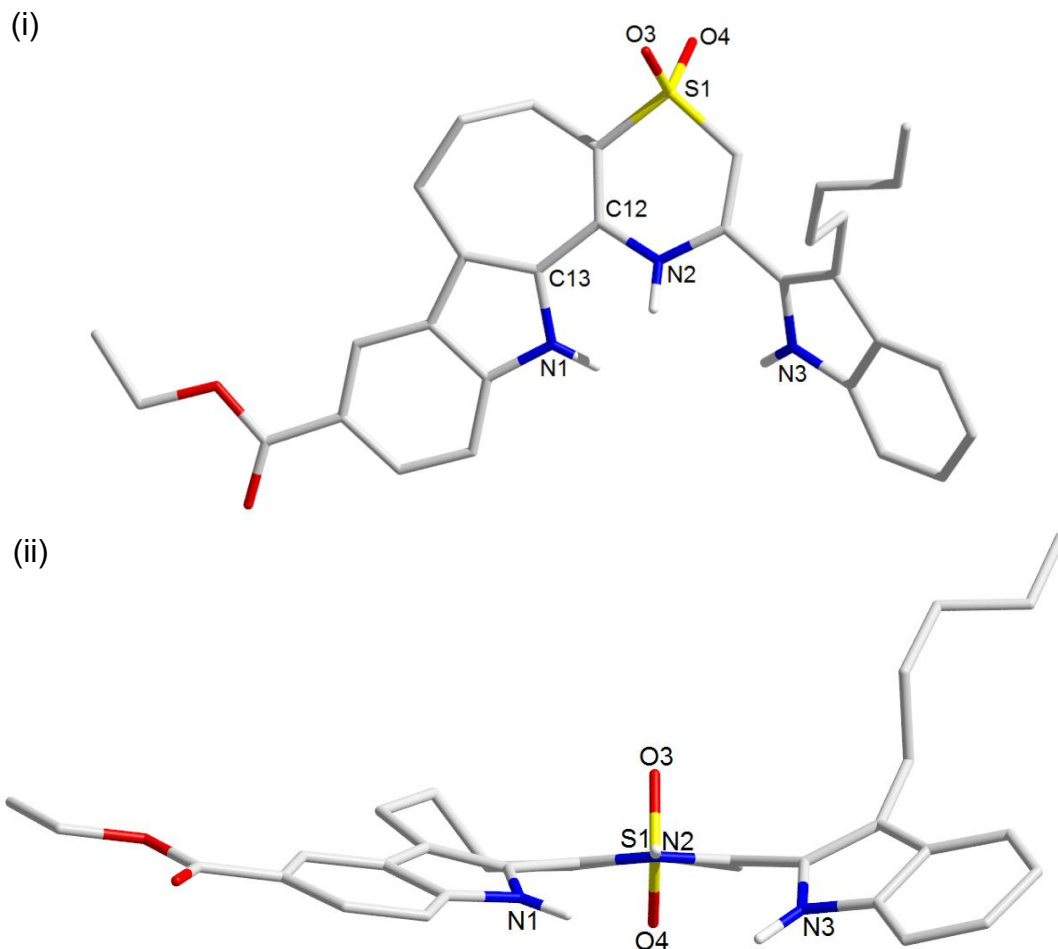


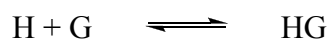
Figure 3-9 Stick representations of X-ray crystal structure of array **3-5b**. (i) Looking down on the plane of the tethered indole ring; (ii) Looking down the axis connecting N2 and S1. The dihedral angle between the tethered indole N-H group and the thiazine dioxide heterocycle ($N1-C13-C12-N2 = 24^\circ$) is similar to that observed in the case of **3-4b**.

The important observations were brought out by comparison with the above discussed structures. The dimer formation of the DDD arrays via hydrogen bonding (between donor N-H groups and carbonyl oxygen atoms) is absent in this case and likely

explains the solubility of this array (and by analogy **3-5a** and **3-6**) in non-polar solvents such CDCl₃. One further observation is the haphazard orientation of the pentyl chain the sterics of which may detrimentally affect the binding constants by hindering the approaching acceptor arrays during complex formation.

3.4 NMR Titration Studies of DDD Arrays

The stabilities of the complexes formed between the DDD and AAA arrays were investigated using ¹H NMR titrations. As the process of titration is a concentration dependant phenomenon, the host and guest concentrations were used to arrive at a set of equations that would define an association constant, K_a as shown below.



$$K_a = \frac{[HG]}{[H][G]} \quad (1)$$

$$\delta_{\text{obs}} = \frac{[HG]}{[H]_0} \delta_{\text{bound}} + \frac{[H]}{[H]_0} \delta_{\text{free}} \quad (2)^{16}$$

$$[H] = [H]_0 - [HG] \quad (3a)$$

$$[G] = [G]_0 - [HG] \quad (3b)$$

Where,

$[H]_0$ = total concentration of host $[G]_0$ = total concentration of guest

$[H]$ = concentration of uncomplexed host $[HG]$ = concentration of complexed
host and guest

δ_{obs} = the chemical shift of N-H observed during the titration experiment

δ_{bound} = the proton chemical shift of the host-guest complex (N-H \cdots N)

δ_{free} = the chemical shift of uncomplexed donor proton (N-H) in the free host

From Eq. 1 and 3a and 3b

$$[\text{HG}] = K_a ([\text{H}]_0 - [\text{HG}]) ([\text{G}]_0 - [\text{HG}]) \quad (4)$$

Squaring the Eq. 4 on both sides and rearranging the equation leads to Eq. 5

$$[\text{HG}]^2 - \left(\frac{1}{K_a} + [\text{H}]_0 + [\text{HG}]\right) [\text{HG}] + [\text{H}]_0 [\text{G}]_0 = 0 \quad (5)$$

When the Eq. 5 is rearranged using the quadratic equation, leads to Eq. 6:

$$[\text{HG}] = \frac{1 + K_a([\text{H}]_0 + [\text{G}]_0) - \sqrt{(1 + K_a([\text{H}]_0 + [\text{G}]_0))^2 - 4 K_a^2 [\text{H}]_0 [\text{G}]_0}}{2 K_a} \quad (6)$$

Substituting the Eq. 6 in Eq. 3a, leads to Eq. 7

$$[\text{H}] = [\text{H}]_0 - \left(\frac{1 + K_a([\text{H}]_0 + [\text{G}]_0) - \sqrt{(1 + K_a([\text{H}]_0 + [\text{G}]_0))^2 - 4 K_a^2 [\text{H}]_0 [\text{G}]_0}}{2 K_a} \right) \quad (7)$$

Substituting the above Eqs. 6 and 7 in Eq. 2 yields the final Eq. 8

$$\delta_{\text{obs}} = \frac{\left(1 + K_a([\text{H}]_0 + [\text{G}]_0) - \sqrt{(1 + K_a([\text{H}]_0 + [\text{G}]_0))^2 - 4 K_a^2 [\text{H}]_0 [\text{G}]_0} \right)}{2 K_a [\text{H}]_0} \delta_{\text{bound}} +$$

$$\frac{\left([\text{H}]_0 - \left(\frac{1 + K_a([\text{H}]_0 + [\text{G}]_0) - \sqrt{(1 + K_a([\text{H}]_0 + [\text{G}]_0))^2 - 4 K_a^2 [\text{H}]_0 [\text{G}]_0}}{2 K_a} \right) \right)}{[\text{H}]_0} \delta_{\text{free}} \quad (8)$$

During the NMR titration experiments, as the concentration of the guest increases, the chemical shift of the donor proton shifts downfield as a result of a decrease in electron density due to participation in hydrogen bonding. Origin is a data analysis software package that uses non-linear regression of the concentration and chemical shift data to plot the titration curves and calculate the K_a values based on the above 1:1 complexation model.

3.4.1 NMR Titration Studies of DDD Array 3-4b.

Though the DDD arrays **3-4a,b** are insoluble in all non-competitive organic solvents such as chloroform, DCM and toluene, they are drawn into chloroform solution when the AAA array is added to it in a 1:2.5 ratio. The ability of the AAA array to draw the insoluble DDD into solution suggests a strongly hydrogen bonded complex. There have been similar solubility issues reported in the literature^{17,18} in which cases titrations were carried out in mixed solvents. Among the DDD arrays synthesized, array **3-4b** should form the strongest complex with acceptor array **3-2a** and was therefore considered the best option to carry out such tests. Determination of these binding constants provides a method to estimate the binding constant in non-polar solution. In the case of **3-4b**, addition of 0.5% CH₃OH to CDCl₃ was sufficient to dissolve the array and therefore different percentages of methanol were added to test, compare and extrapolate the binding constants to solutions containing no CH₃OH. Six different concentrations of glass distilled CH₃OH (non-deuterated) were mixed in CDCl₃ and used in the titrations to give interesting results. There appears to be an exponential decrease in binding constants from 0.5% to 1% CH₃OH in CDCl₃ that tapers off as the amount of CH₃OH added increases (Figure 3-10 and 3-11).

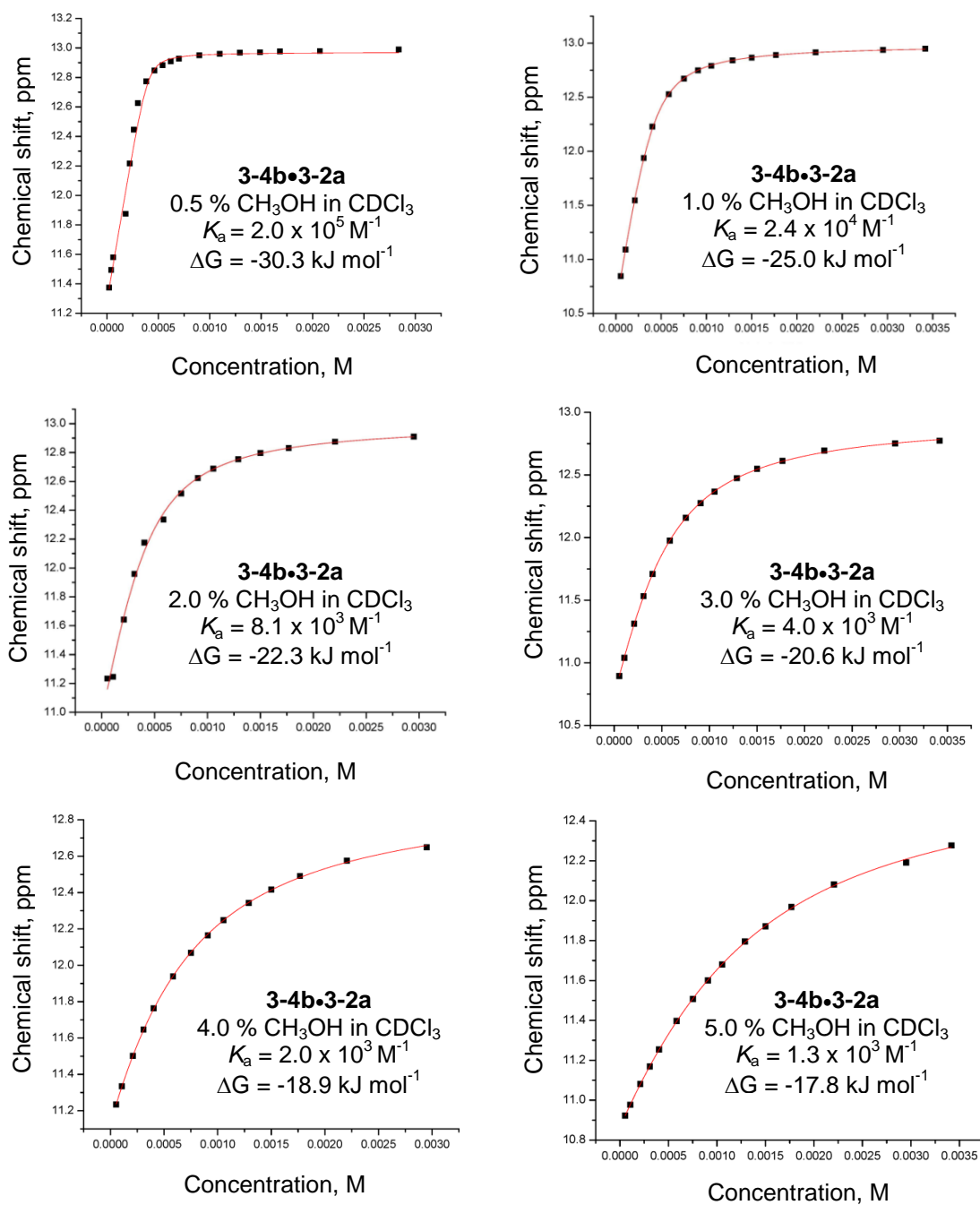


Figure 3-10 Titration curves measured at six different percentages of added CH₃OH (v/v) in CDCl₃, association constants (K_a) and free energies of complexation (ΔG), determined at room temperature.

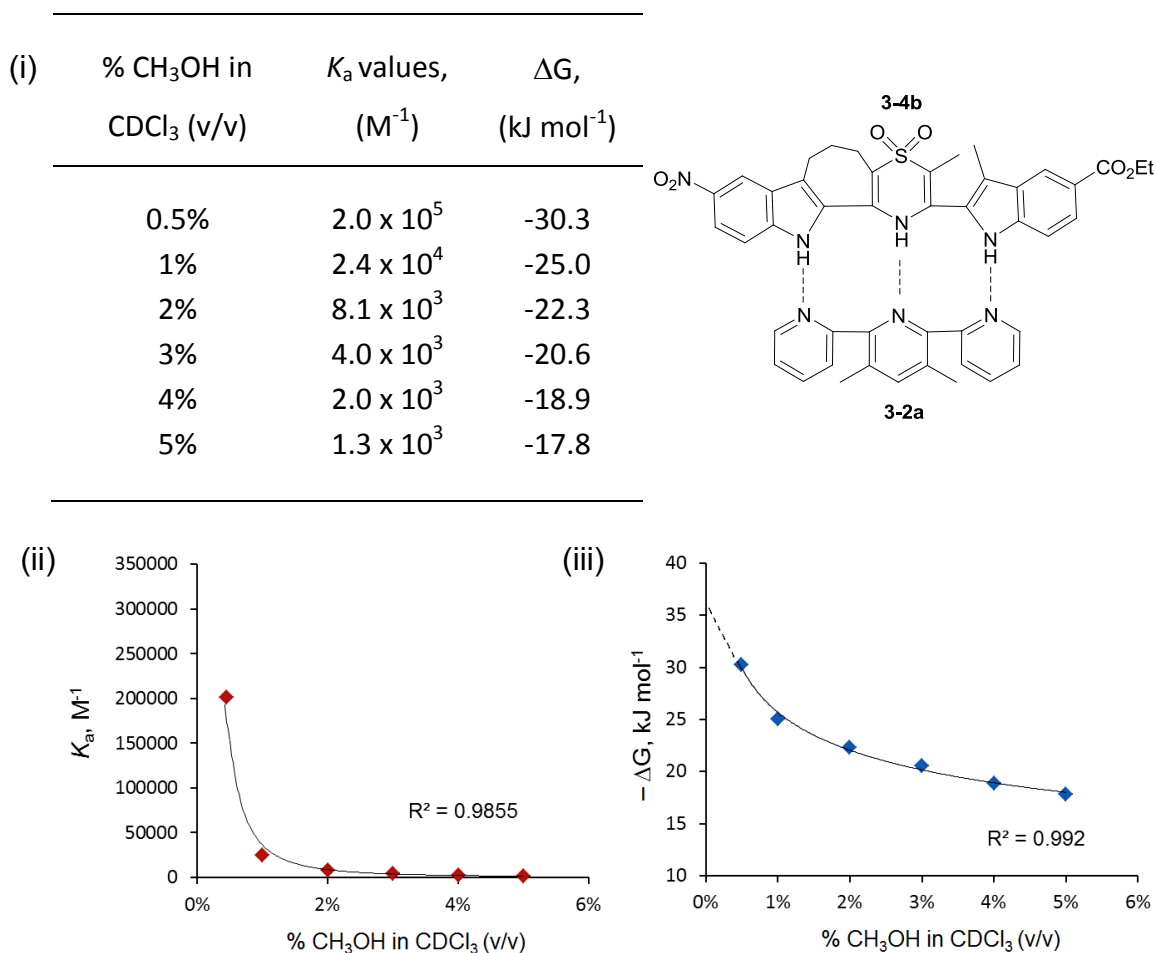


Figure 3-11 (i) K_a and ΔG values measured in solutions with different percentages of added CH₃OH for complex **3-4b-3-2a**; Plots of K_a (ii) and ΔG values (iii) vs. % CH₃OH in CDCl₃. Curves included in the plots are only meant to guide the eye.

The largest association constant for the complex **3-4b-3-2a** was measured to be $2.0 \times 10^5 \text{ M}^{-1}$ with 0.5 % (v/v) CH₃OH in CDCl₃. The exponential nature of the changes in association constants corresponding to 0.5% and 1% added CH₃OH experiments makes it difficult to predict the value at 0% added CH₃OH (pure CDCl₃). However the plots of ΔG vs. added CH₃OH is more easily followed and produces a conservative estimate for the free energy of complexation at 36.0 kJ mol^{-1} or $K_a = 2.0 \times 10^6 \text{ M}^{-1}$. A

steeper approach to the y-axis would give an estimate of closer to 40.0 kJ mol^{-1} or $K_a = 1.0 \times 10^7 \text{ M}^{-1}$.

In previously reported work,⁸ the K_a value of complex **3-1h•3-2a** ($R = \text{CN}$, $R'' = \text{CO}_2\text{Et}$, absent of the tether and considering electron withdrawing nature of CN being similar to NO_2) was reported to be $1.5 \times 10^5 \text{ M}^{-1}$. There is an approximately order of magnitude increase in the association constant estimated here. The increase in K_a value can be attributed to the preorganization by the trimethylene tethering of the donor heterocycles. As mentioned the estimation may not be entirely accurate (in fact likely too low) but is encouraging enough to carry out further comparative studies to establish the higher stabilities of the complexes with these tethers.

3.4.2 NMR Studies of Soluble DDD Arrays **3-5a,b** and **3-6a,b**:

The new DDD arrays **3-5a-b** and **3-6a-b** were synthesized following Scheme 3-2 were found to be soluble (as expected) in non-competitive solvents such as CDCl_3 . Solubility is the important here as it allows determination of exact binding constants through NMR titration experiments with out added polar solvent like the experiment above. All NMR experiments were carried out in CDCl_3 and association constants are determined by fitting the data to the 1:1 complexation model described earlier.

The goal of these experiments is to compare the stabilities of the soluble complexes, and draw correlations between the association constants and individual molecular features. In fact, a correlation of the association constants between the complexes **3-5a,b•3-2a**, **3-6a,b•3-2a** and **3-1a,b•3-2a** is apparent from this limited study.

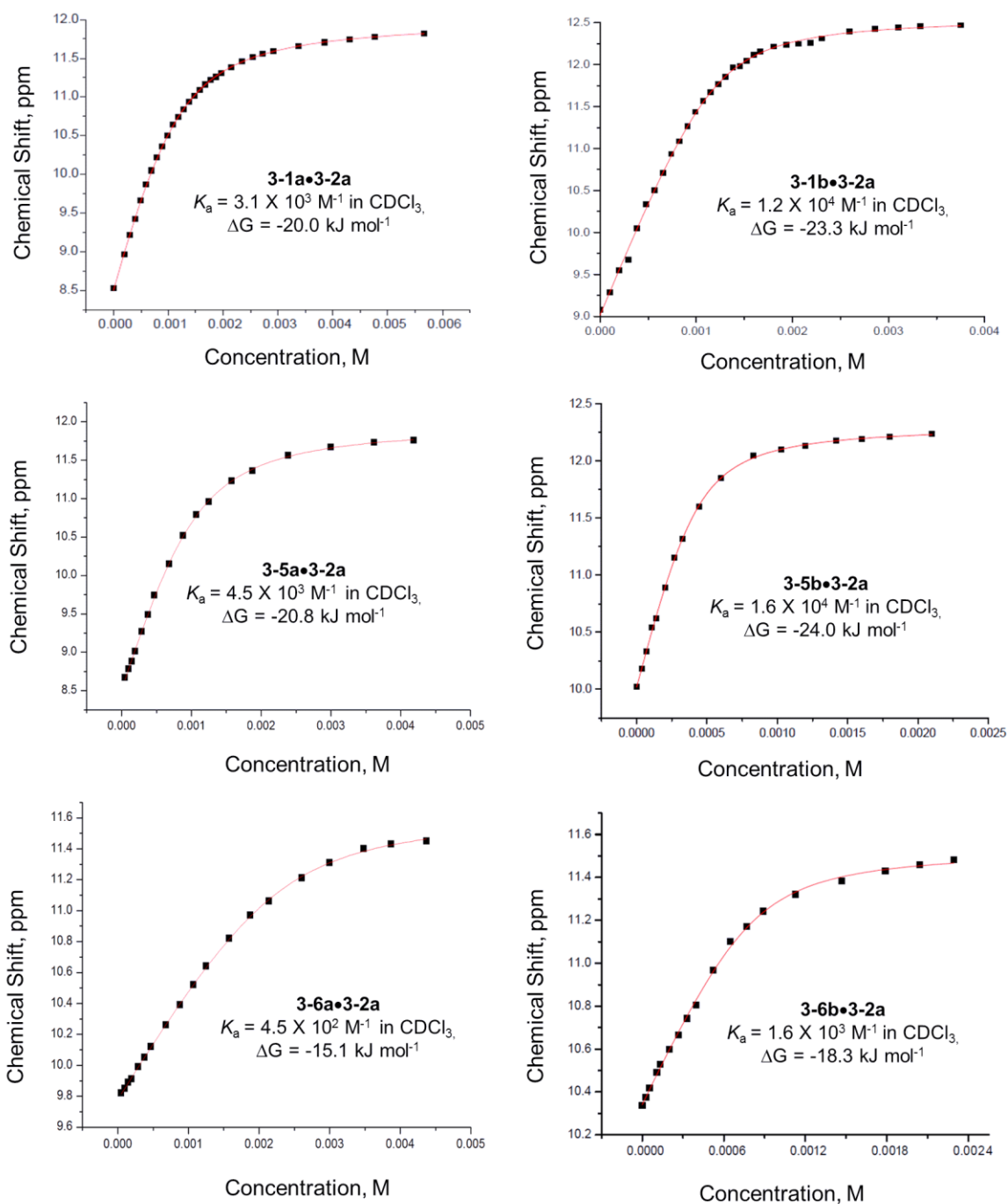


Figure 3-12 Titration curves for three different types of complexes **3-5a,b•3-2a**, **3-6a,b•3-2a** and **3-1a,b•3-2a**, their respective association constants (K_a) and free energies of complexation (ΔG) in CDCl_3 at room temperature.

The association constant of complex **3-1a-3-2a** was determined to be $3.1 (\pm 0.6) \times 10^3 \text{ M}^{-1}$ ($\Delta G = -20.0 \text{ kJ mol}^{-1}$) from previous work⁸ in our lab whereas the association constant of complex **3-5a-3-2a** was determined to be $4.5 (\pm 0.2) \times 10^3 \text{ M}^{-1}$ ($\Delta G = -20.8 \text{ kJ mol}^{-1}$). Though there is an increase in the association constant, it is not significant as the difference in Gibbs free energies of the two complexes is only 0.8 kJ mol^{-1} which appears to be very low considering the anticipated effect of preorganization due to trimethylene tether. However, this observation does not take into account the effect of the pentyl substituents. The K_a value of the complex **3-6a-3-2a** was determined to be $4.5 (\pm 0.6) \times 10^2 \text{ M}^{-1}$ ($\Delta G = -15.1 \text{ kJ mol}^{-1}$) which is significantly lower than the other two complexes. The difference between the Gibbs free energies of complexes **3-1a-3-2a** and **3-6a-3-2a** is 4.9 kJ mol^{-1} (which corresponds to almost an order of magnitude in terms of K_a values), indicating that the pentyl chain, though it induces solubility in the arrays, has a detrimental effect on the stability of complex formation. The net energy difference between complex **3-5a-3-2a** and complex **3-6a-3-2a** is calculated to be 5.7 kJ mol^{-1} which is the combination of the two effects namely, preorganization and pentyl group attachments.

From the comparison of association constant values of the complexes **3-1a-3-2a**, **3-5a-3-2a**, **3-6a-3-2a** and taking the mixed solvent studies of **3-4b-3-2a**, we may conclude that, though preorganization greatly increases the stability of the resultant complexes (by almost an order of magnitude in terms of the association constant) by holding the donor heterocycles in an optimal geometry for complex formation, the incorporation of the pentyl chains at the 3-position of the indole ring can greatly lower the complex stability.

Table 3-2 Four sets of complementary AAA•DDD complexes (**3-5a•3-2a**, **3-5b•3-2a**, **3-6a•3-2a** and **3-6b•3-2a**) compared with the association constants, free energies, their differences and net difference in energies with that of **3-1a•3-2a** and **3-1b•3-2a**, respectively.

Added Molecular Features	Complex	K_a (kJ mol ⁻¹)	ΔG (kJ mol ⁻¹)	$\Delta\Delta G^a$ (kJ mol ⁻¹)	$\Delta\Delta\Delta G^a$ (kJ mol ⁻¹)
Tether + pentyl	3-5a•3-2a	4500	20.8	0.8	
None	3-1a•3-2a	3100	20.0		5.7
Pentyl	3-6a•3-2a	450	15.1	4.9	
Tether + pentyl	3-5b•3-2a	16000	24.0	0.7	
None	3-1b•3-2a	12000	23.3		5.7
Pentyl	3-6b•3-2a	1640	18.3	5.0	

a) difference in values that appear immediately above and below in the column to the left.

Extrapolating the results from the exact values and accurate comparisons we can conclude that preorganization due to the trimethylene tether accounts for an increase in stability of approximately 5.7 kJ mol⁻¹ or over an order of magnitude in terms of the K_a values for complexes **3-4a,b•3-2a**, **3-5a•3-2a** and **3-6a•3-2a**. This conclusion is similar to the estimation derived from the mixed solvent NMR titration experiments and extrapolation to pure CDCl₃ of **3-4a-b•3-2a** complex (K_a value $\cong 10^6$ M⁻¹). However, the pentyl chains at 3-position of indole rings decrease the stability of the complexes **3-6a•3-2a** and **3-6b•3-2a** by approximately 5.0 kJ mol⁻¹. In a similar manner, complexes **3-5b•3-**

2a and **3-6b.3-2a** may be compared with complex **3-1b.3-2a** to yield an almost identical result (Table 3-2).

3.5 Conclusion

In the complementary systems discussed, we have studied both the individual and collective effects of preorganization (due to tethering of the heterocycles) and the introduction of alkyl chains for the induction of solubility. These two modifications produce competing effects. The tethering feature helps to greatly increase the stabilities of the complementary systems by preorganizing the DDD arrays in an optimal helical geometry thereby producing the need to expend energy bringing the array to the required geometry to form the complex. Sterics in the solution phase can effect the stabilities of complex formation significantly as revealed by the effect of the alkyl chains at the 3-positions of the indole rings. From our comparative studies, the preorganization in these complexes appears to increase the complex stability by nearly an order of magnitude. Complexes with very high association constants (in the range of 10^6 M^{-1} for three hydrogen bond arrays) were realized through incorporation of electron withdrawing functional groups and by preorganization via trimethylene tethers between the donor heterocycles.

3.5.1 Experimental

General: All experiments were performed under an atmosphere of nitrogen unless otherwise indicated. Chemicals were purchased from Aldrich and Alfa Aesar and used as received. Solvents (THF, hexanes, dichloromethane, toluene and diethyl ether) were obtained from Caledon Laboratories and dried using an Innovative Technology Inc.

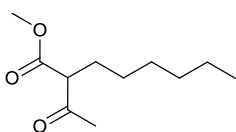
Controlled Atmospheres Solvent Purification System that utilizes dual alumina columns (SPS-400-5), or purchased from Aldrich and used as is. Reactions were monitored by thin layer chromatography (TLC) performed on EM 250 Kieselgel 60 F254 silica gel plates. Column chromatography was performed with 240-400 mesh silica gel-60. Nuclear magnetic resonance spectra were recorded on an INOVA and Mercury 400 MHz spectrometer ($^{13}\text{C} = 100.52$ MHz). Proton and $^{13}\text{C}\{^1\text{H}\}$ NMR spectra were referenced relative to Me_4Si using the NMR solvent (^1H : CHCl_3 , $\delta = 7.26$ ppm, $\text{C}_3\text{HD}_5\text{O}$, $\delta = 2.05$ ppm,; $^{13}\text{C}\{^1\text{H}\}$: CHCl_3 , $\delta = 77.16$ ppm, $\text{C}_3\text{HD}_5\text{O}$, $\delta = 29.84, 206.26$ ppm). Solvents for ^1H NMR spectroscopy (chloroform- D , acetone- D_6 , $\text{DMSO-}\text{D}_6$) were purchased from Cambridge Isotope Laboratories. Mass spectra were recorded using an, electron ionization Finnigan MAT 8200 mass spectrometer and PE-Sciex API 365. X-ray diffraction data were collected on a Bruker Nonius Kappa CCD X-ray diffractometer using graphite monochromated Mo-K_α radiation ($\gamma = 0.71073$ Å).

3.5.2 ^1H NMR Titration Procedure

A host sample (DDD array) of known weight was dissolved in 2.0 mL CDCl_3 to produce a 5×10^{-4} M solution. A portion (0.75 mL) of this solution was transferred into a NMR tube, and a ^1H NMR spectrum was then recorded. An accurately weighed sample of the guest was then dissolved in 1.0 mL of the remaining host solution to produce a 5×10^{-3} M guest solution. Aliquots of guest solution were added successively to the NMR tube containing the host solution ($7.5 \mu\text{L} \times 20$, $15.0 \mu\text{L} \times 5$, $37.5 \mu\text{L} \times 4$, $75.0 \mu\text{L} \times 3$), the tube was well shaken each time to mix the host and guest solutions, and the ^1H NMR spectrum was recorded after each addition. The chemical shifts of the N-H protons from

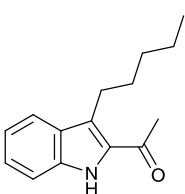
all three hydrogen bond donors in each sample were recorded and fit satisfactorily to a 1:1 binding model using Origin data analysis software (Microcal, USA). The average of the three K_a values determined from these three protons was used as the value for that titration run.

3.5.3 Synthetic Procedures



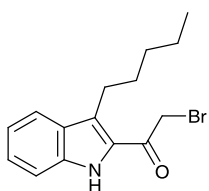
Synthesis of methyl 2-acetyloctanoate: To a mixture of methyl acetylacetate (1.00g, 5.00 mmol) and iodohexane (1.06g, 5.00 mmol) in THF (15 mL), potassium carbonate (2.07g, 15.00 mmol)

was added and the mixture was refluxed for about 60 h. The solids were filtered and the organics were extracted with DCM (3x10 mL) washed with water (3x10 mL) dried over $MgSO_4$ and concentrated under reduced pressure to give pure orange brown oil which was carried on to next reaction step. 1H -NMR ($CDCl_3$) δ : 3.72 (s, 3H), 3.41 (t, $J=8.3$ Hz, 1H), 2.21 (s, 3H), 1.86-1.78 (m, 2H), 1.28-1.21 (m, 8H), 0.86 (t, $J=7.0$ Hz, 3H). ^{13}C NMR (100MHz, $CDCl_3$) δ ppm 203.8, 171.2, 59.8, 52.1, 31.8, 28.7, 28.2, 27.1, 22.2, 13.9. ESI HRMS calcd. for $C_{11}H_{20}O_3$ m/z : 200.1412, found : 200.1410.



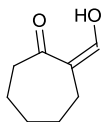
Synthesis of 3-8c: A solution of sodium hydroxide (5M, 12.05 mmol) was added to a solution of methyl 2-acetyloctanoate (2.19 g, 10.95 mmol) in water (7.5 mL) and stirred for about 16 h. and of concentrated hydrochloric acid (1.26 mL, 12.05 mmol) was added drop wise at 0 °C and aged 45 minutes at the same temperature. To a mixture of aniline (1.02 g, 1.0 mL, 10.95 mmol), (3.4 mL, 32.86 mmol) and water (6.6 mL), a solution of sodium nitrite (0.76 g, 10.95 mmol) was added drop wise at 0 °C and stirred for 20 min. at the same temperature. This

mixture was added to the buffered solution of methyl 2-acetyloctanoate at 0 °C and stirred at room temperature for about 1 h. and the entire mixture was added to a saturated solution of sodium acetate (5.0 mL) and stirred for an additional 2 h. before the precipitate was collected by filtration and washed with water to give the intermediate product, 3-(2-phenyl hydrazono)nonan-2-one (2.03g) as red solid granules. A solution of 3-(2-phenyl hydrazono)nonan-2-one (1.90 g) in formic acid (20 mL) was stirred at 100 °C for 16 h. and the mixture was allowed to cool to room temperature. The reaction mixture was poured onto ice cold water (50 mL) stirred for about 30 min. and the resulting residue was filtered and air dried to give pure brown solid beads (1.8 g). ¹H NMR (400 MHz, CDCl₃) δ ppm: 9.21 (s, *br*, 1H), 7.70 (d, *J*=8.2 Hz, 1H), 7.38 - 7.32 (m, 2H), 7.15 - 7.11 (m, 1H), 3.10 (t, *J*=8.2 Hz, 2H), 2.66 (s, 3H), 1.76-1.68 (m, 2H), 1.48 - 1.32 (m, 4H), 0.92 (t, *J*=7.0 Hz, 3H). ¹³C NMR (100MHz, CDCl₃) δ ppm 190.7, 136.3, 132.0, 129.6, 128.5, 126.5, 124.7, 121.5, 120.1, 112.1, 32.3, 31.6, 28.5, 25.7, 22.7, 14.2. ESI HRMS calcd. for C₁₅H₁₉NO *m/z* : 229.1467, found : 229.1466.

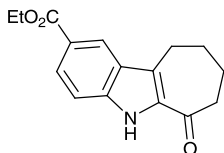


Synthesis of 3-9c: The bromide was made in accordance with the A.N.

Kost *et al.*⁴⁵ method in 80 % yield. ¹H NMR (400 MHz, CDCl₃) δ ppm: 8.96 (s, *br*, 1H), 7.70 (d, *J*=8.2 Hz, 1H), 7.42 - 7.32 (m, 2H), 7.17 - 7.13 (m, 1H), 4.43 (s, 2H), 3.09 (t, *J*=8.2 Hz, 2H), 2.66 (s, 3H), 1.76-1.68 (m, 2H), 1.50 - 1.25 (m, 4H), 0.92 (t, *J*=7.0 Hz, 3H). ¹³C NMR (100MHz, CDCl₃) δ ppm 184.1, 137.1, 132.0, 128.4, 127.4, 126.2, 121.8, 120.6, 120.2, 112.2, 32.8, 31.6, 26.1, 25.7, 22.7, 14.2. ESI HRMS calcd. for C₁₅H₁₈BrNO *m/z* : 307.0572, found : 307.0575.

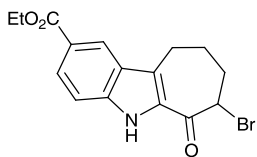


Synthesis of 2-(Hydroxymethylidene)cycloheptanone: To a mixture of cycloheptanone (1.2 mL), diethyl ether (10 mL) and sodium methoxide (1.08 g) was added ethyl formate (1.1 mL), and the mixture was stirred at room temperature for 18 h. 1 N Hydrochloric acid was added to the reaction mixture, and the mixture was extracted with ethyl acetate. The extract washed with saturated brine, dried over anhydrous magnesium sulphate, filtered and concentrated to give the title compound (1.32g) as a yellow liquid. $^1\text{H-NMR}$ (CDCl_3) δ : 14.63 (d, $J=8.7$ Hz, 1H), 7.59 (d, $J=8.3$ Hz, 1H), 2.51-2.48 (2H, m), 2.23-2.20 (2H, m), 1.75-1.53 (6H, m). ^{13}C NMR (100MHz, CDCl_3) δ ppm 204.3, 170.9, 114.7, 42.1, 31.7, 29.8, 28.6, 24.6. ESI HRMS calcd. for $\text{C}_8\text{H}_{12}\text{O}_2$ m/z : 140.0837, found : 140.0838.

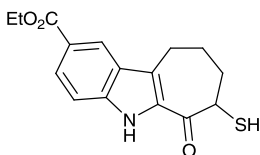


Synthesis of 3-10d: A mixture of ethyl 4-aminobenzoate (1.65 g, 10 mmol), concentrated hydrochloric acid (2.06 g), water (6 mL) and sodium nitrite (0.69 g, 10 mmol) was stirred at 0° C. for 20 min. This mixture was added to a mixed solution of 2-(hydroxymethylene)cyclo-heptanone (1.40 g) in ethanol (16 mL) and a solution of potassium hydroxide (561 mg) in water (0.6 mL) at 0° C., and the mixture was stirred at 0° C. for 10 min and at room temperature for 1 hr and added to water. The precipitate was collected by filtration and washed with water to give the intermediate compound, ethyl 4-(2-(2-oxocycloheptylidene)hydrazinyl)benzoate (2.03 g) as a yellow solid. The title compound was synthesized from the hydrazone as described in the cyclization process above by refluxing in formic acid in 90% yield. ^1H NMR (Acetone- D_6) δ : 10.74 (s, br, 1H), 8.42 (s, 1H), 7.96 (dd, $J=8.6$ Hz, $J=1.6$ Hz, 1H), 7.55 (d, $J=8.6$ Hz, 1H), 4.35 (q, $J=7.0$ Hz, 2H), 3.21-3.18 (m, 2H), 2.81-2.78 (m, 2H), 2.13-1.95 (m, 4H), 1.38 (t, $J=7.0$ Hz, 3H). ^{13}C NMR (100MHz,

Acetone-D6) δ ppm 195.0, 167.8, 140.7, 135.8, 128.8, 127.8, 125.9, 125.3, 123.6, 113.5, 61.6, 43.9, 27.8, 26.3, 23.8, 15.3. ESI HRMS calcd. for $C_{16}H_{17}NO_3$ m/z : 271.1208, found : 271.1210.

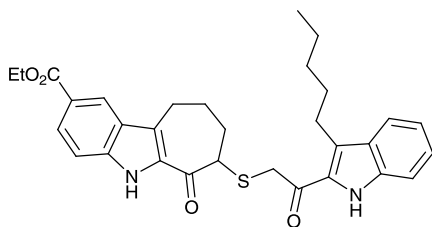


Synthesis of 3-11d: The bromide was made in accordance with the A.N. Kost *et al.*⁴⁵ method in 80 % yield. 1H NMR (400 MHz, $CDCl_3$) δ ppm: 9.37 (s, br, 1H), 8.44 (s, 1H), 8.04 (dd, $J=8.6$ Hz, $J=1.6$ Hz, 1H), 7.40 (d, $J=8.6$ Hz, 1H), 5.01–4.98 (m, 1H), 4.40 (q, $J=7.0$ Hz, 2H), 3.45–3.12 (m, 2H), 2.50–2.45 (m, 3H), 2.20–2.15 (m, 1H), 1.42 (t, $J=7.0$ Hz, 3H). ^{13}C NMR (100MHz, $CDCl_3$) δ ppm 193.8, 189.9, 167.0, 139.1, 132.8, 127.8, 127.3, 126.6, 124.6, 122.8, 111.7, 60.9, 53.3, 30.5, 30.3, 25.1, 14.4. EI HRMS calcd. for $C_{16}H_{16}BrNO_3$ m/z : 349.0314, found : 349.0319.



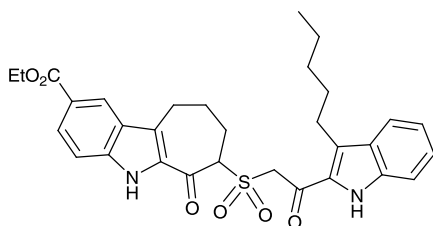
Synthesis of 3-12d: To a solution of Potassium thioacetate (0.97 g, 8.50 mmol) in 10 mL dry DMF, was added a solution of bromide **3-11d** (2.95 g, 8.50 mmol) in 15 mL dry DMF, drop wise over a period of 15 min. and stirred at room temperature for 16 h The reaction mixture was poured in to 50 mL water and stirred for 20 minutes before filtering the yellow solid, corresponding thioacetate. The solid was taken up in 100 mL of acetonitrile solution and to this was added Cysteamine.HCl salt (0.95 g, 8.50 mmol) followed by the addition of sodium bicarbonate. The contents are stirred for about 24 h and acidified with 10% HCl solution and stirred for 2 h to give the title compound as yellowish red solid (90%, 2.29 g, 7.59). 1H NMR (400 MHz, $DMSO-d_6$) δ ppm: 11.82 (s, br, 1H), 8.34 (s, 1H), 7.87 (d, $J=8.6$ Hz, 1H), 7.46 (d, $J=8.6$ Hz, 1H), 4.30 (q, $J=7.0$ Hz, 2H), 4.27–4.20 (m, 1H),

3.28–3.16 (m, 2H), 3.06–2.95 (m, 1H), 2.40–2.28 (m, 1H), 2.12–1.94 (m, 3H), 1.33 (t, $J=7.0$ Hz, 3H). ^{13}C NMR (100MHz, DMSO- d_6) δ ppm 191.3, 166.2, 139.4, 132.5, 126.5, 126.2, 124.6, 123.9, 121.3, 112.4, 60.4, 47.6, 31.9, 24.4, 23.1, 14.3. ESI HRMS calcd. for $\text{C}_{16}\text{H}_{17}\text{NO}_3$ m/z : 303.0929, found : 303.0930.



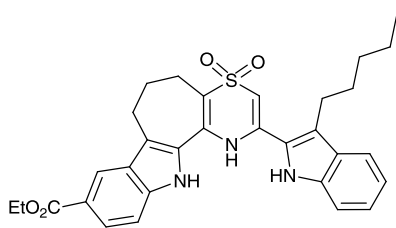
Synthesis of 3-13d: Potassium carbonate (1.42 g, 10.28 mmol) was added to the solution of **3-9c** (1.20 g, 3.42 mmol) and **3-12d** (1.04 g, 3.42 mmol) in acetonitrile and was stirred for a period of 36 h at

room temperature. The resulting mixture was poured into water and stirred for 2 h to give the brownish red precipitate as product (85%, 1.54 g, 2.91 mmol). ^1H NMR (400 MHz, DMSO- d_6) δ ppm: 11.82 (s, br, 1H), 11.58 (s, *br*, 1H), 8.35 (s, 1H), 7.88 (d, $J=8.6$ Hz, 1H), 7.66 (d, $J=8.6$ Hz, 1H), 7.50–7.41 (m, 2H), 7.29 (t, $J=7.4$ Hz, 1H), 7.06 (t, $J=7.4$ Hz, 1H), 4.31 (q, $J=7.0$ Hz, 2H), 4.24–4.10 (m, 2H), 4.05–4.00 (m, 1H), 3.08–3.00 (m, 2H), 2.98–2.62 (m, 2H), 2.40–1.92 (m, 4H), 1.62–1.58 (m, 2H), 1.38–1.25 (m, 6H), 0.80 (t, $J=7.0$ Hz, 3H). ^{13}C NMR (100MHz, DMSO- d_6) δ ppm 190.0, 187.5, 171.3, 166.3, 139.4, 136.5, 132.7, 129.9, 127.4, 126.6, 125.7, 124.5, 124.0, 123.8, 121.4, 120.8, 119.7, 112.6, 112.4, 60.3, 52.0, 31.4, 30.4, 28.6, 24.7, 24.5, 22.8, 22.0, 14.3, 13.9. ESI HRMS calcd. for $\text{C}_{31}\text{H}_{34}\text{N}_2\text{O}_4\text{S}$ m/z : 530.2239, found : 530.2236.



Synthesis of 3-14d: To the solution of **3-13d** (1.50 g, 2.83 mmol) in 15 mL DMF was added a solution of *m*CPBA (2.53 g, 11.32 mmol) in 5 mL DMF was added dropwise. The reaction mixture was stirred

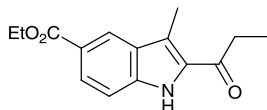
for 12 h and poured into a saturated solution of sodium sulphite and washed with 50 mL water. The product was extracted with dichloromethane and the organic layer was dried using MgSO_4 . The solvent was evaporated to at reduced pressures to give orange brownish precipitate (80 %, 1.27 g, 2.26 mmol). ^1H NMR (400 MHz, DMSO-d_6) δ ppm: 11.26 (s, br, 1H), 11.22 (s, *br*, 1H), 8.33 (s, 1H), 7.89 (d, $J=8.6$ Hz, 1H), 7.59 (d, $J=8.6$ Hz, 1H), 7.40-7.32 (m, 2H), 7.25 (t, $J=7.4$ Hz, 1H), 7.02 (t, $J=7.4$ Hz, 1H), 5.17 (dd, $J=110.2$ Hz, $J=14.5$ Hz, 2H), 4.98-4.93 (m, 2H), 4.30 (q, $J=7.0$ Hz, 1H), 3.30-2.95 (m, 4H), 2.60-2.36 (m, 3H), 2.37-2.12 (m, 1H), 1.60-1.55 (m, 2H), 1.40-1.21 (m, 7H), 0.78 (t, $J=7.0$ Hz, 3H). ^{13}C NMR (100MHz, CDCl_3 and DMSO-d_6 mixture in 1:1 ratio) δ ppm 185.7, 180.9, 166.0, 166.3, 139.4, 136.8, 132.6, 129.7, 127.4, 127.0, 126.8, 126.1, 125.9, 123.7, 121.5, 120.4, 119.4, 111.9, 111.7, 70.1, 61.1, 59.9, 31.1, 29.8, 25.1, 24.3, 22.7, 21.7, 20.8, 13.6, 13.3. ESI HRMS calcd. for $\text{C}_{31}\text{H}_{34}\text{N}_2\text{O}_6\text{S}$ m/z : 562.2138, found : 562.2140.



Synthesis of 3-5b: the title compound is made following the general method for synthesis of thiazine dioxides in 80 % yield. ^1H NMR (400 MHz, DMSO-d_6) δ ppm: 11.57 (s, br, 1H), 11.43 (s, *br*, 1H), 10.45 (s, *br*,

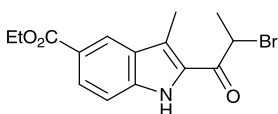
1H), 8.34 (s, 1H), 7.88 (dd, $J=8.6$ Hz, $J=1.6$ Hz, 1H), 7.67-7.61 (m, 2H), 7.51 (d, $J=8.2$ Hz, 1H), 7.26 (t, $J=7.8$ Hz, 1H), 7.10 (t, $J=7.8$ Hz, 1H), 6.17 (s, 1H), 4.35 (q, $J=7.0$ Hz, 2H), 3.12 (t, $J=7.0$ Hz, 2H), 2.95 (t, $J=7.8$ Hz, 2H), 2.64-2.60 (m, 2H), 2.32-2.24 (m, 2H), 1.73-1.64 (m, 2H), 1.40-1.30 (m, 7H), 0.85 (t, $J=7.0$ Hz, 3H). ^{13}C NMR (100MHz, DMSO-d_6) δ ppm 166.5, 138.4, 136.9, 135.9, 132.9, 127.8, 127.6, 127.5, 126.5, 124.4, 123.3, 121.6, 121.3, 119.7, 119.3, 117.2, 115.8, 111.6, 111.5, 99.5, 79.2, 60.3, 31.3, 30.5,

30.2, 23.8, 23.5, 21.9, 20.7, 14.3, 14.0. ESI HRMS calcd. for $C_{31}H_{33}N_3O_4S$ m/z : 543.2192, found : 543.2196.



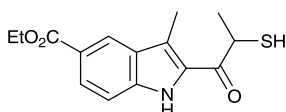
Synthesis of 3-8b: The light yellow brown title compound was made by following the general method for synthesis of Fisher

Indole synthesis starting with Ethyl 4-aminobenzoate in 85 %. 1H NMR (400 MHz, $CDCl_3$) δ ppm: 9.26 (s, *br*, 1H), 8.48 (s, 1H), 8.02 (dd, $J=8.6$ Hz, $J=1.6$ Hz, 1H), 7.38 (d, $J=8.6$ Hz, 1H), 4.41 (q, $J=7.0$ Hz, 2H), 2.99 (q, $J=7.4$ Hz, 2H), 2.68 (s, 3H), 1.43 (t, $J=7.0$ Hz, 3H), 1.29 (t, $J=7.4$ Hz, 3H). ^{13}C NMR (100MHz, $CDCl_3$) δ ppm 193.7, 135.9, 132.3, 128.9, 126.2, 121.1, 124.7, 120.0, 117.8, 111.8, 34.3, 11.2, 8.0. ESI HRMS calcd. for $C_{15}H_{17}NO_3$ m/z : 259.1208, found : 259.1210.



Synthesis of 3-9b: The yellow brown title compound was made by following the general method for synthesis of bromination

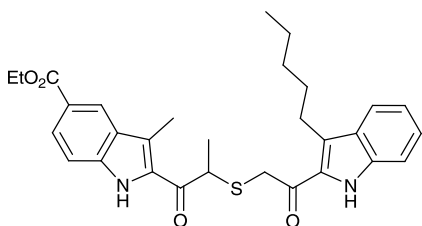
indoles. 1H NMR (400 MHz, $DMSO-d_6$, 298 K) δ (ppm) = 11.98 (s, 1H), 8.38 (m, 1H), 7.88 (m, 1H), 7.51 (m, 1H), 5.50 (q, $J=6.3$ Hz, 1H), 4.31 (q, $J=7.0$ Hz, 2H), 2.65 (s, 3H), 1.82 (d, $J=6.3$ Hz, 2H), 1.34 (t, $J=7.0$ Hz, 3H); ^{13}C NMR (100 MHz, $DMSO-d_6$, 298 K) δ (ppm) = 186.6, 166.2, 138.9, 130.4, 127.4, 126.3, 123.7, 121.6, 121.1, 112.6, 60.4, 45.0, 19.8, 14.3, 10.4; EI-HRMS (m/z) calculated for $C_{15}H_{16}NBrO_3$: 337.0314, found 337.0311.



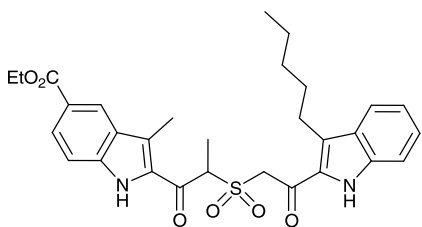
Synthesis of ethyl 2-(2-(bromopropanoyl)-3-methyl-1H-indole-5-carboxylate: The yellow brown title compound was

made by following the general method for synthesis of thiols of indoles. 1H NMR (400 MHz, $CDCl_3$) δ ppm: 9.67 (s, *br*, 1H), 8.47 (s, 1H), 8.02 (dd, $J=8.6$ Hz, $J=1.6$ Hz,

1H), 7.39 (d, $J = 8.6$ Hz, 1H), 4.41 (q, $J = 7.0$ Hz, 2H), 4.26-4.22 (m, 1H), 2.08 (d, $J = 9.8$ Hz, 1H), 2.70 (s, 3H), 1.68 (d, $J = 6.6$ Hz, 3H), 1.42 (t, $J = 7.0$ Hz, 3H). ^{13}C NMR (100MHz, CDCl_3) δ ppm 190.9, 167.1, 138.8, 131.2, 128.5, 127.4, 124.5, 122.6, 120.1, 111.6, 60.8, 38.5, 20.8, 14.3, 11.2. ESI HRMS calcd. for $\text{C}_{15}\text{H}_{17}\text{NO}_3\text{S}$ m/z : 291.0929, found : 291.0926.

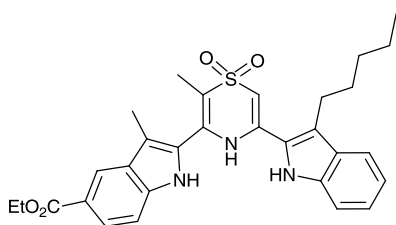


Synthesis of 3-13f: the title compound is made as described for compound **3-13d** in 80 % yield. ^1H NMR (400 MHz, CDCl_3) δ ppm: 10.46 (s, br, 1H), 9.17 (s, br, 1H), 8.48 (s, 1H), 8.42 (s, 1H), 8.04-8.01 (m, 1H), 7.68-7.64 (m, 2H), 7.40-7.32 (m, 3H), 7.15-7.11 (m, 1H), 4.47-4.39 (m, 3H), 4.05 (dd, $J = 40.0$ Hz, $J = 14.5$ Hz, 2H), 4.05-4.00 (m, 1H), 3.14-3.09 (m, 2H), 2.68 (s, 3H), 1.70-1.62 (m, 3H), 1.52-1.43 (m, 6H), 1.29 (t, $J = 7.0$ Hz, 3H), 0.90 (t, $J = 7.0$ Hz, 3H). ^{13}C NMR (100MHz, CDCl_3) δ ppm 193.9, 188.2, 167.2, 138.8, 138.2, 136.9, 136.1, 133.3, 131.6, 129.4, 128.0, 126.9, 126.3, 124.3, 122.8, 122.3, 121.3, 114.3, 111.9, 60.7, 43.7, 37.3, 35.0, 32.0, 25.5, 22.5, 24.7, 24.5, 22.8, 22.0, 16.2, 14.0, 11.1, 7.8. EI HRMS calcd. for $\text{C}_{31}\text{H}_{34}\text{N}_2\text{O}_4\text{S}$ m/z : 518.2239, found : 518.2242.



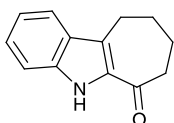
Synthesis of 3-14f: the title compound is made following the general method for synthesis of sulfones in 85 % yield. ^1H NMR (400 MHz, CDCl_3 and DMSO-d_6 mixture in 1:1 ratio) δ ppm: 9.29 (s, br, 1H), 8.48 (s, br, 1H), 8.35 (s, 1H), 7.89 (d, $J = 8.6$ Hz, 1H), 7.69 (d, $J = 8.6$ Hz, 1H), 7.58-7.54 (m, 2H), 7.40-7.28 (m, 1H), 7.14 (t, $J = 7.4$ Hz, 1H), 5.36-5.31 (m, 1H), 4.77 (q,

$J = 7.0$ Hz, 2H), 4.45-4.38 (m, 2H), 3.12-3.08 (m, 2H), 2.69 (s, 3H), 1.86-1.68 (m, 3H), 1.50-1.38 (m, 6H), 1.29 (t, $J = 7.0$ Hz, 3H), 0.89 (t, $J = 7.0$ Hz, 3H). ^{13}C NMR (100MHz, CDCl_3) δ ppm 197.2, 193.6, 164.0, 140.8, 138.7, 136.7, 135.8, 132.6, 131.8, 129.3, 128.1, 127.8, 125.6, 124.8, 122.9, 121.6, 120.7, 113.8, 110.3, 72.3, 62.1, 60.6, 43.9, 38.2, 28.4, 24.6, 16.8, 12.7, 11.6, 8.9. ESI HRMS calcd. for $\text{C}_{30}\text{H}_{34}\text{N}_2\text{O}_6\text{S}$ m/z : 550.2138, found : 550.2141.



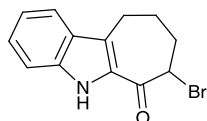
Synthesis of 3-6b: the title compound is made following the general method for synthesis of thiazine dioxides in 80 % yield. ^1H NMR (400 MHz, CDCl_3 with few drops of DMSO-d_6) δ ppm: 10.93 (s, br, 1H), 10.32

(s, br, 1H), 9.79 (s, br, 1H), 7.97 (s, 1H), 7.53 (dd, $J=8.6$ Hz, $J=1.6$ Hz, 1H), 7.27-7.24 (m, 1H), 7.04 (d, $J=8.2$ Hz, 1H), 6.96 (t, $J=7.8$ Hz, 1H), 6.82 (t, $J=7.8$ Hz, 1H), 6.70 (t, $J=7.8$ Hz, 1H), 5.59 (s, 1H), 4.00 (q, $J=7.0$ Hz, 2H), 2.63 (t, $J=7.0$ Hz, 2H), 1.99 (s, 3H), 1.77 (s, 3H), 1.38-1.32 (m, 2H), 1.01-1.07 (m, 4H), 0.85 (t, $J=7.0$ Hz, 3H). ^{13}C NMR (100MHz, DMSO-d_6) δ ppm 166.5, 138.4, 136.9, 135.9, 132.9, 127.8, 127.6, 127.5, 126.5, 124.4, 123.3, 121.6, 121.3, 119.7, 119.3, 117.2, 115.8, 111.6, 111.5, 99.5, 79.2, 60.3, 31.3, 30.5, 30.2, 23.8, 23.5, 21.9, 20.7, 14.3, 14.0. EI HRMS calcd. for $\text{C}_{31}\text{H}_{33}\text{N}_3\text{O}_4\text{S}$ m/z : 543.2192, found : 543.2195.

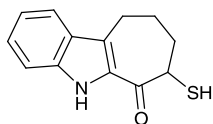


Synthesis of 3-10c : The title compound was synthesized as described for **3-10d**, in 90% yield. ^1H NMR (Acetone- D_6) δ : 10.34 (s, br, 1H), 7.65 (d, $J = 8.2$ Hz, 1H), 7.46 (d, $J = 8.6$ Hz, 1H), 7.27 (t, $J = 7.0$ Hz, 1H), 7.05 (t, $J = 7.0$ Hz, 1H), 3.16-3.08 (m, 2H), 2.78-2.70 (m, 2H), 2.04-1.99 (m, 2H), 1.97-1.88 (m,

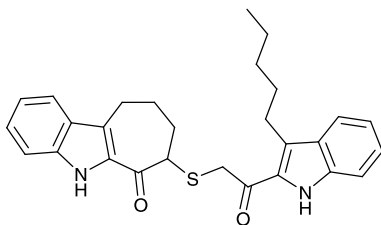
2H). ^{13}C NMR (100MHz, Acetone-D6) δ ppm 195.0, 127.3, 122.4, 121.0, 113.7, 43.9, 27.9, 26.4, 24.0. EI HRMS calcd. for $\text{C}_{13}\text{H}_{13}\text{NO}$ m/z : 199.0997, found : 199.0992.



Synthesis of 3-11c: The bromide was made in accordance with the A.N. Kost *et al.* method in 80 % yield. ^1H NMR (400 MHz, DMSO-d6) δ ppm: 11.44 (s, br, 1H), 7.64 (d, J = 8.2 Hz, 1H), 7.27 (t, J = 7.0 Hz, 1H), 7.03 (t, J = 7.0 Hz, 1H), 5.22–5.16 (m, 1H), 3.30-3.18 (m, 2H), 2.48–2.23 (m, 2H), 2.21–1.98 (m, 2H). ^{13}C NMR (100MHz, DMSO-d6) δ ppm 187.2, 137.6, 130.1, 126.9, 126.4, 123.5, 121.3, 119.7, 112.4, 56.8, 32.1, 24.8, 23.0. EI HRMS calcd. for $\text{C}_{13}\text{H}_{12}\text{BrNO}$ m/z : 277.0102, found : 277.0105.

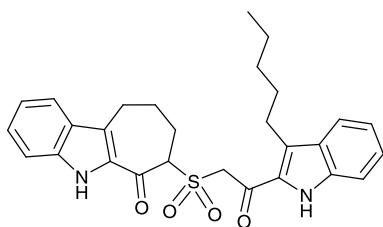


Synthesis of 3-12c: The title compound was made following the method for synthesis of thiols in 85 % yield. ^1H NMR (400 MHz, CDCl_3) δ ppm: 8.98 (s, br, 1H), 7.65 (d, J = 8.6 Hz, 1H), 7.42-7.32 (m, 2H), 7.18-7.09 (m, 1H), 4.18-4.10 (m, 2H), 3.28–3.16 (m, 2H), 3.30-3.00 (m, 2H), 2.52 (d, J = 6.6 Hz, 1H), 2.45-2.37 (m, 1H), 2.27-2.10 (m, 3H). ^{13}C NMR (100MHz, CDCl_3) δ ppm 191.9, 137.3, 130.8, 127.8, 127.1, 124.7, 123.9, 121.4, 120.4, 112.2, 48.0, 31.9, 25.7, 23.6. ESI HRMS calcd. for $\text{C}_{13}\text{H}_{13}\text{NOS}$ m/z : 231.0718, found : 231.0721.



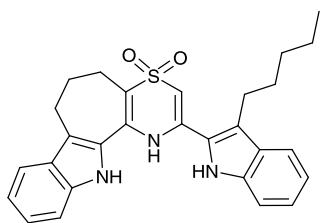
Synthesis of 3-13c: The title compound was synthesized by following the method described for synthesis of **3-13d** in 80 % yield. ^1H NMR (400 MHz, CDCl_3) δ ppm: 11.26 (s, br, 1H), 11.03 (s, br, 1H), 7.65-7.56 (m, 2H), 7.46-7.40 (m, 2H), 7.28-7.20 (m, 2H), 7.08-7.00 (m, 2H), 4.18-3.86 (m, 2H), 4.05-4.01 (m, 1H), 3.46-3.18 (m, 1H), 3.10-2.85 (m, 3H), 2.82-2.70 (m,

1H), 2.37-2.16 (m, 1H), 1.45-1.12 (m, 4H), 0.87 (t, $J=7.0$ Hz, 3H). ^{13}C NMR (100MHz, CDCl_3 and few drops of DMSO-d_6) δ ppm 188.9, 186.2, 136.1, 135.6, 131.7, 130.0, 128.8, 126.4, 125.9, 124.6, 124.4, 124.0, 122.4, 121.6, 119.5, 118.2, 113.2, 111.2, 50.8, 41.2, 36.9, 30.5, 29.5, 27.2, 25.0, 23.7, 21.1, 12.7. EI HRMS calcd. for $\text{C}_{28}\text{H}_{30}\text{N}_2\text{O}_2\text{S}$ m/z : 458.2028, found : 458.2034.



Synthesis of 3-14c: The title compound was synthesized by following the method described for general synthesis of sulfones in 85% yield. ^1H NMR (400 MHz, CDCl_3) δ ppm: 11.82 (s, br, 1H), 11.58

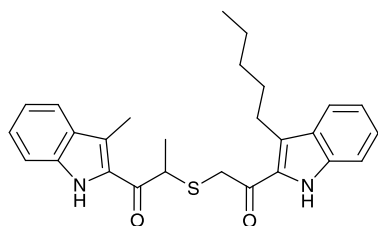
(s, br, 1H), 8.35 (s, 1H), 7.88 (d, $J=8.6$ Hz, 1H), 7.66 (d, $J=8.6$ Hz, 1H), 7.50-7.41 (m, 2H), 7.29 (t, $J=7.4$ Hz, 1H), 7.06 (t, $J=7.4$ Hz, 1H), 4.31 (q, $J=7.0$ Hz, 2H), 4.24-4.10 (m, 2H), 4.05-4.00 (m, 1H), 3.08-3.00 (m, 2H), 2.98-2.62 (m, 2H), 2.40-1.92 (m, 4H), 1.62-1.58 (m, 2H), 1.38-1.25 (m, 7H), 0.80 (t, $J=7.0$ Hz, 3H). ^{13}C NMR (100MHz, CDCl_3 and DMSO-d_6 mixture in 1:1 ratio) δ ppm 185.7, 180.9, 166.0, 166.3, 139.4, 136.8, 132.6, 129.7, 127.4, 127.0, 126.8, 126.1, 125.9, 123.7, 121.5, 120.4, 119.4, 111.9, 111.7, 70.1, 61.1, 59.9, 31.1, 29.8, 25.1, 24.3, 22.7, 21.7, 20.8, 13.6, 13.3. ESI HRMS calcd. for $\text{C}_{28}\text{H}_{30}\text{N}_2\text{O}_4\text{S}$ m/z : 490.1926, found : 490.1930.



Synthesis of 3-5a: the title compound is made following the general method for synthesis of thiazine dioxides in 80 % yield. ^1H NMR (400 MHz, DMSO-d_6) δ ppm: 11.57 (s, br, 1H), 11.43 (s, br, 1H), 10.45

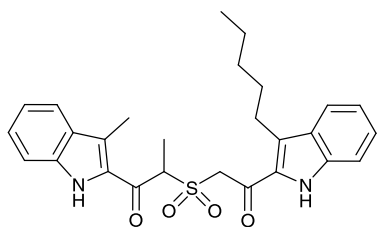
(s, br, 1H), 8.34 (s, 1H), 7.88 (dd, $J=8.6$ Hz, $J=1.6$ Hz, 1H), 7.67-7.61 (m, 2H), 7.51 (d,

$J=8.2$ Hz, 1H), 7.26 (t, $J=7.8$ Hz, 1H), 7.10 (t, $J=7.8$ Hz, 1H), 6.17 (s, 1H), 4.35 (q, $J=7.0$ Hz, 2H), 3.12 (t, $J=7.0$ Hz, 2H), 2.95 (t, $J=7.8$ Hz, 2H), 2.64-2.60 (m, 2H), 2.32-2.24 (m, 2H), 1.73-1.64 (m, 2H), 1.40-1.30 (m, 7H), 0.85 (t, $J=7.0$ Hz, 3H). ^{13}C NMR (100MHz, DMSO- d_6) δ ppm 166.5, 138.4, 136.9, 135.9, 132.9, 127.8, 127.6, 127.5, 126.5, 124.4, 123.3, 121.6, 121.3, 119.7, 119.3, 117.2, 115.8, 111.6, 111.5, 99.5, 79.2, 60.3, 31.3, 30.5, 30.2, 23.8, 23.5, 21.9, 20.7, 14.3, 14.0. ESI HRMS calcd. for $\text{C}_{31}\text{H}_{33}\text{N}_3\text{O}_4\text{S}$ m/z : 543.2192, found : 543.2196.



Synthesis of 3-13e: the title compound is made as described for compound **3-13d** in 80 % yield. ^1H NMR (400 MHz, CDCl_3) δ ppm: 10.06 (s, br, 1H), 9.22 (s, br, 1H), 7.70-7.64 (m, 2H), 7.45-7.32 (m, 4H), 7.16-7.06

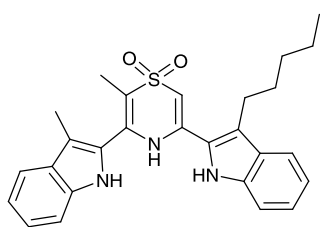
(m, 2H), 4.48 (q, $J = 6.6$ Hz, 1H), 4.10-3.92 (m, 2H), 3.08-3.02 (m, 2H), 2.67 (s, 3H), 1.74-1.65 (m, 2H), 1.62 (d, $J = 6.6$ Hz, 3H), 1.56-1.21 (m, 4H), 0.90 (t, $J=7.0$ Hz, 3H). ^{13}C NMR (100MHz, CDCl_3) δ ppm 189.8, 187.8, 136.7, 136.6, 130.5, 130.1, 128.6, 128.2, 127.0, 126.5, 126.4, 121.5, 121.1, 120.3, 120.1, 120.0, 112.1, 112.0, 111.9, 43.6, 37.2, 32.0, 31.4, 25.8, 22.5, 16.5, 14.0, 11.0. EI HRMS calcd. for $\text{C}_{27}\text{H}_{30}\text{N}_2\text{O}_2\text{S}$ m/z : 446.2028, found : 446.2034.



Synthesis of 3-14e: the title compound is made following the general method for synthesis of sulfones in 85 % yield. ^1H NMR (400 MHz, CDCl_3) δ ppm: 9.89 (s, br, 1H), 9.79 (s, br, 1H), 7.66-7.60 (m, 2H),

7.38-7.27 (m, 4H), 7.17-7.08 (m, 2H), 5.42-5.34 (m, 1H), 4.81 (dd, $J = 40.0$ Hz, $J = 14.5$

Hz, 2H), 3.08-3.04 (m, 2H), 2.67 (s, 3H), 1.82 (d, $J = 6.6$ Hz, 3H), 1.68-1.58 (m, 2H), 1.42-1.30 (m, 4H), 0.87 (t, $J = 7.0$ Hz, 3H). ^{13}C NMR (100MHz, CDCl_3 and a few drops of DMSO-d_6) δ ppm 184.6, 180.2, 137.7, 137.4, 130.8, 130.7, 129.6, 128.5, 128.0, 127.6, 127.5, 123.4, 121.5, 121.4, 120.6, 120.5, 112.5, 112.4, 65.5, 59.5, 36.5, 25.3, 22.5, 14.0, 12.3, 10.9. EI HRMS calcd. for $\text{C}_{27}\text{H}_{30}\text{N}_2\text{O}_4\text{S}$ m/z : 478.1926, found : 478.1928.



Synthesis of 3-6a: the title compound is made following the general method for synthesis of thiazine dioxides in 80 % yield. ^1H NMR (400 MHz, CDCl_3) δ ppm: 9.16 (s, br, 1H), 9.02 (s, br, 1H), 7.68 (s, br, 1H), 7.61-7.56 (m, 2H),

7.37 (d, $J=8.6$ Hz, 2H), 7.28-7.23 (m, 2H), 7.20-7.12 (m, 2H), 5.71 (s, 1H), 2.70-2.64 (m, 2H), 2.22 (s, 3H), 1.93 (s, 3H), 1.45-1.40 (m, 2H), 1.16-1.00 (m, 4H), 0.72 (t, $J=7.0$ Hz, 3H). ^{13}C NMR (100MHz, CDCl_3) δ ppm 137.6, 136.6, 132.9, 128.2, 124.7, 124.3, 120.5, 120.2, 120.0, 119.9, 119.6, 114.4, 112.0, 111.7, 31.8, 30.9, 24.5, 22.3, 13.9, 9.5, 8.6. EI HRMS calcd. for $\text{C}_{27}\text{H}_{29}\text{N}_3\text{O}_2\text{S}$ m/z : 459.1980, found : 459.1984.

3.6 References

1. (a) Jorgensen, W. L.; Pranata, J. *J. Am. Chem. Soc.* **1990**, *112* (5), 2008-2010; (b) Pranata, J.; Wierschke, S. G.; Jorgensen, W. L. *J. Am. Chem. Soc.* **1991**, *113* (8), 2810-2819.
2. (a) Zimmerman, S. C.; Murray, T. J. *Tet. Lett.* **1994**, *35* (24), 4077-4080; (b) Djurdjevic, S.; Leigh, D. A.; McNab, H.; Parsons, S.; Teobaldi, G.; Zerbetto, F. *J. Am. Chem. Soc.* **2006**, *129* (3), 476-477; (c) Blight, B. A.; Camara-Campos, A.;

- Djurdjevic, S.; Kaller, M.; Leigh, D. A.; McMillan, F. M.; McNab, H.; Slawin, A. M. Z. *J. Am. Chem. Soc.* **2009**, *131* (39), 14116-14122; (d) Blight, B. A.; Hunter, C. A.; Leigh, D. A.; McNab, H.; Thomson, P. I. T. *Nat Chem* **2011**, *3* (3), 244-248.
3. (a) Caluwe, P.; Majewicz, T. G. *J. Org. Chem.* **1977**, *42* (21), 3410-3413; (b) Bell, D. A.; Anslyn, E. V. *Tetrahedron* **1995**, *51* (26), 7161-7172.
4. Murray, T. J.; Zimmerman, S. C. *J. Am. Chem. Soc.* **1992**, *114* (10), 4010-4011.
5. Taubitz, J.; Lüning, U. *Aust. J. Chem.* **2009**, *62* (11), 1550-1555.
6. (a) Brunsveld, L.; Folmer, B. J. B.; Meijer, E. W.; Sijbesma, R. P. *Chem. rev.* **2001**, *101* (12), 4071-4098; (b) Brunsveld, L.; Folmer, B. J. B.; Meijer, E. W. *MRS Bull.* **2000**, *25* (04), 49-53.
7. Wang, H.-B.; Mudraboyina, B. P.; Li, J.; Wisner, J. A. *Chem. Commun.* **2010**, *46* (39), 7343-7345.
8. Wang, H.-B.; Mudraboyina, B. P.; Wisner, J. A. *Chem. Eur. J.* **2012**, *18* (5), 1322-1327.
9. (a) Robinson, B. *Chem. Rev.* **1963**, *63* (4), 373-401; (b) Hillier, M. C.; Marcoux, J.-F.; Zhao, D.; Grabowski, E. J. J.; McKeown, A. E.; Tillyer, R. D. *J. Org. Chem.* **2005**, *70* (21), 8385-8394.
10. Kost, A. N.; Gorbunova, S. M.; Budylin, V. A. *Khim. Geterotsykl.* **1971**, *11* 1522-1526.

11. Yamamura, Y.; Toriyama, F.; Kondo, T.; Mori, A. *Tetrahedron: Asymmetry* **2002**, *13* (1), 13-15.
12. (a) Jones, S. M.; Urch, J. E.; Kaiser, M.; Brun, R.; Harwood, J. L.; Berry, C.; Gilbert, I. H. *J. Med. Chem.* **2005**, *48* (19), 5932-5941; (b) Tice, C. M.; Bryman, L. M. *Tetrahedron* **2001**, *57* (14), 2689-2700.
13. Nishikimi, Y.; Fukushi, H.; Miki, H. Indole derivative and use for treatment of cancer. US2007/0254877 A1, 2007.
14. Mascal, M.; Hext, N. M.; Warmuth, R.; Moore, M. H.; Turkenburg, J. P. *Angew. Chem. Int. Ed.* **1996**, *35* (19), 2204-2206.
15. (a) Yu, J.; Zhang, J.; Yang, L.; Chen, W. Method of preparing 3,6-dialkyl-5,6-dihydro-4-hydroxy-2H-pyran-2-one CN 101058569 A 20071024, 2007; (b) Madsen, U.; Bräuner-Osborne, H.; Frydenvang, K.; Hvene, L.; Johansen, T. N.; Nielsen, B.; Sánchez, C.; Stensbøl, T. B.; Bischoff, F.; Krogsgaard-Larsen, P. *J. Med. Chem.* **2001**, *44* (7), 1051-1059.
16. Bisson, A. P.; Carver, F. J.; Eggleston, D. S.; Haltiwanger, R. C.; Hunter, C. A.; Livingstone, D. L.; McCabe, J. F.; Rotger, C.; Rowan, A. E. *J. Am. Chem. Soc.* **2000**, *122* (37), 8856-8868.
17. Li, X.; Fang, Y.; Deng, P.; Hu, J.; Li, T.; Feng, W.; Yuan, L. *Org. Lett.* **2011**, *13* (17), 4628-4631.
18. Zeng, J.; Wang, W.; Deng, P.; Feng, W.; Zhou, J.; Yang, Y.; Yuan, L.; Yamato,

K.; Gong, B. *Org. Lett.* **2011**, *13* (15), 3798-3801.

Chapter 4

4 Synthesis and Binding Studies of a Complementary DDD•AAA Complex and a Self-Associated Double-Helical AAADDD•DDDAAA Complex

The strongest possible hydrogen bonded complexes arise from the contiguous arrangement of the arrays. Numerous examples have been provided and discussed in detail in the preceding chapter. Recently, several examples have been developed in our research group and reported.¹ Among them, of particular interest was the AAA•DDD hydrogen bonded double complex **4-1•4-2**, (Figure 4-1) stabilized by three hydrogen bonds that exhibits a very high binding constant ($K_a \geq 10^5 \text{ M}^{-1}$).²

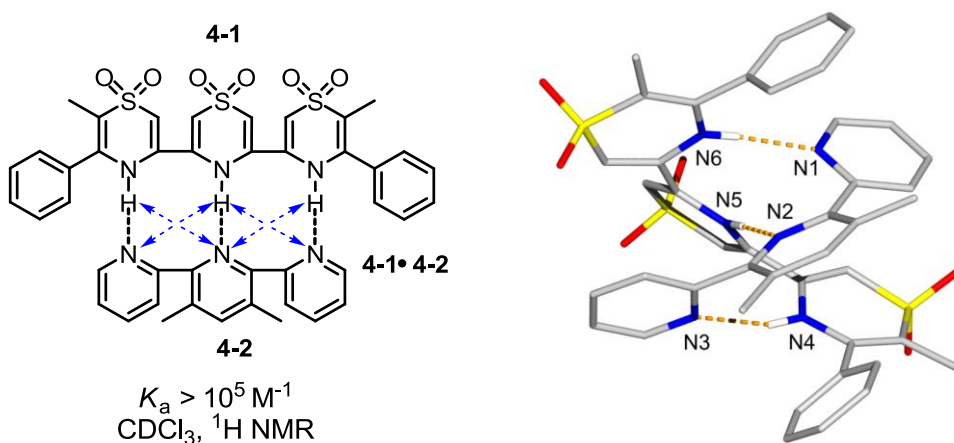


Figure 4-1 An AAA•DDD complementary complex with high stability ($K_a \geq 10^5 \text{ M}^{-1}$) in CDCl_3 . Stick representation of X-ray crystal structure of **4-1•4-2** displaying the double helical arrangement of the complex.

Donor array **4-1** can be drawn into a solution of non-polar, non-competitive solvent CDCl_3 in the presence of a molar equivalent of complementary **4-2**. Unfortunately, the donor array **4-1** alone is completely insoluble in all non-polar solvents

examined. This insolubility prevents a proper binding study and thus the evaluation of the donor array as a potential monomer in building supramolecular assemblies.

A potential reason behind the accompanying solubility issue was evident from the solid state structure of a similarly insoluble DDD array **4-3a**, (Figure 4-2). Array **4-3a** (R = H) was completely insoluble in non-polar solvents such as CDCl_3 . Introduction of a methyl group for R in **4-3b** induced solubility in CDCl_3 . Presumably this methyl group provides enough steric hindrance to avoid the undesirable intermolecular hydrogen bonds between the DDD monomers observed in solid state **4-3a**.

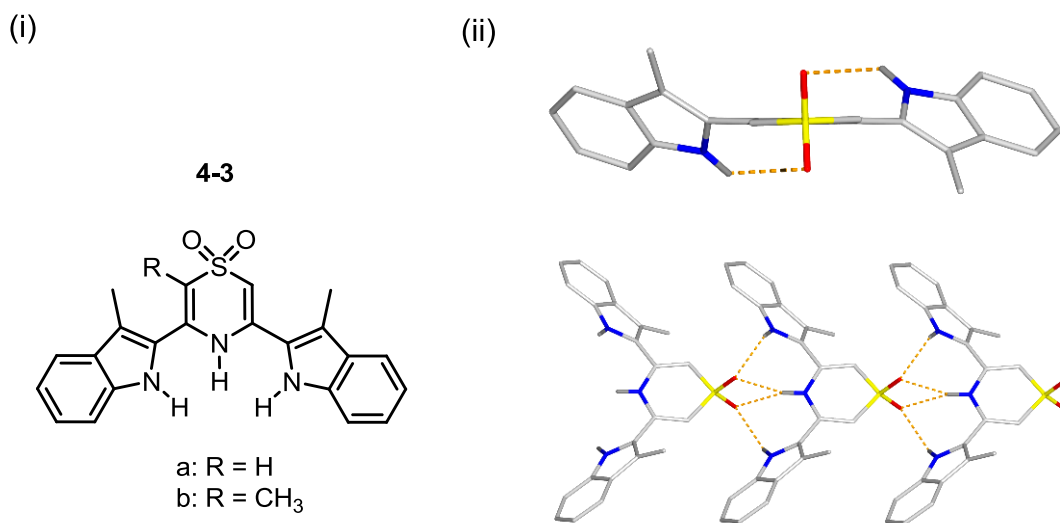


Figure 4-2 (i) Thiazine dioxide and indole containing DDD arrays. (ii) Crystal structure of the insoluble array **4-3a** (R = H) displaying the intermolecular hydrogen bonds between N-H donors of the thiazine dioxide and indole heterocycles and oxygen acceptors of the thiazine dioxide sulfones forming an infinite columnar array.^{1a}

Following these encouraging results, we considered incorporating an alkyl group on the central thiazine dioxide heterocycle to induce solubility in the DDD array **4-1**. Since the design consists of three thiazine dioxide rings (i.e. stronger hydrogen bonding compared to indole donor subunits) it was assumed that the degree of intermolecular

interaction might be greater in this particular case. Thus a more demanding steric encumbrance than one methyl group was estimated to be necessary to prevent unintended intermolecular hydrogen bonding. In the previous chapter, pentyl chains were successful in inducing a great degree of solubility and hence an alkyl chain was introduced instead of a methyl group on the central thiazine dioxide heterocycle.

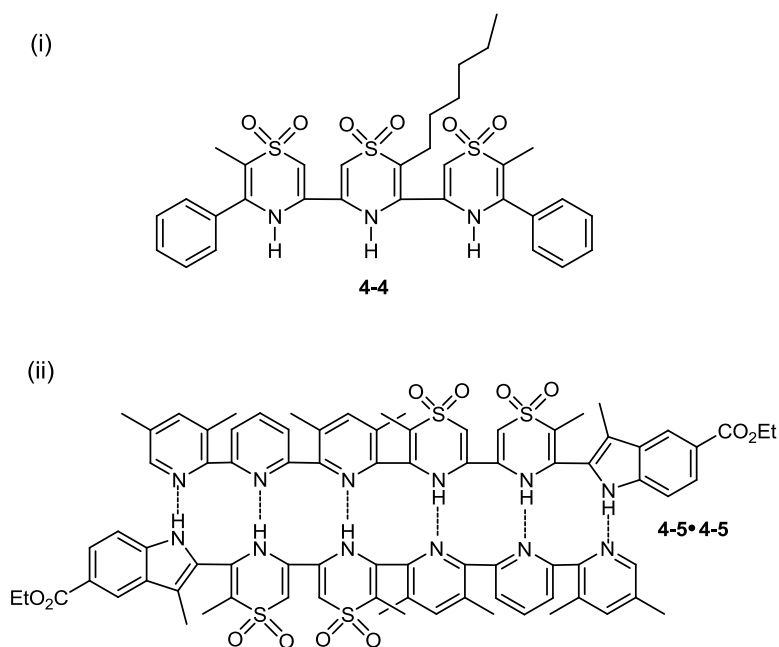
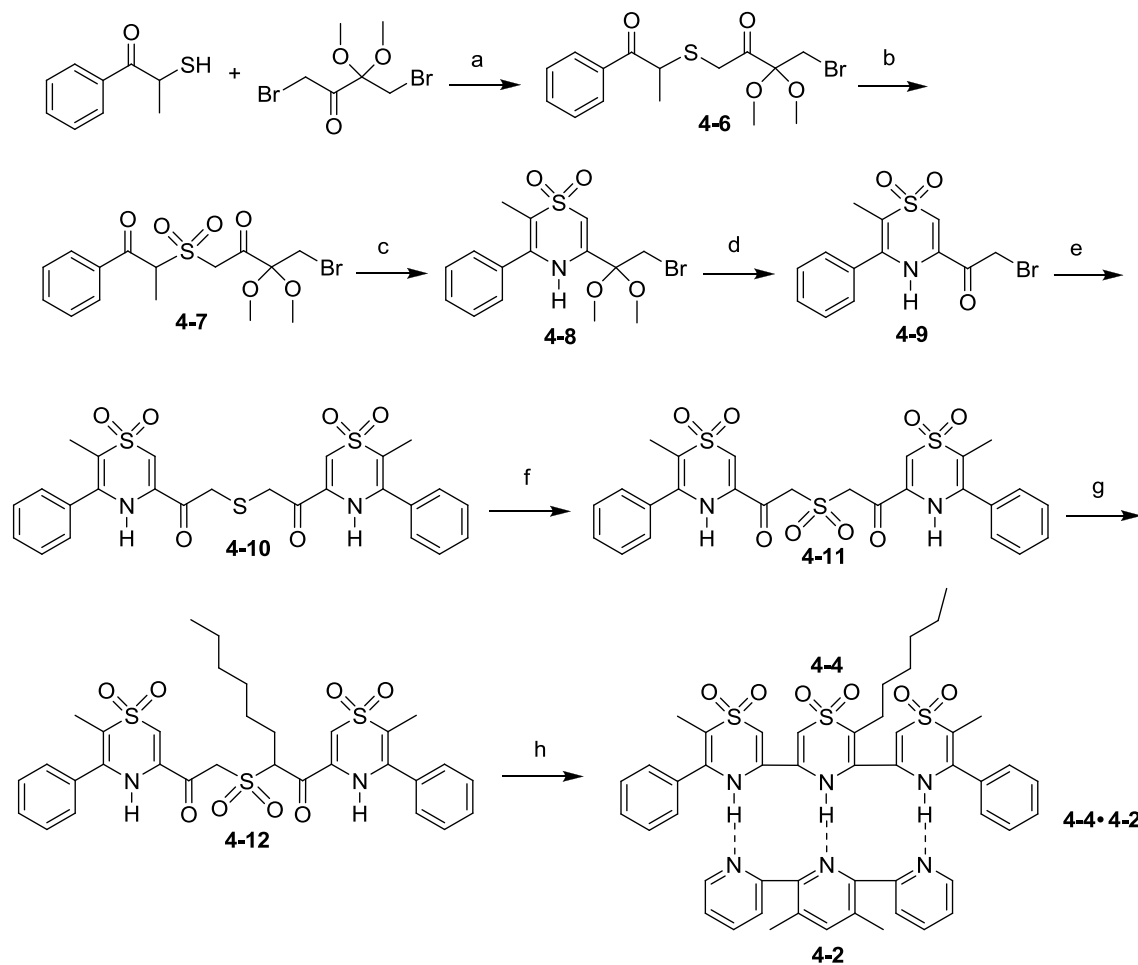


Figure 4-3 (i) Ter(thiazine dioxide) based DDD array **4-4** including a hexyl chain attached to the central donor heterocycle to induce solubility in CDCl_3 ; (ii) a six-hydrogen bond self-complementary AAADDD array **4-5**.

Apart from employing entirely contiguous arrays, extremely stable complexes can be also be constructed by increasing the number of hydrogen bonds.^{3,4} As the number of hydrogen bonds increases, cooperativity generally results in an increasing association constant.⁵ Taking the successful AADD designs from chapter 2 we wished to test their extensibility and resulting binding behavior by a synthesizing six hydrogen bond self-complementary complex. Toward this end, a six membered AAADDD array was

designed to study such a system. Thus, schemes were drawn up to synthesize arrays **4-4** and **4-5** (Figure 4-3).

4.1 Synthesis of Alkylated DDD Array 4-4



Scheme 4-1 Synthetic pathway for the preparation of alkylated DDD array **4-4** which undergoes complementary helical complex formation with **4-2**. Reaction conditions: a) K_2CO_3 , CH_3CN , 12-16 h; b) 4 eq. UHP, 3 eq. TFAA, CH_3CN , 90 minutes; c) 8 eq. NH_4OAc , AcOH, reflux, 12-16 h; d) formic acid, reflux; e) $\text{Na}_2\text{S}\cdot 9\text{H}_2\text{O}$, H_2O , acetone 3 h; f) 4 eq. UHP, 3 eq. TFAA, CH_3CN , 90 minutes (g) 4 portions of 2eq. 1-iodohexane and 2eq. DBU, CH_3CN , approximately 7 days; (h) 8 eq. NH_4OAc , AcOH, reflux, 3 days.

The synthetic steps involved in preparation of the alkylated donor array are largely the same as previously reported.^{1a} The scheme is unaltered until the alkylation of sulfone **4-11**, followed by the cyclization (Scheme 4-1).

Some modifications were made in terms of reaction conditions, purifications and isolations, thereby giving better results. The condensation of the protected dibromide and the 2-mercapto-propiofenone was carried out in the presence of an excess of potassium carbonate (3 eq.) and the reaction time was reduced to 12 h (from 2 days as originally reported) and extracted with DCM to give clean product. Thioether **4-6**, was oxidized using urea hydrogen peroxide (UHP) and trifluoro acetic anhydride (TFAA) in a 4:3 ratio at room temperature in acetonitrile over 2 h. The product was cleaner compared to the one obtained using *m*CPBA as oxidant, with no side products observed. Cyclization of the sulfone was performed in glacial acetic acid in the presence of 6-8 eq. of ammonium acetate. Best results are obtained when heated at 100 °C to 110 °C. Any temperature above this leads to cleavage of the cyclized product producing propiofenone.

The protected bromide **4-8** was deprotected by refluxing the reaction mixture in formic acid for approximately an hour. Letting the reaction run for longer times leads to formation of the cleaved product again. The deprotected bromide (**4-9**) was dissolved in acetone and added drop wise to an aqueous solution containing a half an equivalent of sodium sulfide (nonahydrate) at 0 °C and the reaction mixture was stirred at room temperature for 3 h to yield thioether **4-10**. The change in reagent from sodium hydrogen sulfide (original procedure) to sodium sulfide allowed shorter reaction times and resulted in cleaner products. Thioether **4-10** was oxidized using the 4:3 UHP/TFAA mixture in

acetonitrile. The reaction mixture was extracted with DCM, washed with water and sodium bicarbonate solution to yield pure sulfone **4-11**, in high yield. The alkylation with the hexyl chain was carried out in basic medium using excess DBU^{6,7} and 1-iodohexane. Sterics play a significant role as the alkylation took approximately a week stirring at room temperature. Heating the reaction mixture resulted in decomposition. The reaction mixture was washed with 10 % HCl solution, extracted with DCM and carried forward to the cyclization step⁸ without any further purification.^{1a, 9} The final DDD array **4-4** was obtained upon treatment of the alkylated sulfone with 6-8 equivalents of ammonium acetate at reflux in acetic acid for 3 days. The reaction times were likely a result of sterics of the alkyl chain. The final product was purified by preparatory thin layer chromatography using 5% CH₃OH in CH₂Cl₂ as eluent.

4.2 NMR Titration Studies of the AAA•DDD Array

The solubility induced by the hexyl chain allowed the execution of binding studies and analysis of its complexation with acceptor array **4-2**. ¹H NMR titrations conducted in CDCl₃ show significant downfield shifts of the N-H protons of the thiazine dioxide heterocycles. Proton peaks corresponding to amine groups, N-H^{abc} are shifted from 8.30, 7.86 and 8.12 ppm to 12.76, 11.89 and 12.08 ppm ($\Delta\delta = 4.46, 4.03$ and 3.96 ppm) respectively. The large values of downfield chemical shifts are suggestive of very strong binding between the participating acceptor and donor arrays. The upfield shifts of phenyl ring protons are indicative of either π stacking with the pyridyl rings of **4-2**, induction due to hydrogen bonding or combination of both the effects. The other peak movements are less definitive of particular interactions.

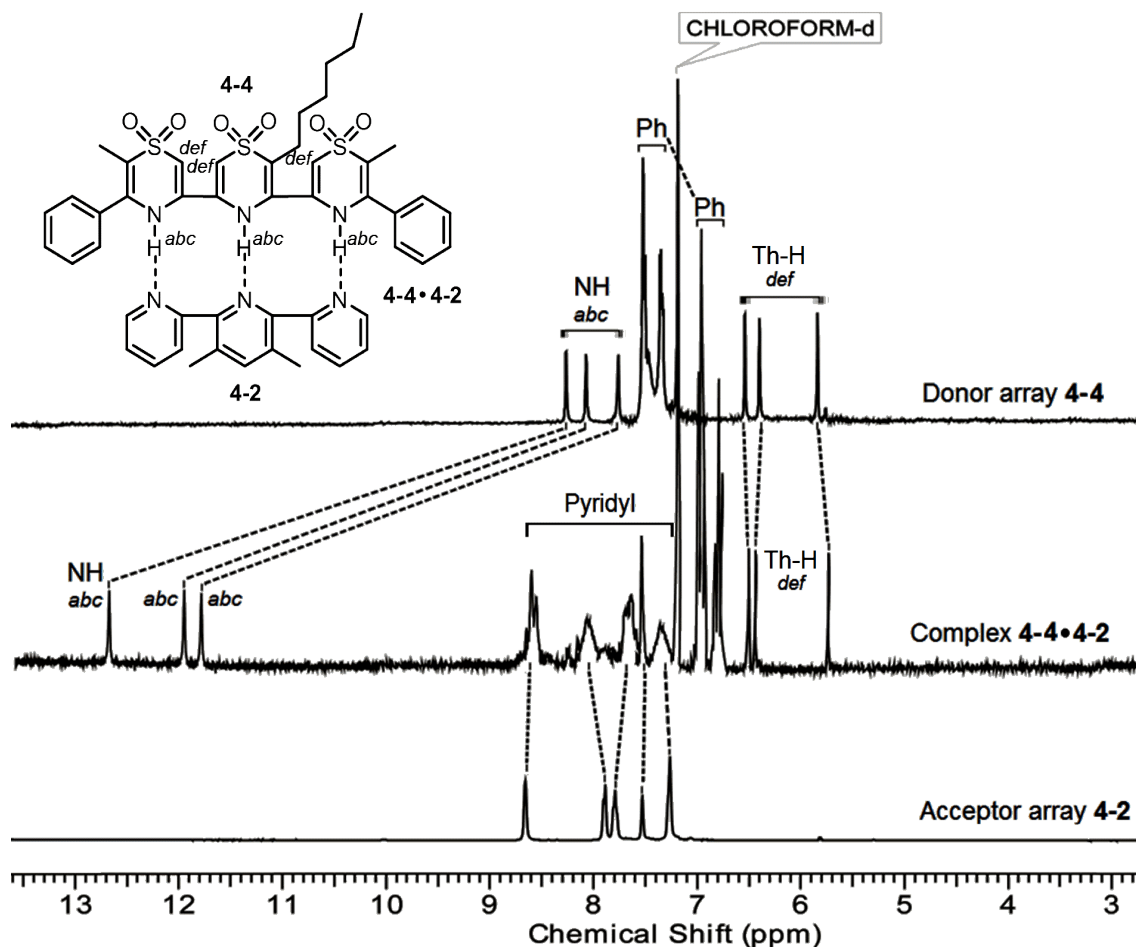


Figure 4-4 Stacked plot of the downfield region of the ¹H NMR spectra of alkylated donor array 4-4, acceptor array 4-2 and the complex 4-4.4-2 in CDCl₃ at room temperature. Chemical shift changes of the three thiazine dioxide NH groups, (NH, *abc*), three thiazine ring protons (Th-H, *def*), phenyl ring protons (Ph, upfield shifts) and pyridyl protons (Pyridyl-Hs) are indicated by dotted lines. It is apparent that the addition of the hexyl chain solubilizes array 4-4 in CDCl₃.

In our recent report^{1a} the K_a value for complex **4-1.4-2** was determined to have a lower limit² of 10^5 M^{-1} and the K_a value of the complex **4-4.4-2** was determined using NMR titration (performed thrice) to be $1.40 (\pm 0.75) \times 10^5 \text{ M}^{-1}$.

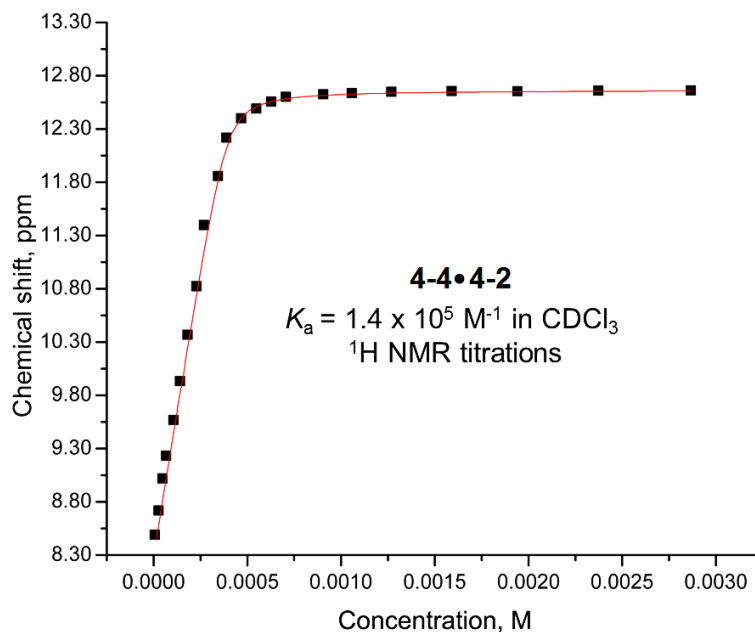


Figure 4-5 Titration curve displaying the concentration dependent chemical shifts of the amine proton of thiazine dioxide of **4-4** when titrated with **4-2**. For clarity only one of the three NH protons is shown here.

Further analysis of the complexation was conducted employing Isothermal Titration Calorimetry (ITC). Titration was carried out in undeuterated HPLC grade chloroform (performed three times) and a K_a value of $1.35 (\pm 0.10) \times 10^5 \text{ M}^{-1}$ was determined by fitting the data satisfactorily to a 1:1 binding model (Figure 4-4). Analysis of the data provides the thermodynamic quantities $\Delta G = -28.68 (\pm 0.6) \text{ kJ mol}^{-1}$, $\Delta H = -56.19 (\pm 0.6) \text{ kJ mol}^{-1}$ and $\Delta S = -92.88 \text{ J mol}^{-1}$. We observe that the free energy of complexation is enthalpy driven as one would expect for hydrogen bond driven complexation in non-polar solution.

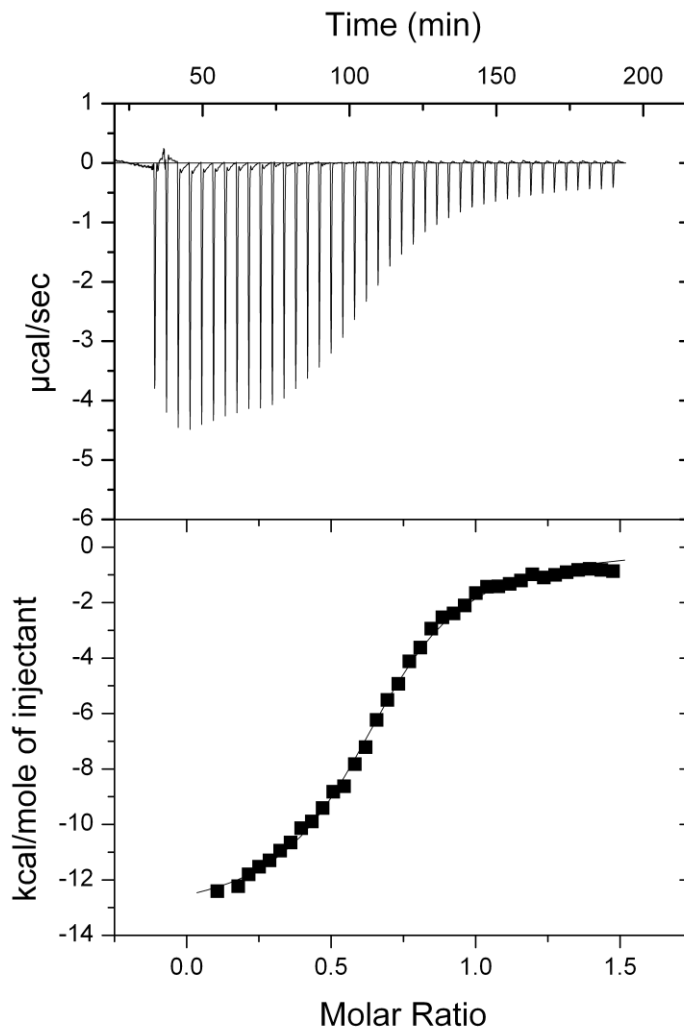


Figure 4-6 ITC data for the binding of **4-4** and **4-2** in CDCl_3 at 22°C . The upper plot illustrates the power as a function of time and the bottom plot displays integrated enthalpy values as a function of the molar ratio of **4-2** titrated into **4-4**.

Though the K_a value indicates strong complexation, three thiazine dioxides are expected to result in formation of a stronger complex probably with a likely binding constant approximately an order of magnitude higher. The reason for the attenuation of the K_a value in this case may be explained based on the observations from the previous chapter, where the inclusion of an alkyl group not only contributed to an increase in solubility of the DDD arrays but also a decrease in the association constant by

approximately an order of magnitude. It is reasonable to expect a similar effect at work here. Applied to the present AAA•DDD complex we may estimate a K_a value $\geq 1 \times 10^6$ M^{-1} for the non-alkylated complex **4-1.4-2**. Hence, an extra amount of energy is required to bring the DDD array in to right conformation to form the complex.

4.3 Synthesis of a Double Helical Self-Complementary AAADDD Array

Although self-complementary complexes have been well studied in literature, there are very few examples of six or more hydrogen bond arrays that form self-complementary complexes. These are highly stable due to the number of hydrogen bonds present in the complex. Based on these considerations, a six hydrogen bonding self-complementary AAADDD•DDDAAA system was selected to test the binding strength and extensibility of our self-complementary design.

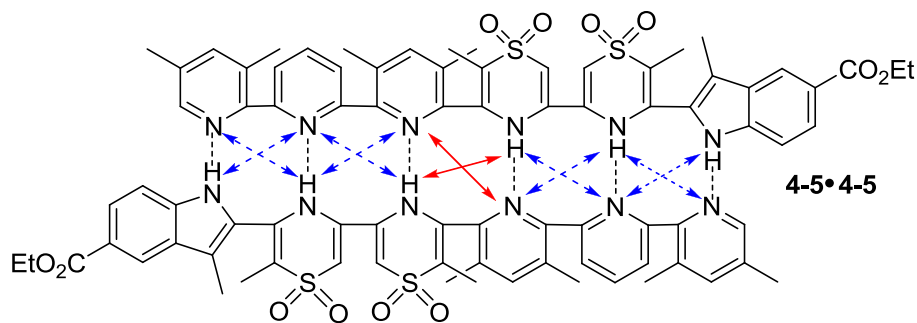
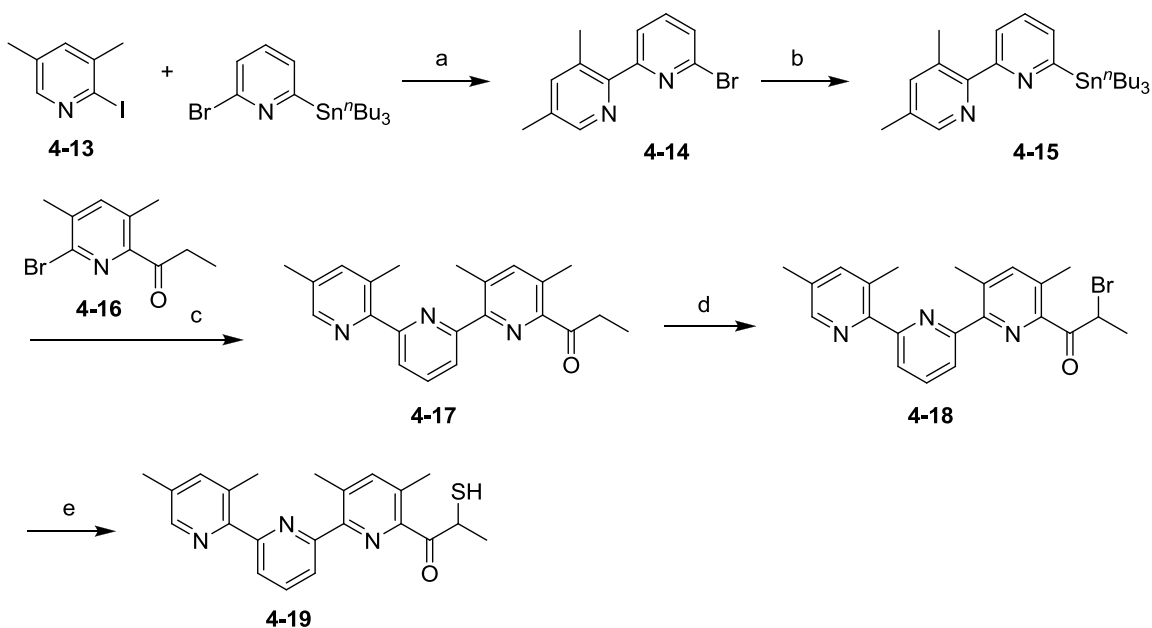


Figure 4-7 A double-helical six hydrogen bonded self-complementary system **4-5.4-5** based on thiazine dioxide, indole and pyridine heterocycles.

The design consists of two lutidines sandwiching a pyridine connected to two thiazine dioxides terminated by an indole donor.^{1b,10} An ester appended indole was preferred to enhance the solubility of the complex and also as a mild electron withdrawing group for additional stability. Methyl groups of the lutidine heterocycle

should increase the electron donating nature of the acceptor components and to induce an angular twist to aid in formation of the double helical complex. There are eight attractive secondary interactions and two repulsive secondary interactions and so overall the stabilizing factors should greatly outweigh the number of destabilizing factors.

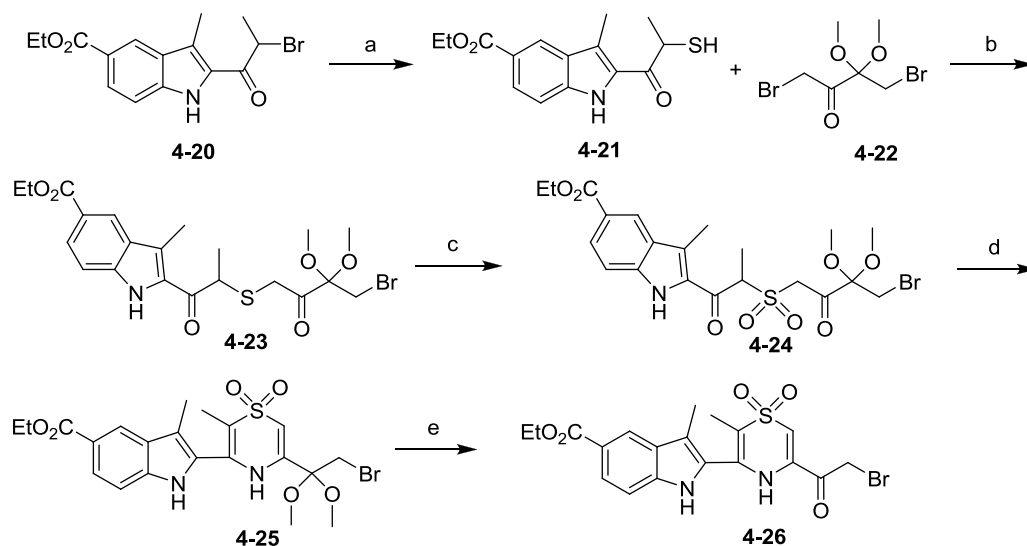


Scheme 4-2 Synthetic scheme leading to preparation of acceptor component **4-19**. Reaction conditions: (a) 5 % $\text{Pd}(\text{PPh}_3)_4$, toluene, reflux 16 h., 85%; (b) 2.4 eq. $n\text{BuLi}$, THF, $-78\text{ }^\circ\text{C}$, 2 h. 2.2 eq. $\text{Sn}^n\text{Bu}_3\text{Cl}$, THF, $-78\text{ }^\circ\text{C}$ to $21\text{ }^\circ\text{C}$, 80 %; (c) 5 % $\text{Pd}(\text{PPh}_3)_4$, toluene, reflux 16 h., 85%; (d) 1.2 eq. Br_2 , anhy. THF, 16 h., 70%. (e) (i) 1 eq. potassium thioacetate, absolute ethanol, 3h. (ii) 1 eq. cysteamine. HCl, acetonitrile, 4 h. 85%.

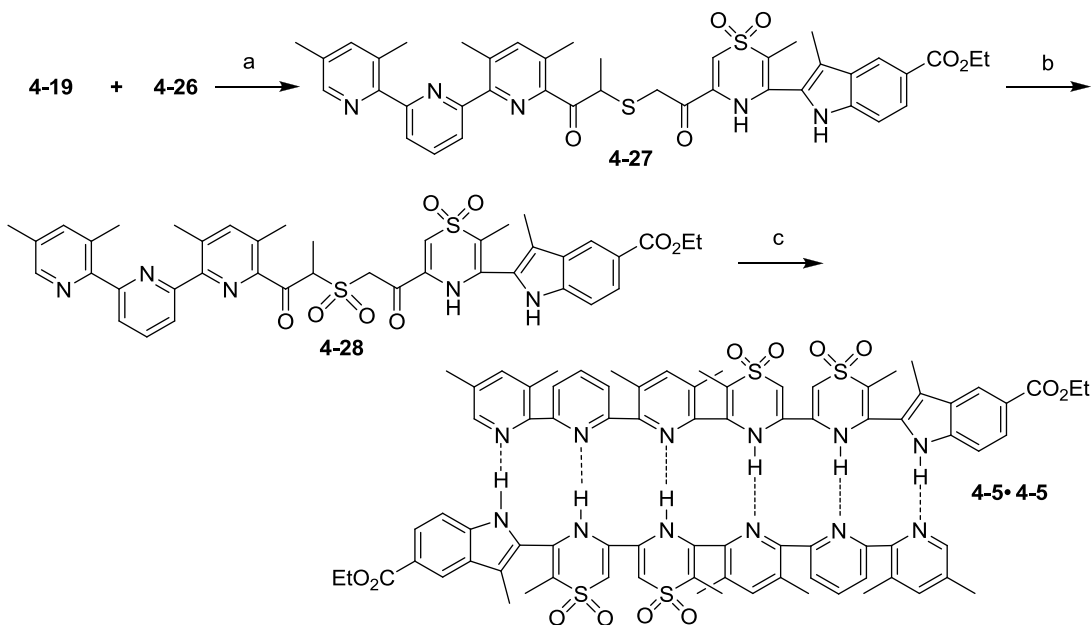
The synthesis is straight forward and most of the steps are derived from the synthetic schemes of the self-complementary and complementary arrays reported in chapter 2 and 3. The acceptor fragment (**4-19**, Scheme 4-2) was largely synthesized by Stille coupling of suitably functionalized heterocycles. Lutidine-*N*-oxide was deprotonated with $i\text{PrMgCl}^{11}$ followed by addition of iodine. A selective monohalogenation was observed which stands in contrast to the reaction performed using

alkyllithium, which gave mainly dihalogenated products. 2-Bromo-6-tri-*n*-butylstannyl pyridine (synthesized according to literature)¹² and 2-iodo-3,5-lutidine were coupled under standard Stille coupling conditions in the presence of 5% tetrakis (triphenylphosphine)palladium to yield fine crystals of **4-14**. The dimethyl substituted halo bipyridine was lithiated using *n*BuLi at -65 °C and after stabilizing the lithium intermediate (dark brown color) tributyltin chloride was added at -78 °C. The pale yellow organo-tin compound **4-15**, was coupled to halide **4-16** using standard Stille conditions. The resulting **4-17** was brominated in anhy. THF solution using 1.2 eq. of bromine solution in the presence of a lewis acid (AlCl₃). Thioacetate was obtained from compound **4-18**, by employing potassium thioacetate which was hydrolysed using cysteamine.HCl to produce a pale yellow solid, **4-19**. Though the reactions are simple to execute, almost every step required purification either by chromatography or recrystallization in ethanol.

α -Bromoacylindole **4-20** (Scheme 4-3), was relatively simple to synthesize¹³ with no requirement for purification by column chromatography or recrystallization to produce pure material. The synthesis of this component was performed in a similar manner as described in scheme 4-1. The bromide was converted to the corresponding thiol which was condensed with the protected dibromide **4-21** to form thioether **4-23**. The thioether was oxidized and cyclized to produce protected intermediate **4-25**. Deprotection of **4-25** was carried out in formic acid yielding **4-26** as a brownish white powder. Synthesis of donor fragment **4-26** utilized methods developed in the previous chapters.



Scheme 4-3 Synthetic scheme leading to 4-26. Reaction conditions: (a) (i) 1 eq. potassium thioacetate, absolute ethanol, 3h. (ii) 1 eq. cysteamine. HCl, acetonitrile, 4 h. 80 %; (b) 3 eq. potassium thioacetate, acetonitrile, 12 h. 80 %; (c) 4 eq. UHP, 3 eq. TFAA in acetonitrile, 90 minutes, 85% (d) 6-8 eq. ammonium acetate, glacial acetic acid, reflux 16 h., 85%; (e) formic acid (20 mL for per gram) reflux 1 h., 90%.



Scheme 4-4 Synthetic scheme leading to preparation of 4-5 and its homodimer. Reaction conditions: (a) 1 eq. 2,6-lutidine, MeCN, 3 h., 70%; (b) 4 eq. urea hydrogen peroxide, 3 eq. TFAA, MeCN, 90 minutes, 85%; (c) 6 eq. NH₄OAc, AcOH, reflux 18-36 h., 65%.

The final steps of the synthesis connected the acceptor and donor fragments **4-19** and **4-26** in the presence of a mild base such as 2,6-lutidine. The thioether was then oxidized using UHP/TFAA in the ratio of 4:3 equivalents and cyclized under acidic conditions using 6-8 equivalents of ammonium acetate to give the final array **4-5**.

4.4 Self-Association of the Double-Helical AAADDD•DDDAAA Complex

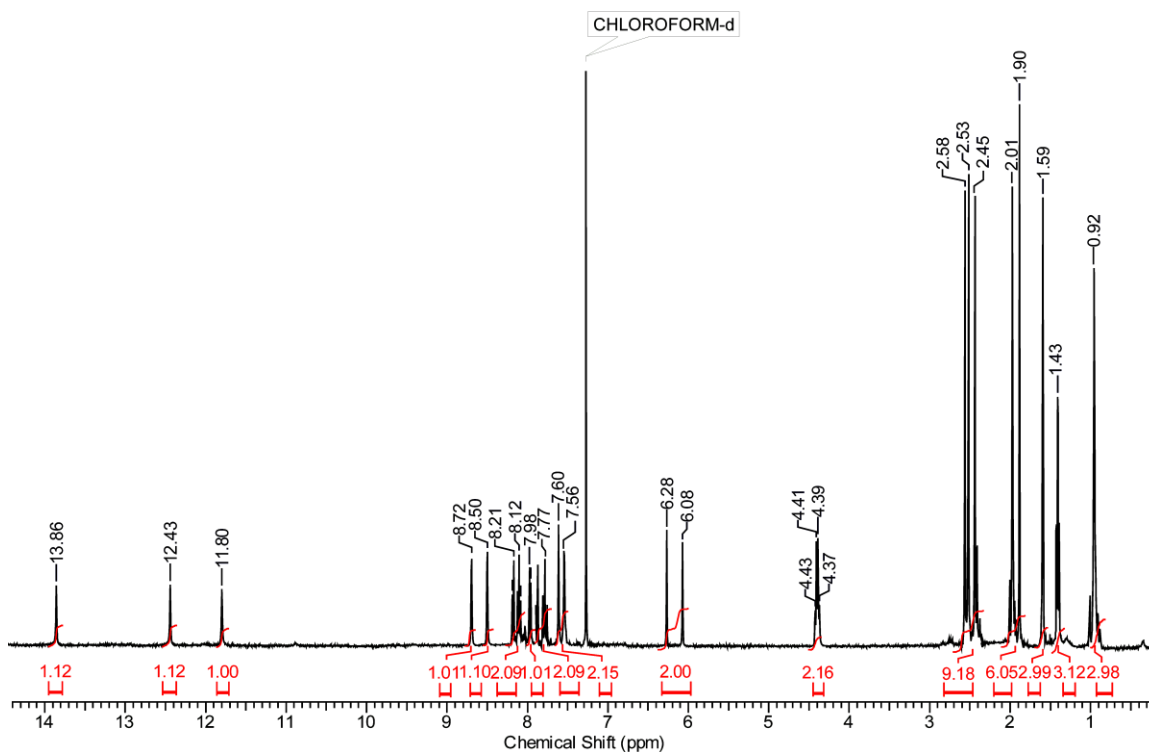


Figure 4-8 ^1H NMR spectrum of the double-helical AAADDD•DDDAAA **4-5.4-5** Complex, in 1.0×10^{-3} M solution of CDCl_3 at room temperature.

Multiple arrays usually display extremely strong binding propensities during complex formation in solution phase.^{4a,14} Often the dimerization constants (K_{dimer}) exceed the upper limit of values that can be measured through NMR dilution studies. The self-assembly of the AAADDD array displays exceptionally strong binding behaviour in CDCl_3 solution (Figure 4-8) as the peaks corresponding to the three protons of N-H peaks

(at 13.86, 12.43 and 11.80 ppm) show no movement upfield over a range NMR dilutions starting from 3.2 mM to 1 μ M, suggesting extremely strong dimerization of the array.

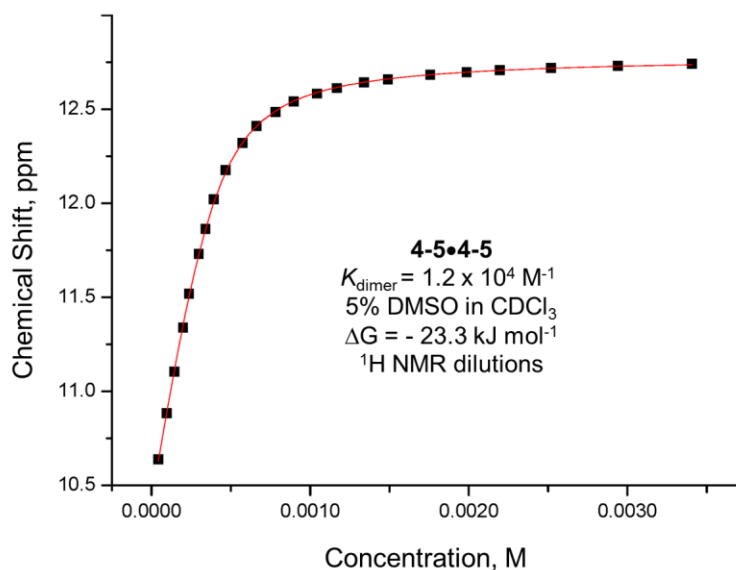


Figure 4-9 ^1H NMR dilution curve of array **4-5** with a K_{dimer} value of $1.2 \times 10^4 \text{ M}^{-1}$, calculated from fitting of the data to a 1:1 dimerization model with 5% DMSO in CDCl_3 .

Though a definitive binding constant cannot be determined in CDCl_3 , a K_{dimer} with a lower limit of $4.5 \times 10^7 \text{ M}^{-1}$ can be calculated with a conservative assumption of 10% dissociation at 1 μM . However, a definitive K_{dimer} value of $1.2 (\pm 0.1) \times 10^4 \text{ M}^{-1}$ was obtained by performing the dilution in 5% DMSO (a highly competitive solvent) in CDCl_3 solution (v/v) (figure 4-9). The mixed solvent experiment was carried out to estimate the dimerization values and compare them with the literature dimerization strengths of complexes with similar reported K_{dimer} values. Despite significant competition from 5% DMSO- d_6 the fact that the array still forms a stable dimer indicates extreme binding strength of the array in the absence of competitive solvents. When

compared to the literature^{4b,15} (with four three center hydrogen bonds, Figure 4-10), the K_{dimer} value of the array can be few orders of magnitude higher than the calculated lower limit K_{dimer} value ($4.5 \times 10^7 \text{ M}^{-1}$).

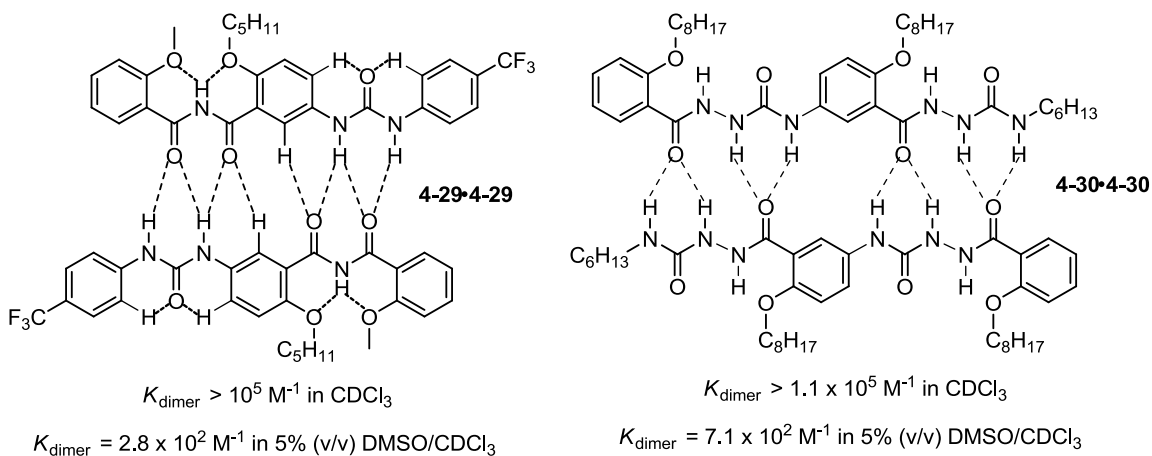


Figure 4-10 Examples of dimers with their definitive K_{dimer} values determined in 5% DMSO (v/v)/ CDCl_3 solvent mixture.

4.5 Conclusion

Complementary and self-complementary arrays were synthesized which display exceptionally strong hydrogen bonding based complexation studied employing NMR and ITC titrations. Their extreme strengths (K_{dimer} on the orders of 10^5 and 10^7 M^{-1}) and high binding constants are direct result of the attractive secondary interactions and also the number of hydrogen bonded heterocycles. Also these systems demonstrate the extendibility of our donor and acceptor heterocycles into longer oligomeric chains and may potentially be employed in the construction of supramolecular polymers and smart materials.

4.6 Experimental

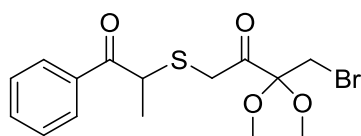
General. All experiments were performed under an atmosphere of nitrogen unless otherwise indicated. Chemicals were purchased from Aldrich and Alfa aesar and used as received. Solvents (THF, hexanes, dichloromethane, toluene and diethyl ether) were obtained from Caledon Laboratories and dried using an Innovative Technology Inc. Controlled Atmospheres Solvent Purification System that utilizes dual alumina columns (SPS-400-5), or purchased from Aldrich and used as is. Reactions were monitored by thin layer chromatography (TLC) performed on EM 250 Kieselgel 60 F254 silica gel plates. Column chromatography was performed with 240-400 mesh silica gel-60. Nuclear magnetic resonance spectra were recorded on an INOVA and Mercury 400 MHz spectrometer ($^{13}\text{C} = 100.52$ MHz). Proton and $^{13}\text{C}\{^1\text{H}\}$ NMR spectra were referenced relative to Me_4Si using the NMR solvent (^1H : CHCl_3 , $\delta = 7.26$ ppm, $\text{C}_3\text{HD}_5\text{O}$, $\delta = 2.05$ ppm,; $^{13}\text{C}\{^1\text{H}\}$: CHCl_3 , $\delta = 77.16$ ppm, $\text{C}_3\text{HD}_5\text{O}$, $\delta = 29.84, 206.26$ ppm). Solvents for ^1H NMR spectroscopy (chloroform- D , acetone- D_6 , DMSO- D_6) were purchased from Cambridge Isotope Laboratories. Mass spectra were recorded using an, electron ionization Finnigan MAT 8200 mass spectrometer and PE-Sciex API 365. X-ray diffraction data were collected on a Bruker Nonius Kappa CCD X-ray diffractometer using graphite monochromated Mo-K_α radiation ($\gamma = 0.71073 \text{ \AA}$).

4.6.1 Isothermal Titration Calorimetry Procedure

Isothermal titration calorimetry experiments were carried out using a Microcal VP-ITC microcalorimeter. The sample cell was charged with a 2.0×10^{-4} M solution of the donor

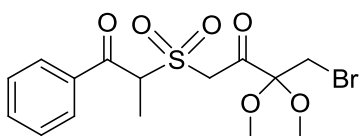
(4-1) dissolved in dry CHCl_3 (4Å mol. sieves) and the reference cell with the same pure solvent. The injector syringe was loaded with a 2×10^{-3} M solution of the acceptor dissolved in dry CHCl_3 . The instrument was equilibrated for 1 hour and then a series of $40 \times 5 \mu\text{L}$ injections were executed. A similar experiment was executed with a neat CHCl_3 solution in the sample cell (i.e. no host present) and this background run was subtracted from the analogous run containing host to give a corrected data set. The data was then integrated and fit satisfactorily to a 1:1 binding model. Each set of experiments was repeated three times to arrive at the average value and error quoted.

4.6.2 Synthetic Procedures



Synthesis of 4-6: Phenylpropiethiol (4.15 g, 25.00 mmol) and 1,4-Dibromo-3,3-dimethoxybutan-2-one (1) (7.25 g, 25.00 mmol) were dissolved in CH_3CN (75 mL) and

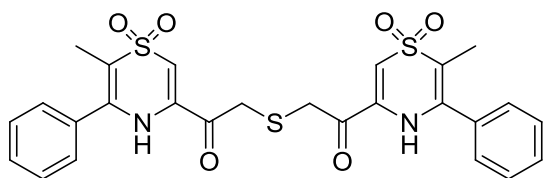
potassium carbonate (10.36 g, 75 mmol) was all added at once. The reaction mixture was stirred for 12 h before the slurry was filtered through celite, and the filtrate was concentrated under reduced pressure to give pure product, yellowish brown oil (9 g, 96%). ^1H NMR (400 MHz, CDCl_3) δ ppm 8.02 (d, $J = 7.2$ Hz, 2H), 7.57 (t, $J = 7.5$ Hz, 1H), 7.47 (t, $J = 7.8$ Hz, 2H), 4.52 (q, $J = 6.8$ Hz, 1H), 3.73 (m, 2H), 3.47 (s, 2H), 3.27 (s, 3H), 3.23 (s, 3H), 1.55 (d, $J = 7.0$ Hz, 3H); ^{13}C NMR (100 MHz, CDCl_3) δ ppm 202.6, 196.2, 135.1, 132.9, 128.4, 128.3, 101.7, 50.0, 49.8, 41.2, 37.6, 29.4, 16.4; EI HRMS calculated for $\text{C}_{15}\text{H}_{19}\text{BrO}_4\text{S}$ m/z : 375.0266, found 375.0272.



Synthesis of 4-7: To a 50 mL solution of acetonitrile, solid urea hydrogen peroxide (UHP) (8.52 g, 90.66 mmol) was

added followed by drop wise addition of TFAA (9.7 mL, 68.00 mmol). The reagent mixture was stirred to dissolve UHP and the mixture was added dropwise to a 50 mL acetonitrile solution of **4-6** (8.5 g, 22.66 mmol). The mixture was stirred vigorously for 90 minutes. The reaction solution was quenched with ice cold water, extracted with DCM (3 × 30 mL). The combined organic layers were washed with water and dried over anhydrous MgSO₄. The crude product was concentrated under reduced pressure to give the pure waxy orange product in 95% (8.70 g, 21.53 mmol). ¹H NMR (400 MHz, CDCl₃) δ ppm 8.03 (d, *J* = 8.2 Hz, 2H), 7.64 (t, *J* = 7.7 Hz, 1H), 7.52 (t, *J* = 7.7 Hz, 2H), 5.47 (q, *J* = 7.2 Hz, 1H), 4.68-4.64 (m, 2H), 3.47-3.43 (m, 2H), 3.32 (s, 3H), 3.26 (s, 3H), 1.75 (d, *J* = 7.2 Hz, 3H). ¹³C NMR (100 MHz, CDCl₃) δ ppm 199.1, 193.5, 135.3, 134.4, 129.0, 109.8, 101.6, 64.2, 59.2, 50.4, 40.2, 28.9, 12.3; EI HRMS calculated for C₁₅H₁₉BrO₆S *m/z* : 407.0164; found 407.0157.

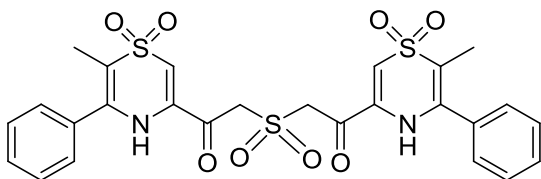
Compounds **4-8**, **4-9** are synthesized as according to the procedures mentioned in our recent publication.^{1a}



Synthesis of 4-10: To an aqueous solution of sodium sulfide (nonahydrate) (1.41 g, 5.87 mmol) a solution of **4-9** (4.00 g, 11.73

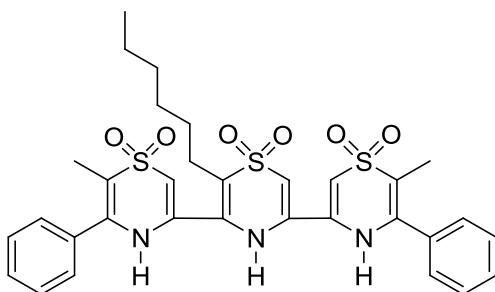
mmol) in 35 mL of acetone was added drop wise at 0 °C. The reaction mixture was brought to room temperature and was stirred for 3 h to give the condensed product. The reaction mixture was poured into 100 mL of ice cold water and acidified with 10% HCl solution, extracted with 3 x 30 mL of DCM. The organic layers were combined, dried over MgSO₄ and concentrated under reduced pressure to yield the desired product in 90% (2.93 g, 10.96 mmol). ¹H NMR (400 MHz, CDCl₃) δ ppm 7.96 (s, 2H), 7.46 (m, 6H),

7.35 (m, 4H), 6.77 (s, 2H), 3.93 (s, 4H), 2.02 (s, 6H); ^{13}C NMR (100 MHz, CDCl_3) δ ppm 188.9, 139.5, 134.9, 132.9, 130.3, 129.1, 128.4, 110.9, 104.2, 35.8, 8.7; EI HRMS calculated for $\text{C}_{26}\text{H}_{24}\text{N}_2\text{O}_6\text{S}_3$ m/z : 556.0796; found 556.0781.



Synthesis of 4-11: The title compound **4-11** was synthesized following the same procedure outlined for the synthesis of **4-7**

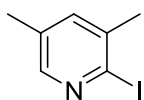
in 80 %. ^1H NMR (400 MHz, CDCl_3) δ ppm 8.03 (s, 2H), 7.50-7.40 (m, 6H), 7.38-7.28 (m, 4H), 6.89 (s, 2H), 5.00 (s, 4H), 2.04 (s, 6H); ^{13}C NMR (100 MHz, CDCl_3) δ ppm 194.3, 142.6, 135.7, 133.3, 131.9, 129.7, 128.1, 111.2, 105.6, 61.7, 9.1; EI HRMS calculated for $\text{C}_{26}\text{H}_{24}\text{N}_2\text{O}_8\text{S}_3$ m/z : 588.0695; found 588.0702.



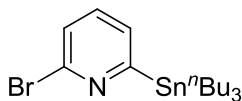
Synthesis of 4-4: To a solution of **4-11** (1.50 g, 2.55 mmol) in 40 mL acetonitrile, DBU (0.76 mL, 5.10 mmol) was added drop wise followed by slow addition of 1-iodohexane (0.75 mL, 5.10 mmol). The base and reagent was added

several times during the course of reaction to drive it towards product formation. After stirring the reaction mixture approximately a week, the reaction went to completion and the reaction mixture was quenched with 10% aqueous HCl solution and poured into 100 mL ice cold water and stirred for 12 h. The resulting precipitate was vacuum filtered, dried and carried forwards to cyclization reaction. To the crude residue solution in 15 mL of glacial acetic acid, 8 eq. of ammonium acetate was added in single portion and refluxed for approximately 3 days and the reaction mixture was cooled to room temperature and poured into 100 mL of ice cold solution and stirred for 2 h. The solids

were collected under vacuum filtration and the dried crude was purified by flash column chromatography using 5% methanol in DCM as eluent yielding pale yellow solid in overall 50 % (for two steps, 0.82 g, 1.25 mmol). ^1H NMR (400 MHz, CDCl_3) δ ppm 8.30 (s, 1H), 8.12 (s, 1H), 7.86 (s, 1H), 7.54-7.35 (m, 10H), 6.79 (s, 1H), 6.64 (s, 1H), 5.72 (s, 1H), 2.56 (t, $J = 7.0$ Hz, 2H), 2.32 (s, 3H), 2.21 (s, 3H), 1.52-1.38 (m, 2H), 1.12-0.89 (m, 6H), 0.72 (t, $J = 7.0$ Hz, 3H). ^{13}C NMR (100 MHz, CDCl_3) δ ppm 155.8, 155.3, 154.6, 147.8, 146.6, 146.0, 135.9, 134.6, 128.3, 18.0, 127.8, 118.1, 108.9, 107.3, 102.4, 102.0, 100.6, 32.4, 29.6, 26.8, 22.3, 21.6, 14.7, 9.1, 8.9; EI HRMS calculated for $\text{C}_{32}\text{H}_{35}\text{N}_3\text{O}_6\text{S}_3$ m/z : 653.1688; found 653.1696.

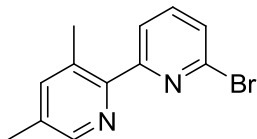


Synthesis of 4-13: The title compound was synthesized according to the method developed by Almqvist,¹¹ and deoxygenated using phosphorous trichloride as described previously, in overall 80 % yield. The ^1H , ^{13}C NMR studies matches with the known compound.¹⁶



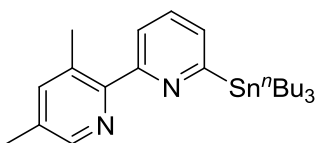
Synthesis of 2-bromo-6-(tributylstannyl)pyridine^{12a}: A solution of 2,6-dibromopyridine (3.00 g, 12.66 mmol) in anhy. THF was added drop wise to a solution $^n\text{BuLi}$ (1.2 eq. 15.19 mmol) at -10 °C. After the mixture was stirred for 45 minutes, at the same temperature, the orange solution was further cooled to -75 °C and treated with a solution of tributyltin chloride (1.2 eq., 3.32 mL, 15.19 mmol). After 1 h at -78 °C, the reaction mixture was warmed to room temperature. Hydrolysis was carried at 0 °C with water (20 mL). The organic layer was then extracted with diethylether (2x15 mL) and dried over MgSO_4 , and the solvents were evaporated under vacuum. The crude product was then purified by column chromatography with

hexanes:EtOAc, 4:1 mixtures as eluents giving pure product as yellow liquid in 90% (5.10 g, 11.39 mmol). The NMR spectral studies match with the reported literature values.^{12b}



Synthesis of 4-14: 2-bromo-6-tri-*n*-butylstannylpyridine (3.50 g, 7.83 mmol) and 2-iodo-3,5-lutidine (1.82 g, 7.83 mmol) were dissolved in anhy. toluene under nitrogen and refluxed in the

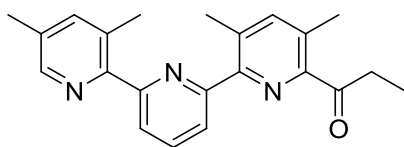
presence of 5% Pd(PPh₃)₄ (0.45 g, 0.39 mmol) for about 16 h and filtered. After removing the solvent under reduced pressure, flash column chromatography was done on the residue, using 1 : 1 ; EtOAc : Hexanes, as eluent system, yielded white needle like crystals (85%, 1.74 g, 2.01 mmol). ¹H NMR (400 MHz, CDCl₃) δ ppm 8.33 (s, 1H), 7.84 (d, *J* = 7.8 Hz, 1H), 7.65 (t, *J* = 7.8 Hz, 1H), 7.46 (d, *J* = 7.8 Hz, 1H), 7.41 (s, 1H), 2.53 (s, 3H), 2.35 (s, 3H); ¹³C NMR (100MHz,) δ CDCl₃ 156.3, 154.1, 147.6, 142.4, 140.2, 135.6, 133.3, 130.9, 128.3, 126.2, 122.7, 19.8, 18.7. EI HRMS calcd. for C₁₂H₁₁BrN₂ *m/z* : 262.0106, found : 262.0110.



Synthesis of 4-15: The title compound was synthesized following the same method as described for synthesis of **2** in 80 % yield. The product was purified by flash column

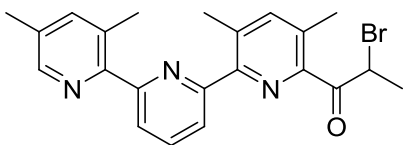
chromatography using 25:1 ratio of hexanes to ethyl acetate producing a pale yellow colour solution. ¹H NMR (400 MHz, CDCl₃) δ ppm 8.33 (s, 1H), 7.71 (d, *J* = 8.2 Hz, 1H), 7.60 (t, *J* = 8.2 Hz, 1H), 7.40 (s, 1H), 7.35 (d, *J* = 7.0 Hz, 1H), 2.55 (s, 3H), 2.35 (s, 3H), 1.66-1.52 (m, 4H), 1.40-1.27 (m, 10H), 1.15-1.08 (m, 4H), 0.89-0.85 (m, 9H); ¹³C NMR (100MHz,) δ CDCl₃ 168.4, 155.7, 154.9, 146.4, 138.7, 136.3, 132.5, 128.1, 126.8,

120.2, 27.3, 27.2, 26.2, 26.1, 19.9, 18.2, 16.2, 16.0, 14.0, 13.9. EI HRMS calcd. for $C_{24}H_{38}N_2Sn$ m/z : 474.2057, found : 474.2061.



Synthesis of 4-17: The title compound was synthesized following the same method as described for synthesis of **3** in 85% yield. The white crude solid was subjected to

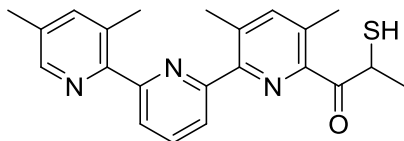
flash column chromatography using 1 : 1 ; EtOAc : Hexanes, as eluent system, yielded white needle like crystals. ¹H NMR (400 MHz, CDCl₃) δ ppm 8.37 (s, 1H), 7.99-7.91 (m, 1H), 7.84 (d, *J* = 8.2 Hz, 1H), 7.60-7.54 (m, 1H), 7.46 (s, 1H), 7.35-7.28 (m, 1H), 3.29 (q, *J* = 7.4 Hz, 2H), 2.60 (s, 6H), 2.51 (s, 3H), 2.36 (s, 3H), 1.20 (t, *J* = 7.4 Hz, 3H); ¹³C NMR (100MHz,) δ CDCl₃ 204.8, 157.7, 157.0, 153.7, 152.3, 148.7, 147.0, 143.4, 139.8, 138.7, 137.1, 135.7, 134.6, 133.6, 132.5, 131.7, 129.8, 1276.8, 123.2, 122.9, 32.9, 20.6, 20.1, 19.8, 18.0, 8.1. EI HRMS calcd. for $C_{22}H_{23}N_3O$ m/z : 345.1841, found : 345.1844.



Synthesis of 4-18: White crystalline needles of **7** (1.6 g, 4.78 mmol) were dissolved in 50 mL of anhy. THF followed by addition of 2% AlCl₃ under nitrogen.

Bromine solution, (0.26 mL, 5.72 mmol) was added drop wise to the reaction mixture over 15 minutes. The reaction mixture was stirred for 16 h. and was washed with sodium bicarbonate solution followed by extraction with 2x30 mL of dichloromethane. The organic layers were combined washed with 2x30 mL of water and dried over MgSO₄. The solvent is removed by roto-vaporation and subjected to flash column chromatography using EtOAc : DCM; 1: 9, as eluent system. The product was obtained in the form of yellowish white crystals (70 %, 1.41 g, 3.31 mmol). ¹H NMR (400 MHz, CDCl₃) δ ppm 8.36 (s, 1H), 8.00-7.93 (m, 2H), 7.85 (d, *J* = 8.2 Hz, 1H), 7.51 (s, 1H), 7.42 (s, 1H), 6.18

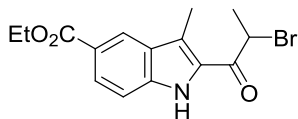
(q, $J = 6.4$ Hz, 1H), 2.62 (s, 3H), 2.61 (s, 3H), 2.50 (s, 3H), 2.36 (s, 3H), 1.88 (d, $J = 6.4$ Hz, 3H); ^{13}C NMR (100MHz,) δ CDCl_3 195.7, 157.6, 157.0, 156.7, 153.5, 152.5, 147.0, 143.5, 139.8, 137.2, 136.7, 132.6, 131.7, 123.4, 120.1, 43.6, 20.7, 20.1, 19.8, 19.5, 18.0. EI HRMS calcd. for $\text{C}_{22}\text{H}_{22}\text{BrN}_3\text{O}$ m/z : 423.0946, found : 423.0952.



Synthesis of 4-19: To a solution of potassium thioacetate (0.37 g, 3.20 mmol) dissolved in 25 mL of anhydrous ethanol was added a solution of the

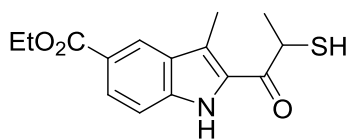
bromide **7** (1.35 g, 3.20 mmol) dissolved in 25 mL of anhydrous Ethanol drop wise over a period of 5 minutes. The reaction mixture was stirred for 4 h and solid contents were filtered through celite. The mixture was extracted with 3x15 mL of diethylether and the solids were again filtered through celite to give pure thioacetate of **7**. The organic layers were combined and concentrated by rotary evaporation, to obtain the thioacetate. The crude thioacetate was dissolved in 75 mL of dry DCM and an equivalent of cysteamine hydrochloride was added to the solution followed by addition of an equivalent of sodium bicarbonate under nitrogen blanket. The reaction mixture was stirred for 3 h and the reaction was quenched by 10% hydrochloride solution followed by the addition of 100 mL of water. Then, 3 x 40 mL of DCM was used to extract the organic layers and washed with 3 x 50 mL of water before the organic layers were pooled and dried over MgSO_4 . Reduction of solvent was carried out under reduced pressure to yield the title compound **4-19** (1.02 g, 2.27 mmol, 85% overall yield) as a pale yellow solid. ^1H NMR (400 MHz, CDCl_3) δ ppm 8.41 (s, 1H), 8.00-7.92 (m, 2H), 7.92-7.85 (m, 1H), 7.51 (s, 1H), 7.50 (s, 1H), 5.20-5.15 (m, 1H), 2.64 (s, 3H), 2.61 (s, 3H), 2.53 (s, 3H), 2.39 (s, 3H), 2.01 (d, $J = 8.2$ Hz, 1H), 1.59 (d, $J = 7.0$ Hz, 3H); ^{13}C NMR (100MHz,) δ CDCl_3 199.4, 158.3, 150.7,

148.3, 147.2, 144.0, 139.5, 138.5, 136.8, 136.4, 136.2, 126.1, 125.1, 42.4, 36.5, 20.7, 19.7, 19.5, 18.2. EI HRMS calcd. for $C_{22}H_{23}N_3OS$ m/z : 377.1562, found : 377.1566.



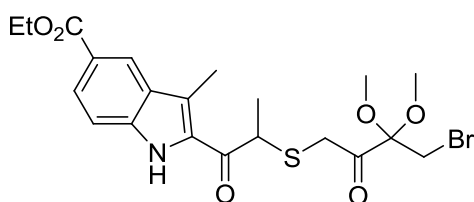
Synthesis of 4-20: The yellow brown title compound was made in accordance with the A.N. Kost *et al.*^{13b} method in 80 % yield

1H NMR (400 MHz, DMSO- d_6 , 298 K) δ (ppm) = 11.98 (s, 1H), 8.38 (m, 1H), 7.88 (m, 1H), 7.51 (m, 1H), 5.50 (q, J = 6.3Hz, 1H), 4.31 (q, J = 7.0Hz, 2H), 2.65 (s, 3H), 1.82 (d, J =6.3Hz, 2H), 1.34 (t, J =7.0Hz, 3H); ^{13}C NMR (100 MHz, DMSO- d_6 , 298 K) δ (ppm) = 186.6, 166.2, 138.9, 130.4, 127.4, 126.3, 123.7, 121.6, 121.1, 112.6, 60.4, 45.0, 19.8, 14.3, 10.4; EI-HRMS (m/z) calculated for $C_{15}H_{16}NBrO_3$: 337.0314, found 337.0311.



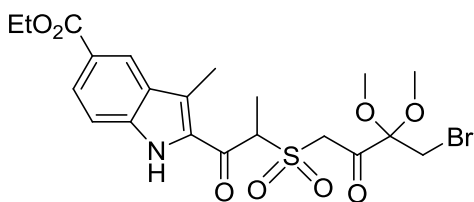
Synthesis of 4-21: The yellow brown title compound was made by following the general method for synthesis of thiols in 80 % described in the previous chapter. 1H NMR

(400 MHz, $CDCl_3$) δ ppm: 9.67 (s, *br*, 1H), 8.47 (s, 1H), 8.02 (dd, J = 8.6 Hz, J = 1.6 Hz, 1H), 7.39 (d, J = 8.6 Hz, 1H), 4.41 (q, J = 7.0 Hz, 2H), 4.26-4.22 (m, 1H), 2.08 (d, J = 9.8 Hz, 1H), 2.70 (s, 3H), 1.68 (d, J = 6.6 Hz, 3H), 1.42 (t, J =7.0 Hz, 3H). ^{13}C NMR (100MHz, $CDCl_3$) δ ppm 190.9, 167.1, 138.8, 131.2, 128.5, 127.4, 124.5, 122.6, 120.1, 111.6, 60.8, 38.5, 20.8, 14.3, 11.2. EI HRMS calcd. for $C_{15}H_{17}NO_3S$ m/z : 291.0929, found : 291.0926.



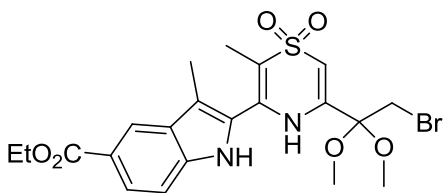
Synthesis of 4-23: The title compound was synthesized following the same method as

described for synthesis of **4-6** in 80 % yield. ^1H NMR (400 MHz, CDCl_3) δ ppm 10.06 (s, 1H), 8.47 (s, 1H), 8.07-8.00 (m, 1H), 7.48-7.36 (m, 1H), 4.41 (q, $J = 7.0$ Hz, 2H), 4.30 (q, $J = 6.6$ Hz, 1H), 3.90 (dd, $J = 97.9$ Hz, $J = 18.0$ Hz, 2H), 3.56-3.47 (m, 2H), 3.30 (s, 3H), 3.26 (s, 3H), 2.68 (s, 3H), 1.57 (d, $J = 6.6$ Hz, 3H), 1.42 (t, $J = 7.0$ Hz, 3H); ^{13}C NMR (100 MHz, CDCl_3 and $\text{DMSO}-d_6$, 1:1 ratio) δ ppm 190.4, 180.5, 168.3, 137.2, 131.6, 126.8, 126.1, 124.2, 121.1, 119.6, 112.5, 59.7, 49.8, 36.6, 28.5, 24.1, 23.7, 18.2, 14.7, 8.9. EI HRMS calcd. for $\text{C}_{21}\text{H}_{26}\text{BrO}_6\text{S}$ m/z : 499.0664; found 499.0669.



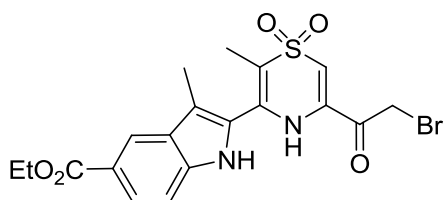
Synthesis of 4-24: The title compound was synthesized following the same method as described for synthesis of **4-7** in 85% yield. ^1H NMR (400 MHz, CDCl_3) δ ppm 9.63 (s, 1H), 8.46

(s, 1H), 8.06-7.97 (m, 1H), 7.43-7.36 (m, 1H), 5.31 (q, $J = 6.6$ Hz, 1H), 4.68 (s, 2H), 4.40 (q, $J = 7.0$ Hz, 2H), 3.46-3.41 (m, 2H), 3.31 (s, 3H), 3.26 (s, 3H), 2.76 (s, 3H), 1.79 (d, $J = 6.6$ Hz, 3H), 1.42 (t, $J = 7.0$ Hz, 3H); ^{13}C NMR (100 MHz, CDCl_3) δ ppm 198.7, 184.8, 166.9, 139.3, 131.9, 128.3, 128.0, 126.8, 124.6, 119.4, 112.0, 101.5, 66.0, 60.8, 50.4, 50.1, 34.2, 28.9, 14.3, 10.9. EI HRMS calcd. for $\text{C}_{21}\text{H}_{26}\text{BrO}_8\text{S}$ m/z : 531.0563; found 531.0565.



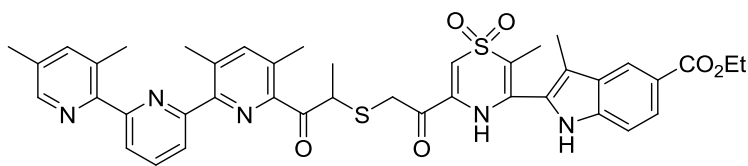
Synthesis of 4-25: The title compound was synthesized following the same method as described for synthesis of **4-8** in 85% yield. ^1H NMR (400 MHz, CDCl_3) δ ppm 9.23 (s, 1H), 8.85 (s, 1H), 8.48 (s, 1H), 8.07-7.95 (m, 1H), 7.45-7.39 (m, 1H), 6.04 (s, 1H), 4.40 (q, $J = 7.0$ Hz, 2H), 3.55 (s, 2H), 3.29 (s, 6H), 2.36 (s, 3H), 2.14 (s, 3H), 1.42 (t, $J = 7.0$ Hz, 3H); ^{13}C NMR (100 MHz, CDCl_3) δ ppm 164.3, 150.3,

147.7, 136.2, 131.4, 130.4, 127.8, 126.8, 121.5, 116.3, 111.4, 100.1, 66.0, 61.2, 52.6, 50.1, 35.2, 28.9, 14.3, 10.9, 8.1. EI HRMS calcd. for $C_{21}H_{25}BrN_2O_6S$ m/z : 512.0617; found 512.0620.



Synthesis of 4-26: The title compound was synthesized following the same method as described for synthesis of **4-9** in 90% yield. 1H NMR (400 MHz, $CDCl_3$) δ ppm 9.31 (s, 1H), 9.26

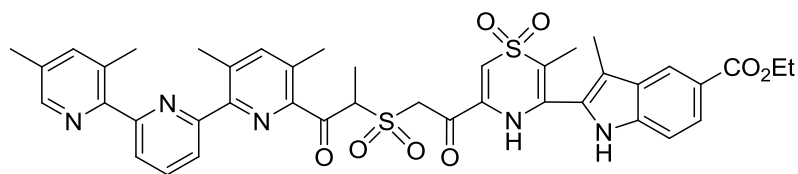
(s, 1H), 8.46 (s, 1H), 8.04-7.95 (m, 1H), 7.42-7.38 (m, 1H), 6.66 (s, 1H), 4.40 (q, $J = 7.0$ Hz, 2H), 4.30 (s, 2H), 2.32 (s, 3H), 2.15 (s, 3H), 1.42 (t, $J = 7.0$ Hz, 3H); ^{13}C NMR (100 MHz, $CDCl_3$) δ ppm 197.8, 164.3, 153.8, 148.2, 134.3, 131.6, 130.4, 127.1, 126.5, 121.4, 116.3, 114.5, 112.8, 111.8, 110.4, 62.5, 30.1, 14.3, 11.2, 8.6. EI HRMS calcd. for $C_{21}H_{25}BrN_2O_6S$ m/z : 512.0617; found 512.0620.



Synthesis of 4-27: To the thiol (1.00 g, 2.65 mmol) (**4-19**) solution in 25 mL of

anhy. DCM, the solution of bromide (**4-26**) (1.24 g, 2.65 mmol) in 40 mL anhy. DCM was added drop wise at 0 °C. After the addition the reaction mixture was brought to room temperature and after half an hour of stirring, 2,6-lutidine (0.32 mL, 2.75 mmol) was added and stirred for a period of 2 h. The reaction was quenched using 10% aqueous HCl solution and extracted using 2 x 20 mL of DCM and the organic layers were combined, dried over $MgSO_4$. The dried DCM layer was evaporated under reduced pressure yielding a yellow sticky compound. Flash column chromatography carried on the thioethers crude using 2% methanol in DCM as eluent system afforded white solid in

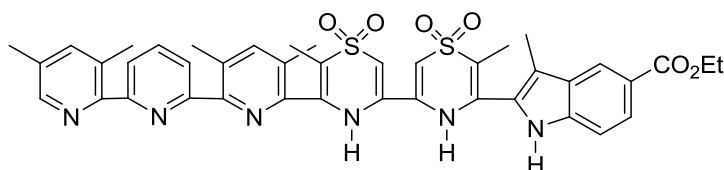
70% yield (1.42 g, 1.86 mmol). ^1H NMR (400 MHz, CDCl_3) δ ppm 11.15 (s, 1H), 8.68 (s, 1H), 8.32-8.26 (m, 2H), 7.95-7.80 (m, 2H), 7.72 (d, $J = 7.8$ Hz, 1H), 7.60 (d, $J = 7.8$ Hz, 1H), 7.43 (s, 2H), 7.25-7.21 (m, 1H), 6.26 (s, 1H), 5.24-5.17 (m, 1H), 4.40 (q, $J = 7.0$ Hz, 2H), 3.68 (dd, $J = 99.5$ Hz, $J = 15.6$ Hz, 2H), 2.58 (s, 3H), 2.43 (s, 3H), 2.34 (s, 6H), 2.18 (s, 3H), 2.03 (s, 3H), 1.46 (d, $J = 7.4$ Hz, 3H), 1.42 (t, $J = 7.0$ Hz, 3H); ^{13}C NMR (100MHz,) δ CDCl_3 198.6, 188.8, 167.5, 156.4, 153.1, 150.9, 147.2, 146.2, 143.7, 138.8, 136.9, 136.4, 135.8, 133.4, 131.7, 127.7, 126.5, 124.6, 123.5, 123.0, 122.4, 122.1, 114.4, 113.6, 111.1, 102.8, 60.7, 41.7, 35.4, 21.0, 20.3, 19.7, 19.3, 18.0, 16.5, 14.4, 9.1. EI HRMS calcd. for $\text{C}_{41}\text{H}_{41}\text{N}_5\text{O}_6\text{S}_2$ m/z : 763.2498, found :763.



Synthesis of 4-28: To a

solution of **4-27** (1.20 g, 1.57 mmol) in 30 mL of acetonitrile, a mixture of UHP (0.60 g, 6.29 mmol) and TFAA (0.70 mL, 4.72 mmol) dissolved in 10 mL of acetonitrile was added drop wise and the reaction was stirred at room temperature for 90 minutes. The reaction mixture was poured in a beaker containing 100 mL of ice cold water and stirred to precipitate the yellowish white product in 85% yield (1.00 g, 1.33 mmol). ^1H NMR (400 MHz, CDCl_3) δ ppm 10.61 (s, 1H), 9.90 (s, 1H), 8.34 (s, 1H), 8.18-8.12 (m, 2H), 7.97-7.90 (m, 1H), 7.78 (d, $J = 7.8$ Hz, 1H), 7.69 (d, $J = 7.8$ Hz, 1H), 7.58 (s, 1H), 7.56 (s, 1H), 7.34-7.30 (m, 1H), 6.31 (s, 1H), 6.28-6.22 (m, 1H), 4.68 (dd, $J = 124.5$ Hz, $J = 15.6$ Hz, 2H), 4.42 (q, $J = 7.0$ Hz, 2H), 2.52 (s, 3H), 2.47 (s, 3H), 2.38 (s, 6H), 2.17 (s, 3H), 2.05 (s, 3H), 1.65 (d, $J = 7.4$ Hz, 3H), 1.43 (t, $J = 7.0$ Hz, 3H); ^{13}C NMR (100MHz,) δ CDCl_3 197.8, 189.6, 166.9, 156.3, 153.4, 150.3, 146.9, 146.1, 142.5, 139.0, 137.2, 136.5, 136.1, 133.8, 131.1, 127.4, 126.6, 125.2, 123.3,

122.7, 122.5, 121.8, 115.1, 113.8, 111.6, 103.7, 74.6, 62.4, 60.8, 21.5, 20.8, 19.1, 18.5, 17.9, 16.1, 14.8, 9.6. EI HRMS calcd. for $C_{41}H_{41}N_5O_8S_2$ m/z : 795.2397, found :795.



Synthesis of 4-5: To a solution of **4-28** (0.85 g, 1.07 mmol) in 15 mL of glacial

acetic acid, solid ammonium acetate (0.50 g, 6.40 mmol) was added in portions and the reaction mixture was refluxed for approximately 16 h. The mixture was cooled to room temperature and poured in to a beaker containing 150 mL of ice cold water to precipitate the crude product. The crude was purified using preparatory thin layer chromatography using 5% methanol in DCM as eluent to give pale yellowish crystals in 65 % yield (0.52 g, 0.69 mmol). 1H NMR (400 MHz, $CDCl_3$) δ ppm 13.86 (s, 1H), 12.43 (s, 1H), 11.80 (s, 1H), 8.72 (s, 1H), 8.50 (s, 1H), 8.24-8.10 (m, 2H), 7.99-7.95 (m, 1H), 7.92-7.68 (m, 2H), 7.60 (s, 1H), 7.56 (s, 1H), 6.28 (s, 1H), 6.08 (s, 1H), 4.40 (q, $J = 7.0$ Hz, 2H), 2.58 (s, 3H), 2.53 (s, 3H), 2.45 (s, 3H), 2.01 (s, 3H), 1.90 (s, 3H), 1.59 (s, 3H), 1.43 (t, $J = 7.0$ Hz, 3H), 0.92 (s, 3H); ^{13}C NMR (100MHz,) δ $CDCl_3$ 165.8, 156.3, 156.2, 156.0, 155.7, 155.6, 155.2, 154.9, 150.5, 148.2, 146.6, 141.3, 137.0, 136.1, 131.8, 130.4, 130.0, 127.8, 126.5, 127.1, 122.3, 121.8, 121.2, 118.5, 116.2, 115.4, 112.8, 112.1, 111.6, 101.1, 100.7, 61.8, 60.8, 20.8, 20.1, 19.6, 19.3, 15.1, 14.7, 9.6, 8.7. EI HRMS calcd. for $C_{41}H_{40}N_6O_6S_2$ m/z : 776.2451, found :776.2457.

4.7 References

1. (a) Wang, H.-B.; Mudraboyina, B. P.; Li, J.; Wisner, J. A. *Chem. Commun.* **2010**, 46 (39), 7343-7345; (b) Wang, H.-B.; Mudraboyina, B. P.; Wisner, J. A. *Chem.*

- Eur. J.* **2012**, *18* (5), 1322-1327.
2. Beijer, F. H.; Sijbesma, R. P.; Kooijman, H.; Spek, A. L.; Meijer, E. W. *J. Am. Chem. Soc.* **1998**, *120* (27), 6761-6769.
 3. Zeng, H.; Yang, X.; Brown, A. L.; Martinovic, S.; Smith, R. D.; Gong, B. *Chem. Commun.* **2003**, (13), 1556-1557.
 4. (a) Mayer, M. F.; Nakashima, S.; Zimmerman, S. C. *Org. Lett.* **2005**, *7* (14), 3005-3008; (b) Chu, W.-J.; Yang, Y.; Chen, C.-F. *Org. Lett.* **2010**, *12* (14), 3156-3159.
 5. (a) Prins, L. J.; Reinhoudt, D. N.; Timmerman, P. *Angew. Chem. Int. Ed.* **2001**, *40* (13), 2382-2426; (b) Cooke, G.; Rotello, V. M. *Chem. Soc. Rev.* **2002**, *31* (5), 275-286; (c) Hunter, C. A.; Anderson, H. L. *Angew. Chem. Int. Ed.* **2009**, *48* (41), 7488-7499; (d) Misuraca, M. C.; Grecu, T.; Freixa, Z.; Garavini, V.; Hunter, C. A.; van Leeuwen, P. W. N. M.; Segarra-Maset, M. D.; Turega, S. M. *J. Org. Chem.* **2011**, *76* (8), 2723-2732.
 6. Bulger, P. G.; Cottrell, I. F.; Cowden, C. J.; Davies *, A. J.; Dolling, U.-H. *Tet. Lett.* **2000**, *41* (8), 1297-1301.
 7. Ho, T.-L.; Fieser, M.; Fieser, L.; Smith, J.; Fieser, L. F., 1,8-Diazabicyclo[5.4.0]undec-7-ene, DBU. In *Fieser and Fieser's Reagents for Organic Synthesis*, John Wiley & Sons, Inc.: 2006.
 8. Baliah, V.; Rangarajan, T. *J. Org. Chem.* **1961**, *26* (3), 969-970.

9. Li, J. The design of hydrogen bonded double helices. monograph, University of Western Ontario, London Ontario, 2009.
10. (a) Gooch, A.; McGhee, A. M.; Pellizzaro, M. L.; Lindsay, C. I.; Wilson, A. J. *Org. Lett.* **2010**, *13* (2), 240-243; (b) Beijer, F. H.; Sijbesma, R. P.; Kooijman, H.; Spek, A. L.; Meijer, E. W. *J. Am. Chem. Soc.* **1998**, *120* (27), 6761-6769; (c) Chien, C.-H.; Leung, M.-k.; Su, J.-K.; Li, G.-H.; Liu, Y.-H.; Wang, Y. *J. Org. Chem.* **2004**, *69* (6), 1866-1871; (d) Lafitte, V. G. H.; Aliev, A. E.; Hailes, H. C.; Bala, K.; Golding, P. *J. Org. Chem.* **2005**, *70* (7), 2701-2707.
11. Andersson, H.; Gustafsson, M.; Olsson, R.; Almqvist, F. *Tet. Lett.* **2008**, *49* (48), 6901-6903.
12. (a) Verniest, G.; Wang, X.; Kimpe, N. D.; Padwa, A. *J. Org. Chem.* **2009**, *75* (2), 424-433; (b) Getmanenko, Y. A.; Twieg, R. J. *J. Org. Chem.* **2008**, *73* (3), 830-839; (c) Zoppellaro, G.; Ivanova, A.; Enkelmann, V.; Geies, A.; Baumgarten, M. *Polyhedron* **2003**, *22* (14-17), 2099-2110.
13. (a) Yudin, L.; Budylin, V.; Kost, A. *Chem. Heterocycl. Compd.* **1967**, *3* (2), 561-563; (b) Kost, A. N.; Gorbunova, S. M.; Budylin, V. A. *Khim. Geterotsykl.* **1971**, *11*, 1522-1526.
14. Zeng, H.; Miller, R. S.; Flowers, R. A.; Gong, B. *J. Am. Chem. Soc.* **2000**, *122* (11), 2635-2644.
15. Li, X.; Fang, Y.; Deng, P.; Hu, J.; Li, T.; Feng, W.; Yuan, L. *Org. Lett.* **2011**, *13*

(17), 4628-4631.

16. Gros, P.; Viney, C.; Fort, Y. *Synlett* **2002**, (4), 628-630.

Chapter 5

5 Conclusions

Linear self-complementary AADD arrays are some of the most studied in the literature of hydrogen bonded complexes and they are widely used in supramolecular polymers and nano- materials. We report a new non-linear self-complementary design of AADD arrays **2-1a-d** whose synthesis, design and binding propensities (in solid state and solution) were investigated. The importance of unwanted intramolecular hydrogen bonding that prevents double-helical complex formation and the elimination of this intramolecular interaction through steric interference was examined. Dimerization constants as function of array substitution (electron donating groups on acceptor components and electron withdrawing groups on donor components) were measured and discussed. A preorganization effect due to trimethylene tether group between the donor components of **2-1d** was highlighted. ¹H NMR dilution studies indicated that the dimerization constants of **2-1a-d** range from $9.0 \times 10^1 \text{ M}^{-1}$ to $> 4.5 \times 10^7 \text{ M}^{-1}$. This demonstrates a wide range ($>10^5 \text{ M}^{-1}$ or $\Delta\Delta G \geq 32.6 \text{ kJ mol}^{-1}$) of stabilities with respect to substitutions and preorganization of the AADD oligomers.

Secondly, how substituent groups, alkyl chain incorporation and preorganization affect the binding stabilities of the AAA•DDD complexes **3-5a,b**•**3-2a** and **3-6a,b**•**3-2a** was investigated. The electron withdrawing effects of an ester group was studied in comparison to unsubstituted DDD arrays. Not only the solubilizing effect of an appended pentyl group was examined, but also the destabilization effect (X-ray structure of **3-5b**) due to steric hindrance caused by the alkyl chain resulting in expenditure of energy in

bringing the donor array in to optimal geometry for complexation. This was reflected in a great decrease in complex stability. On the other hand, the preorganization effect compensated for the loss in terms of increased binding constants (5.0 kJ mol⁻¹ or at least an order of magnitude per tether). The comparison studies allowed calculation of exact amounts of stabilizing energies due to preorganization and substitution groups which indicate that triple hydrogen bond complexes with association constants up to at least 10⁶ M⁻¹ can be synthesized and used in construction of reversible supramolecular polymers.

As a final study, synthesis of a soluble DDD array **4-4** was realized through incorporation of a hexyl group on the central donor heterocycle. Formation of a highly stable complementary complex ($K_a = 1.4 \times 10^5 \text{ M}^{-1}$ for triple hydrogen bonded complex) was examined, despite the destabilizing effect of the corresponding bulky hexyl group. Comparison with our previous studies allowed a calculated K_a value $\geq 10^6 \text{ M}^{-1}$ for the non-alkylated complex **4-1-4-2**. In addition, a self-complementary complex AAADDD•DDDAAA was synthesized to test the extensibility and the binding propensity of longer arrays. The ¹H NMR studies display similar results as in the case of array **2-1d** and a $K_{\text{dimer}} \geq 4.5 \times 10^7 \text{ M}^{-1}$ was estimated as the lower limit in CDCl₃ and a $K_{\text{dimer}} = 1.2 \times 10^4 \text{ M}^{-1}$ was determined in 5% DMSO/CDCl₃. The extreme stabilities of the complex are the direct outcome of an increased number of hydrogen bonding components and attractive secondary hydrogen bonding interactions. The values are similar to literature values of multi hydrogen bonded complexes.

In conclusion, we have constructed highly stable complementary and self-complementary double helical complexes (K_a and $K_{\text{dimer}} > 10^5 \text{ M}^{-1}$) which can likely be used as hydrogen-bonded motifs for supramolecular polymerization.

5.1 Scope for Future Work

The main disadvantage of the DDD arrays was their insolubility which can be prevented by incorporation of alkyl chains at 3-position of indoles or on the thiazine dioxides. However, appending the alkyl chains led to destabilization of the complexation due to the bulky nature of the alkyl chain. It may be that appending shorter alkyl chains such as ethyl or propyl (Figure 5-1) could induce the required solubility but still not be too sterically demanding to avoid unwanted destabilization of the resulting complex with the AAA array.

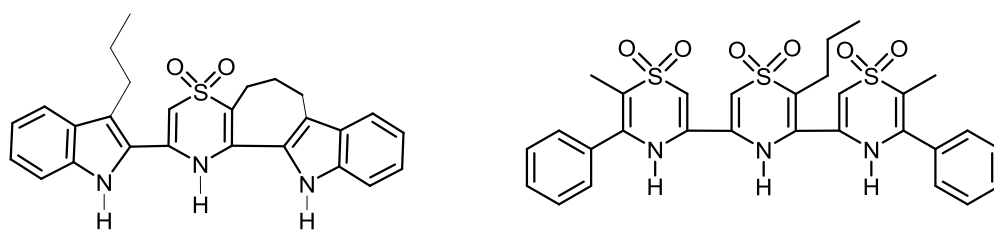


Figure 5-1 Propyl chain incorporated DDD arrays.

In addition a modification could be made to the acceptor arrays. For example a dimethylamine group can be incorporated at the 4-position of the pyridyl heterocycles and preorganization could be introduced by adding trimethylene tethers to connect one or two of the pyridyl rings (Figure 5-2).

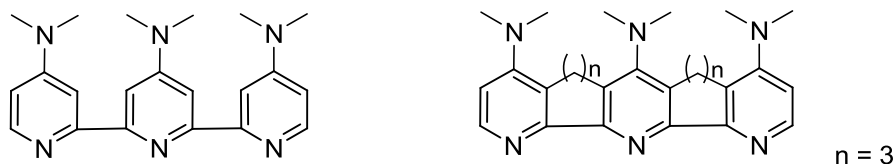


Figure 5-2 : *N,N'*-dimethylamine functionalized and preorganized DDD arrays.

All the above DDD and AAA arrays are potential motifs for synthesizing supramolecular reversible polymers and therefore it would be very interesting to study the synthesis and macromolecular behaviour of main-chain polymers derived from these hydrogen bonding complementary motifs.

As an application of the complexes towards construct of supramolecular smart materials, reversible polymers can be synthesized based on the hydrogen bonding utilizing the complex arrays discussed in previous chapters as depicted in Figure 5-3.

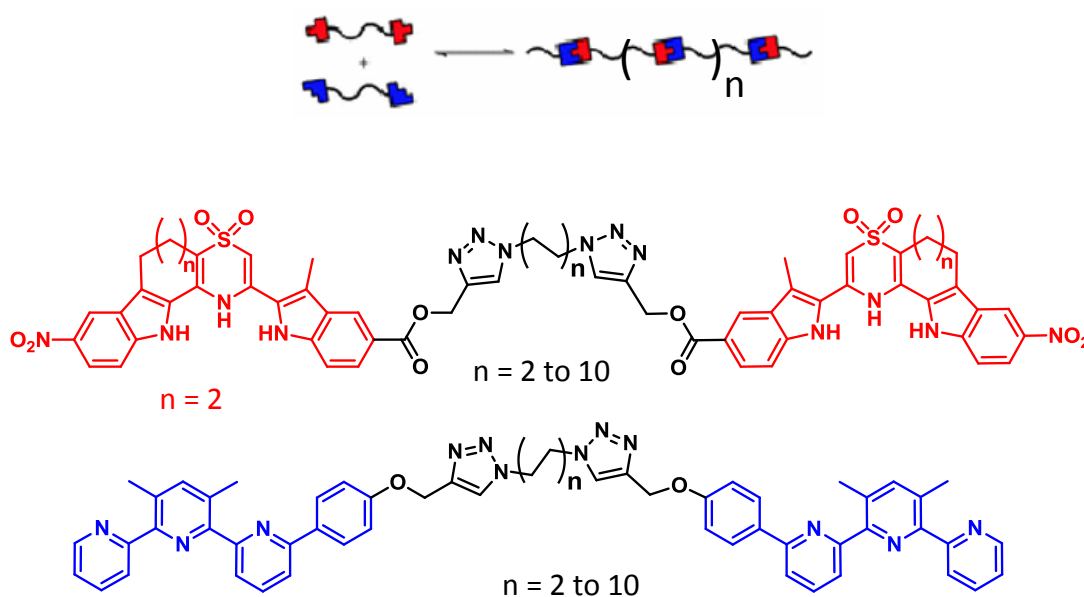


Figure 5-3 : Supramolecular polymers formed on the basis of DDD-Linker-DDD and AAA-Linker-AAA.

Apart from the reversible polymers, hydrogen bonded complexes found applications relating to hot-melt inks,¹ aqueous based inks formulated with supramolecular polymers (Xerox),² polychrome graphics³ (Kodak) and coatings for glass fibers (DSM)⁴. Our new arrays with extreme stabilities are very promising in displaying stimuli responsive

behavior and would present a very interesting research study to enhance the desirable properties.

5.2 References

1. Goodbrand, H. B., et al., Phase change ink composition. Patent No: US2003/0105185 A1, 2003.
2. Smith, T. W., et al., Aqueous ink compositions. Patent No: US2003/0079644 A1, 2003.
3. Pappas, S. P., et al., Imageable element and composition comprising thermally reversible polymers. Patent No: WO02053626 A1, 2002.
4. Loontjens, J. A., et al., *Supramolecular compound*. Patent No: EP1031589 A1, 2000.

Appendices

Permission to Reproduce Material from the literature

This is a License Agreement between Bhanu Mudraboyina and John Wiley and Sons ("John Wiley and Sons"). The license consists of your order details, the terms and conditions provided by John Wiley and Sons, and the payment terms and conditions.

License Number	2884821367687
License date	Apr 09, 2012
Licensed content publisher	John Wiley and Sons
Licensed content publication	Angewandte Chemie International Edition
Licensed content title	Quantifying Intermolecular Interactions: Guidelines for the Molecular Recognition Toolbox
Licensed content author	Christopher A. Hunter
Licensed content date	Oct 11, 2004
Start page	5310
End page	5324
Type of use	Dissertation/Thesis
Requestor type	University/Academic
Format	Electronic
Portion	Figure/table
Number of figures/tables	2
Original Wiley figure/table number(s)	Figure3 and figure-4

This is a License Agreement between Bhanu Mudraboyina and John Wiley and Sons ("John Wiley and Sons") provided by Copyright Clearance Center ("CCC"). The license consists of your order details, the terms and conditions provided by John Wiley and Sons, and the payment terms and conditions.

License Number	2884830331253
License date	Apr 09, 2012
Licensed content publisher	John Wiley and Sons
Licensed content publication	Angewandte Chemie International Edition
Licensed content title	Quantifying Intermolecular Interactions: Guidelines for the Molecular Recognition Toolbox
Licensed content author	Christopher A. Hunter
Licensed content date	Oct 11, 2004
Start page	5310
End page	5324
Type of use	Dissertation/Thesis
Requestor type	University/Academic
Format	Print and electronic
Portion	Figure/table
Number of figures/tables	1
Number of extracts	None

This is a License Agreement between Bhanu Mudraboyina and Nature Publishing Group ("Nature Publishing Group") provided by Copyright Clearance Center ("CCC"). The license consists of your order details, the terms and conditions provided by Nature Publishing Group, and the payment terms and conditions.

License Number	2884831447557
License date	Apr 09, 2012
Licensed content publisher	Nature Publishing Group
Licensed content publication	Nature Chemistry
Licensed content title	An AAAA–DDDD quadruple hydrogen-bond array
Licensed content author	Barry A. Blight, Christopher A. Hunter, David A. Leigh, Hamish McNab, Patrick I. T. Thomson
Licensed content date	Feb 21, 2011
Volume number	3
Issue number	3
Type of Use	reuse in a thesis/dissertation
Requestor type	non-commercial (non-profit)
Format	print and electronic
Portion	figures/tables/illustrations
Number of figures/tables/illustrations	1
High-res required	no
Figures	Figure-5
Author of this NPG article	no
Your reference number	None
Title of your thesis / dissertation	Complementary and self-complementary hydrogen bonded double-helices
Expected completion date	May 2012
Estimated size (number of pages)	250

This is a License Agreement between Bhanu Mudraboyina and Nature Publishing Group ("Nature Publishing Group") provided by Copyright Clearance Center ("CCC"). The license consists of your order details, the terms and conditions provided by Nature Publishing Group, and the payment terms and conditions.

License Number	2884840403685
License date	Apr 09, 2012
Licensed content publisher	Nature Publishing Group
Licensed content publication	Nature
Licensed content title	Interconversion of single and double helices formed from synthetic molecularstrands
Licensed content author	Volker Berl, Ivan Huc, Richard G. Khoury, Michael J. Krische and Jean-Marie Lehn
Licensed content date	Oct 12, 2000
Volume number	407
Issue number	6805
Type of Use	reuse in a thesis/dissertation
Requestor type	non-commercial (non-profit)
Format	print and electronic
Portion	figures/tables/illustrations
Number of figures/tables/illustrations	1
Figures	Figure-3
Author of this NPG article	no
Your reference number	None
Title of your thesis / dissertation	Complementary and self-complementary hydrogen bonded double-helices
Expected completion date	May 2012
Estimated size (number of pages)	250

This is a License Agreement between Bhanu Mudraboyina and John Wiley and Sons ("John Wiley and Sons") provided by Copyright Clearance Center ("CCC"). The license consists of your order details, the terms and conditions provided by John Wiley and Sons, and the payment terms and conditions.

License Number	2884860256656
License date	Apr 09, 2012
Licensed content publisher	John Wiley and Sons
Licensed content publication	Advanced Materials
Licensed content title	Supramolecular Polymer Materials: Chain Extension of Telechelic Polymers Using a Reactive Hydrogen-Bonding Synthone
Licensed content author	B. J. B. Folmer,R. P. Sijbesma,R. M. Versteegen,J. A. J. van der Rijt,E. W. Meijer
Licensed content date	Jun 1, 2000
Start page	874
End page	878
Type of use	Dissertation/Thesis
Requestor type	University/Academic
Format	Print and electronic
Portion	Figure/table
Number of figures/tables	1
Number of extracts	None
Original Wiley figure/table number(s)	Figure-2

Curriculum Vitae

- Name:** Bhanu Prakash Mudraboyina
- Post-secondary Education and Degrees:** University of Western Ontario
London, Ontario, Canada
1996-1999 B.Sc. Honors in Chemistry
- Sri Sathya Sai Institute of Higher Learning
Prasanthinilayam, Andhra Pradesh, India
1999-2001 M.Sc. Honors in Chemistry
- The University of Western Ontario
London, Ontario, Canada
2007-2012 Ph.D.
- Honours and Awards:** International Graduate Student Scholarship (IGSS) 2007-2008
Western Graduate Research Scholarship (WGRS) 2008-2009
Western Graduate Research Scholarship (WGRS) 2010-2011
Western Graduate Research Scholarship (WGRS) 2011-2012
Best Research Project Award in M.Sc. 2002
January **2004** – Qualified the joint CSIR-UGC
National Eligibility Test (NET) for Lectureship (India)
- Related Work Experience** Teaching Assistant
The University of Western Ontario 2007-2012
Doctoral Research Associate 2008-2009
Research Associate, IIT Kanpur, India 2005-2006
Founder and Lecturer, CSIR Coaching Center, India 2002-2004
- Publications:**
1. Wang, H. -B.; **Mudraboyina, B. P.**; Li, J.; Wisner, J. A.* Minimal complementary hydrogen-bonded double helices. *Chem. Commun.* **2010**, 46 (39), 7343-7345.
 2. **Mudraboyina, B. P.**; Wang, H. -B.; Newbury, R.; Wisner, J. A.* 2,6-Diaminopyridinium tetra-phenyl-borate-1,2-bis-(5,7-dimethyl-1,8-naphthyridin-2-yl)diazene. *Acta crystallographica E.* **2011**, 67, o1222.
 3. Wang, H. -B.; **Mudraboyina, B. P.**; Wisner, J. A.* Substituent effects in double-helical hydrogen-bonded AAA-DDD complexes. *Chem. Eur. J.* 2012, 18, 1322-1327.
 4. **Mudraboyina, B. P.**; Wisner, J. A.* Synthesis and Self-association of Double-Helical AADD Arrays *Chem. Eur. J. under review.*

Conference Presentations:

1. **Mudraboyina, B. P.**; Wisner, J. A.* The Effect of Sterics and Preorganization on Stability in Double Helical AAA-DDD Complexes. 39th Physical Organic Minisymposium, London, Ontario, Canada, November 4-6, 2011. (Oral)
2. **Mudraboyina, B. P.**; Wisner, J. A.* Double-helical hydrogen bonded AAA-DDD complexes. 94th Canadian Chemistry Conference and Exhibition, Montréal, Québec, Canada, June 5-9, 2011. (Poster)
3. **Mudraboyina, B. P.**; Wisner, J. A.* Double Helical AAA-DDD Hydrogen Bond Complexes. 3rd French-Canadian Workshop in Supramolecular Chemistry, Université de Montréal, Montréal, Québec, Canada, June 21-23, 2010. (Oral)
4. Wisner, J. A.*; **Mudraboyina, B. P.** Synthesis and Self-association of AADD Hydrogen Bonded Double Helices. 5th International Symposium On Macrocyclic & Supramolecular Chemistry, Nara, Japan, June 6-10, 2010. (Poster)
5. **Mudraboyina, B. P.**; Wisner, J. A.* Very Strong Hydrogen Bonding in Double Helical AAA-DDD Complexes. 93rd Canadian Chemistry Conference and Exhibition, Toronto, Ontario, Canada, May 29-June 2, 2010. (Poster)
6. **Mudraboyina, B. P.**; Wisner, J. A.* Synthesis and Complimentary Studies of AADDs and DDD, Double Helical Molecular Recognising Motifs. 92nd Canadian Chemistry Conference and Exhibition, Hamilton, Ontario, Canada, May 30-June 4, 2009. (Poster)
7. Wisner, J. A.*; Li, J.; **Mudraboyina, B. P.** Hydrogen-bonded double helices. 91th Canadian Chemistry Conference and Exhibition, Edmonton, AB. May 24-June 28, 2008, (Oral)